



**HAL**  
open science

# Ionic liquids for the separation of gaseous hydrocarbons

Leila Moura

► **To cite this version:**

Leila Moura. Ionic liquids for the separation of gaseous hydrocarbons. Theoretical and/or physical chemistry. Université Claude Bernard - Lyon I, 2014. English. NNT : 2014LYO10097 . tel-01064777

**HAL Id: tel-01064777**

**<https://theses.hal.science/tel-01064777>**

Submitted on 17 Sep 2014

**HAL** is a multi-disciplinary open access archive for the deposit and dissemination of scientific research documents, whether they are published or not. The documents may come from teaching and research institutions in France or abroad, or from public or private research centers.

L'archive ouverte pluridisciplinaire **HAL**, est destinée au dépôt et à la diffusion de documents scientifiques de niveau recherche, publiés ou non, émanant des établissements d'enseignement et de recherche français ou étrangers, des laboratoires publics ou privés.

N° d'ordre 97-2014  
2014

Année

THESE DE L'UNIVERSITE DE LYON

Délivrée par

L'UNIVERSITE CLAUDE BERNARD LYON 1

ECOLE DOCTORALE DE CHIMIE

DIPLOME DE DOCTORAT

(arrêté du 7 août 2006)

soutenue publiquement le 16 Juin 2014

par

**Mlle Leila MOURA**

## **Ionic liquids for the separation of gaseous hydrocarbons**

Directeur de thèse : Catherine SANTINI  
(Directeur de recherche CNRS, Université de Lyon 1)

Co-directeur de thèse : Margarida COSTA GOMES  
(Directeur de recherche CNRS, Université Blaise Pascal, Clermont-Ferrand)

**JURY:** Pr. Dr. Anja-Verena MUDRING (Ruhr-Universität, Bochum), rapporteur  
Dr. John D. HOLBREY (Queen's University, Belfast), rapporteur  
Pr. Stéphane DANIELE (Professeur, Université Lyon 1), examinateur  
Dr. Alain BERTHOD (Directeur de recherche CNRS, Lyon), examinateur  
Dr. Isabelle BILLARD (Directeur de recherche CNRS, IPHC) examinateur  
Dr. Alain METHIVIER (Directeur de recherche, IFPEN Lyon), membre invité  
Dr. Catherine SANTINI (Directeur de recherche CNRS, CPE Lyon)  
Dr. Margarida COSTA GOMES (Directeur de recherche CNRS, ICCF)



# UNIVERSITE CLAUDE BERNARD - LYON 1

## **Président de l'Université**

Vice-président du Conseil d'Administration  
Vice-président du Conseil des Etudes et de la Vie  
Universitaire  
Vice-président du Conseil Scientifique  
Directeur Général des Services

## **M. François-Noël GILLY**

M. le Professeur Hamda BEN HADID  
M. le Professeur Philippe LALLE  
M. le Professeur Germain GILLET  
M. Alain HELLEU

## **COMPOSANTES SANTE**

Faculté de Médecine Lyon Est – Claude Bernard  
Faculté de Médecine et de Maïeutique Lyon Sud – Charles  
Mérieux  
Faculté d'Odontologie  
Institut des Sciences Pharmaceutiques et Biologiques  
Institut des Sciences et Techniques de la Réadaptation  
Département de formation et Centre de Recherche en  
Biologie Humaine

Directeur : M. le Professeur J. ETIENNE  
Directeur : Mme la Professeure C. BURILLON  
Directeur : M. le Professeur D. BOURGEOIS  
Directeur : Mme la Professeure C.  
VINCIGUERRA  
Directeur : M. le Professeur Y. MATILLON  
Directeur : Mme. la Professeure A-M. SCHOTT

## **COMPOSANTES ET DEPARTEMENTS DE SCIENCES ET TECHNOLOGIE**

Faculté des Sciences et Technologies  
Département Biologie  
Département Chimie Biochimie  
Département GEP  
Département Informatique  
Département Mathématiques  
Département Mécanique  
Département Physique  
UFR Sciences et Techniques des Activités Physiques et  
Sportives  
Observatoire des Sciences de l'Univers de Lyon  
Polytech Lyon  
Ecole Supérieure de Chimie Physique Electronique  
Institut Universitaire de Technologie de Lyon 1  
Ecole Supérieure du Professorat et de l'Education  
Institut de Science Financière et d'Assurances

Directeur : M. F. DE MARCHI  
Directeur : M. le Professeur F. FLEURY  
Directeur : Mme Caroline FELIX  
Directeur : M. Hassan HAMMOURI  
Directeur : M. le Professeur S. AKKOUICHE  
Directeur : M. Georges TOMANOV  
Directeur : M. le Professeur H. BEN HADID  
Directeur : M. Jean-Claude PLENET  
Directeur : M. Y. VANPOULLE  
Directeur : M. B. GUIDERDONI  
Directeur : M. P. FOURNIER  
Directeur : M. G. PIGNAULT  
Directeur : M. C. VITON  
Directeur : M. A. MOUGNIOTTE  
Directeur : M. N. LEBOISNE



*For Carolina, my grandma*



*Necessity is the mother of invention*

*Proverb*



# Résumé

L'objectif de ces travaux était de synthétiser, caractériser et étudier le potentiel d'une sélection de liquides ioniques, pour la séparation de l'éthane et de l'éthène. L'influence dans l'absorption de l'éthène de la présence de trois cations métalliques, le lithium (I), le nickel (II) et le cuivre (II) dans un liquide ionique était également étudiée.

Les liquides ioniques sélectionnés sont basés sur le cation imidazolium contenant des groupes fonctionnels au niveau de la chaîne alkyle latérale. Les anions choisis sont le bis(trifluorométhylsulfonyl)imide, [NTf<sub>2</sub>], la dicyanamide, [DCA] et le méthylphosphite, [C<sub>1</sub>HPO<sub>3</sub>].

Sachant qu'un solvant de séparation idéale doit avoir une capacité d'absorption et une sélectivité de séparation élevées, une faible viscosité, une haute stabilité thermique et une cinétique d'absorption rapide pour le gaz sélectionné. Pour évaluer ces propriétés pour les milieux sélectionnés, plusieurs paramètres ont été déterminés la densité et la viscosité des liquides ioniques ainsi que l'absorption de chaque gaz dans les liquides ioniques.

L'absorption de l'éthane et de l'éthène dans les liquides ioniques purs ainsi que dans les solutions de liquide ionique + sel métallique a été mesurée dans une gamme de températures comprises entre 303.15 K et 353.15 K et pour des pressions proches de l'atmosphérique. La sélectivité idéale des liquides ioniques pour l'absorption de l'éthane par rapport à l'éthène a ainsi pu être déterminée.

La détermination de l'absorption en fonction de la température a permis d'accéder aux propriétés thermodynamiques de solvation de ces gaz dans des liquides ioniques et à comprendre la manière dont les liquides ioniques interagissent avec ces solutés comment les liquides ioniques se structurent autour de ces molécules.

**Mots clefs**: liquides ioniques, absorption de gaz, séparation d'hydrocarbures gazeux, synthèse de liquides ioniques, éthane, éthène, sels métalliques

# Abstract

The goal of this research was to synthesize, characterize and study the potential of selected ionic liquids as solvents for the separation of ethane and ethene. The influence on ethene absorption of the presence of three different metallic cations, lithium (I), nickel (II) and copper (II) in an ionic liquid was also studied.

The selected ionic liquids are based in the imidazolium cation containing a functionalization in the alkyl side chain. The chosen anions were the bis(trifluorosulfonyl)imide, [NTf<sub>2</sub>], the dicyanamide, [DCA] and the methylphosphite, [C<sub>1</sub>HPO<sub>3</sub>].

Several parameters were taken into account for this primary evaluation, such as measurements of density, viscosity and absorption of each gas in the ionic liquids, since an ideal separation solvent should have a high absorption capacity and gas selectivity, low viscosity, high thermal stability and fast absorption kinetics for the selected gas.

The absorption of the 2 gases in the pure ionic liquids and ionic liquid + metallic salt solutions was measured in the temperature range between 303.15 K and 353.15 K and for pressures close to atmospheric. The ideal selectivity of the ionic liquid for the absorption of ethane compared to ethene was determined.

The determination of the gas solubility in function of the temperature allowed access to the thermodynamic properties of solvation of the gases in the ionic liquids, and a deeper understanding of the gas-ionic liquid interactions and the structure of the solution.

**Keywords:** ionic liquid, gas absorption, hydrocarbon gas separation, synthesis of ionic liquids, ethane, ethene, metallic salts

# Acknowledgments

New project, new country, new language, new life. I made it! The end of a great adventure and the start of a new one.

The work presented in this thesis was carried out between October 2010 and January 2014 in the “*Laboratoire de Chimie, Catalyse, Polymères et Procédés*” in the team “*Chimie OrganoMétallique de Surface*”, in Lyon and in the “*Institut de Chimie de Clermont-Ferrand*” in the team “*Thermodynamique et Interactions Moleculaires*”, in Clermont-Ferrand.

This work would not have been possible without the funding provided by the “*Région Rhône-Alpes*” and IFP Energies Nouvelles. I would like to thank Mr. Alain Methivier, Mr. Arnaud Baudot and Mr. Javier Pérez Pellitero from IFP Energies Nouvelles for the great interest demonstrated in my work, the interesting discussions and the advices provided.

I want to thank my thesis director Catherine Santini, for trusting me with this project, for the guidance, help, teachings, support and precious advices.

I want to express my deepest gratitude to my co-director, Margarida Costa Gomes with whom I spent the last 2 and half years. You never gave up on me and your patience, teachings and support allowed me to grow as a scientist and as a person.

I thank Pr. Dr. Anja-Verena Mudring, Dr. John D. Holbrey, Pr. Stéphane Daniele, Dr. Alain Berthod, Dr. Isabelle Billard and Dr. Alain Methivier for agreeing to be part of the jury for my defense.

I thank the lab directors of C2P2 and ICCF and directors of the doctoral schools in Lyon and Clermont-Ferrand, Prof. Delort, Prof. Charleux, Prof McKenna, Prof. Malfreyt and Prof. Lancelin for welcoming me.

I am very grateful to Laure Pisson for her teachings and unconditional help in the lab, you are more than a colleague, you are a friend. A big thank you to Pascale Husson, who was always there to help me with a smile, whether we discussed science or correcting my French.

I have no words to thank my dear friend Catarina Mendonça. Your friendship, support, kind help and advices were especially precious to me during this time. Thank you.

I wish to thank Prof. Agílio Padua, Varinia Bernales and Manas Mistra for the work collaboration.

The friends I made in France became such an important part of my life and I know our friendship will last no matter where we are in this world: Inga Helgadottir, Laurent Mathey, Hassan Srour, Gaëlle Phillipini, João França, Hannah Dunckley and Bárbara Libório. I am grateful to everyone from CPE, TIM and ICCF for making my stay so enjoyable.

I want to thank Antoine, who always helps, supports and encourages me. You made my life so much brighter. I would also like to thank his family for welcoming me in their lives with such warmth.

The support of my friends in Portugal whom didn't let the distance affect our friendship was very important for me, especially Andreia Loureiro, Tânia Ribeiro and Catarina Rodrigues.

A part of me never left Portugal. To my family who always trusted me and supported all my decisions, thank you. This adventure would not have been possible without them.

## List of symbols and abbreviations

$\alpha$	Ideal selectivity
$\gamma$	Activity coefficient
$\rho$	Density
$\Delta\rho$	Density correction factor for high viscosities
$\tau$	Vibration period
$\delta$	Relative deviation
$\eta$	Dynamic viscosity
$\eta_\infty$	Viscosity at infinite temperature
$\mu$	Chemical potential
$\phi$	Fugacity coefficient
$\Delta_{solv}G^\infty$	Gibbs energy of solvation
$\Delta_{solv}H^\infty$	Enthalpy of solvation
$\Delta_{solv}S^\infty$	Entropy of solvation
$A$	Densimeter calibration constant
$a$	Density fitting parameter
$A_i$	Adjustable parameters of the empirical equation of gas absorption correlation
$B$	Densimeter calibration constant
$B_n$	Second virial coefficient
$b$	Density fitting parameter
$C_i$	Fitting parameters of group contribution molar volume variation with temperature
$f$	Fugacity
$k$	Adjustable parameter of VFT equation
$K_H$	Henry's law constant
$n$	Number of moles
$p^0$	Standard-state pressure
$pVT$	Pressure-Volume-Temperature
$R$	Gas constant
$V$	Volume
$x, y$	Molar fraction
$C$	Adjustable parameter of VFT equation
$^{13}\text{C}$	Carbon-13
$^1\text{H}$	Hydrogen-1
AMVn	Automated Micro Viscosimeter
Ar	Argon
BrBud	4-Bromo-1-butene
BrProp	3-Bromo-1-propyne
BTU	British thermal units

C1, C2	Vacuum o-ring connections
C <sub>1</sub> C <sub>1</sub> Im	1,2-Dimethylimidazole
C <sub>1</sub> Im	Methylimidazole
C <sub>2</sub> H <sub>2</sub>	Ethyne
C <sub>2</sub> H <sub>4</sub>	Ethene
C <sub>2</sub> H <sub>6</sub>	Ethane
C <sub>3</sub> H <sub>4</sub>	Propyne
C <sub>3</sub> H <sub>6</sub>	Propene
C <sub>3</sub> H <sub>8</sub>	Propane
C <sub>4</sub> Im	Butylimidazole
CD <sub>2</sub> Cl <sub>2</sub>	Dichloromethane- <i>D</i> <sub>6</sub>
CH <sub>4</sub>	Methane
CIBCN	4-Chlorobutyronitrile
CIBu	1-Chlorobutane
CIBz	Benzylchloride
CIHx	1-Chlorohexane
CO	Carbon monoxide
CO <sub>2</sub>	Carbon dioxide
DBS	Dodecylbenzenesulfonate
DMA	Density meter from Anton Paar
DMP	Dimethylphosphate
DMS	Dimethylsulfate
DMSO	Dimethylsulphoxide
E2	Bi-molecular elimination reaction
<i>E</i> <sub>a</sub>	Activation energy
EC	Equilibrium cell
ESCPE	École Supérieure de Chimie Physique Électronique de Lyon
g	grams
GB	Glass bulb
h	hour(s)
H <sub>2</sub>	Molecular hydrogen
HRMS	High resolution mass spectra
ICCF	Institut de Chimie de Clermont-Ferrand
IL(s)	Ionic liquid(s)
K	Degrees Kelvin
Kcal	Kilocalories
Kg	Kilograms
LC2P2	Équipe Chimie Organométallique de Surface
LMOPS	Laboratoire Matériaux Organiques à Propriétés Spécifiques
M	Manometer
m	meters

mL	milliliter
mmol	milimol
Mpa	MegaPascal
mPa	miliPascal
N <sub>2</sub>	Molecular nitrogen
N <sub>2</sub> O	Nitrous oxide
NMR	Nuclear magnetic resonance
O <sub>2</sub>	Molecular oxygen
Pa	Pascal
PID	Proportional-integral-derivative
ppm	Parts <i>per</i> million
PRT	Platinum resistance thermometer
QUILL	Queen's University Ionic Liquid Laboratory
<i>R</i>	Gas constant
RT	Room temperature
SiO <sub>2</sub>	Silica
S <sub>N</sub> 2	Bi-molecular nucleophilic substitution reaction
SO <sub>2</sub>	Sulfur dioxide
T	Temperature
T <sub>0</sub>	Vogel temperature or ideal gas transition temperature
TB	Thermostated water bath
T <sub>g</sub>	Glass transition temperature
TIM	Équipe Thermodynamique et Interactions Moléculaires
TMP	Trimethylphosphate
V1, V2	Constant volume glass valves
VFT	Vogel–Fulcher–Tammann
VG	Vaccum gauge
VP	Vaccum pump
Z	Compressibility factor

## List of anions and cations

$(C_2SO_2C_2)C_1Im^+$	1-Diethylsulfonyl-3-methylimidazolium
$(C_3CN)_2Im^+$	1,3-Dicyanopropylimidazolium
$Al^{3+}$	Aluminum
BETI	Bis(perfluoroethylsulfonyl)imide
$BF_4^-$	Tetrafluoroborate
$Br^-$	Bromide
$C_1(C_2H_2CH)Im^+$	1-Methyl-3-(propyn-3-yl)imidazolium
$C_1(C_3H_5CH_2)Im^+$	1-(Buten-3-yl)-3-methylimidazolium
$C_1(CH_2C_6H_5)Im^+$	1-Benzyl-3-methylimidazolium
$C_1C_1COOC_2OC_2Im^+$	3-Methyl-1-(ethoxyethoxycarbonylmethyl)imidazolium
$C_1C_1COOC_2OC_2OC_4Im^+$	3-Methyl-1-(2-(2-butoxyethoxy)ethoxycarbonylmethyl)imidazolium
$C_1C_1COOC_5Im^+$	3-Methyl-1-(pentoxycarbonylmethyl)imidazolium
$C_1C_3CNIm^+$	1-(3-Cyanopropyl)-3-methylimidazolium
$CF_3SO_3^-$	Trifluoromethanesulfonate
$Cl^-$	Chloride
$NC_nC_mC_pC_q^+$	AlkylAmmonium
$PC_nC_mC_pC_q^+$	AlkylPhosphonium
$C_nC_mIm^+$	1-alkyl,3-alkylimidazolium
$C_nC_mPO_4^-$	Alkylphosphate
$C_nC_mPyr^+$	AlkylPyrrolidinium
$C_nCO_2^-$	Carboxylate
$C_nHPO_3^-$	Alkylphosphite
$C_nPyr^+$	AlkylPyridinium
$C_nSO_4^-$	Alkylsulfate
$Cu^{2+}$	Copper
DBS <sup>-</sup>	Dodecylbenzenesulfonate
DCA <sup>-</sup>	Dicyanamide
FAP <sup>-</sup>	Tris(pentafluoroethyl)trifluorophosphate
$I^-$	Iodide
Iso <sup>-</sup>	Isobutyrate
Lev <sup>-</sup>	Levulinate
$Li^+$	Lithium
$N_{1132-OH}^+$	Propylcholinium
$n-C_{15}H_{31}COO^-$	Palmitate
$n-C_{17}H_{35}COO^-$	Stearate
$Ni^{2+}$	Nickel
$NO_3^-$	Nitrate
$NTf_2^-$	Bis((trifluoromethyl)sulfonyl)imide
OAc <sup>-</sup>	Acetate
$PF_6^-$	Hexafluorophosphate
Pro <sup>-</sup>	Propionate
TFA <sup>-</sup>	Trifluoroacetate
TMP <sup>-</sup>	Trimethylphosphate
TMPP <sup>-</sup>	Bis(2,4,4-trimethylpentyl)phosphinate

# Table of contents

<b>Introduction</b>		1
<b>Chapter 1</b>	<b>Ionic Liquids for Light Hydrocarbon Separation</b>	5
	1. Gas solubility	13
	1.1 <i>Solubility of ethane and propane</i>	18
	1.2 <i>Solubility of ethene and propene</i>	24
	1.3 <i>Solubility of ethyne and propyne</i>	33
	1.4 <i>Selectivity</i>	37
	1.5 <i>Ionic liquids containing metal salts</i>	40
	Conclusions	42
	References	44
<b>Chapter 2</b>	<b>Synthesis and Characterization of Ionic Liquids</b>	51
	A. Synthesis of ionic liquids	53
	2.1 <i>One-step synthesis of ionic liquids</i>	55
	2.2 <i>Two-step synthesis of ionic liquids</i>	57
	2.3 <i>Materials and synthesis procedures</i>	61
	2.4 <i>Ionic liquid and metallic salt solutions</i>	77
	B. Physicochemical characterization	78
	2.5 <i>Density measurement</i>	79
	2.6 <i>Viscosity measurement</i>	94
	Conclusions	104
	References	105
<b>Chapter 3</b>	<b>Ethane and Ethene Solubility in Ionic Liquids</b>	113
	3. Gas Solubility in ionic liquids	117
	3.1 <i>Materials</i>	123
	3.2 <i>Ethane and ethene solubility</i>	125
	3.3 <i>Ethane and ethene separation selectivity</i>	142
	Conclusions	144
	References	145
<b>Chapter 4</b>	<b>Conclusions and Perspectives</b>	149
<b>Appendix 1</b>	List of ionic liquids synthesized	165
<b>Appendix 2</b>	NMR and HRMS spectra of the Ionic Liquids	169
<b>Appendix 3</b>	Collection of Publications	193



# Introduction

---



The interest of using ionic liquids for a potential industrial application in gas separations is related to their negligible vapor pressure and their ability to selectively dissolve certain families of gases. Furthermore, it is generally accepted that ionic liquids preferentially absorb an unsaturated gas hydrocarbon compared with its saturated counterpart<sup>1,2,3,4</sup>. The goal of this work is to use physicochemical characterization, gas solubility and thermodynamic properties of solvation to propose ionic liquids to optimize an alternative gas separation process. Since most of the alternative processes proposed in the literature comprise the use of a transition metal that selectively reacts with a gas, the combination of a transition metal salt with ionic liquids will also be explored.<sup>5,6,7,8,9</sup>

Therefore interdisciplinary collaborations were essential in this work and the combination of skills of the laboratory TIM at ICCF in the field of physicochemical properties and solubility experiments and the expertise of C2P2 in the synthesis of ionic liquids and the use of NMR techniques is essential to characterize the molecular interactions involved.

**Chapter 1** consists of a review of the experimental data on the absorption of ethane, ethene, ethyne, propane, propene and propyne in ionic liquids. The influence of the different cations, anions and their size and/or functionalization was analyzed. The ideal separation selectivity for ethane/ethene, ethene/ethyne, propane/propene and propene/propyne, for the reviewed ionic liquids was calculated and, whenever possible, related to the structure of the ions. In **chapter 2** the synthesis and characterization of several ionic liquids and of different solutions of metal salts in ionic liquids are described. The syntheses were performed in one or two steps and the ionic liquids were characterized by NMR and HRMS. The density and viscosity of the ionic liquids and of the solutions of metal salts in ionic liquid were measured. In **chapter 3**, the solubility of ethane and ethene solubility in selected ionic liquids and metallic salt-ionic liquid solutions is reported. The influence in ethane and ethene solubility of the length and functionalization of the alkyl side chain of the cation and the use of a phosphite based anion was studied. The thermodynamic properties of solvation of each gas in each solvent were determined and compared. **Chapter 4** consists of an overview of conclusion of the present work and of the perspectives it offers for future development.

## References

---

- <sup>1</sup> Palgunadi, J.; Hong, S. Y.; Lee, J. K.; Lee, H.; Lee, S. D.; Cheong, M. and Kim, H. S. Correlation between Hydrogen Bond Basicity and Acetylene Solubility in Room Temperature Ionic Liquids, *J. Phys. Chem. B* **2011**, 115, 1067-1074
- <sup>2</sup> Mokrushin, V.; Assenbaum, D.; Paape, N.; Gerhard, D.; Mokrushina, L.; Wasserscheid, P.; Arlt, W.; Kistenmacher, H.; Neuendorf, S. and Göke, V. Ionic Liquids for Propene-Propane Separation. *Chem. Eng. Technol.* **2010**, 33, 63-73
- <sup>3</sup> Anthony, J. L.; Anderson, J. L.; Maginn, E. J. and Brennecke, J. F. Anion Effects on Gas Solubility in Ionic Liquids, *J. Phys. Chem. B* **2005**, 109, 6366-6374
- <sup>4</sup> Kilaru, P. K.; Scovazzo, P. Correlations of Low-Pressure Carbon Dioxide and Hydrocarbon Solubilities in Imidazolium-, Phosphonium-, and Ammonium-Based Room-Temperature Ionic Liquids. Part 2. Using Activation Energy of Viscosity, *Ind. Eng. Chem. Res.* **2008**, 47, 910-919
- <sup>5</sup> Kim, J. H.; Kang, S. W.; Kang, Y. S. Threshold Silver concentration for Facilitated Olefin Transport in Polymer/Silver Salt Membranes, *J. Polym. Res.* **2012**, 19, 9753-9760
- <sup>6</sup> Weston, M. H.; Colón, Y. J.; Bae, Y.; Garibay, S. J.; Snurr, R. Q.; Farha, O. K.; Hupp, J. T. and Nguyen, S. T. High Propylene/Propane Adsorption Selectivity in a Copper(catecholate)-decorated Porous Organic Polymer, *J. Mater. Chem. A* **2014**, 2, 299-302
- <sup>7</sup> Pan, Y and Lai, Z. Sharp Separation of C2/C3 Hydrocarbon Mixtures by Zeolitic Imidazolate Framework-8 (ZIF-8) Membranes Synthesized in Aqueous Solutions, *Chem. Commun.* **2011**, **47**, 10275–10277
- <sup>8</sup> Geier, S. J.; Mason, J. A.; Bloch, E. D.; Queen, W. L.; Hudson, M. R.; Brown, C. M. and Long, J. R. Selective Adsorption of Ethylene Over Ethane and Propylene Over Propane in the Metal–Organic Frameworks  $M_2(\text{dobdc})$  (M = Mg, Mn, Fe, Co, Ni, Zn), *Chem. Sci.* **2013**, 4, 2054-2061
- <sup>9</sup> Bloch, E. D.; Queen, W. L.; Krishna, R.; Zadrozny, J. M.; Brown, C. M. and Long, J. R. Hydrocarbon Separations in a Metal–Organic Framework with Open Iron(II) Coordination Sites, *Science* **2012**, 335, 1606-1610

# Chapter 1

---

Ionic Liquids for Light Hydrocarbon Separation



Separation explores differences in properties of the species, either molecular (molar mass, van der Waals volume or dipole moment), thermodynamic (vapor pressure or solubility) or transport (diffusivity). Common separation techniques rely on creating or adding a new phase, on introducing a barrier or a solid agent, or on using a force field or a gradient.<sup>1</sup>

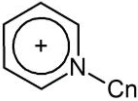
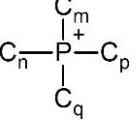
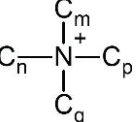
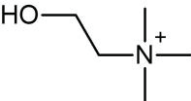
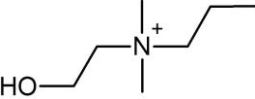
Distillation, crystallization, liquid-liquid extraction and absorption are the most common examples of separation techniques based on the creation or on the addition of a new phase that require an energy transfer or the use of a mass-transfer agent, respectively. Changing from an energy-separating agent to a mass-separating agent can potentially reduce the process energy requirements, but the selected absorbent should be easy to recycle, have low volatility, and the solubilities of the species to separate should be significantly different. Membranes make use of liquid or solid (frequently polymeric) barriers to separate species that present different permeabilities. Membranes are used in small, compact and clean units that require low energy to achieve separation, but are still difficult to scale-up. Adsorption is a surface-based process that frequently relies on a solid agent to achieve separation. The separation is achieved due to different interacting forces at the interface (originating physisorption or chemisorption processes) that selectively interacts with certain components in detriment of others from a liquid or gas mixture. The adsorbent material should have high surface area, good mechanical properties, fast adsorption kinetics and the ability to be regenerated without loss of its properties. Commonly used supports are alumina, ion exchanging resins, high-surface-area SiO<sub>2</sub>, zeolites and molecular sieves. Electrophoresis and centrifugation are examples of separation techniques that exploit the differences in the responses of the constituents of a feed to an external force or gradient. They are especially useful and versatile for separating biochemicals.<sup>1</sup>

Ethene and propene are the largest-volume organic chemical feedstock, being used as precursors for the production of polymers, lubricants, rubbers, solvents and fuel components.<sup>1,2,3</sup> These are mostly obtained from the separation of the light hydrocarbons components of naphtha, separated through cryogenic distillation. Cryogenic distillation has been in use since the 1960's, for the ethane/ethene and propane/propene separation.<sup>1,4</sup> It requires large distillation towers (120-180 trays), low temperatures (-114°C) and high pressures (15-30 bar), resulting in a high capital and energy demanding process needing up to  $120 \times 10^{12}$  BTU/year.<sup>5,6</sup> The high

demand (25 trillion tons of ethene per annum)<sup>2</sup> and high purity<sup>7</sup> required for industrial applications of ethene and propene imply effective and reliable separation methods which are often difficult to implement. The implementation of an alternative process to cryogenic distillation with improved economic and environmental performance would represent a major advance in the sector.

Table 1.1 - Abbreviation, full designation and structure of some cations of ionic liquids. C<sub>n/m</sub> represent carbon chains of variable size

Abbreviation	Full designation	Structure
C <sub>n</sub> C <sub>m</sub> Im <sup>+</sup>	1-C <sub>n</sub> -3-C <sub>m</sub> imidazolium	
C <sub>1</sub> C <sub>2-OH</sub> Im <sup>+</sup>	1-(2-hydroxyethyl)-3-methylimidazolium	
(C <sub>2</sub> SO <sub>2</sub> C <sub>2</sub> )C <sub>1</sub> Im <sup>+</sup>	1-diethylsulfonyl-3-methylimidazolium	
C <sub>1</sub> C <sub>3</sub> CNI <sup>+</sup>	1-(3-cyanopropyl)-3-methylimidazolium	
C <sub>1</sub> C <sub>1</sub> C <sub>3</sub> CNI <sup>+</sup>	1-(3-cyanopropyl)-2,3-dimethylimidazolium	
(C <sub>3</sub> CN) <sub>2</sub> Im <sup>+</sup>	1,3-(3-cyanopropyl)imidazolium	
C <sub>1</sub> C <sub>1</sub> COOC <sub>5</sub> Im <sup>+</sup>	1-(pentoxycarbonylmethyl)-3-methylimidazolium	
C <sub>1</sub> C <sub>1</sub> COOC <sub>2</sub> OC <sub>2</sub> Im <sup>+</sup>	1-(ethoxyethoxycarbonylmethyl)-3-methylimidazolium	
C <sub>1</sub> C <sub>1</sub> COOC <sub>2</sub> OC <sub>2</sub> OC <sub>4</sub> Im <sup>+</sup>	1-(2-(2-butoxyethoxy)ethoxycarbonylmethyl)-3-methylimidazolium	
C <sub>n</sub> C <sub>m</sub> Pyrr <sup>+</sup>	C <sub>n</sub> C <sub>m</sub> pyrrolidinium	

Abbreviation	Full designation	Structure
$C_n\text{Pyr}^+$	$C_n$ pyridinium	
$P_{nmpq}^+$	$C_nC_mC_pC_q$ phosphonium	
$N_{nmpq}^+$	$C_nC_mC_pC_q$ ammonium	
$N_{1112\text{-OH}}$	Cholinium	
$N_{1132\text{-OH}}$	Propylcholinium	

Ionic liquids have been suggested as new separating agents for olefin/paraffin gas separation, as absorbents or as solvents for the chemical complexation of olefins with silver or copper salts. Ionic liquids are composed uniquely of ions and have a melting point below 100°C. Many present unique properties such as negligible vapor pressure, high thermal, chemical and electrochemical stability, non-flammability and high ionic conductivity. Ionic liquid are also called “designer solvents” due to the large variety of combination possibilities of cations and anions, leading to tunable physical chemical properties. The cations and anions that constitute the ionic liquids mentioned in this review are listed in tables 1.1 and 1.2.

In figure 1.1 the Henry’s law constants,  $K_H$ , of different gases in  $[\text{C}_1\text{C}_4\text{Im}][\text{BF}_4]$  are represented. Monoatomic, diatomic, non-polar or gases with low polarizability present the lowest solubilities. Unsaturated hydrocarbons frequently present a higher solubility in ionic liquids than their saturated counterparts. The exact reasons for the observed trends are still poorly understood, but essential for the development of new alkane/alkene/alkyne separation processes.<sup>8</sup> In this chapter we review the current knowledge on the solubility of ethane, ethene, ethyne, propane, propene and propyne in pure ionic liquids. Whenever possible we calculate the ionic liquid absorption capacity and ideal selectivity for ethane/ethene, ethene/ethyne,

propane/propene and propene/propyne mixtures and so assess the potential of a particular ionic liquid as separating agent.

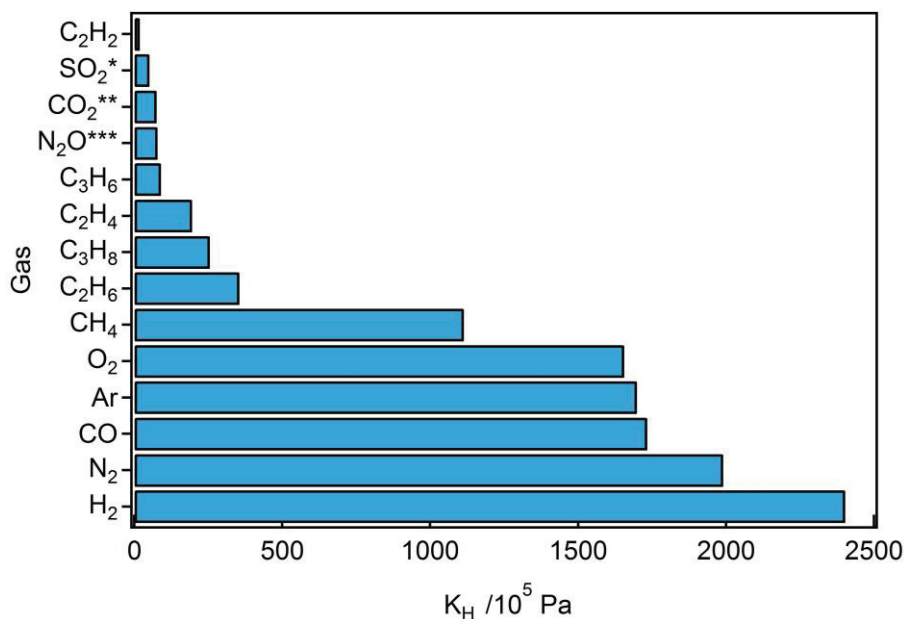
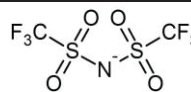
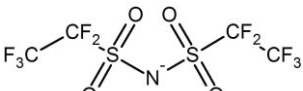
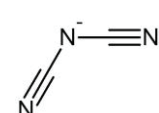
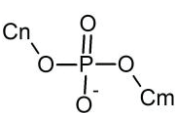
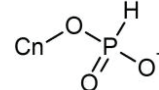
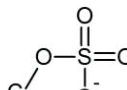
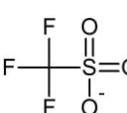
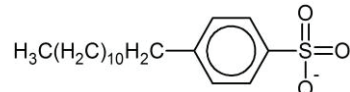
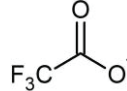


Figure 1.1 - Henry's law constant,  $K_H$ , for several gases in ionic liquid  $[\text{C}_1\text{C}_4\text{Im}][\text{BF}_4]$ <sup>7,9,10,11,12</sup> at 313 K. \* - 293 K; \*\* - 314 K; \*\*\* - 298 K.

The reviewed data are expressed in Henry's law constant,  $K_H$ . The absorption capacity of gaseous hydrocarbons by pure ionic liquids is relatively low because, in most cases, it is only a physical process. The use of silver (I) and copper (I) salts can improve the amount of unsaturated hydrocarbon absorbed by the ionic liquid phase as these metal cations are capable of selecting and reversibly reacting with it.<sup>5,13,14,15,16</sup> This concept has been explored for the separation of ethene from ethane and propene from propane.<sup>6,17,18,19,20,21,22</sup>

Table 1.2 - Abbreviation, full designation and structure of some anions of ionic liquids. R<sub>n</sub> represents carbon chains of variable size

Abbreviation	Full designation	Structure
NTf <sub>2</sub> <sup>-</sup>	Bis(trifluoromethylsulfonyl)imide	
BETf <sup>-</sup>	Bis(perfluoroethylsulfonyl)imide	
DCA <sup>-</sup>	Dicyanamide	
NO <sub>3</sub> <sup>-</sup>	Nitrate	
C <sub>n</sub> C <sub>m</sub> PO <sub>4</sub> <sup>-</sup>	C <sub>n</sub> C <sub>m</sub> phosphate	
C <sub>n</sub> HPO <sub>3</sub> <sup>-</sup>	C <sub>n</sub> phosphite	
PF <sub>6</sub> <sup>-</sup>	Hexafluorophosphate	
C <sub>n</sub> SO <sub>4</sub> <sup>-</sup>	C <sub>n</sub> sulfate	
CF <sub>3</sub> SO <sub>3</sub> <sup>-</sup>	Trifluoromethanesulfonate	
DBS <sup>-</sup>	Dodecylbenzenesulfonate	
C <sub>n</sub> CO <sub>2</sub> <sup>-</sup>	Carboxylate	
OAc <sup>-</sup>	Acetate	
TFA <sup>-</sup>	Trifluoroacetate	
AlCl <sub>4</sub> <sup>-</sup>	Tetrachloroaluminate	

Abbreviation	Full designation	Structure
BF <sub>4</sub> <sup>-</sup>	Tetrafluoroborate	
TMPP <sup>-</sup>	Bis(2,4,4-trimethylpentyl)phosphinate	
FAP <sup>-</sup>	Tris(pentafluoroethyl)trifluorophosphate	

# 1. Gas Solubility

The chemical potential of component  $i$  in a mixture is defined as<sup>23,24</sup>

$$\mu_i = \mu_i^{ref} + RT \ln(\gamma_i x_i) \quad (1.1)$$

where  $\mu_i^{ref}$  is the chemical potential of component  $i$  in a chosen reference state and  $\gamma_i$  its activity coefficient. Two conventions are usually adopted to choose the appropriate combination of the reference state chemical potential and the activity coefficient, the choice depending of the physical state of the pure components at the thermodynamic conditions of the mixture.

The asymmetric convention is usually applied to solutions where the solute(s) or the solvent are not in the physical state of the solution at a given temperature and pressure, as in the case of the solutions of gases in ionic liquids considered herein. For the solvent, the activity coefficient approaches unity when its mole fraction is approximately unity and for the solute its activity becomes unity when the solute is present at very low concentrations,  $\gamma_i^H \rightarrow 1$  when  $x_i \rightarrow 0$ . In this case, the solute is present in the limit of infinite dilution and the solution approaches ideal behavior in the sense of Henry's law. The reference state adopted for the calculation of the chemical potential in this case is that of the pure solute at infinite dilution.<sup>25,26</sup>

$$\mu_i = \mu_i^{ref} + RT \ln(\gamma_i x_i) \quad x_i \rightarrow 0 \Rightarrow \gamma_i^H \rightarrow 1 \quad (1.2)$$

the activity coefficient in the asymmetric convention,  $\gamma_i^H$ , being a measure of the solute intermolecular interactions, the solvent and solute-solvent interactions are accounted for in the reference state.

The Gibbs energy of solutions is defined as the difference in chemical potential when the solute is transferred, at constant pressure and temperature, from its pure state into the infinite dilution solution. If the solute remains pure at equilibrium

with the solution<sup>†</sup> and the solubility is enough that  $\gamma_i^H \approx 1$  the following approximate relation can be used:

$$\Delta_{\text{sol}}G_i \approx -RT\ln x_i \quad (1.3)$$

The Gibbs energy of solution expresses the difference between the solute-solute interactions in the pure species, which may be a condensed phase, and the solute-solvent interactions in an infinitely dilute solution. In order to isolate the role of the solute-solvent interactions in the process of dissolution, a thermodynamic transformation called solvation can be defined as the difference in chemical potential when the solute is transferred from an ideal gas at standard pressure into the reference state at infinite dilution, equation 1.3 leading to:

$$\Delta_{\text{solv}}G_i = RT\ln\left(\frac{K_{H,i}}{p^0}\right) \quad (1.4)$$

in which  $K_{H,i}$  is the Henry's law constant defined as:

$$K_{H,i} \equiv \lim_{x_i \rightarrow 0} (f_i/x_i) \quad (1.5)$$

From the behavior with temperature or with pressure of the Gibbs energy of solvation it is possible to calculate the other thermodynamic properties:

$$\Delta_{\text{solv}}H_i = -T^2 \frac{\partial}{\partial T} \left( \frac{\Delta_{\text{solv}}G_i}{T} \right)_p \quad (1.6)$$

$$\Delta_{\text{solv}}S_i = - \left( \frac{\partial \Delta_{\text{solv}}G_i}{\partial T} \right)_p \quad (1.7)$$

$$\Delta_{\text{solv}}V_i = - \left( \frac{\partial \Delta_{\text{solv}}G_i}{\partial T} \right)_T \quad (1.8)$$

The thermodynamic properties of solvation provide insights into the molecular mechanisms determining the solution behavior - the enthalpy of solvation reflects the

---

<sup>†</sup> This is the case for the solutions of gases in ionic liquids because the solvent does not have any measurable vapor pressure at moderate temperatures.

energy of solute-solvent interactions and the entropic contribution is related to structural organization of the solution. These thermodynamic properties of solvation are approximately equal to the thermodynamic properties of solution in the case of gaseous solutes at low pressure, the differences becoming more important for liquid and solid solutes. These solvation properties can be determined through experimentally accessible quantities namely from solubility measurements and the calculation of Henry's law constants.

The techniques reported in the literature to determine the solubility of light hydrocarbon gases in pure ionic liquids can be assembled in three groups: gravimetric, *pVT* and permeation methods.

In the gravimetric method,<sup>27</sup> a high-resolution microbalance is used to determine the mass increase of a liquid sample, when in contact with a gas, at a certain pressure and temperature. The mass increase is monitored as a function of time and the equilibrium is detected when the mass does not change significantly for a period of time. The microbalance does not have a stirring mechanism, and so, relies solely on the diffusion of the gas into the ionic liquid. This method requires solvent amounts as small as 70 mg since the balance can have a 1  $\mu\text{g}$  stable resolution, but it requires large amounts of gas, especially at high pressures. The absorption process can be reversed, yielding a complete absorption/desorption isotherm. A correction for buoyancy effects has to be taken into account to calculate the solubility, which requires accurate knowledge of the gas and solution density. The main advantage of this method is that it requires only small amounts of ionic liquid.<sup>28,29,30</sup>

*pVT* methods<sup>31,32,33,34,35</sup> are, by far, the most used for determining the solubility of light hydrocarbon in ionic liquids. In these methods, a known amount of gas is put in contact with a known amount of ionic liquid, and makes use of pressure, volume and temperature measurements to determine solubility. These measurements can be made at constant volume (isochoric method) or at constant pressure. The isochoric method consists in accurately measuring the volume of the cell and the volume of the vapor and liquid phases. This information is used to determine the quantity of gas remaining in the gas phase and, by difference, the amount of gas dissolved in the liquid, by difference. When measuring at constant pressure, the difference between the total volume of gas delivered to the system and

the vapor phase is used to determine the solubility. The amount of ionic liquid sample required for the  $pVT$  methods is usually larger than the one needed for the gravimetric microbalance method. A few milliliters are necessary to measure the solubility from pressures close to atmospheric up to 550 bar. The advantages of this method are its simplicity and the capability of delivering high-precision data for scarcely, as well as for very soluble gases.<sup>28,29,30,36</sup>

Gas chromatography and the lag-time technique belong to the group of permeation methods. Gas chromatography<sup>37</sup> makes use of columns that are either coated or contain inert solid supports coated with ionic liquid. The sample gas is introduced with a carrier gas (such as H<sub>2</sub>, Ar or He) and passes through the column, where it is more or less retained according to the affinity between the gas phase and the coating phase. A detector is placed at the end of the column to detect the components of the gas phase and create the chromatogram. The peak exit time and size is related to the component identity and amount. From the retention volume (volume of sample gas retained in the column) and column characteristics, the partition coefficients are determined. Knowing the column dimensions and amount of ionic liquid, we can determine the gas solubility in the ionic liquid. However it should be taken into consideration that the solubility is determined for a gas in a film of liquid and in which the carrier gas is already equilibrated; the process involves steady states and transient equilibriums as the carried component is swept through the column; and it is difficult to ascertain the carried component partial pressure. Few milliliters of ionic liquid are needed to create the column and small amounts of solute gas are required.<sup>28,38,39</sup>

The lag-time technique<sup>40</sup> makes use of a supported ionic liquid film to evaluate the diffusivity and solubility of the gas through the measurement of its permeability in the ionic liquid. The liquid film is placed between a feed chamber and a permeate chamber with known volumes and the entire unit is thermostated. The solute gas is injected in the feed chamber through a syringe, passes through the membrane onto the permeate chamber and the resulting pressure increase in the permeate chamber with time is read by a pressure transducer. The lag time refers to the difference between the time at which the gas enters the membrane and the time at which the flow rate of diffusing species into the closed volume reaches a steady state of permeation. The liquid film is immobilized in porous glass fiber supports, which limits mass transport to molecular diffusion. The liquid membrane is considered the

rate-limiting step, so it is assumed that no boundary layer resistance occurs at the membrane interface. Assuming these two conditions, and by analyzing both the transient and steady-state regimes of permeation, an expression for the pressure rise in the permeate chamber with time can be obtained. The experimental permeation data is analyzed in the light of this expression, and the slope and abscissa intercept (designated lag time) allow the determination of solubility and diffusivity, respectively. The advantage of this method is that it allows the determination of both gas diffusivity and solubility in a single experiment with an ionic liquid sample of less than 1 milliliter. However, the solubility of the gas in the ionic liquid greatly limits the precision of the results. The solubility can only be determined when over  $0.01 \text{ mol L}^{-1} \text{ atm}^{-1}$ , with a 10% deviation.<sup>41</sup>

The solubility of ethane was measured in a total of 34 samples, of 26 different ionic liquids. Ethane is by far the most studied gas from ethane, ethene, ethyne, propane, propene and propyne. 70 ethane solubility measurements were performed using 55 different ionic liquids. In the case of ethyne 42 measurements were made in 30 different ionic liquids. The solubility of propane was measured in 10 samples of 8 different ionic liquids. For propene, 33 measurements were performed in 30 different ionic liquids. In the case of propyne 5 measurements were made in 5 ionic liquids. Imidazolium-based ionic liquids present the largest variety of anions tested and represent the major part of the ionic liquids tested for each gas, more than 70%.

The results are organized in three groups with solubility results in ionic liquids for ethane and propane, ethene and propene and finally ethyne and propyne.

For each group the analysis of the results is done in 7 steps:

1. Full solubility range
2. Influence in solubility of ionic liquids with different cations and same anion
3. Solubility range for imidazolium-based ionic liquids
4. Influence on solubility of increasing alkyl side chain length of the cation
5. Influence on solubility of increasing alkyl side chain length of the anion
6. Influence on solubility of functionalizing the alkyl side chain of the cation
7. Influence in solubility of ionic liquids with different anions and same cation.

## 1.1 Solubility of ethane and propane

The Henry's law constants,  $K_H$ , for ethane and propane in several ionic liquids at 313 K are depicted in figures 1.2 to 1.4 and tables 1.3 and 1.4.  $K_H$  ranges from  $665.2 \times 10^5$  Pa for  $[\text{C}_1\text{C}_2\text{Im}][\text{DCA}]$  to  $19 \times 10^5$  Pa for  $[\text{P}_{(14)666}][\text{TMPP}]$  for ethane at 313 K. For propane  $K_H$  ranges from  $308.5 \times 10^5$  Pa for  $[\text{C}_1\text{C}_2\text{Im}][\text{DCA}]$  and  $6.4 \times 10^5$  Pa for  $[\text{P}_{(14)666}][\text{TMPP}]$ , at 313 K.

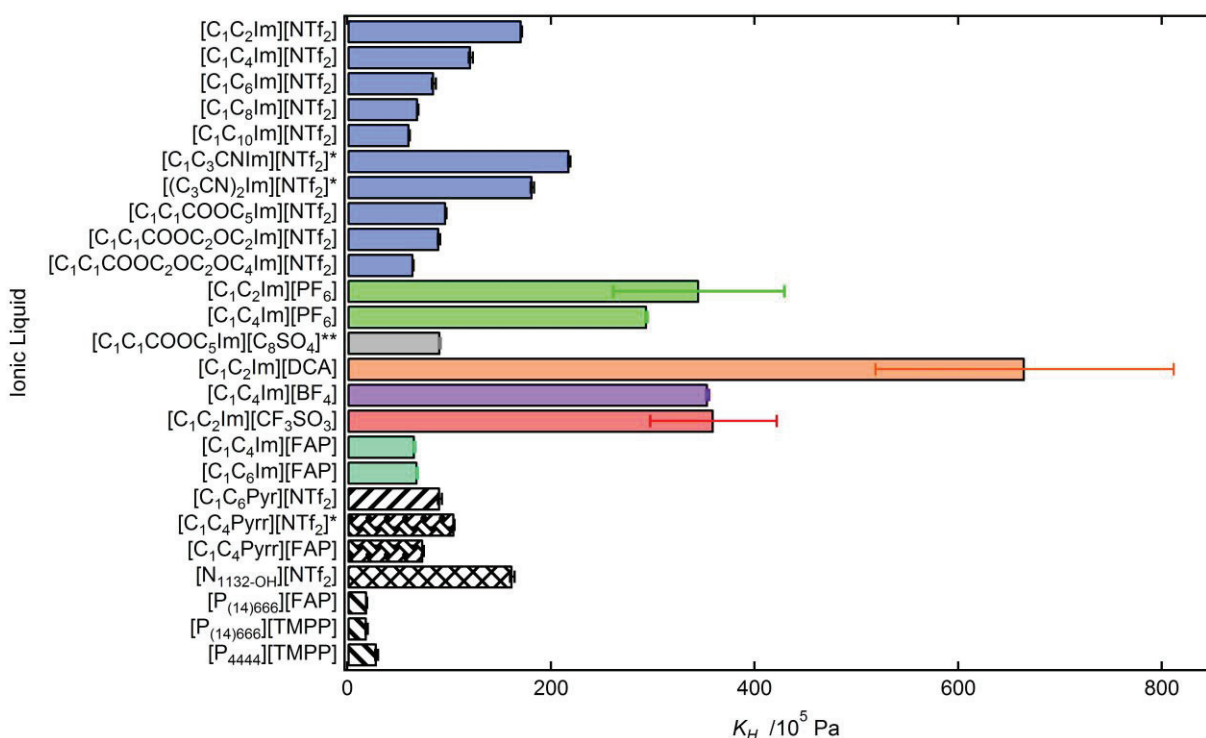


Figure 1.2 - Henry's law constant,  $K_H$ , for ethane in several ionic liquids at 313 K. \* - at 303 K; \*\* - at 323 K.  $[\text{C}_1\text{C}_2\text{Im}][\text{NTf}_2]$ <sup>42</sup>;  $[\text{C}_1\text{C}_4\text{Im}][\text{NTf}_2]$ <sup>34</sup>;  $[\text{C}_1\text{C}_6\text{Im}][\text{NTf}_2]$ <sup>43</sup>;  $[\text{C}_1\text{C}_8\text{Im}][\text{NTf}_2]$ <sup>34</sup>;  $[\text{C}_1\text{C}_{10}\text{Im}][\text{NTf}_2]$ <sup>34</sup>;  $[\text{C}_1\text{C}_3\text{CNIm}][\text{NTf}_2]$ <sup>33</sup>;  $[(\text{C}_3\text{CN})_2\text{Im}][\text{NTf}_2]$ <sup>33</sup>;  $[\text{C}_1\text{C}_1\text{COOC}_5\text{Im}][\text{NTf}_2]$ <sup>44</sup>;  $[\text{C}_1\text{C}_1\text{COOC}_2\text{OC}_2\text{Im}][\text{NTf}_2]$ <sup>44</sup>;  $[\text{C}_1\text{C}_1\text{COOC}_2\text{OC}_2\text{OC}_4\text{Im}][\text{NTf}_2]$ <sup>44</sup>;  $[\text{C}_1\text{C}_2\text{Im}][\text{PF}_6]$ <sup>11</sup>;  $[\text{C}_1\text{C}_4\text{Im}][\text{PF}_6]$ <sup>45</sup>;  $[\text{C}_1\text{C}_1\text{COOC}_5\text{Im}][\text{C}_8\text{SO}_4]$ <sup>44</sup>;  $[\text{C}_1\text{C}_2\text{Im}][\text{DCA}]$ <sup>11</sup>;  $[\text{C}_1\text{C}_4\text{Im}][\text{BF}_4]$ <sup>12</sup>;  $[\text{C}_1\text{C}_2\text{Im}][\text{CF}_3\text{SO}_3]$ <sup>11</sup>;  $[\text{C}_1\text{C}_4\text{Im}][\text{FAP}]$ <sup>46</sup>;  $[\text{C}_1\text{C}_6\text{Im}][\text{FAP}]$ <sup>27</sup>;  $[\text{C}_1\text{C}_6\text{Pyr}][\text{NTf}_2]$ <sup>27</sup>;  $[\text{C}_1\text{C}_4\text{Pyr}][\text{NTf}_2]$ <sup>42</sup>;  $[\text{C}_1\text{C}_4\text{Pyr}][\text{FAP}]$ <sup>47</sup>;  $[\text{N}_{1132-\text{OH}}][\text{NTf}_2]$ <sup>42</sup>;  $[\text{P}_{(14)666}][\text{FAP}]$ <sup>47</sup>;  $[\text{P}_{(14)666}][\text{TMPP}]$ <sup>32,48</sup>;  $[\text{P}_{4444}][\text{TMPP}]$ <sup>32</sup>.

The ionic liquids that present the highest ethane and propane solubility are based in the phosphonium cation followed by those based in the imidazolium, the pyridinium, the pyrrolidinium and the ammonium cations (only one measurement with ammonium-based ionic liquids for ethane and none for propane were reported).

The ethane and/or propane solubility data reported by Mokrushin *et al.*<sup>49</sup>, by Scovazzo,<sup>50</sup> by Kang *et al.*,<sup>51</sup> by Ortiz *et al.*,<sup>52</sup> and by Dreisbach *et al.*<sup>53</sup> were not taken into consideration, due to lack of information for the calculation of Henry's law constants. The high-pressure solubility data reported by Bermejo, Fieback and Martín<sup>54</sup> presented deviations of 34% from the literature, as claimed by the authors.

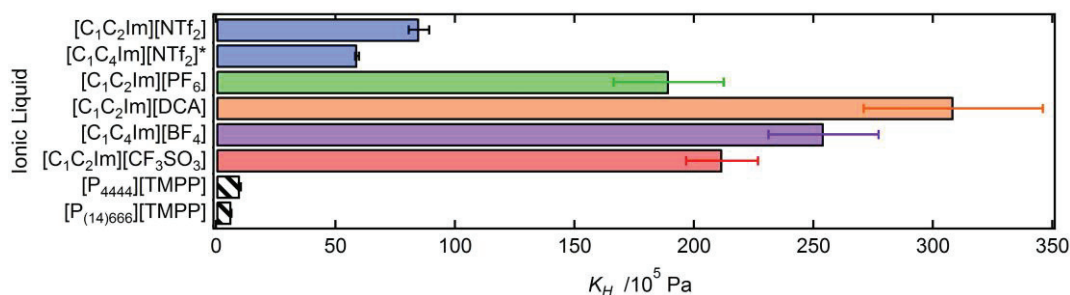


Figure 1.3 - Henry's law constant,  $K_H$ , for propane in several ionic liquids at 313 K. \* - at 320 K. [C<sub>1</sub>C<sub>2</sub>Im][NTf<sub>2</sub>]<sup>32</sup>; [C<sub>1</sub>C<sub>4</sub>Im][NTf<sub>2</sub>]<sup>55</sup>; [C<sub>1</sub>C<sub>2</sub>Im][PF<sub>6</sub>]<sup>11</sup>; [C<sub>1</sub>C<sub>2</sub>Im][DCA]<sup>11</sup>; [C<sub>1</sub>C<sub>4</sub>Im][BF<sub>4</sub>]<sup>11</sup>; [C<sub>1</sub>C<sub>2</sub>Im][CF<sub>3</sub>SO<sub>3</sub>]<sup>11</sup>; [P<sub>4444</sub>][TMPP]<sup>32</sup>; [P<sub>(14)666</sub>][TMPP]<sup>48</sup>.

Phosphonium based ionic liquids present a Henry's law constant 35 times lower for ethane and 48 times lower for propane relative to imidazolium based ones. These ratios are lower when the solubility is expressed in mass fraction instead of mole fraction or Henry's law constant<sup>41</sup>, as observed in figure 1.4.

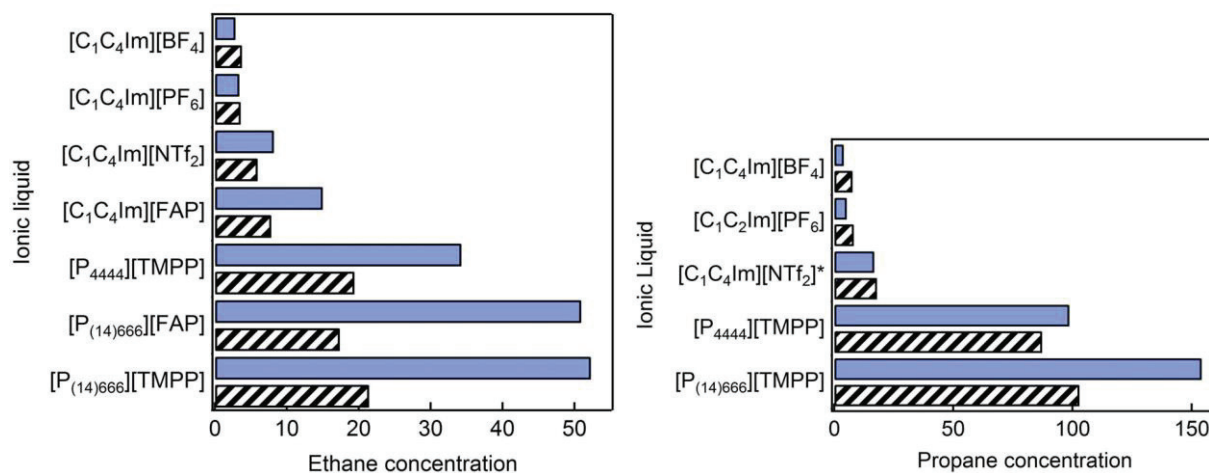


Figure 1.4 - Mole fraction ( $\times 10^3$ , full bars) and mass fraction ( $\times 10^4$ , patterned bars) of ethane (on the left) or propane (on the right) in several ionic liquids at  $10^5$  Pa and 313 K. \* - at 320 K. When mole fraction values were not available for 0.1 MPa, they were recalculated using Henry's law constant values given by the authors. Mass fractions were calculated from mole fraction values. [C<sub>1</sub>C<sub>4</sub>Im][BF<sub>4</sub>]<sup>11,12</sup>; [C<sub>1</sub>C<sub>4</sub>Im][PF<sub>6</sub>]<sup>34,56</sup>; [C<sub>1</sub>C<sub>4</sub>Im][NTf<sub>2</sub>]<sup>34,55</sup>; [C<sub>1</sub>C<sub>4</sub>Im][FAP]<sup>46</sup>; [P<sub>4444</sub>][TMPP]<sup>32</sup>; [P<sub>(14)666</sub>][FAP]<sup>47</sup>; [P<sub>(14)666</sub>][TMPP]<sup>32,48</sup>.

$[N_{1132-OH}][NTf_2]$  presents an average of 34% less ethane solubility than  $[C_1C_4Im][NTf_2]$ . From the analysis of the thermodynamic properties of solvation we conclude that the solubility difference is due to less favorable solute-solvent interactions in the ammonium based ionic liquid.<sup>34,42</sup>  $[C_1C_6Pyr][NTf_2]$  and  $[C_1C_4Pyrr][NTf_2]$  present similar performances to their imidazolium counterparts.  $[C_1C_4Pyrr][FAP]$  presents 13% less ethane solubility than  $[C_1C_4Im][FAP]$ , due to slightly less favorable solute-solvent interactions.<sup>46,47</sup>

In imidazolium based ionic liquids the minimum  $K_H$  for ethane is  $60.9 \times 10^5$  Pa obtained for  $[C_1C_{10}Im][NTf_2]$  at 313 K and for propane is  $59 \times 10^5$  Pa for  $[C_1C_4Im][NTf_2]$  at 320 K.

The solubility of ethane increases with the increase of the alkyl chain length of the cation, 63% from  $[C_1C_2Im][NTf_2]$  to  $[C_1C_{10}Im][NTf_2]$ , in the temperature range covered. On average, a 22% increase in solubility of ethane for each  $-C_2H_4-$  added in the cation alkyl chain of the imidazolium is obtained, at 303 K. The increase in solubility is not due to more favorable interactions between ethane and the increasing alkyl chain of the cation, but to increasingly more favorable entropies of solvation. Using molecular simulation, it was observed that ethane is solvated in the non-polar domains of the ionic liquid.<sup>34</sup> So, increasing the amount of the non-polar domains in the ionic liquid will lead to an increase in the solubility of ethane. The same effect is observed for ionic liquids based in the  $PF_6^-$  anion. The ethane solubility increase between  $[C_1C_4Im][FAP]$  and  $[C_1C_6Im][FAP]$  is smaller than the one found for their  $NTf_2^-$  or  $PF_6^-$  equivalents. The smaller difference is due to a balancing effect between a more favorable enthalpy and less favorable entropy for the  $C_1C_6Im^+$  containing ionic liquids, resulting in similar Gibbs energies of solvation for both.<sup>46</sup> An increase in solubility of propane is observed from  $[C_1C_2Im][NTf_2]$  to  $[C_1C_4Im][NTf_2]$ , although the comparison temperatures are slightly different, 303 K for the first and 300 K for the second. A 35% increase in ethane and propane solubility is observed from  $[P_{4444}][TMPP]$  to  $[P_{(14)666}][TMPP]$ .

Table 1.3 - Henry's law constant,  $K_H$ , or Henry's law constant range for ethane in several ionic liquids. Uncertainty included when possible for single measurements.

Ionic liquid	Temperature /K	$K_H$ /10 <sup>5</sup> Pa	Data points	Measuring method	Reference
[C <sub>1</sub> C <sub>2</sub> Im][NTf <sub>2</sub> ]	303	107.4±1.8	1	<i>pVT</i> - isochoric	31
[C <sub>1</sub> C <sub>2</sub> Im][NTf <sub>2</sub> ]	313	167.69±17	1	<i>pVT</i> - isochoric	11
[C <sub>1</sub> C <sub>2</sub> Im][NTf <sub>2</sub> ]	303-333	152-206	3	<i>pVT</i> - isochoric	32
[C <sub>1</sub> C <sub>2</sub> Im][NTf <sub>2</sub> ]	303-343	150.05-261.80	5	<i>pVT</i> - isochoric	42
[C <sub>1</sub> C <sub>4</sub> Im][NTf <sub>2</sub> ]	283-323	86-141	3	Gravimetric microbalance	57
[C <sub>1</sub> C <sub>4</sub> Im][NTf <sub>2</sub> ]	303	104.4±1	1	<i>pVT</i> - isochoric	33
[C <sub>1</sub> C <sub>4</sub> Im][NTf <sub>2</sub> ]	303-343	104.17-192.10	5	<i>pVT</i> - isochoric	34
[C <sub>1</sub> C <sub>4</sub> Im][NTf <sub>2</sub> ]	303-334	105.7-165.5	4	<i>pVT</i> - isochoric	58
[C <sub>1</sub> C <sub>6</sub> Im][NTf <sub>2</sub> ]	298-353	79.243-148.206	4	<i>pVT</i> - constant pressure	35
[C <sub>1</sub> C <sub>6</sub> Im][NTf <sub>2</sub> ]	283-343	55.34-116.0	7	<i>pVT</i> - isochoric	43
[C <sub>1</sub> C <sub>8</sub> Im][NTf <sub>2</sub> ]	303-343	59.864- 112.53	5	<i>pVT</i> - isochoric	34
[C <sub>1</sub> C <sub>10</sub> Im][NTf <sub>2</sub> ]	303-343	53.068- 98.300	5	<i>pVT</i> - isochoric	34
[C <sub>1</sub> C <sub>3</sub> CNIm][NTf <sub>2</sub> ]	303	218±1.1	1	<i>pVT</i> - isochoric	33
[(C <sub>3</sub> CN) <sub>2</sub> Im][NTf <sub>2</sub> ]	303	282±1.8	1	<i>pVT</i> - isochoric	33
[C <sub>1</sub> C <sub>1</sub> COOC <sub>5</sub> Im][NTf <sub>2</sub> ]	303-343	85.53-7.367	5	<i>pVT</i> - isochoric	44
[C <sub>1</sub> C <sub>1</sub> COOC <sub>2</sub> OC <sub>2</sub> Im][ NTf <sub>2</sub> ]	303-343	83.33-9.007	5	<i>pVT</i> - isochoric	44
[C <sub>1</sub> C <sub>1</sub> COOC <sub>2</sub> OC <sub>2</sub> OC <sub>4</sub> Im][ NTf <sub>2</sub> ]	303-343	58.13-11.16	5	<i>pVT</i> - isochoric	44
[C <sub>1</sub> C <sub>2</sub> Im][PF <sub>6</sub> ]	313	345.52±84	1	<i>pVT</i> - isochoric	11
[C <sub>1</sub> C <sub>4</sub> Im][PF <sub>6</sub> ]	283-323	234-363	3	Gravimetric microbalance	33, 45
[C <sub>1</sub> C <sub>4</sub> Im][PF <sub>6</sub> ]	283-343	199-521.25	7	<i>pVT</i> - isochoric	56
[C <sub>1</sub> C <sub>1</sub> COOC <sub>5</sub> Im][ C <sub>8</sub> SO <sub>4</sub> ]	323-343	91.45-115.0	6	<i>pVT</i> - isochoric	56
[C <sub>1</sub> C <sub>2</sub> Im][DCA]	313	665.2±146.5	1	<i>pVT</i> - isochoric	11
[C <sub>1</sub> C <sub>4</sub> Im][BF <sub>4</sub> ]	283-343	257.6-503.8	7	<i>pVT</i> - isochoric	12
[C <sub>1</sub> C <sub>4</sub> Im][BF <sub>4</sub> ]	313	421.01±64	1	<i>pVT</i> - isochoric	11
[C <sub>1</sub> C <sub>2</sub> Im][CF <sub>3</sub> SO <sub>3</sub> ]	313	359.7±62	1	<i>pVT</i> - isochoric	11
[C <sub>1</sub> C <sub>4</sub> Im][eFAP]	303-343	59.2-95.5	5	<i>pVT</i> - isochoric	46
[C <sub>1</sub> C <sub>6</sub> Im][eFAP]	303-343	60.27±109.67	5	<i>pVT</i> - isochoric	46
[C <sub>1</sub> C <sub>6</sub> Pyrr][NTf <sub>2</sub> ]	298-333	72-118	3	Gravimetric microbalance	27
[C <sub>1</sub> C <sub>4</sub> Pyrr][NTf <sub>2</sub> ]	303-343	105.2-173.7	5	<i>pVT</i> - isochoric	11
[C <sub>1</sub> C <sub>4</sub> Pyrr][eFAP]	303-343	67.67-100.4	5	<i>pVT</i> - isochoric	47
[N <sub>1132</sub> -OH][NTf <sub>2</sub> ]	303-343	162.05-278.4	5	<i>pVT</i> - isochoric	11

Ionic liquid	Temperature /K	$K_H / 10^5 \text{ Pa}$	Data points	Measuring method	Reference
$[\text{P}_{(14)666}][\text{eFAP}]$	303-343	16.87-29.77	5	$pVT$ - isochoric	47
$[\text{P}_{(14)666}][\text{TMPP}]$	303-353	16.0-30.3	4	$pVT$ - isochoric	32, 48
$[\text{P}_{4444}][\text{TMPP}]$	303-333	26-36	3	$pVT$ - isochoric	32

When the alkyl chain of the cation of the  $\text{NTf}_2^-$ -based ionic liquid is functionalized with a cyano group, like in the case of  $[\text{C}_1\text{C}_3\text{CNIm}][\text{NTf}_2]$ , the solubility of ethane is 37% less than in  $[\text{C}_1\text{C}_2\text{Im}][\text{NTf}_2]$ , 50% lower than  $[\text{C}_1\text{C}_4\text{Im}][\text{NTf}_2]$  and 69% lower than  $[\text{C}_1\text{C}_6\text{Im}][\text{NTf}_2]$ , at 303 K. Additional functionalization of the cation,  $[(\text{C}_3\text{CN})_2\text{Im}][\text{NTf}_2]$ , results in a further 23% decrease in ethane solubility. These differences are due to the increase of polarity upon functionalization of the ionic liquid, affecting the solubility of the apolar ethane.<sup>33</sup> The increase in solubility of ethane is more important when adding  $-\text{C}_2\text{H}_4-$  segments to the alkyl chain than when adding ester and/or ether functionalized segments. For example, the solubility of ethane increases less than 3% from  $[\text{C}_1\text{C}_1\text{COOC}_5\text{Im}][\text{NTf}_2]$  to  $[\text{C}_1\text{C}_1\text{COOC}_2\text{OC}_2\text{Im}][\text{NTf}_2]$ , at 303 K. The solubility of ethane decreases when the functionalization of the chain is done with an ester function,  $[\text{C}_1\text{C}_1\text{COOC}_5\text{Im}][\text{NTf}_2]$  presents an ethane solubility 13% inferior to  $[\text{C}_1\text{C}_6\text{Im}][\text{NTf}_2]$ .<sup>44</sup>

Imidazolium-based ionic liquids containing large anions such as  $\text{FAP}^-$ ,  $\text{C}_8\text{SO}_4^-$  and  $\text{NTf}_2^-$  present higher ethane and propane solubility (for each common anion), followed by  $\text{PF}_6^-$ ,  $\text{CF}_3\text{SO}_3^-$ ,  $\text{BF}_4^-$  and  $\text{DCA}^-$ . Changing the anion from  $\text{NTf}_2^-$  to  $\text{FAP}^-$  leads to 40% increase in ethane solubility when the cation is  $\text{C}_1\text{C}_4\text{Im}^+$  or  $\text{C}_1\text{C}_4\text{Pyrr}^+$  and of 18% for  $\text{C}_1\text{C}_6\text{Im}^+$ , at 303 K. Comparing  $[\text{C}_1\text{C}_1\text{COOC}_5\text{Im}][\text{NTf}_2]$  and  $[\text{C}_1\text{C}_1\text{COOC}_5\text{Im}][\text{C}_8\text{SO}_4]$ , we observe an ethane solubility increase of 15%, due to slightly more favorable enthalpies and entropies of solvation.<sup>44</sup> Ethane and propane solubility decreases to less than half when the anion is changed from  $\text{NTf}_2^-$  to  $\text{PF}_6^-$ , for cations  $\text{C}_1\text{C}_2\text{Im}^+$  and  $\text{C}_1\text{C}_4\text{Im}^+$ . Comparing the thermodynamic properties of solvation for ethane in the ionic liquid with the larger cation we observe that this is due to a more favorable entropy of solvation, although compensated by a less favorable enthalpy of solvation.<sup>27,34</sup> Ethane and propane solubility decreases by more than 50% when the anion is changed from  $\text{NTf}_2^-$  to  $\text{CF}_3\text{SO}_3^-$ , and over 70% when changed from  $\text{NTf}_2^-$  to  $\text{DCA}^-$ , for the  $\text{C}_1\text{C}_2\text{Im}^+$  cation.

Table 1.4 - Henry's law constant,  $K_H$ , or Henry's law constant range for propane in several ionic liquids. Uncertainty included when possible for single measurements.

Ionic liquid	Temperature /K	$K_H$ /10 <sup>5</sup> Pa	Data points	Measuring method	Reference
[C <sub>1</sub> C <sub>2</sub> Im][NTf <sub>2</sub> ]	303	70.93±1.1	1	<i>pVT</i> - isochoric	31
[C <sub>1</sub> C <sub>2</sub> Im][NTf <sub>2</sub> ]	313	94.28±5.8	1	<i>pVT</i> - isochoric	11
[C <sub>1</sub> C <sub>2</sub> Im][NTf <sub>2</sub> ]	303-333	73-111	3	<i>pVT</i> - isochoric	32
[C <sub>1</sub> C <sub>4</sub> Im][NTf <sub>2</sub> ]	280-340	35.7-80.9	4	<i>pVT</i> - isochoric	55
[C <sub>1</sub> C <sub>2</sub> Im][PF <sub>6</sub> ]	313	189.48±23	1	<i>pVT</i> - isochoric	11
[C <sub>1</sub> C <sub>2</sub> Im][DCA]	313	308.53±37.5	1	<i>pVT</i> - isochoric	11
[C <sub>1</sub> C <sub>4</sub> Im][BF <sub>4</sub> ]	313	254.33±23	1	<i>pVT</i> - isochoric	11
[C <sub>1</sub> C <sub>2</sub> Im][CF <sub>3</sub> SO <sub>3</sub> ]	313	211.77±15	1	<i>pVT</i> - isochoric	11
[P <sub>4444</sub> ][TMPP]	303-333	8.2-14	3	<i>pVT</i> - isochoric	32
[P <sub>(14)666</sub> ][TMPP]	303-353	5.1-13	4	<i>pVT</i> - isochoric	32, 48

Ethane solubility decreases 70% and propane 80% when the anion is changed from NTf<sub>2</sub><sup>-</sup> to BF<sub>4</sub><sup>-</sup>, for C<sub>1</sub>C<sub>4</sub>Im<sup>+</sup>. In the case of ethane this is due to a less favorable enthalpy of solvation of ethane in [C<sub>1</sub>C<sub>4</sub>Im][BF<sub>4</sub>].<sup>‡ 12,34</sup> In the case of the phosphonium cation, we observe that the TMPP<sup>-</sup> and FAP<sup>-</sup> anions have similar ethane solubility. [P<sub>(14)666</sub>][FAP] presents 72% more ethane solubility comparing to [C<sub>1</sub>C<sub>6</sub>Im][FAP], due to a more favorable entropy of solvation.<sup>46,47</sup>

In summary, the solubility of ethane and propane is higher in ionic liquids with larger non polar domains, such as phosphonium-based ionic liquids compared to imidazolium-based ones. The solubility of both gases is much less affected by the change of anion type.

<sup>‡</sup> The comparison temperature for the propane measurements was 320 K for NTf<sub>2</sub><sup>-</sup> and 313 K for BF<sub>4</sub><sup>-</sup> based ionic liquids

## 1.2 Solubility of ethene and propene

The Henry's law constants of ethene and propene in several ionic liquids are reported in figures 1.5 to 1.8 and tables 1.5 and 1.6.

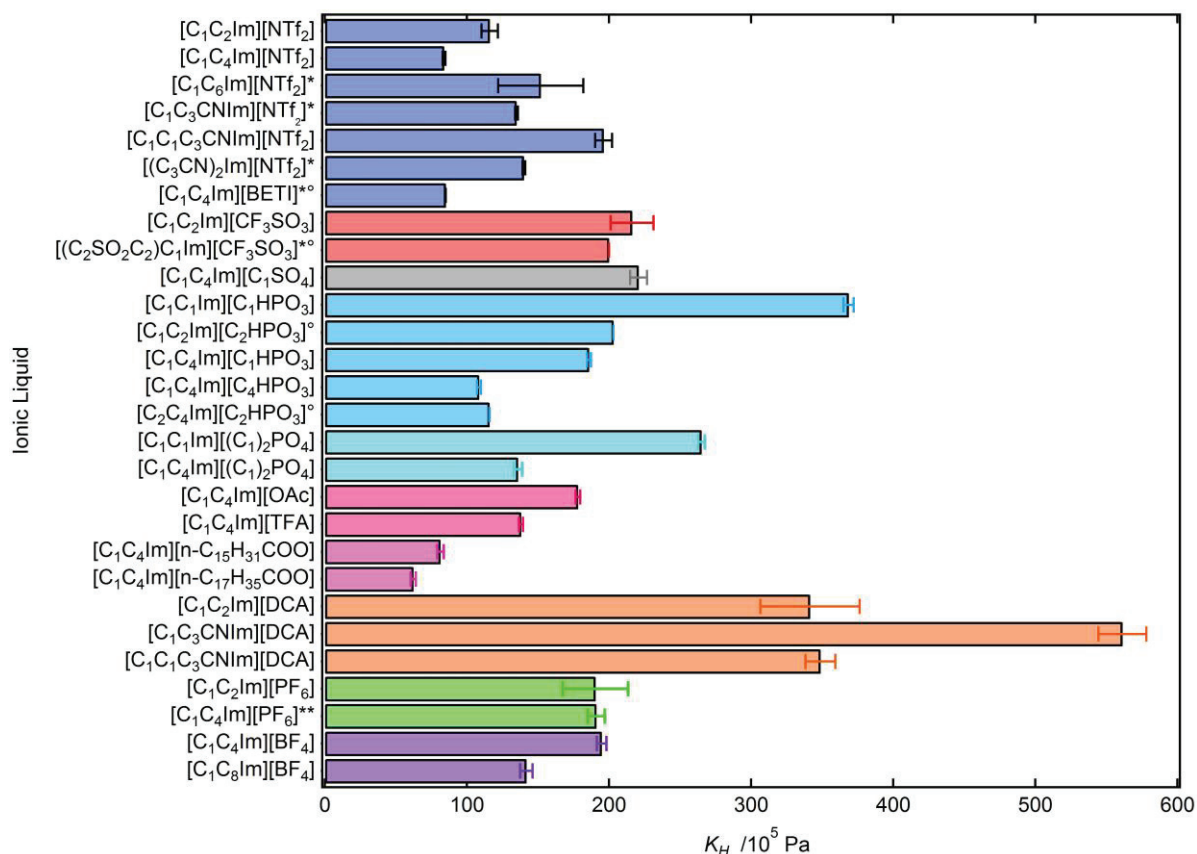


Figure 1.5 - Henry's law constant,  $K_H$ , for ethene in several imidazolium ionic liquids at 313 K.

\* - at 303 K; \*\* - at 323 K; ° - Uncertainty not indicated by the authors. [C<sub>1</sub>C<sub>2</sub>Im][NTf<sub>2</sub>]<sup>32</sup>; [C<sub>1</sub>C<sub>4</sub>Im][NTf<sub>2</sub>]<sup>7</sup>; [C<sub>1</sub>C<sub>6</sub>Im][NTf<sub>2</sub>]<sup>40,60</sup>; [C<sub>1</sub>C<sub>3</sub>CNIm][NTf<sub>2</sub>]<sup>33</sup>; [C<sub>1</sub>C<sub>1</sub>C<sub>3</sub>CNIm][NTf<sub>2</sub>]<sup>37,61</sup>; [(C<sub>3</sub>CN)<sub>2</sub>Im][NTf<sub>2</sub>]<sup>33</sup>; [C<sub>1</sub>C<sub>4</sub>Im][BETI]<sup>40</sup>; [C<sub>1</sub>C<sub>2</sub>Im][CF<sub>3</sub>SO<sub>3</sub>]<sup>11</sup>; [(C<sub>2</sub>SO<sub>2</sub>C<sub>2</sub>)C<sub>1</sub>Im][CF<sub>3</sub>SO<sub>3</sub>]<sup>40,60</sup>; [C<sub>1</sub>C<sub>4</sub>Im][C<sub>1</sub>SO<sub>4</sub>]<sup>7</sup>; [C<sub>1</sub>C<sub>1</sub>Im][C<sub>1</sub>HPO<sub>3</sub>]<sup>7</sup>; [C<sub>1</sub>C<sub>2</sub>Im][C<sub>2</sub>HPO<sub>3</sub>]<sup>62</sup>; [C<sub>1</sub>C<sub>4</sub>Im][C<sub>1</sub>HPO<sub>3</sub>]<sup>7</sup>; [C<sub>1</sub>C<sub>4</sub>Im][C<sub>4</sub>HPO<sub>3</sub>]<sup>7</sup>; [C<sub>2</sub>C<sub>4</sub>Im][C<sub>2</sub>HPO<sub>3</sub>]<sup>62</sup>; [C<sub>1</sub>C<sub>1</sub>Im][(C<sub>1</sub>)<sub>2</sub>PO<sub>4</sub>]<sup>7</sup>; [C<sub>1</sub>C<sub>4</sub>Im][(C<sub>1</sub>)<sub>2</sub>PO<sub>4</sub>]<sup>7</sup>; [C<sub>1</sub>C<sub>4</sub>Im][OAc]<sup>7</sup>; [C<sub>1</sub>C<sub>4</sub>Im][TFA]<sup>7</sup>; [C<sub>1</sub>C<sub>4</sub>Im][n-C<sub>15</sub>H<sub>31</sub>COO]<sup>37</sup>; [C<sub>1</sub>C<sub>4</sub>Im][n-C<sub>17</sub>H<sub>35</sub>COO]<sup>37</sup>; [C<sub>1</sub>C<sub>2</sub>Im][DCA]<sup>11</sup>; [C<sub>1</sub>C<sub>3</sub>CNIm][DCA]<sup>37,61</sup>; [C<sub>1</sub>C<sub>1</sub>C<sub>3</sub>CNIm][DCA]<sup>37,61</sup>;

Henry's law constants,  $K_H$  for ethene range from  $561.3 \times 10^5 \text{ Pa}$  for [C<sub>1</sub>C<sub>3</sub>CNIm][DCA] to  $26 \times 10^5 \text{ Pa}$  for [P<sub>(14)666</sub>][TMPP], at 313 K. For propene it ranges from  $241.4 \times 10^5 \text{ Pa}$  for [C<sub>1</sub>C<sub>1</sub>Im][C<sub>1</sub>SO<sub>4</sub>] to  $7.5 \times 10^5 \text{ Pa}$  for [P<sub>(14)666</sub>][TMPP], at 313 K. Ethene and propene solubility is less affected when changing from [C<sub>1</sub>C<sub>2</sub>Im][DCA] to [P<sub>(14)666</sub>][TMPP] than the solubility of ethane or propane. Solubility

is higher in phosphonium-based ionic liquids than imidazolium-based ones, up to 13 times for ethene and 17 times for propene.

The ethene and/or propene solubility data reported by Mokrushin *et al.*,<sup>49</sup> by Scovazzo,<sup>50</sup> by Kang *et al.*<sup>51</sup> and by Ortiz *et al.*<sup>52</sup> were not taken into consideration, due to lack of information for the calculation of Henry's law constants. The ethene solubility measurement in [C<sub>1</sub>C<sub>6</sub>Im][NTf<sub>2</sub>] reported by Kilaru and Scovazzo<sup>40</sup>, and by Kilaru, Condemarin and Scovazzo<sup>60</sup> is not consistent with other reported results and tendencies observed, and will not be considered in this analysis.<sup>40</sup>

Phosphonium-based ionic liquids present the highest ethene and propene solubility and are followed by ammonium, pyridinium, pyrrolidinium and imidazolium ones. In the case of phosphonium based ionic liquids, several anions were studied and both ethylene and propylene solubility follow the order: [P<sub>(14)666</sub>][DCA] < [P<sub>(14)666</sub>][Cl] < [P<sub>4444</sub>][TMPP] < [P<sub>(14)444</sub>][DBS] < [P<sub>(14)666</sub>][TMPP]. In the case of imidazolium and ammonium based ionic liquids, ethylene is more soluble in [C<sub>1</sub>C<sub>4</sub>Im][NTf<sub>2</sub>] than in [N<sub>(4)111</sub>][NTf<sub>2</sub>] but significantly less soluble than in [N<sub>(1)888</sub>][NTf<sub>2</sub>], at 303K.

When changing from an imidazolium-based cation for a pyrrolidinium one, no tendencies were observed.

Henry's law constant for ethene in imidazolium-based ionic liquids ranges from  $561.3 \times 10^5$  Pa for [C<sub>1</sub>C<sub>3</sub>CNIIm][DCA] to  $62 \times 10^5$  Pa for [C<sub>1</sub>C<sub>4</sub>Im][n-C<sub>17</sub>H<sub>35</sub>COO], at 313 K. For propene the range goes from  $189.3 \times 10^5$  Pa for [C<sub>1</sub>C<sub>1</sub>Im][C<sub>1</sub>HPO<sub>3</sub>] to  $7.5 \times 10^5$  Pa for [P<sub>(14)666</sub>][TMPP], at 313 K.

The solubility of ethene and propene increases from 30% to 60% with the increase of the alkyl chain of the cation or anion, for imidazolium, pyrrolidinium and phosphonium based ionic liquids based in NTf<sub>2</sub><sup>-</sup>, BF<sub>4</sub><sup>-</sup>, phosphate and phosphite anions. For small increases in the total number of carbons in the alkyl chain of ammonium-based ionic liquids containing the NTf<sub>2</sub><sup>-</sup> anion, no ethene solubility difference is observed within the expected uncertainties. An increase in ethene solubility starts to be visible for [N<sub>(4)111</sub>][NTf<sub>2</sub>] and [N<sub>(10)111</sub>][NTf<sub>2</sub>], 27% and [N<sub>(6)111</sub>][NTf<sub>2</sub>] and [N<sub>(6)222</sub>][NTf<sub>2</sub>], 30%. The largest ethene solubility increase is 61% between [N<sub>(4)111</sub>][NTf<sub>2</sub>] and [N<sub>(1)888</sub>][NTf<sub>2</sub>].

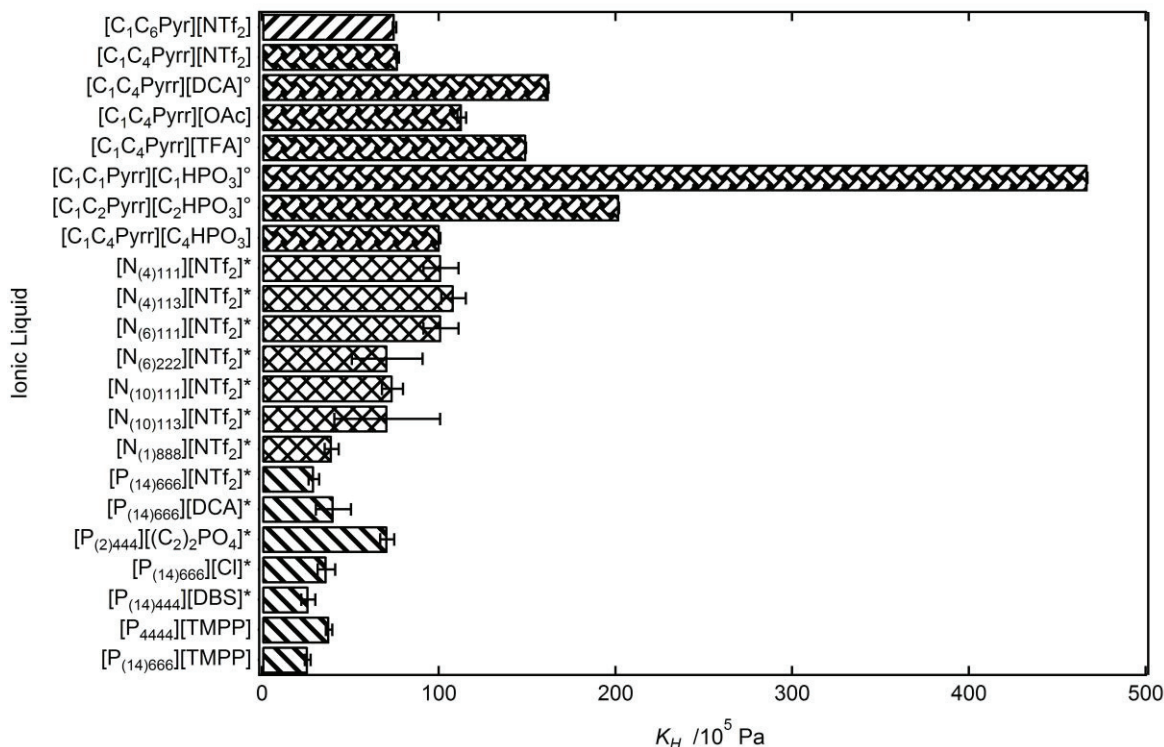


Figure 1.6 - Henry's law constant,  $K_H$ , for ethene in several non-imidazolium ionic liquids at 313 K.

\* - at 303 K; ° - Uncertainty not indicated by the authors. [C<sub>1</sub>C<sub>6</sub>Pyrr][NTf<sub>2</sub>]<sup>40</sup>; [C<sub>1</sub>C<sub>4</sub>Pyrr][NTf<sub>2</sub>]<sup>7</sup>; [C<sub>1</sub>C<sub>4</sub>Pyrr][DCA]<sup>65</sup>; [C<sub>1</sub>C<sub>4</sub>Pyrr][OAc]<sup>7,65</sup>; [C<sub>1</sub>C<sub>4</sub>Pyrr][TFA]<sup>65</sup>; [C<sub>1</sub>C<sub>1</sub>Pyrr][C<sub>1</sub>HPO<sub>3</sub>]<sup>65</sup>; [C<sub>1</sub>C<sub>2</sub>Pyrr][C<sub>2</sub>HPO<sub>3</sub>]<sup>65</sup>; [C<sub>1</sub>C<sub>4</sub>Pyrr][C<sub>4</sub>HPO<sub>3</sub>]<sup>7</sup>; [N<sub>(4)111</sub>][NTf<sub>2</sub>]<sup>40,60,64</sup>; [N<sub>(4)113</sub>][NTf<sub>2</sub>]<sup>40,60,64</sup>; [N<sub>(6)111</sub>][NTf<sub>2</sub>]<sup>40,60,64</sup>; [N<sub>(6)222</sub>][NTf<sub>2</sub>]<sup>40,60,64</sup>; [N<sub>(10)111</sub>][NTf<sub>2</sub>]<sup>40,60,64</sup>; [N<sub>(10)113</sub>][NTf<sub>2</sub>]<sup>40,60,64</sup>; [N<sub>(1)888</sub>][NTf<sub>2</sub>]<sup>40,60,64</sup>; [P<sub>(14)666</sub>][NTf<sub>2</sub>]<sup>40,60,63</sup>; [P<sub>(14)666</sub>][DCA]<sup>40,60,63</sup>; [P<sub>(2)444</sub>][(C<sub>2</sub>)<sub>2</sub>PO<sub>4</sub>]<sup>40,60,63</sup>; [P<sub>(14)666</sub>][Cl]<sup>40, 41,60,63</sup>; [P<sub>(14)444</sub>][DBS]<sup>40,63</sup>; [P<sub>4444</sub>][TMPP]<sup>32</sup>; [P<sub>(14)666</sub>][TMPP]<sup>32,48</sup>

The addition of a polar group in the side chain of the cation of the ionic liquid can increase or decrease ethene solubility. Functionalizing the side chain of the ionic liquid [C<sub>1</sub>C<sub>2</sub>Im][CF<sub>3</sub>SO<sub>3</sub>], resulting in [(C<sub>2</sub>SO<sub>2</sub>C<sub>2</sub>)C<sub>1</sub>Im][CF<sub>3</sub>SO<sub>3</sub>] leads to a 25% increase of ethene solubility, while [C<sub>1</sub>C<sub>3</sub>CNIm][DCA] presents 57% less ethene solubility than [C<sub>1</sub>C<sub>4</sub>Im][NTf<sub>2</sub>], at 313 K.

Removing the imidazolium acidic proton of [C<sub>1</sub>C<sub>3</sub>CNIm][DCA] to [C<sub>1</sub>C<sub>1</sub>C<sub>3</sub>CNIm][DCA] increases the solubility of ethene by 51% at 303 K (to 25% at 323 K).

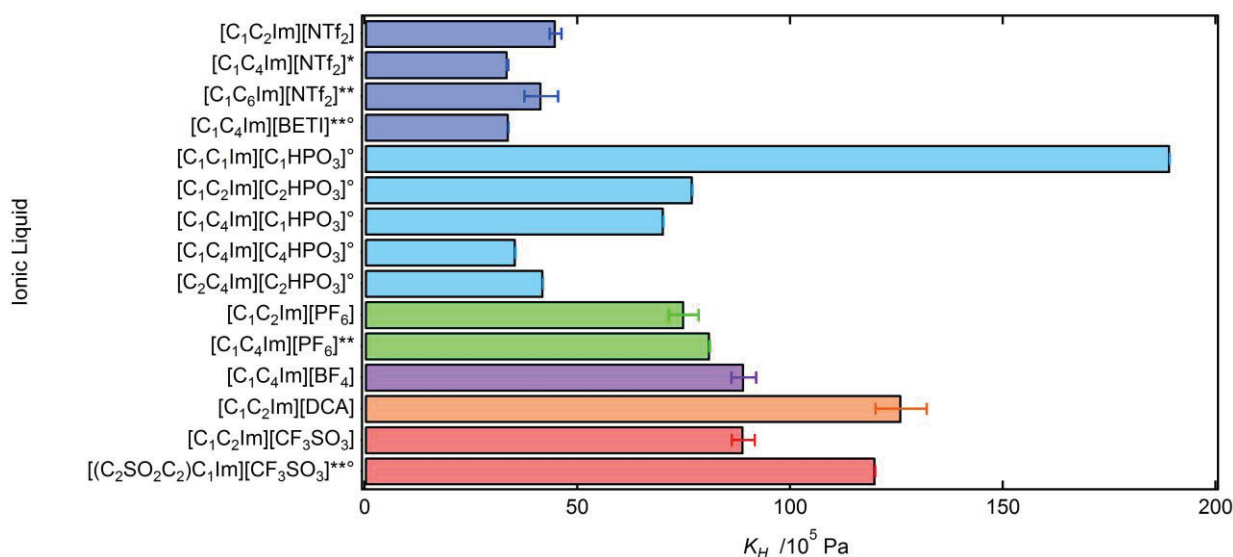


Figure 1.7 - Henry's law constant,  $K_H$ , for propene in several imidazolium ionic liquids at 313 K. \* - at 320 K; \*\* - at 303 K; ° - Uncertainty not indicated by the authors. [C<sub>1</sub>C<sub>2</sub>Im][NTf<sub>2</sub>]<sup>11</sup>; [C<sub>1</sub>C<sub>4</sub>Im][NTf<sub>2</sub>]<sup>62</sup>; [C<sub>1</sub>C<sub>6</sub>Im][NTf<sub>2</sub>]<sup>40, 60</sup>; [C<sub>1</sub>C<sub>4</sub>Im][BETI]<sup>40</sup>; [C<sub>1</sub>C<sub>1</sub>Im][C<sub>1</sub>HPO<sub>3</sub>]<sup>62</sup>; [C<sub>1</sub>C<sub>2</sub>Im][C<sub>2</sub>HPO<sub>3</sub>]<sup>62</sup>; [C<sub>1</sub>C<sub>4</sub>Im][C<sub>1</sub>HPO<sub>3</sub>]<sup>62</sup>; [C<sub>1</sub>C<sub>4</sub>Im][C<sub>4</sub>HPO<sub>3</sub>]<sup>62</sup>; [C<sub>2</sub>C<sub>4</sub>Im][C<sub>2</sub>HPO<sub>3</sub>]<sup>62</sup>; [C<sub>1</sub>C<sub>2</sub>Im][PF<sub>6</sub>]<sup>11</sup>; [C<sub>1</sub>C<sub>4</sub>Im][PF<sub>6</sub>]<sup>40,41,60</sup>; [C<sub>1</sub>C<sub>4</sub>Im][BF<sub>4</sub>]<sup>11</sup>; [C<sub>1</sub>C<sub>2</sub>Im][DCA]<sup>11</sup>; [C<sub>1</sub>C<sub>2</sub>Im][CF<sub>3</sub>SO<sub>3</sub>]<sup>11</sup>; [(C<sub>2</sub>SO<sub>2</sub>C<sub>2</sub>)C<sub>1</sub>Im][CF<sub>3</sub>SO<sub>3</sub>]<sup>40,60</sup>.

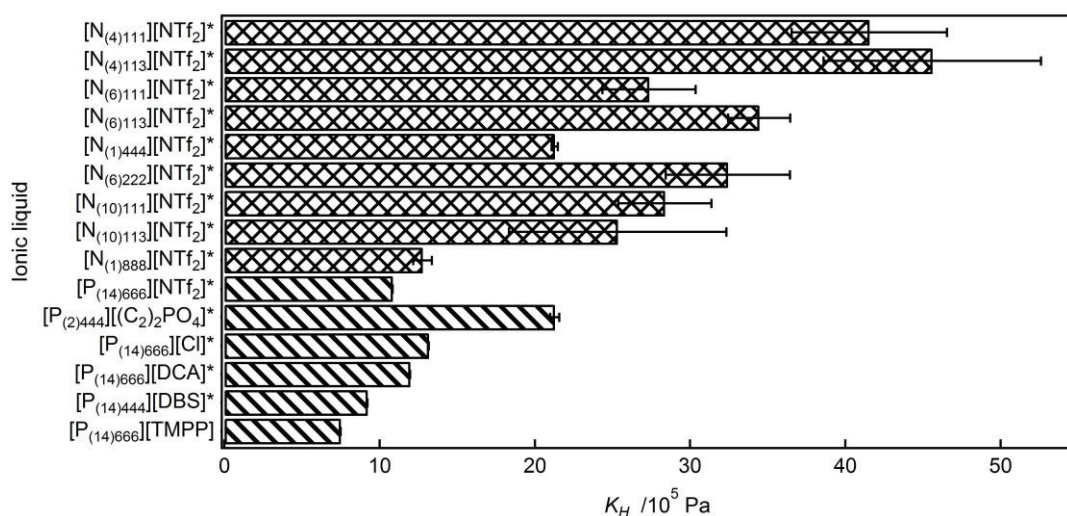


Figure 1.8 - Henry's law constant,  $K_H$ , for propene in several non-imidazolium ionic liquids at 313 K. \* - at 303 K. ° - Uncertainty not indicated by the authors. [N<sub>(4)111</sub>][NTf<sub>2</sub>]<sup>40,60,64</sup>; [N<sub>(4)113</sub>][NTf<sub>2</sub>]<sup>40,60,64</sup>; [N<sub>(6)111</sub>][NTf<sub>2</sub>]<sup>40,60,64</sup>; [N<sub>(6)113</sub>][NTf<sub>2</sub>]<sup>40,60,64</sup>; [N<sub>(1)444</sub>][NTf<sub>2</sub>]<sup>64</sup>; [N<sub>(6)222</sub>][NTf<sub>2</sub>]<sup>40,60,64</sup>; [N<sub>(10)111</sub>][NTf<sub>2</sub>]<sup>40,60,64</sup>; [N<sub>(10)113</sub>][NTf<sub>2</sub>]<sup>40,60,64</sup>; [N<sub>(1)888</sub>][NTf<sub>2</sub>]<sup>40,60,64</sup>; [P<sub>(14)666</sub>][NTf<sub>2</sub>]<sup>40,60,63</sup>; [P<sub>(2)444</sub>][(C<sub>2</sub>)<sub>2</sub>PO<sub>4</sub>]<sup>40,60,63</sup>; [P<sub>(14)666</sub>][Cl]<sup>40,60,63</sup>; [P<sub>(14)666</sub>][DCA]<sup>40,60,63</sup>; [P<sub>(14)444</sub>][DBS]<sup>40,63</sup>; [P<sub>(14)666</sub>][TMPP]<sup>48</sup>.

Imidazolium ionic liquids containing  $\text{NTf}_2^-$ ,  $\text{BETI}^-$  or long chain carboxylate anions present the highest ethene and propene solubility (for each common anion), followed by heavy phosphates and phosphites,  $\text{PF}_6^-$ ,  $\text{CF}_3\text{SO}_3^-$ ,  $\text{BF}_4^-$ , sulphates and finally  $\text{DCA}^-$ .

For  $\text{C}_1\text{C}_2\text{Im}^+$  the ethene solubility order is  $\text{NTf}_2^- > \text{PF}_6^-$  (the decrease is larger for  $\text{C}_1\text{C}_4\text{Im}^+$ )  $> \text{C}_2\text{HPO}_3^- > \text{CF}_3\text{SO}_3^- > \text{DCA}^-$ , at 313 K.

For  $\text{C}_1\text{C}_2\text{Im}^+$  the propene solubility order is  $\text{NTf}_2^- > \text{PF}_6^-$  (the decrease is larger for  $\text{C}_1\text{C}_4\text{Im}^+$ )  $> \text{CF}_3\text{SO}_3^- \approx \text{C}_2\text{HPO}_3^- > \text{DCA}^- > \text{BF}_4^-$ , between the temperatures of 303 K to 333 K (303 K and 308 K for  $\text{CF}_3\text{SO}_3^-$  and at 313 K for  $\text{PF}_6^-$  and  $\text{DCA}^-$ ).

$[\text{C}_1\text{C}_4\text{Im}][\text{NTf}_2]$  and  $[\text{C}_1\text{C}_4\text{Im}][\text{BETI}]$  present a solubility difference of 4% for ethene and 47% for propene with higher solubility for  $[\text{C}_1\text{C}_4\text{Im}][\text{NTf}_2]$ , at 303 K.

For all the following comparisons, the solubility measurement temperature of propene in  $[\text{C}_1\text{C}_4\text{Im}][\text{NTf}_2]$  is 320 K.

The ethene solubility order for  $\text{C}_1\text{C}_4\text{Im}^+$  is  $\text{NTf}_2^- > \text{C}_4\text{HPO}_3^- > (\text{C}_1)_2\text{PO}_4^- \approx \text{TFA}^- \approx \text{C}_2\text{HPO}_3^- > 50\%$  for  $\text{CF}_3\text{SO}_3^- \approx \text{OAc}^- \approx \text{C}_1\text{HPO}_3^- > \text{C}_1\text{SO}_4^- \approx \text{BF}_4^- > \text{DCA}^-$ , at 313 K.

The propene solubility order for  $\text{C}_1\text{C}_4\text{Im}^+$  is  $\text{NTf}_2^- > \text{C}_4\text{HPO}_3^- \approx (\text{C}_4)_2\text{PO}_4^- > \text{C}_1\text{HPO}_3^- > \text{PF}_6^-$  (at 303K)  $> \text{BF}_4^- \approx \text{C}_1\text{SO}_4^-$ , at 318 K.

From the imidazolium ionic liquids reported, the only ones with ethene solubility greater than  $[\text{C}_1\text{C}_4\text{Im}][\text{NTf}_2]$  are  $[\text{C}_1\text{C}_4\text{Im}][n\text{-C}_{15}\text{H}_{31}\text{COO}]$  and  $[\text{C}_1\text{C}_4\text{Im}][n\text{-C}_{17}\text{H}_{35}\text{COO}]$ , by 8% and 29% at 313 K.

The ethene solubility order for  $\text{C}_1\text{C}_4\text{Pyrr}^+$  is  $\text{NTf}_2^- > \text{C}_4\text{HPO}_3^- > \text{OAc}^- \approx \text{TFA}^- \approx \text{DCA}^-$ , at 313 K, following a similar trend then their imidazolium counterparts, with the exception of  $\text{OAc}^-$  anion.

The ethene solubility order for phosphonium-based ionic liquids is  $[\text{P}_{(14)666}][\text{TMPP}] \approx [\text{P}_{(14)444}][\text{DBS}] \approx [\text{P}_{(14)666}][\text{NTf}_2] > [\text{P}_{4444}][\text{TMPP}] \approx [\text{P}_{(14)666}][\text{Cl}] > [\text{P}_{(14)666}][\text{DCA}] > [\text{P}_{(2)444}][(\text{C}_2)_2\text{PO}_4]$ , at 303K.

The propene solubility order for phosphonium-based ionic liquids is  $[\text{P}_{(14)666}][\text{TMPP}] > [\text{P}_{(14)444}][\text{DBS}] > [\text{P}_{(14)666}][\text{NTf}_2] > [\text{P}_{(14)666}][\text{DCA}] > [\text{P}_{(14)666}][\text{Cl}] > [\text{P}_{(2)444}][(\text{C}_2)_2\text{PO}_4]$ , at 303K.

Table 1.5 - Henry's law constant,  $K_H$ , or Henry's law constant range for ethene in several ionic liquids. Uncertainty included when possible for single measurements.

Ionic liquid	Temperature /K	$K_H / 10^5$ Pa	Data points	Measuring method	Reference
[C <sub>1</sub> C <sub>2</sub> Im][NTf <sub>2</sub> ]	303	111±7	1	$pVT$ - isochoric	59
[C <sub>1</sub> C <sub>2</sub> Im][NTf <sub>2</sub> ]	303	151.48±2.8	1	$pVT$ - isochoric	31
[C <sub>1</sub> C <sub>2</sub> Im][NTf <sub>2</sub> ]	313	123.62±8	1	$pVT$ - isochoric	11
[C <sub>1</sub> C <sub>2</sub> Im][NTf <sub>2</sub> ]	303	134.7	1	Lag-time technique	40, 41, 60
[C <sub>1</sub> C <sub>2</sub> Im][NTf <sub>2</sub> ]	303-333	100-154	3	$pVT$ - isochoric	32
[C <sub>1</sub> C <sub>4</sub> Im][NTf <sub>2</sub> ]	283-323	61-97	3	Gravimetric microbalance	45
[C <sub>1</sub> C <sub>4</sub> Im][NTf <sub>2</sub> ]	303	75.7±0.5	1	$pVT$ - isochoric	33
[C <sub>1</sub> C <sub>4</sub> Im][NTf <sub>2</sub> ]	303-323	87.3-108	3	Gas chromatography	37, 61
[C <sub>1</sub> C <sub>4</sub> Im][NTf <sub>2</sub> ]	313	84.0±1.0	1	$pVT$ - isochoric	7
[C <sub>1</sub> C <sub>6</sub> Im][NTf <sub>2</sub> ]	303	152±30	1	Lag-time technique	40, 60
[C <sub>1</sub> C <sub>3</sub> CNIm][NTf <sub>2</sub> ]	303	135±0.9	1	$pVT$ - isochoric	33
[C <sub>1</sub> C <sub>3</sub> CNIm][NTf <sub>2</sub> ]	303-323	195.3-214.5	3	Gas chromatography	37, 61
[C <sub>1</sub> C <sub>1</sub> C <sub>3</sub> CNIm][NTf <sub>2</sub> ]	303-323	182.1-203.1	3	Gas chromatography	37, 61
[(C <sub>3</sub> CN) <sub>2</sub> Im][NTf <sub>2</sub> ]	303	140.1±0.9	1	$pVT$ - isochoric	33
[C <sub>1</sub> C <sub>4</sub> Im][BETI]	303	85	1	Lag-time technique	40
[C <sub>1</sub> C <sub>2</sub> Im][CF <sub>3</sub> SO <sub>3</sub> ]	303	223±21	1	$pVT$ - isochoric	37
[C <sub>1</sub> C <sub>2</sub> Im][CF <sub>3</sub> SO <sub>3</sub> ]	313	216±15	1	$pVT$ - isochoric	11
[C <sub>1</sub> C <sub>2</sub> Im][CF <sub>3</sub> SO <sub>3</sub> ]	303	265.3	1	Lag-time technique	40, 41, 60
[(C <sub>2</sub> SO <sub>2</sub> C <sub>2</sub> )C <sub>1</sub> Im][CF <sub>3</sub> SO <sub>3</sub> ]	303	200.2	1	Lag-time technique	40, 60
[C <sub>1</sub> C <sub>4</sub> Im][C <sub>1</sub> SO <sub>4</sub> ]	313	220.8±6.0	1	$pVT$ - isochoric	7
[C <sub>1</sub> C <sub>1</sub> Im][C <sub>1</sub> HPO <sub>3</sub> ]	313	368.7±3.5	1	$pVT$ - isochoric	7
[C <sub>1</sub> C <sub>1</sub> Im][C <sub>1</sub> HPO <sub>3</sub> ]	313	367.3	1	$pVT$ - isochoric	62
[C <sub>1</sub> C <sub>2</sub> Im][C <sub>2</sub> HPO <sub>3</sub> ]	313	203.1	1	$pVT$ - isochoric	62
[C <sub>1</sub> C <sub>4</sub> Im][C <sub>1</sub> HPO <sub>3</sub> ]	313	183.4	1	$pVT$ - isochoric	62
[C <sub>1</sub> C <sub>4</sub> Im][C <sub>1</sub> HPO <sub>3</sub> ]	313	185.8±1.3	1	$pVT$ - isochoric	7
[C <sub>1</sub> C <sub>4</sub> Im][C <sub>4</sub> HPO <sub>3</sub> ]	313	107.1	1	$pVT$ - isochoric	62
[C <sub>1</sub> C <sub>4</sub> Im][C <sub>4</sub> HPO <sub>3</sub> ]	313	108.5±1.4	1	$pVT$ - isochoric	7
[C <sub>2</sub> C <sub>4</sub> Im][C <sub>2</sub> HPO <sub>3</sub> ]	313	115.8	1	$pVT$ - isochoric	62
[C <sub>1</sub> C <sub>1</sub> Im][(C <sub>1</sub> ) <sub>2</sub> PO <sub>4</sub> ]	313	265.1±2.4	1	$pVT$ - isochoric	7
[C <sub>1</sub> C <sub>4</sub> Im][(C <sub>1</sub> ) <sub>2</sub> PO <sub>4</sub> ]	313	136.0±3.0	1	$pVT$ - isochoric	7
[C <sub>1</sub> C <sub>4</sub> Im][OAc]	313	178.2±1.6	1	$pVT$ - isochoric	7
[C <sub>1</sub> C <sub>4</sub> Im][TFA]	313	138.1±1.4	1	$pVT$ - isochoric	7

Ionic liquid	Temperature /K	$K_H / 10^5 \text{ Pa}$	Data points	Measuring method	Reference
[C <sub>1</sub> C <sub>4</sub> Im][n-C <sub>15</sub> H <sub>31</sub> COO]	313-323	81.4-72.2	2	Gas chromatography	37
[C <sub>1</sub> C <sub>4</sub> Im][n-C <sub>17</sub> H <sub>35</sub> COO]	313	62.3-59.3	2	Gas chromatography	37
[C <sub>1</sub> C <sub>2</sub> Im][DCA]	313	341±35	1	<i>pVT</i> - isochoric	11
[C <sub>1</sub> C <sub>2</sub> Im][DCA]	303	314±38	1	<i>pVT</i> - isochoric	37
[C <sub>1</sub> C <sub>3</sub> CNIm][DCA]	303-323	546.3-636.6	3	Gas chromatography	37, 61
[C <sub>1</sub> C <sub>1</sub> C <sub>3</sub> CNIm][DCA]	303-323	266.6-475.9	3	Gas chromatography	37, 61
[C <sub>1</sub> C <sub>2</sub> Im][PF <sub>6</sub> ]	313	190±23	1	<i>pVT</i> - isochoric	11
[C <sub>1</sub> C <sub>4</sub> Im][PF <sub>6</sub> ]	283-323	125-191	3	Gravimetric microbalance	45, 57
[C <sub>1</sub> C <sub>4</sub> Im][PF <sub>6</sub> ]	303	182±16	1	<i>pVT</i> - isochoric	37
[C <sub>1</sub> C <sub>4</sub> Im][PF <sub>6</sub> ]	303	205.9	1	Lag-time technique	40, 41, 60
[C <sub>1</sub> C <sub>4</sub> Im][BF <sub>4</sub> ]	313	194.7±3.4	1	<i>pVT</i> - isochoric	7
[C <sub>1</sub> C <sub>4</sub> Im][BF <sub>4</sub> ]	303-323	206.5-255.2	3	Gas chromatography	37
[C <sub>1</sub> C <sub>4</sub> Im][BF <sub>4</sub> ]	303	256.4±22.5	1	<i>pVT</i> - isochoric	11
[C <sub>1</sub> C <sub>8</sub> Im][BF <sub>4</sub> ]	303-323	134.6-151.2	3	Gas chromatography	37
[P <sub>(2)444</sub> ][(C <sub>2</sub> ) <sub>2</sub> PO <sub>4</sub> ]	303	71±4	1	Lag-time technique	40, 60, 63
[P <sub>4444</sub> ][TMPP]	303-323	35-45	3	<i>pVT</i> - isochoric	32
[P <sub>(14)444</sub> ][DBS]	303	26±4	1	Lag-time technique	40, 63
[P <sub>(14)666</sub> ][TMPP]	303-353	23.0-4.01	3	<i>pVT</i> - isochoric	32, 48
[P <sub>(14)666</sub> ][Cl]	303	36±5	1	Lag-time technique	40, 41, 60, 63
[P <sub>(14)666</sub> ][DCA]	303	41±10	1	Lag-time technique	40, 60, 63
[P <sub>(14)666</sub> ][NTf <sub>2</sub> ]	303	29±3	1	Lag-time technique	40, 60, 63
[N <sub>(4)111</sub> ][NTf <sub>2</sub> ]	303	101±10	1	Lag-time technique	40, 60, 64
[N <sub>(4)113</sub> ][NTf <sub>2</sub> ]	303	108±7	1	Lag-time technique	40, 60, 64
[N <sub>(6)111</sub> ][NTf <sub>2</sub> ]	303	101±10	1	Lag-time technique	40, 60, 64
[N <sub>(10)111</sub> ][NTf <sub>2</sub> ]	303	74±6	1	Lag-time technique	40, 60, 64
[N <sub>(6)222</sub> ][NTf <sub>2</sub> ]	303	71±20	1	Lag-time technique	40, 60, 64
[N <sub>(10)113</sub> ][NTf <sub>2</sub> ]	303	71±30	1	Lag-time technique	40, 60, 64
[N <sub>(1)888</sub> ][NTf <sub>2</sub> ]	303	40±4	1	Lag-time technique	40, 60, 64
[C <sub>1</sub> C <sub>1</sub> Pyrr][C <sub>1</sub> HPO <sub>3</sub> ]	313	467.1	1	<i>pVT</i> - isochoric	65
[C <sub>1</sub> C <sub>2</sub> Pyrr][C <sub>2</sub> HPO <sub>3</sub> ]	313	202	1	<i>pVT</i> - isochoric	65
[C <sub>1</sub> C <sub>4</sub> Pyrr][NTf <sub>2</sub> ]	313	76.8±0.6	1	<i>pVT</i> - isochoric	7
[C <sub>1</sub> C <sub>4</sub> Pyrr][C <sub>4</sub> HPO <sub>3</sub> ]	313	101±0.5	1	<i>pVT</i> - isochoric	7
[C <sub>1</sub> C <sub>4</sub> Pyrr][C <sub>4</sub> HPO <sub>3</sub> ]	313	99.9	1	<i>pVT</i> - isochoric	65

Ionic liquid	Temperature /K	$K_H / 10^5$ Pa	Data points	Measuring method	Reference
[C <sub>1</sub> C <sub>4</sub> Pyrr][OAc]	313	113.8±2.5	1	<i>pVT</i> - isochoric	7
[C <sub>1</sub> C <sub>4</sub> Pyrr][OAc]	313	112.3	1	<i>pVT</i> - isochoric	65
[C <sub>1</sub> C <sub>4</sub> Pyrr][TFA]	313	149.4	1	<i>pVT</i> - isochoric	65
[C <sub>1</sub> C <sub>4</sub> Pyrr][DCA]	313	162.2	1	<i>pVT</i> - isochoric	65
[C <sub>1</sub> C <sub>6</sub> Pyrr][NTf <sub>2</sub> ]	298-333	58-96	3	Gravimetric microbalance	40

Table 1.6 - Henry's law constant,  $K_H$ , or Henry's law constant range for propene in several ionic liquids. Uncertainty included when possible for single measurements.

Ionic liquid	Temperature /K	$K_H / 10^5$ Pa	Data points	Measuring method	Reference
[C <sub>1</sub> C <sub>2</sub> Im][NTf <sub>2</sub> ]	303	37.54±0.5	1	<i>pVT</i> - isochoric	31
[C <sub>1</sub> C <sub>2</sub> Im][NTf <sub>2</sub> ]	313	44.94±1.4	1	<i>pVT</i> - isochoric	11
[C <sub>1</sub> C <sub>2</sub> Im][NTf <sub>2</sub> ]	303	47.1	1	Lag-time technique	40, 41, 60
[C <sub>1</sub> C <sub>4</sub> Im][NTf <sub>2</sub> ]	280-340	15.3-45.8	4	<i>pVT</i> - isochoric	62
[C <sub>1</sub> C <sub>6</sub> Im][NTf <sub>2</sub> ]	303	42±4	1	Lag-time technique	40, 60
[C <sub>1</sub> C <sub>4</sub> Im][BETI]	303	33.8	1	Lag-time technique	40
[C <sub>1</sub> C <sub>1</sub> Im][C <sub>1</sub> HPO <sub>3</sub> ]	313	189.3	1	<i>pVT</i> - isochoric	62
[C <sub>1</sub> C <sub>2</sub> Im][C <sub>2</sub> HPO <sub>3</sub> ]	313	77.1	1	<i>pVT</i> - isochoric	62
[C <sub>1</sub> C <sub>4</sub> Im][C <sub>1</sub> HPO <sub>3</sub> ]	313	70.3	1	<i>pVT</i> - isochoric	62
[C <sub>1</sub> C <sub>4</sub> Im][C <sub>4</sub> HPO <sub>3</sub> ]	313	35.5	1	<i>pVT</i> - isochoric	62
[C <sub>2</sub> C <sub>4</sub> Im][C <sub>2</sub> HPO <sub>3</sub> ]	313	42	1	<i>pVT</i> - isochoric	62
[C <sub>1</sub> C <sub>2</sub> Im][PF <sub>6</sub> ]	313	75.08±3.5	1	<i>pVT</i> - isochoric	11
[C <sub>1</sub> C <sub>4</sub> Im][PF <sub>6</sub> ]	303	81.2	1	Lag-time technique	40, 41, 60
[C <sub>1</sub> C <sub>4</sub> Im][BF <sub>4</sub> ]	313	89.17±2.9	1	<i>pVT</i> - isochoric	11
[C <sub>1</sub> C <sub>2</sub> Im][DCA]	313	126.15±6	1	<i>pVT</i> - isochoric	11
[C <sub>1</sub> C <sub>2</sub> Im][CF <sub>3</sub> SO <sub>3</sub> ]	313	89.01±2.7	1	<i>pVT</i> - isochoric	11
[C <sub>1</sub> C <sub>2</sub> Im][CF <sub>3</sub> SO <sub>3</sub> ]	303	89.1	1	Lag-time technique	40, 41, 60
[(C <sub>2</sub> SO <sub>2</sub> C <sub>2</sub> )C <sub>1</sub> Im][CF <sub>3</sub> SO <sub>3</sub> ]	303	120.1	1	Lag-time technique	40, 60
[P <sub>(2)444</sub> ][(C <sub>2</sub> ) <sub>2</sub> PO <sub>4</sub> ]	303	21±0.3	1	Lag-time technique	40, 60, 63
[P <sub>(14)444</sub> ][DBS]	303	9.2±0.007	1	Lag-time technique	40, 63
[P <sub>(14)666</sub> ][TMPP]	313-353	7.5-16	3	<i>pVT</i> - isochoric	48
[P <sub>(14)666</sub> ][Cl]	303	13±0.01	1	Lag-time technique	40, 60, 63
[P <sub>(14)666</sub> ][DCA]	303	12.0±0.01	1	Lag-time technique	40, 60, 63
[P <sub>(14)666</sub> ][NTf <sub>2</sub> ]	303	10.8±0.003	1	Lag-time technique	40, 60, 63
[N <sub>(4)111</sub> ][NTf <sub>2</sub> ]	303	42±5	1	Lag-time technique	40, 60, 64

<b>Ionic liquid</b>	<b>Temperature /K</b>	<b><math>K_H / 10^5</math> Pa</b>	<b>Data points</b>	<b>Measuring method</b>	<b>Reference</b>
[N <sub>(4)113</sub> ][NTf <sub>2</sub> ]	303	46±7	1	Lag-time technique	40, 60, 64
[N <sub>(6)113</sub> ][NTf <sub>2</sub> ]	303	34±2	1	Lag-time technique	40, 60, 64
[N <sub>(6)111</sub> ][NTf <sub>2</sub> ]	303	27±3	1	Lag-time technique	40, 60, 64
[N <sub>(1)444</sub> ][NTf <sub>2</sub> ]	303	21±0.2	1	Lag-time technique	64
[N <sub>(6)222</sub> ][NTf <sub>2</sub> ]	303	32±4	1	Lag-time technique	40, 60, 64
[N <sub>(10)111</sub> ][NTf <sub>2</sub> ]	303	28±3	1	Lag-time technique	40, 60, 64
[N <sub>(10)113</sub> ][NTf <sub>2</sub> ]	303	25±7	1	Lag-time technique	40, 60, 64
[N <sub>(1)888</sub> ][NTf <sub>2</sub> ]	303	12.8±0.6	1	Lag-time technique	40, 60, 64

In summary, we observed the same tendencies for ethene and propene solubility in ionic liquids than for ethane and propane. Ionic liquids containing larger non polar domains such as phosphonium and ammonium-based ionic liquids present higher ethene and propene solubility. The solubility of both gases is much less affected by the change of anion type.

### 1.3 Solubility of ethyne and propyne

In figures 1.9 and 1.10 and tables 1.7 and 1.8, the Henry's constants for ethyne and propyne in several ionic liquids is reported. Henry's law constants for ethyne range from  $23.6 \times 10^5$  Pa for  $[\text{C}_1\text{C}_2\text{Im}][\text{NTf}_2]$  to at  $4.9 \times 10^5$  Pa for  $[\text{C}_1\text{C}_4\text{Im}][(\text{C}_1)_2\text{PO}_4]$  and  $[\text{C}_1\text{C}_4\text{Pyrr}][\text{C}_4\text{HPO}_3]$ . For propyne it ranges from  $11 \times 10^5$  Pa for  $[\text{C}_1\text{C}_1\text{Im}][\text{C}_1\text{HPO}_3]$  to  $5.7 \times 10^5$  Pa for  $[\text{C}_2\text{C}_4\text{Im}][\text{C}_2\text{HPO}_3]$ , at 313 K.

The solubility range for ethyne and propyne in ionic liquids is much larger than for ethane, ethene, propane and propene.

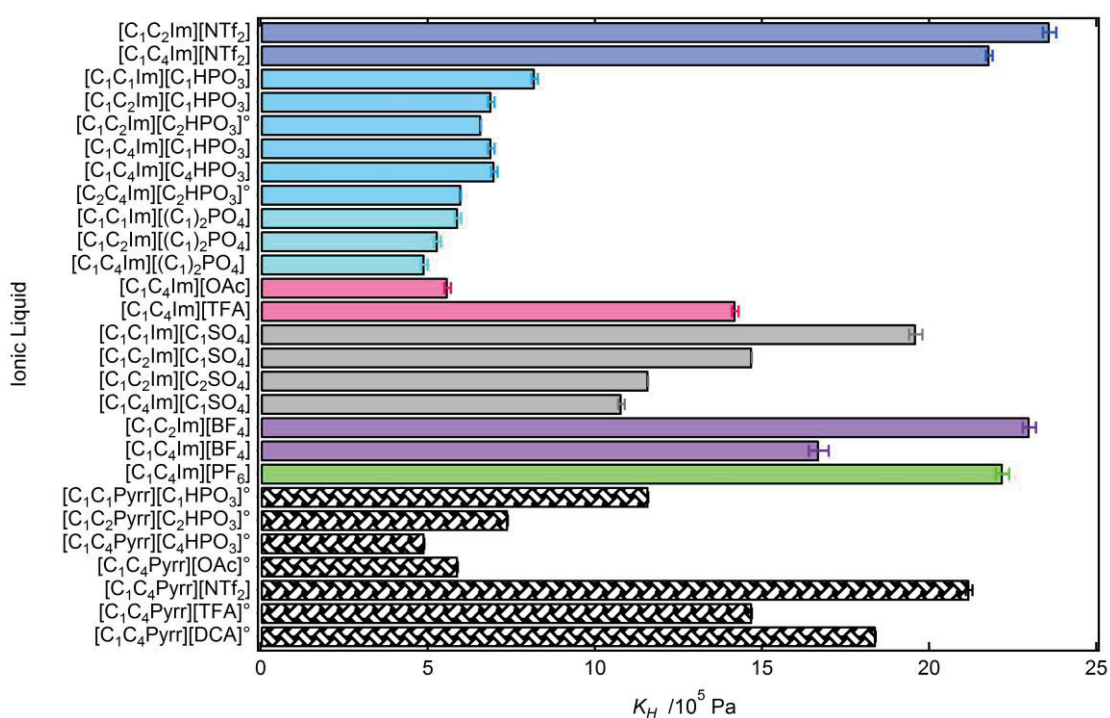


Figure 1.9 - Henry's law constant,  $K_H$ , for ethyne in several ionic liquids at 313 K. ° - Uncertainty not indicated by the authors.  $[\text{C}_1\text{C}_2\text{Im}][\text{NTf}_2]^{66}$ ;  $[\text{C}_1\text{C}_4\text{Im}][\text{NTf}_2]^{66}$ ;  $[\text{C}_1\text{C}_1\text{Im}][\text{C}_1\text{HPO}_3]^{66}$ ;  $[\text{C}_1\text{C}_2\text{Im}][\text{C}_1\text{HPO}_3]^{66}$ ;  $[\text{C}_1\text{C}_2\text{Im}][\text{C}_2\text{HPO}_3]^{62}$ ;  $[\text{C}_1\text{C}_4\text{Im}][\text{C}_1\text{HPO}_3]^{66}$ ;  $[\text{C}_1\text{C}_4\text{Im}][\text{C}_4\text{HPO}_3]^7$ ;  $[\text{C}_2\text{C}_4\text{Im}][\text{C}_2\text{HPO}_3]^{62}$ ;  $[\text{C}_1\text{C}_1\text{Im}][(\text{C}_1)_2\text{PO}_4]^{66}$ ;  $[\text{C}_1\text{C}_2\text{Im}][(\text{C}_1)_2\text{PO}_4]^{66}$ ;  $[\text{C}_1\text{C}_4\text{Im}][(\text{C}_1)_2\text{PO}_4]^{66}$ ;  $[\text{C}_1\text{C}_4\text{Im}][\text{OAc}]^{66}$ ;  $[\text{C}_1\text{C}_4\text{Im}][\text{TFA}]^{66}$ ;  $[\text{C}_1\text{C}_1\text{Im}][\text{C}_1\text{SO}_4]^{66}$ ;  $[\text{C}_1\text{C}_1\text{Im}][\text{C}_1\text{SO}_4]^{66}$ ;  $[\text{C}_1\text{C}_1\text{Im}][\text{C}_1\text{SO}_4]^{66}$ ;  $[\text{C}_1\text{C}_1\text{Im}][\text{C}_1\text{SO}_4]^{66}$ ;  $[\text{C}_1\text{C}_2\text{Im}][\text{BF}_4]^{66}$ ;  $[\text{C}_1\text{C}_4\text{Im}][\text{BF}_4]^{66}$ ;  $[\text{C}_1\text{C}_4\text{Im}][\text{PF}_6]^{66}$ ;  $[\text{C}_1\text{C}_1\text{Pyrr}][\text{C}_1\text{HPO}_3]^{65}$ ;  $[\text{C}_1\text{C}_2\text{Pyrr}][\text{C}_2\text{HPO}_3]^{65}$ ;  $[\text{C}_1\text{C}_4\text{Pyrr}][\text{C}_4\text{HPO}_3]^{65}$ ;  $[\text{C}_1\text{C}_4\text{Pyrr}][\text{OAc}]^{65}$ ;  $[\text{C}_1\text{C}_4\text{Pyrr}][\text{NTf}_2]^{66}$ ;  $[\text{C}_1\text{C}_4\text{Pyrr}][\text{TFA}]^{65}$ ;  $[\text{C}_1\text{C}_4\text{Pyrr}][\text{DCA}]^{65}$ .

The solubility of ethyne was only measured in imidazolium and pyrrolidinium-based ionic liquids. They present similar ethyne solubilities. For propyne, only imidazolium-based ionic liquids were studied.

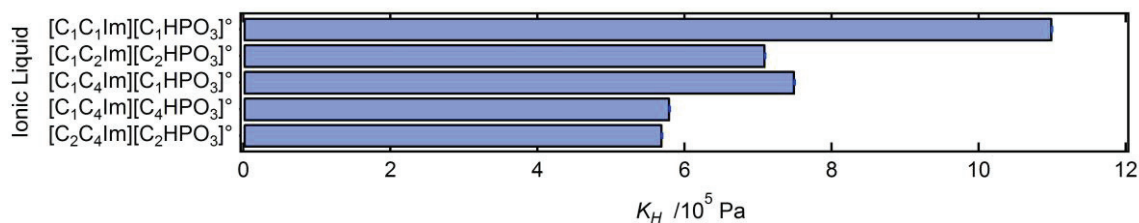


Figure 1.10 - Henry's law constant,  $K_H$ , for propyne in several ionic liquids at 313K.  $^\circ$  - Uncertainty not indicated by the authors.  $[\text{C}_1\text{C}_1\text{Im}][\text{C}_1\text{HPO}_3]^{62}$ ;  $[\text{C}_1\text{C}_2\text{Im}][\text{C}_2\text{HPO}_3]^{62}$ ;  $[\text{C}_1\text{C}_4\text{Im}][\text{C}_1\text{HPO}_3]^{62}$ ;  $[\text{C}_1\text{C}_4\text{Im}][\text{C}_4\text{HPO}_3]^{62}$ ;  $[\text{C}_2\text{C}_4\text{Im}][\text{C}_2\text{HPO}_3]^{62}$ .

Changing the cation from  $\text{C}_1\text{C}_4\text{Im}^+$  to  $\text{C}_1\text{C}_4\text{Pyr}^+$  in ionic liquids based in the  $\text{NTf}_2^-$ ,  $\text{TFA}^-$  and  $\text{OAc}^-$  anions leads to changes in ethyne solubility of less than 3%.

Changing the imidazolium cation for a pyrrolidinium in ionic liquids containing the phosphite anion causes a decrease in ethyne solubility between 10% and 30%.

Contrary to what was found for ethane, ethylene, propane and propylene, the solubility of acetylene does not always increase when the side alkyl chain of the cation or of the anion increases. There is almost no change in solubility of ethyne between, for example  $[\text{C}_1\text{C}_2\text{Im}][\text{NTf}_2]$  and  $[\text{C}_1\text{C}_4\text{Im}][\text{NTf}_2]$  or  $[\text{C}_1\text{C}_4\text{Im}][\text{C}_1\text{HPO}_3]$  and  $[\text{C}_1\text{C}_4\text{Im}][\text{C}_4\text{HPO}_3]$ . Other examples present a 15%-25% increase in ethyne solubility, such as from  $[\text{C}_1\text{C}_2\text{Im}][\text{C}_1\text{SO}_4]$  to  $[\text{C}_1\text{C}_4\text{Im}][\text{C}_1\text{SO}_4]$  or  $[\text{C}_1\text{C}_2\text{Im}][\text{BF}_4]$  and  $[\text{C}_1\text{C}_4\text{Im}][\text{BF}_4]$ . There is a 35% increase in ethyne solubility for pyrrolidinium-based ionic liquids: from  $[\text{C}_1\text{C}_1\text{Pyr}][\text{C}_1\text{HPO}_3]$  to  $[\text{C}_1\text{C}_2\text{Pyr}][\text{C}_2\text{HPO}_3]$  or from  $[\text{C}_1\text{C}_2\text{Pyr}][\text{C}_2\text{HPO}_3]$  to  $[\text{C}_1\text{C}_4\text{Pyr}][\text{C}_4\text{HPO}_3]$ . Propyne seems to follow the general tendency found for ethane, propane, ethene and propene and its solubility increased when the total amount of carbons in the alkyl side chain of the anion or cation is increased, at least for phosphite based ionic liquids.

The order of solubility of ethyne for  $\text{C}_1\text{C}_2\text{Im}^+$ ,  $\text{C}_1\text{C}_4\text{Im}^+$  or  $\text{C}_1\text{C}_4\text{Pyr}^+$  is phosphate >  $\text{OAc}^-$  > phosphite > sulphate >  $\text{TFA}^-$  >  $\text{BF}_4^- \approx \text{PF}_6^- \approx \text{NTf}_2^-$ , for the anions in common.

Table 1.7 - Henry's law constant,  $K_H$ , or Henry's law constant range for ethyne in several ionic liquids. Uncertainty included when possible for single measurements.

Ionic liquid	Temperature /K	$K_H$ /10 <sup>5</sup> Pa	Data points	Measuring method	Reference
[C <sub>1</sub> C <sub>2</sub> Im][NTf <sub>2</sub> ]	303-333	22.2-33.1	7	$pVT$ - isochoric	66
[C <sub>1</sub> C <sub>4</sub> Im][NTf <sub>2</sub> ]	313	21.8±0.1	1	$pVT$ - isochoric	66
[C <sub>1</sub> C <sub>4</sub> Im][NTf <sub>2</sub> ]	313	22.1±0.1	1	$pVT$ - isochoric	7
[C <sub>1</sub> C <sub>1</sub> Im][C <sub>1</sub> HPO <sub>3</sub> ]	303-333	6.1-13.9	7	$pVT$ - isochoric	66
[C <sub>1</sub> C <sub>1</sub> Im][C <sub>1</sub> HPO <sub>3</sub> ]	313	8.7±0.1	1	$pVT$ - isochoric	7
[C <sub>1</sub> C <sub>1</sub> Im][C <sub>1</sub> HPO <sub>3</sub> ]	313	8.5	1	$pVT$ - isochoric	62
[C <sub>1</sub> C <sub>2</sub> Im][C <sub>1</sub> HPO <sub>3</sub> ]	303-333	5.2-11.8	7	$pVT$ - isochoric	66
[C <sub>1</sub> C <sub>2</sub> Im][C <sub>2</sub> HPO <sub>3</sub> ]	313	6.6	1	$pVT$ - isochoric	62
[C <sub>1</sub> C <sub>4</sub> Im][C <sub>1</sub> HPO <sub>3</sub> ]	303-333	5.3±11.8	7	$pVT$ - isochoric	66
[C <sub>1</sub> C <sub>4</sub> Im][C <sub>1</sub> HPO <sub>3</sub> ]	313	7.1	1	$pVT$ - isochoric	62
[C <sub>1</sub> C <sub>4</sub> Im][C <sub>1</sub> HPO <sub>3</sub> ]	313	7.2±0.1	1	$pVT$ - isochoric	7
[C <sub>1</sub> C <sub>4</sub> Im][C <sub>4</sub> HPO <sub>3</sub> ]	313	7.0±0.1	1	$pVT$ - isochoric	7
[C <sub>1</sub> C <sub>4</sub> Im][C <sub>4</sub> HPO <sub>3</sub> ]	313	6.9	1	$pVT$ - isochoric	62
[C <sub>2</sub> C <sub>4</sub> Im][C <sub>2</sub> HPO <sub>3</sub> ]	313	6.0	1	$pVT$ - isochoric	62
[C <sub>1</sub> C <sub>1</sub> Im][(C <sub>1</sub> ) <sub>2</sub> PO <sub>4</sub> ]	313	6.5±0.2	1	$pVT$ - isochoric	7
[C <sub>1</sub> C <sub>1</sub> Im][(C <sub>1</sub> ) <sub>2</sub> PO <sub>4</sub> ]	313	5.9±0.1	1	$pVT$ - isochoric	66
[C <sub>1</sub> C <sub>2</sub> Im][(C <sub>1</sub> ) <sub>2</sub> PO <sub>4</sub> ]	308-333	4.6-9.3	6	$pVT$ - isochoric	66
[C <sub>1</sub> C <sub>4</sub> Im][(C <sub>1</sub> ) <sub>2</sub> PO <sub>4</sub> ]	313	5.0±0.1	1	$pVT$ - isochoric	7
[C <sub>1</sub> C <sub>4</sub> Im][(C <sub>1</sub> ) <sub>2</sub> PO <sub>4</sub> ]	313	4.9±0.1	1	$pVT$ - isochoric	66
[C <sub>1</sub> C <sub>4</sub> Im][OAc]	313	6.5±0.1	1	$pVT$ - isochoric	7
[C <sub>1</sub> C <sub>4</sub> Im][OAc]	313	5.6±0.1	1	$pVT$ - isochoric	66
[C <sub>1</sub> C <sub>4</sub> Im][TFA]	313	14.4±0.1	1	$pVT$ - isochoric	7
[C <sub>1</sub> C <sub>4</sub> Im][TFA]	313	14.2±0.1	1	$pVT$ - isochoric	66
[C <sub>1</sub> C <sub>1</sub> Im][C <sub>1</sub> SO <sub>4</sub> ]	313	19.6±0.2	1	$pVT$ - isochoric	66
[C <sub>1</sub> C <sub>2</sub> Im][C <sub>1</sub> SO <sub>4</sub> ]	303-333	11.4-23.7	7	$pVT$ - isochoric	66
[C <sub>1</sub> C <sub>2</sub> Im][C <sub>2</sub> SO <sub>4</sub> ]	303-333	8.9-18.6	7	$pVT$ - isochoric	66
[C <sub>1</sub> C <sub>4</sub> Im][C <sub>1</sub> SO <sub>4</sub> ]	313	11.0±0.1	1	$pVT$ - isochoric	7
[C <sub>1</sub> C <sub>4</sub> Im][C <sub>1</sub> SO <sub>4</sub> ]	313	10.8±0.1	1	$pVT$ - isochoric	66
[C <sub>1</sub> C <sub>2</sub> Im][BF <sub>4</sub> ]	303-333	20.9-35.1	7	$pVT$ - isochoric	66
[C <sub>1</sub> C <sub>4</sub> Im][BF <sub>4</sub> ]	313	17.7±0.1	1	$pVT$ - isochoric	7
[C <sub>1</sub> C <sub>4</sub> Im][BF <sub>4</sub> ]	303-333	13.2-25.5	7	$pVT$ - isochoric	66
[C <sub>1</sub> C <sub>4</sub> Im][PF <sub>6</sub> ]	303-333	18.8-32.5	7	$pVT$ - isochoric	66

Ionic liquid	Temperature /K	$K_H$ /10 <sup>5</sup> Pa	Data points	Measuring method	Reference
[C <sub>1</sub> C <sub>1</sub> Pyrr][C <sub>1</sub> HPO <sub>3</sub> ]	313	11.6	1	<i>pVT</i> - isochoric	65
[C <sub>1</sub> C <sub>2</sub> Pyrr][C <sub>2</sub> HPO <sub>3</sub> ]	313	7.4	1	<i>pVT</i> - isochoric	65
[C <sub>1</sub> C <sub>4</sub> Pyrr][C <sub>4</sub> HPO <sub>3</sub> ]	313	5.0±0.1	1	<i>pVT</i> - isochoric	7
[C <sub>1</sub> C <sub>4</sub> Pyrr][OAc]	313	6.0±0.2	1	<i>pVT</i> - isochoric	7
[C <sub>1</sub> C <sub>4</sub> Pyrr][NTf <sub>2</sub> ]	313	21.6±0.1	1	<i>pVT</i> - isochoric	7
[C <sub>1</sub> C <sub>4</sub> Pyrr][NTf <sub>2</sub> ]	313	21.2±0.1	1	<i>pVT</i> - isochoric	66
[C <sub>1</sub> C <sub>4</sub> Pyrr][TFA]	313	14.7	1	<i>pVT</i> - isochoric	65
[C <sub>1</sub> C <sub>4</sub> Pyrr][DCA]	313	18.4	1	<i>pVT</i> - isochoric	65
[C <sub>1</sub> C <sub>4</sub> Pyrr][OAc]	313	5.9	1	<i>pVT</i> - isochoric	65
[C <sub>1</sub> C <sub>4</sub> Pyrr][C <sub>4</sub> HPO <sub>3</sub> ]	313	4.9	1	<i>pVT</i> - isochoric	65

Table 1.8 - Henry's law constant,  $K_H$ , or Henry's law constant range for propyne in several ionic liquids. Uncertainty included when possible for single measurements.

Ionic liquid	Temperature /K	$K_H$ /10 <sup>5</sup> Pa	Data points	Measuring method	Reference
[C <sub>1</sub> C <sub>1</sub> Im][C <sub>1</sub> HPO <sub>3</sub> ]	313	11	1	<i>pVT</i> - isochoric	62
[C <sub>1</sub> C <sub>2</sub> Im][C <sub>2</sub> HPO <sub>3</sub> ]	313	7.1	1	<i>pVT</i> - isochoric	62
[C <sub>1</sub> C <sub>4</sub> Im][C <sub>1</sub> HPO <sub>3</sub> ]	313	7.5	1	<i>pVT</i> - isochoric	62
[C <sub>1</sub> C <sub>4</sub> Im][C <sub>4</sub> HPO <sub>3</sub> ]	313	5.8	1	<i>pVT</i> - isochoric	62
[C <sub>2</sub> C <sub>4</sub> Im][C <sub>2</sub> HPO <sub>3</sub> ]	313	5.7	1	<i>pVT</i> - isochoric	62

Contrary to what was observed for ethane, ethene, propane and propene, the change of anion type has a large influence on the solubility of ethyne and propyne. The highest solubilities are found in ionic liquids containing anions with a Lewis base character, such as alkylphosphates, alkylphosphites and alkylsulphates.

## 1.4 Selectivity

The ideal selectivity,  $\alpha$ , can be defined as the ratio of Henry's law constant for two gases in a certain ionic liquid:

$$\alpha = \frac{K_H^1}{K_H^2} \quad (1.9)$$

where,  $K_H^1$  and  $K_H^2$  represent Henry's law constant of the two gases. The ideal selectivity was used to evaluate the potential of the absorbent to act as a gas separating agent. The calculated ideal selectivities were plotted against Henry's law constant for the more unsaturated gas for the separations of ethane/ethene, ethene/ethyne, propane/propene and propene/propyne, in figures 1.11 and 1.12.

In general, the highest ideal selectivities are found for the separation of unsaturated gases and the increase of the ionic liquid unsaturated gas absorption corresponds to a lower selectivity for this gas.

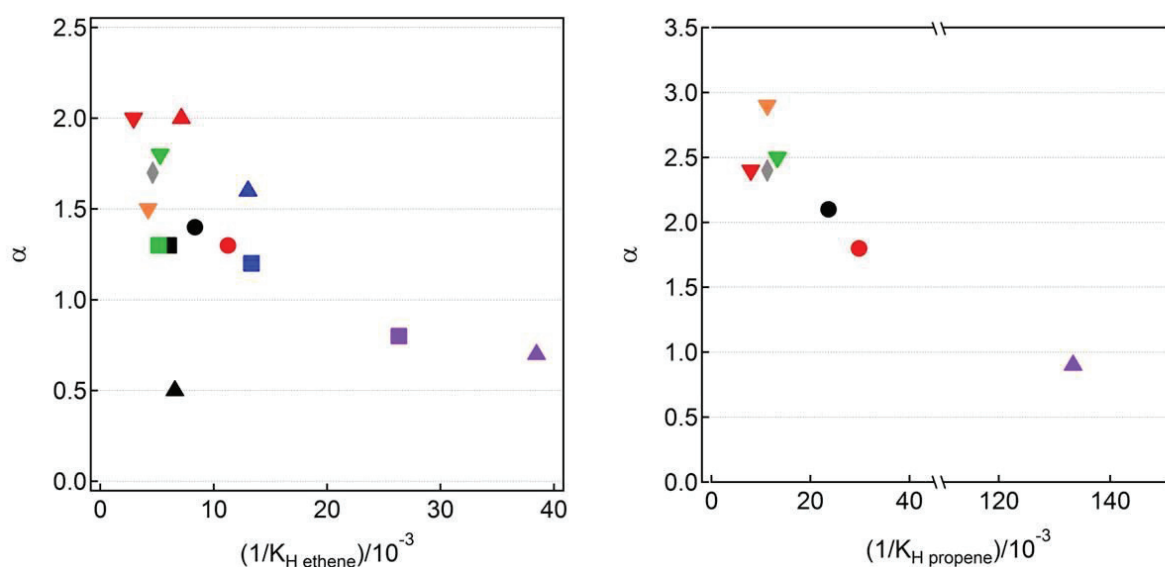


Figure 1.11 - Ethane/ethene and propane/propene ideal selectivity versus Henry's law constant,  $K_H$ , of ethene or propene in the ionic liquids ●,  $[\text{C}_1\text{C}_2\text{Im}][\text{NTf}_2]$ ; ●,  $[\text{C}_1\text{C}_4\text{Im}][\text{NTf}_2]$  (at 320 K for the propane/propene separation); ▲,  $[\text{C}_1\text{C}_6\text{Im}][\text{NTf}_2]^*$ ; ■,  $[\text{C}_1\text{C}_3\text{CNIm}][\text{NTf}_2]^*$ ; ▲,  $[(\text{C}_3\text{CN})_2\text{Im}][\text{NTf}_2]^*$ ; ▼,  $[\text{C}_1\text{C}_2\text{Im}][\text{PF}_6]$ ; ■,  $[\text{C}_1\text{C}_4\text{Im}][\text{PF}_6]^*$ ; ▼,  $[\text{C}_1\text{C}_2\text{Im}][\text{DCA}]$ ; ▼,  $[\text{C}_1\text{C}_4\text{Im}][\text{BF}_4]$ ; ◆,  $[\text{C}_1\text{C}_2\text{Im}][\text{CF}_3\text{SO}_3]$ ; ■,  $[\text{P}_{4444}][\text{TMPP}]$ ; ▲,  $[\text{P}_{(14)666}][\text{TMPP}]$ ; ▲,  $[\text{C}_1\text{C}_4\text{Pyrri}][\text{NTf}_2]$  and ■,  $[\text{C}_1\text{C}_6\text{Pyr}][\text{NTf}_2]$  at 313 K. \* at 303 K for the ethane/ethene separation

The highest ideal selectivities are found for the separation of the two unsaturated gases, ethene and ethyne and propene and propyne.  $[C_1C_1Im][C_1HPO_3]$  and  $[C_1C_1Pyrr][C_1HPO_3]$  present the highest ethene/ethyne ideal selectivities, 43 and 40, respectively. Ionic liquids containing the  $NTf_2^-$ ,  $DCA^-$ ,  $TFA^-$ ,  $BF_4^-$  or  $PF_6^-$  anions present both low ethyne absorption capacities and low ideal selectivity for the ethene and ethyne separation.

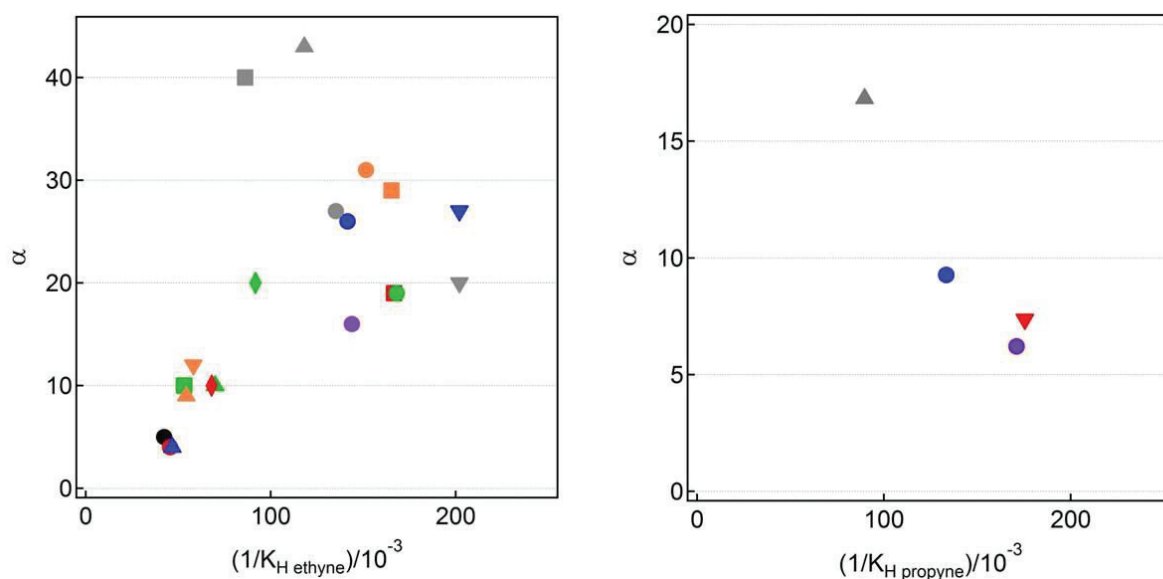


Figure 1.12 - Ethene/ethyne and propene/propyne ideal selectivity versus Henry's law constant,  $K_H$ , of ethyne or propyne in the ionic liquids ●,  $[C_1C_2Im][NTf_2]$ ; ●,  $[C_1C_4Im][NTf_2]$ ; ■,  $[C_1C_4Im][PF_6]^*$ ; ▼,  $[C_1C_4Im][BF_4]$ ; ▲,  $[C_1C_4Im][TFA]$ ; ■,  $[C_1C_4Im][OAc]$ ; ▲,  $[C_1C_1Im][C_1HPO_3]$ ; ●,  $[C_1C_2Im][C_2HPO_3]$ ; ●,  $[C_1C_4Im][C_1HPO_3]$ ; ●,  $[C_1C_4Im][C_4HPO_3]$ ; ▼,  $[C_2C_4Im][C_2HPO_3]$ ; ▼,  $[C_1C_4Im][(C_1)_2PO_4]$ ; ◆,  $[C_1C_4Im][C_1SO_4]$ ; ■,  $[C_1C_1Pyrr][C_1HPO_3]$ ; ●,  $[C_1C_2Pyrr][C_2HPO_3]$ ; ▼,  $[C_1C_4Pyrr][C_4HPO_3]$ ; ●,  $[C_1C_4Pyrr][OAc]$ ; ▲,  $[C_1C_4Pyrr][NTf_2]$ ; ◆,  $[C_1C_4Pyrr][TFA]$  and ▲,  $[C_1C_4Pyrr][DCA]$  at 313 K. \* at 303 K for the ethene/ethyne separation

The maximum ideal selectivities for propene/propyne separation are half of those found for ethene/ethyne separation. As for ethene/ethyne separation, they are obtained for ionic liquids with imidazolium cations containing short alkyl chains associated to a phosphorous anion, like  $[C_1C_1Im][C_1HPO_3]$  that presents a selectivity of 17.

With the lowest values for the ideal selectivity and absorption capacity, the ethane/ethylene separation seems to be the most difficult to perform with ionic liquids as far as these criteria are concerned. The  $[C_1C_2Im][DCA]$  and  $[(C_3CN)_2Im][NTf_2]$  presents the highest ethane/ethene ideal separation selectivity, 2.  $[C_1C_2Im][PF_6]$

presents the second highest 1.8. The presence of a CN group seems to increase the ideal selectivity of ethane and ethene, however leading to lower absorption capacities. The increase of the separation selectivity due to the presence of CN group(s) was also observed by Mokrushin *et al.*<sup>49</sup> for the separation of propane and propene.

[C<sub>1</sub>C<sub>4</sub>Im][BF<sub>4</sub>], [C<sub>1</sub>C<sub>2</sub>Im][DCA] and [C<sub>1</sub>C<sub>2</sub>Im][PF<sub>6</sub>] present the highest ideal selectivities for the propane/propene separation, 2.9, 2.4 and 2.5, respectively.

For all separations, the increase of the alkyl chain in the cation or in the anion, leads to a decrease in the ideal selectivity, and to an increase in the absorption capacity of the ionic liquid. This increase seems to be less important for the ethane/ethene separation.

## 1.5 Ionic liquids containing metal salts

Certain metal transition cations, such as Cu(I) or Ag(I) are able to form  $\pi$ -complexes with unsaturated hydrocarbons. The metal and alkene act as an electron donor and acceptor, forming a double bond if the orbitals involved present the correct symmetry and if the metal possesses high electron affinity for good  $\sigma$ -bond accepting properties and low promotion energy for good  $\pi$ -backbonding.<sup>5</sup> This complexation reaction is used to increase the absorption capacity of the ionic liquid for unsaturated light hydrocarbons.

Ortiz *et al.*<sup>52</sup> studied the selective absorption of propene from propane/propene mixtures in  $[\text{C}_1\text{C}_4\text{Im}][\text{BF}_4]$  with, and without, silver ions, at several temperatures and pressures. They demonstrated that the propene selectivity is less than 3 in absence of the silver salt in the ionic liquid and 8 to 16 upon addition of 0.25 M silver salt in the ionic liquid at 298 K and between 1 and 3 bar. Higher pressures proved to lower the selectivity for the silver salt containing ionic liquid, probably due to the saturation of the silver ions. The propene absorption capacity for the ionic liquids-silver salt solution was compared to aqueous solutions with the same silver salt concentration and it was found that the aqueous solutions presented lower propene capacities. The authors studied the system in further detail obtaining data for the absorption kinetics of propene, the influence of the concentration of the silver salt and the performances of a membrane contractor and of a semi-batch stirred tank reactor.<sup>67,68,69</sup>

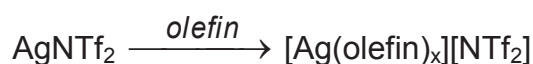
Sánchez *et al.*<sup>70</sup> studied the absorption of ethane and ethene in silver salt solutions with the ionic liquids  $[\text{C}_1\text{C}_2\text{Im}][\text{NTf}_2]$ ,  $[\text{C}_1\text{C}_2\text{Im}][\text{CF}_3\text{SO}_3^-]$ ,  $[\text{C}_1\text{C}_4\text{Im}][\text{NO}_3^-]$ ,  $[\text{C}_0\text{C}_2\text{Im}][\text{NO}_3^-]$ ,  $[\text{C}_1\text{C}_2\text{-OHIm}][\text{NO}_3^-]$ ,  $[\text{4-butyl-C}_4\text{Pyr}][\text{NO}_3^-]$  and  $[\text{N}_{1112\text{-OH}}][\text{NO}_3^-]$  with  $\text{Ag}^+$  concentrations ranging from 0.45 M to 4.4 M. The results were compared to the solubility of ethane and ethene in  $[\text{C}_1\text{C}_2\text{Im}][\text{NTf}_2]$ . The gas absorption was studied at 303 K and 333 K and pressures up to 10 bar. The authors observed that the ionic liquid-silver salt solution selectivities were always higher than for  $[\text{C}_1\text{C}_2\text{Im}][\text{NTf}_2]$ , which presents an ethene selectivity under 2, at 303K and 1 bar. The highest selectivity was obtained for the 1.8 M silver solution in  $[\text{C}_1\text{C}_2\text{Im}][\text{CF}_3\text{SO}_3^-]$ , with a selectivity of 100 at 1 bar and 333 K. The authors defined selectivity as the proportion between mol of ethene and the mol of ethane at a certain pressure.

Mortaheb *et al.*<sup>71</sup> studied the effect of temperature and silver salt concentration on the absorption of ethane and ethene in ionic liquid [C<sub>1</sub>C<sub>4</sub>Im][NO<sub>3</sub>]. The silver salt concentration ranged from 1 to 5 M and temperatures between 283 K and 308 K. A maximum selectivity of 15 was obtained for 5 M silver salt at 278 K. The authors defined selectivity as the proportion between amount of ethene and the amount of ethane.

Kim *et al.*<sup>72</sup> used a cuprous chloride-containing [C<sub>1</sub>C<sub>1</sub>Im][C<sub>1</sub>HPO<sub>3</sub>] and [C<sub>1</sub>C<sub>4</sub>Im][CuCl<sub>2</sub>] as absorbents for propyne over propene and compared to [C<sub>1</sub>C<sub>1</sub>Im][C<sub>1</sub>HPO<sub>3</sub>]. The propyne/propene selectivity of the pure ionic liquid was of 17, 11 for [C<sub>1</sub>C<sub>4</sub>Im][CuCl<sub>2</sub>] and 243 for the cuprous chloride-containing [C<sub>1</sub>C<sub>1</sub>Im][C<sub>1</sub>HPO<sub>3</sub>], all at 313 K.

Faiz and Li<sup>16</sup> reviewed the application of ionic liquid/metal salt composite membranes for olefin/paraffin separations. They concluded that even though the concept was successfully applied for separation, the long term stability of the membranes is still a major issue.

A task specific ionic liquid complex salt, [Ag(olefin)<sub>x</sub>][NTf<sub>2</sub>], formed as described in scheme 1.1, provided a selectivity of 40, a much larger selectivity when compared to the silver salt-[C<sub>1</sub>C<sub>4</sub>Im][BF<sub>4</sub>] solution of 16, at 298 K.



Scheme 1.1 - Synthesis of ionic liquid [Ag(olefin)<sub>x</sub>][NTf<sub>2</sub>]

This salt was also successfully used to create an adaptive self-healing propane/propene separation membrane, although the details of its long term stability were not provided.<sup>73,74</sup>

Although allowing the increase of the capacity and selectivity of the selected support for the unsaturated gas, the use of metals presents drawbacks due to their cost, contamination, degradation, safety problems, limited metal salt solubility and high viscosities of the resulting liquid absorbent.<sup>4,5,6,74,75,76,77</sup>

## Conclusions

Henry's law constants of ethane, ethene, ethyne, propane, propene and propyne in pure ionic liquids were critically reviewed and the general trends were described. The potential of the use of different ionic liquids as separating agents for gaseous mixtures of saturated and unsaturated gases was analysed on the basis of their ideal selectivities and absorption capacities.

Contrary to what is suggested in the literature, the solubility of unsaturated gases, such as ethene and propene is not always higher than of their saturated counterparts, ethane and propane. In fact, their solubilities range overlap.

The highest light hydrocarbon gas solubilities are obtained for ethyne in  $[\text{C}_1\text{C}_4\text{Im}][(\text{C}_1)_2\text{PO}_4]$  and  $[\text{C}_1\text{C}_4\text{Pyr}][\text{C}_4\text{HPO}_3]$  and for propyne in  $[\text{C}_2\text{C}_4\text{Im}][\text{C}_2\text{HPO}_3]$ , with 0.20 and 0.18 mole fraction, respectively. The maximum mole fraction solubilities obtained for propane and propene were 0.15 and 0.13, respectively, in  $[\text{P}_{(14)666}][\text{TMPP}]$ . Ethane and ethene are at least one order of magnitude less soluble than ethyne, with maximum mole fraction solubilities of 0.052 and 0.038 in  $[\text{P}_{(14)666}][\text{TMPP}]$ , all at 313 K and 1 bar.

For ethane, ethene, propane and propene, the highest solubilities are found in ionic liquids containing cations or anions with large non-polar domains. The solubility order in terms of cations is  $\text{P}_{\text{nmpq}}^+ > \text{N}_{\text{nmpq}}^+ > \text{C}_n\text{Pyr}^+ > \text{C}_n\text{C}_m\text{Pyr}^+ > \text{C}_n\text{C}_m\text{Im}^+$ . The influence of the cation size is less important in the solubility of ethyne.

Imidazolium-based ionic liquids containing large anions such as long-chain carboxylates,  $\text{BETI}^-$ ,  $\text{FAP}^-$ ,  $\text{C}_8\text{SO}_4^-$ ,  $\text{NTf}_2^-$ ,  $\text{C}_n\text{C}_m\text{PO}_4^-$  and  $\text{C}_n\text{HPO}_3^-$  (with n and m bigger than 6) present higher ethane, ethene, propane and propene solubility, followed by  $\text{PF}_6^-$ ,  $\text{CF}_3\text{SO}_3^-$ ,  $\text{BF}_4^-$  and  $\text{DCA}^-$ . However, the influence of the nature of the anion is less important than the influence of the size of the cation in the solubility of these 4 gases. The order of solubility of ethyne relative to anions for imidazolium and pyrrolidinium-based cations is very different from what was found for its saturated counterparts:  $\text{C}_n\text{C}_m\text{PO}_4^- > \text{OAc}^- > \text{C}_n\text{HPO}_3^- > \text{C}_n\text{SO}_4^- > \text{TFA}^- > \text{BF}_4^- > \text{PF}_6^- \approx \text{NTf}_2^-$ . The highest ethyne solubilities are found in ionic liquids containing anions with a Lewis base character, such as alkylphosphates, alkylphosphites and alkylsulphates. This is probably due to the presence of a relatively acidic proton in ethyne.

The largest variety of ionic liquids was tested for ethene and propene solubility. The existing data can be completed by additional solubility measurements of ethane, ethyne, propane and propyne in a greater variety of imidazolium, phosphonium and ammonium ionic liquids.

Ionic liquids present great potential for light hydrocarbon separation, especially in the case of ethene/ethyne and propene/propyne separations, with ideal selectivities of over 40 in the first case and over 15 in the second and mole fraction solubilities between 0.1 and 0.2, respectively.

## References

---

- <sup>1</sup> Henley, E. J.; Seader, J. D. and Roper, D. K. Separation Process Principles: Third Edition, John Wiley & Sons, **2011**
- <sup>2</sup> Baker, R. W. Future Directions of Membrane Gas Separation Technology. *Ind. Eng. Chem. Res.* **2002**, 41, 1393-1411
- <sup>3</sup> Keyvanloo, K.; Towfighi, J.; Sadrameli, S. M.; Mohamadalizadeh, A. Investigating the Effect of Key Factors, Their Interactions and Optimization of Naphtha Steam Cracking by Statistical Design of Experiments. *J. Anal. Appl. Pyrol.* **2010**, 87, 224-230
- <sup>4</sup> Eldridge, R. B. Olefin/Paraffin Separation Technology: A Review. *Ind. Eng. Chem. Res.* **1993**, 32, 2208-2212
- <sup>5</sup> Safarik, D. J.; Eldridge, R. B. Olefin/Paraffin Separations by Reactive Absorption: A Review. *Ind. Eng. Chem. Res.* **1998**, 37, 2571-2581
- <sup>6</sup> Asaro, M. F. Sorbents and Processes for Separation of Olefins from Paraffins. US20090143632A1, **2009**
- <sup>7</sup> Palgunadi, J.; Kim, H. S.; Lee, J. M. and Jung, S. Ionic Liquids for Ethyne and Ethene Separation: Material Selection and Solubility Investigation. *Chem. Eng. Process.* **2010**, 49, 192-198
- <sup>8</sup> Hu, Y.; Liu, Z.; Xu, C. and Zhang, X. The Molecular Characteristics Dominating the Solubility of Gases in Ionic Liquids. *Chem. Soc. Rev.* **2011**, 40, 3802-3823
- <sup>9</sup> Jin, M.; Hou, Y.; Wu, W.; Ren, S.; Tian, S.; Xiao, L. and Lei, Z. Solubilities and Thermodynamic Properties of SO<sub>2</sub> in Ionic Liquids, *J. Phys. Chem. B* **2011**, 115, 6585-6591
- <sup>10</sup> Shiflett, M. B.; Niehaus, A. M. S. and Yokozeki, A. Separation of N<sub>2</sub>O and CO<sub>2</sub> Using Room-Temperature Ionic Liquid [bmim][BF<sub>4</sub>], *J. Phys. Chem. B* **2011**, 115, 3478-3487
- <sup>11</sup> Camper, D.; Becker, C.; Koval, C. and Noble, R. Low Pressure Hydrocarbon Solubility in Room Temperature Ionic Liquids Containing Imidazolium Rings Interpreted Using Regular Solution Theory, *Ind. Eng. Chem. Res.* **2005**, 44, 1928-1933
- <sup>12</sup> Jacquemin, J.; Costa Gomes, M. F.; Husson, P. and Majer, V. Solubility of Carbon Dioxide, Ethane, Methane, Oxygen, Nitrogen, Hydrogen, Argon, and Carbon Monoxide in 1-Butyl-3-methylimidazolium Tetrafluoroborate Between Temperatures

---

283 K and 343 K and at Pressures Close to Atmospheric, *J. Chem. Thermodyn.* **2006**, 38, 490-502

<sup>13</sup> Stricker, M.; Oelkers, B.; Rosenau, C. P. and Sundermeyer, J. Copper(I) and Silver(I) Bis(trifluoromethanesulfonyl)imide and Their Interaction with an Arene, Diverse Olefins, and an NTf<sub>2</sub>-Based Ionic Liquid, *Chem. Eur. J.* **2013**, 19, 1042-1057

<sup>14</sup> Premkumar, J. R.; Vijay, D. and Sastry, G. N. The Significance of the Alkene Size and the Nature of the Metal Ion in Metal-Alkene Complexes: a Theoretical Study. *Dalton Trans.* **2012**, 41, 4965-4975

<sup>15</sup> Azhin, M.; Kaghazchi, T.; Rahmani, M. A Review on Olefin/Paraffin Separation Using Reversible Chemical Complexation Technology. *J. Ind. Eng. Chem.* **2008**, 14, 622-638

<sup>16</sup> Faiz, R.; Li, K. Olefin/Paraffin Separation Using Membrane Based Facilitated Transport/Chemical Absorption Techniques. *Chem. Eng. Sci.* **2012**, 73, 261-284

<sup>17</sup> Brown, R. E.; Hair, R. L. and Phillips Petroleum Company. Monoolefin/Paraffin Separation by Selective Absorption. Patent US5202521A, US, **1993**

<sup>18</sup> Andison; D. D. and EXXON Chemical Patents Inc. Transition Metal Exchanged Ionomer Membrane for Hydrocarbon Separation, Patent EP0404416A1, **1990**, Europe

<sup>19</sup> Munson, C. L.; Boudreau, L. C. ; Driver, M. S. ; Schinski, W. L. and Chevron USA Inc. Separation of Olefins from Paraffins Using ionic Liquid Solutions, Patent US6623659B2, **2003**, US

<sup>20</sup> Boudreau, L. C. ; Driver, M. S. ; Munson, C. L.; Schinski, W. L. and Chevron USA Inc. Separation of dienes from Olefins Using Ionic Liquids, Patent US6849774B2, **2005**, US

<sup>21</sup> Gorke, J. T.; Feist, S. D.; Matteucci, S. T.; Nickias, P. N. Olefin Selective Membrane Comprising one ionic Liquid and a Complexing Agent, Patent WO2011/037820A1, **2011**

<sup>22</sup> Munson, C. L.; Boudreau, L. C. ; Driver, M. S. ; Schinski, W. L. Process for the Purification of Olefins, Patent WO0198239A1, **2001**

<sup>23</sup> Atkins, P. and Paula, J. Physical Chemistry: Ninth edition, Oxford University Press, Oxford, **2010**

<sup>24</sup> Costa Gomes, M. F.; Pádua, A. A. H. Developments and Applications in Solubility, Chapter 10: Solubility and Molecular Modelling **2007**, 153-170

- 
- <sup>25</sup> Denbigh, K. *The Principles of Chemical Equilibrium*, 4th edition, CUP, Cambridge, 1981
- <sup>26</sup> Prausnitz, J. M.; Lichtenthaler, R. N.; Gomes de Azevedo, E., *Molecular Thermodynamics of Fluid-Phase Equilibria*, 3rd edition, Prentice Hall, NJ, **1999**
- <sup>27</sup> Anderson, J. L.; Dixon, J. K. and Brennecke, J. F. Solubility of CO<sub>2</sub>, CH<sub>4</sub>, C<sub>2</sub>H<sub>6</sub>, C<sub>2</sub>H<sub>4</sub>, O<sub>2</sub>, and N<sub>2</sub> in 1-Hexyl-3-methylpyridinium Bis(trifluoromethylsulfonyl)imide: Comparison to Other Ionic Liquids, *Acc. Chem. Res.* **2007**, 40, 1208-1216
- <sup>28</sup> Wasserscheid, P. and Welton, T. *Ionic Liquid in Synthesis*, Wiley-VCH, Weinheim, **2002**
- <sup>29</sup> Maurer, M. and Tuma, D. *Ionic Liquids: From Knowledge to Application*, ACS Symposium Series, American Chemical Society, Washington, DC, **2010**
- <sup>30</sup> Koel, M. *Ionic Liquids in Chemical Analysis*, CRC Press, Boca Raton, **2009**
- <sup>31</sup> Camper, D.; Becker, C.; Koval, C. and Noble, R. Diffusion and Solubility Measurements in Room Temperature Ionic Liquids, *Ind. Eng. Chem. Res.* **2006**, 445-450
- <sup>32</sup> Liu, X.; Afzal, W. and Prausnitz, J. M. Solubilities of Small Hydrocarbons in Tetrabutylphosphonium Bis(2,4,4-trimethylpentyl) Phosphinate and in 1-Ethyl-3-methylimidazolium Bis(trifluoromethylsulfonyl)imide, *Ind. Eng. Chem. Res.* **2013**, 52, 14975-14978
- <sup>33</sup> Xing, H.; Zhao, X.; Li, R.; Yang, Y.; Su, B.; Bao, Z.; Yang, Y. and Ren, Q. Improved Efficiency of Ethylene/Ethane Separation Using a Symmetrical Dual Nitrile-Functionalized Ionic Liquid, *ACS Sustainable Chem. Eng.* **2013**, 1, 1357-1363
- <sup>34</sup> Costa Gomes, M. F.; Pison, L.; Pensado, A. S. and Padua, A. A. H. Using Ethane and Butane as Probes to the Molecular Structure of 1-Alkyl-3-methylimidazolium Bis[(trifluoromethyl)sulfonyl]imide Ionic Liquids, *Faraday Discuss.* **2012**, 154, 41-52
- <sup>35</sup> Florusse, L. J.; Raelssi, S. and Peters, C. J. High-Pressure Phase Behavior of Ethane with 1-Hexyl-3-methylimidazolium Bis(trifluoromethylsulfonyl)imide, *J. Chem. Eng. Data* **2008**, 53, 1283-1285
- <sup>36</sup> Battino, R., Clever, H. L. The Solubility of Gases in Liquids *Chem. Rev.* **1966**, 66, 395-463
- <sup>37</sup> Zhang, J.; Zhang, Q.; Qiao, B. and Deng, Y. Solubilities of the Gaseous and Liquid Solutes and Their Thermodynamics of Solubilization in the Novel Room-Temperature

---

Ionic Liquids at Infinite Dilution by Gas Chromatography, *J. Chem. Eng. Data* **2007**, 52, 2277-2283

<sup>38</sup> Ignatiadis, I., Gonnord, M. F. and Vidal-Madjar, C. Measurement of Thermodynamic Equilibria by Chromatography, *Chromatographia* **1987**, 23, 215-219

<sup>39</sup> Ian D. Wilson, Cooke, M. and Poole, C. F. Encyclopedia of Separation Science, Academic, Michigan, **2000**

<sup>40</sup> Kilaru, P. K.; Scovazzo, P. Correlations of Low-Pressure Carbon Dioxide and Hydrocarbon Solubilities in Imidazolium-, Phosphonium-, and Ammonium-Based Room-Temperature Ionic Liquids. Part 2. Using Activation Energy of Viscosity, *Ind. Eng. Chem. Res.* **2008**, 47, 910-919

<sup>41</sup> Morgan, D.; Ferguson, L. and Scovazzo, P. Diffusivities of Gases in Room Temperature Ionic Liquids: Data and Correlations Obtained Using a Lag-Time Technique, *Ind. Eng. Chem. Res.* **2005**, 44, 4815-4823

<sup>42</sup> Hong, G.; Jacquemin, J.; Deetlefs, M.; Hardacre, C.; Husson, P.; Costa Gomes, M. F. Solubility of Carbon Dioxide and Ethane in Three Ionic Liquids Based on the Bis{(trifluoromethyl)sulfonyl}imide Anion, *Fluid Phase Equilibr.* **2007**, 257, 27-34

<sup>43</sup> Costa Gomes, M. F. Low-Pressure Solubility and Thermodynamics of Solvation of Carbon Dioxide, Ethane, and Hydrogen in 1-Hexyl-3-methylimidazolium Bis(trifluoromethylsulfonyl)amide between Temperatures of 283 K and 343 K, *J. Chem. Eng. Data* **2007**, 52, 472-475

<sup>44</sup> Deng, Y.; Morrissey, S.; Gathergood, N.; Delort, A.; Husson, P. and Costa Gomes, M. F. The Presence of Functional Groups Key for Biodegradation in Ionic Liquids: Effect on Gas Solubility, *ChemSusChem* **2010**, 3, 377-385

<sup>45</sup> Anthony, J. L.; Maginn, E. J. and Brennecke, J. F. Solubilities and Thermodynamic Properties of Gases in the Ionic Liquid 1-*n*-Butyl-3-methylimidazolium Hexafluorophosphate, *J. Phys. Chem. B* **2002**, 106, 7315-7320

<sup>46</sup> Almantariotis, D.; Stevanovic, S.; Fandiño, O.; Pensado, A. S.; Padua, A. A. H.; Coxam, J.-Y and Costa Gomes, M. F. Absorption of Carbon Dioxide, Nitrous Oxide, Ethane and Nitrogen by 1-Alkyl-3-methylimidazolium (C<sub>n</sub>mim, n = 2, 4, 6) Tris(pentafluoroethyl)trifluorophosphate Ionic Liquids (eFAP), *J. Phys. Chem. B* **2012**, 116, 7728-7738

<sup>47</sup> Stevanovic, S.; Costa Gomes, M. F. Solubility of Carbon Dioxide, Nitrous Oxide, Ethane, and Nitrogen in 1-Butyl-1-methylpyrrolidinium and

---

Trihexyl(tetradecyl)phosphonium Tris(pentafluoroethyl)trifluorophosphate (eFAP) Ionic Liquids, *J. Chem. Thermodyn.* **2013**, 59, 65-71

<sup>48</sup> Liu, X.; Afzal, W.; Yu, G.; He, M. and Prausnitz, J. M. High Solubilities of Small Hydrocarbons in Trihexyl Tetradecylphosphonium Bis(2,4,4-trimethylpentyl) Phosphinate, *J. Phys. Chem. B* **2013**, 117, 10534-10539

<sup>49</sup> Mokrushin, V.; Assenbaum, D.; Paape, N.; Gerhard, D.; Mokrushina, L.; Wasserscheid, P.; Arlt, W.; Kistenmacher, H.; Neuendorf, S. and Göke, V. Ionic Liquids for Propene-Propane Separation. *Chem. Eng. Technol.* **2010**, 33, 63-73

<sup>50</sup> Scovazzo, P. Determination of the Upper Limits, Benchmarks, and Critical Properties for Gas Separations Using Stabilized Room Temperature Ionic Liquid Membranes (SILMs) for the Purpose of Guiding Future Research. *J. Membrane Sci.* **2009**, 343, 199-211

<sup>51</sup> Lee, J. H.; Kang, S. W.; Song, D.; Wond, J. and Kang, Y. S. Facilitated Olefin Transport Through Room Temperature Ionic Liquids for Separation of Olefin/Paraffin Mixtures. *J. Membrane Sci.* **2012**, 423-424, 159-164

<sup>52</sup> Ortiz, A.; Ruiz, A.; Gorri, D.; Ortiz, I. Room Temperature Ionic Liquid with Silver Salt as Efficient Reaction Media for Propene/Propane Separation: Absorption Equilibrium. *Sep. Purif. Technol.* **2008**, 63, 311-318

<sup>53</sup> Petermann, M.; Weissert, T.; Kareth, S.; Lösch, H. W.; Dreisbach, F. New Instrument to Measure the Selective Sorption of Gas Mixtures Under High Pressures, *J. Supercrit. Fluid.* **2008**, 45, 156-160

<sup>54</sup> Bermejo, M. D.; Fieback, T. M. and Martín, A. Solubility of Gases in 1-Alkyl-3-methylimidazolium Alkyl Sulfate Ionic Liquids: Experimental Determination and Modeling, *J. Chem. Thermodyn.* **2013**, 58, 237-244

<sup>55</sup> Lee, B. and Outcalt, S. L. Solubilities of Gases in the Ionic Liquid 1-*n*-Butyl-3-methylimidazolium Bis(trifluoromethylsulfonyl)imide, *J. Chem. Eng. Data* **2006**, 51, 892-897

<sup>56</sup> Jacquemin, J.; Husson, P.; Majer, V.; Costa Gomes, M. F. Low-Pressure Solubilities and Thermodynamics of Solvation of Eight Gases in 1-Butyl-3-methylimidazolium Hexafluorophosphate, *Fluid Phase Equilib.* **2006**, 240, 87-95

<sup>57</sup> Anthony, J. L.; Anderson, J. L.; Maginn, E. J. and Brennecke, J. F. Anion Effects on Gas Solubility in Ionic Liquids, *J. Phys. Chem. B* **2005**, 109, 6366-6374

- 
- <sup>58</sup> Gan, Q.; Zou, Y.; Rooney, D.; Nancarrow, P.; Thompson, J.; Liang, L. and Lewis, M. Theoretical and Experimental Correlations of Gas Dissolution, Diffusion, and Thermodynamic Properties in Determination of Gas Permeability and Selectivity in Supported Ionic Liquid Membranes, *Adv. Colloid Interfac.* **2011**, 164, 45-55
- <sup>59</sup> Camper, D.; Scovazzo, P.; Koval, C. and Noble, R. Gas Solubilities in Room-Temperature Ionic Liquids, *Ind. Eng. Chem. Res.* **2004**, 43, 3049-3054
- <sup>60</sup> Kilaru, P. K.; Condemarin, R. A. and Scovazzo, P. Correlations of Low-Pressure Carbon Dioxide and Hydrocarbon Solubilities in Imidazolium-, Phosphonium-, and Ammonium-Based Room-Temperature Ionic Liquids. Part 1. Using Surface Tension, *Ind. Eng. Chem. Res.* **2008**, 47, 900-909
- <sup>61</sup> Zhang, Q.; Li, Z.; Zhang, J.; Zhang, S.; Zhu, L.; Yang, J.; Zhang, X. and Deng, Y. Physicochemical Properties of Nitrile-Functionalized Ionic Liquids, *J. Phys. Chem. B* **2007**, 111, 2864-2872
- <sup>62</sup> Lee, J. M.; Palgunadi, J.; Kim, J. H.; Jung, S.; Choi, Y.; Cheong, M. and Kim, H. S. Selective Removal of Acetylenes from Olefin Mixtures Through Specific Physicochemical Interactions of Ionic Liquids with Acetylenes, *Phys. Chem. Chem. Phys.* **2010**, 12, 1812-1816
- <sup>63</sup> Ferguson, L. and Scovazzo, P. Solubility, Diffusivity, and Permeability of Gases in Phosphonium-Based Room Temperature Ionic Liquids: Data and Correlations, *Ind. Eng. Chem. Res.* **2007**, 46, 1369-1374
- <sup>64</sup> Condemarin, R.; Scovazzo, P. Gas Permeabilities, Solubilities, Diffusivities, and Diffusivity Correlations for Ammonium-Based Room Temperature Ionic Liquids with Comparison to Imidazolium and Phosphonium RTIL Data, *Chem. Eng. J.* **2009**, 147, 51-57
- <sup>65</sup> Jung, S. ; Palgunadi, J.; Kim, J. H.; Lee, H.; Ahn, B. S.; Cheong, M. and Kim, H. S. Highly Efficient Metal-Free Membranes for the Separation of Acetylene/Olefin Mixtures: Pyrrolidinium-Based Ionic Liquids as Acetylene Transport Carriers, *J. Membrane Sci.* **2010**, 354, 63-67
- <sup>66</sup> Palgunadi, J.; Hong, S. Y.; Lee, J. K.; Lee, H.; Lee, S. D.; Cheong, M. and Kim, H. S. Correlation between Hydrogen Bond Basicity and Acetylene Solubility in Room Temperature Ionic Liquids, *J. Phys. Chem. B* **2011**, 115, 1067-1074
- <sup>67</sup> Ortiz, A.; Galán, L. M.; Gorri, D.; de Haan, A. B. and Ortiz, I. Kinetics of Reactive Absorption of Propene in RTIL-Ag<sup>+</sup> Media, *Sep. Purif. Technol.* **2010**, 73, 106-113

- 
- <sup>68</sup> Ortiz, A.; Gorri, D.; Irabien, A.; Ortiz, I. Separation of Propene/Propane mixtures Using Ag<sup>+</sup>-RTIL Solutions. Evaluation and Comparison of the Performance of Gas-Liquid Contactors. *J. Membrane Sci.* **2010**, 360, 130-141
- <sup>69</sup> Fallanza, M.; Ortiz, A.; Gorri, D. and Ortiz, I. Experimental Study of the Separation of Propane/Propene Mixtures by Supported Ionic Liquid Membranes Containing Ag<sup>+</sup>-RTILs as Sarrier, *Sep. Purif. Technol.* **2012**, 97, 83-89
- <sup>70</sup> Sánchez, L. M. G.; Meindersma, G. W. and Haan, A. B. Potential of Silver-Based Room-Temperature Ionic Liquids for Ethene/Ethane Separation, *Ind. Eng. Chem. Res.* **2009**, 48, 10650-10656
- <sup>71</sup> Mortaheb, H. R., Mafi, M.; Mokhtarani, B.; Sharifi, A.; Mirzaei, M.; Khodapanah, N. and Ghaemmaghani, F. Experimental Kinetic Analysis of Ethene Absorption in Ionic Liquid [Bmim]NO<sub>3</sub> with Dissolved AgNO<sub>3</sub> by a Semi-Continuous Process, *Chem. Eng. J.* **2010**, 158, 384-392
- <sup>72</sup> Kim, J. H.; Palgunadi, J.; Mukherjee, D. K.; Lee, H. J.; Kim, H.; Ahn, B. S.; Cheong, M. and Kim, H. S. Cu(I)-Containing Room Temperature Ionic Liquids as Selective and Reversible Absorbents for Propyne. *Phys. Chem. Chem. Phys.* **2010**, 12, 14196-14202
- <sup>73</sup> Pitsch, F.; Krull, F. F.; Agel, F.; Schulz, P.; Wasserscheid, P.; Melin, T. and Wessling, M. An Adaptive Self-Healing Ionic Liquid Nanocomposite Membrane for Olefin-Paraffin Separations, *Adv. Mater.* **2012**, 24, 4306-4310
- <sup>74</sup> Agel, F.; Pitsch, F.; Krull, F. F.; Schulz, P.; Wessling, M.; Melin, T. and Wasserscheid, P. Ionic Liquid Silver Salt Complexes for Propene/Propane Separation. *Phys. Chem. Chem. Phys.* **2011**, 13, 725-731
- <sup>75</sup> Staudt-Bickel, C.; Koros, W. J. Olefin/paraffin Gas Separations with 6FDA-Based Polyimide Membranes, *J. Membrane Sci.* **2000**, 170, 205-214
- <sup>76</sup> Morisato, A.; He, Z.; Pinnau, I.; Merkel, T. C. Transport Properties of PA12-PTMO/AgBF<sub>4</sub> Solid Polymer Electrolyte Membranes for Olefin/Paraffin Separation. *Desalination* **2002**, 145, 347-351
- <sup>77</sup> Hsiue, G and Yang, J. Novel Methods in Separation of Olefin/Paraffin Mixtures by Functional Polymeric Membranes. *J. Membrane Sci.* **1993**, 92, 117-128

# Chapter 2

---

Synthesis and Characterization of Ionic Liquids

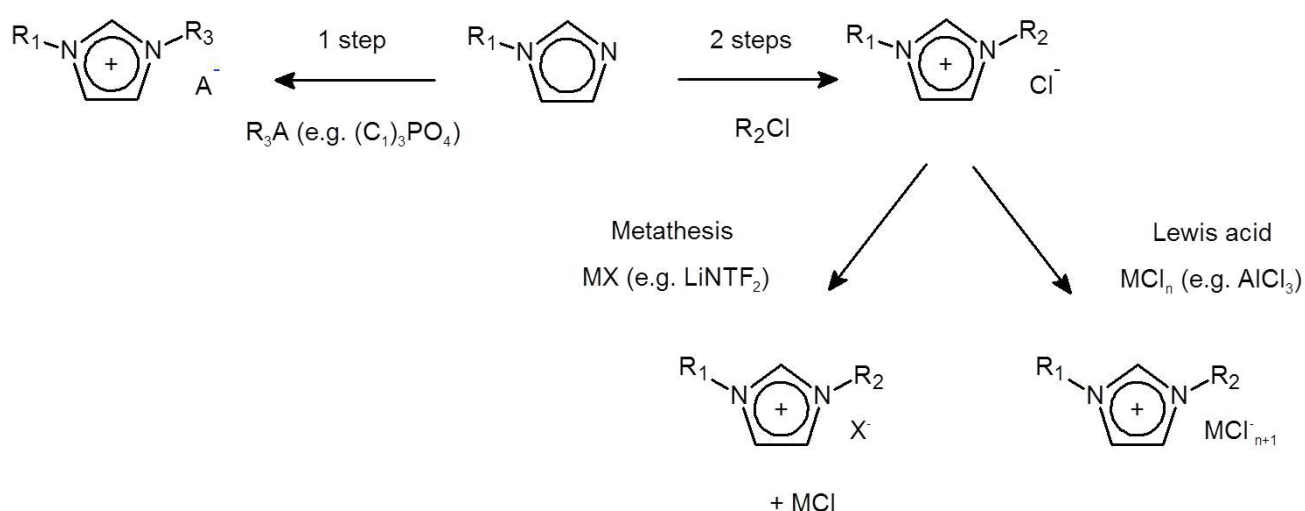


## A. Synthesis of ionic liquids

All the ionic liquids synthesized in this work were based in the imidazolium cation and are described in appendix 1 along with full name, abbreviation and CAS number.

The majority of ionic liquids are usually prepared by quaternization of imidazole, alkylamines or phosphine, often employing alkyl halides as alkylating agents, followed by anion metathesis (scheme 2.1). The anion metathesis methods produce a large number of ILs in good yield, but the contamination by residual halide could limit the production of high purity materials.<sup>1,2</sup>

Halide free synthetic routes have been developed to avoid these contaminations.<sup>3,4</sup> Such is the case the direct alkylation reaction of phosphine, amine, pyridine, or azole yielding ILs based on alkylsulfates,<sup>5,6</sup> alkylsulfonate,<sup>7</sup> alkylphosphate,<sup>8,9</sup> and alkylphosphite<sup>9</sup> or alkyltriflates<sup>9</sup>. Other examples are use of the reaction between imidazole carbenes and the conjugate protic acid of the anion of interest<sup>10</sup>, alkylation with a trifluoroethanoic acid ester, the direct alkylation of the cation precursor with dimethylcarbonate<sup>1</sup> and use of aqueous hydroxide solutions of organic cations, which are then neutralized with organic acids<sup>11</sup>.



Scheme 2.1 - One and two-step synthesis paths based in the imidazolium cation

However each of these alternatives is only applicable to certain families of ionic liquids and the procedures may be complicated or expensive. Even with the risk of contamination, the traditional synthetic routes are still widely used because they apply to a very large range of ionic liquids, their simplicity, relative low reagent price and high yields.

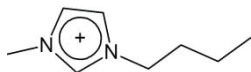
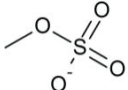
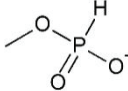
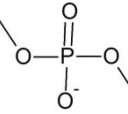
The most common difficulty is to obtain high yield or high purity ionic liquids. To avoid extensive purification of the product it's essential to start with the highest purity reagents. Liquid reagents are distilled prior to use and kept refrigerated under inert atmosphere, to avoid contamination or degradation.

Ionic liquid solutions with metallic salts of lithium (I), nickel (II) and copper (II) were prepared and characterized.

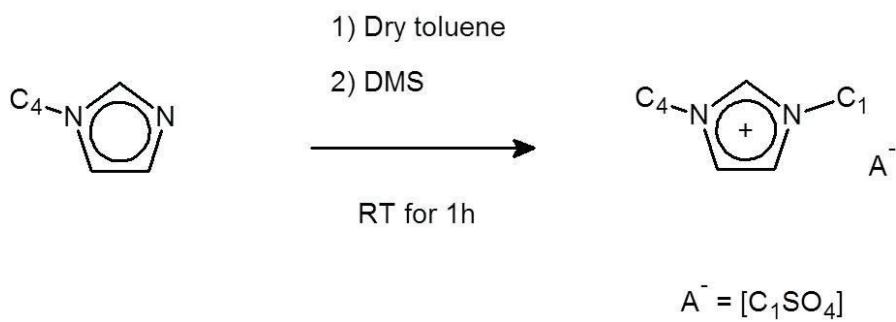
## 2.1 One-step synthesis of ionic liquids

The ionic liquids 1-butyl-3-methylimidazolium methylsulfate,  $[\text{C}_1\text{C}_4\text{Im}][\text{C}_1\text{SO}_4]$ , 1-butyl-3-methylimidazolium methylphosphite,  $[\text{C}_1\text{C}_4\text{Im}][\text{C}_1\text{HPO}_3]$  and 1-butyl-3-methylimidazolium dimethylphosphate,  $[\text{C}_1\text{C}_4\text{Im}][(\text{C}_1)_2\text{PO}_4]$  were synthesized by direct alkylation of butylimidazole with appropriate precursors. The products are described in table 2.1 have been synthesized following a procedure reported in the literature.<sup>12</sup>

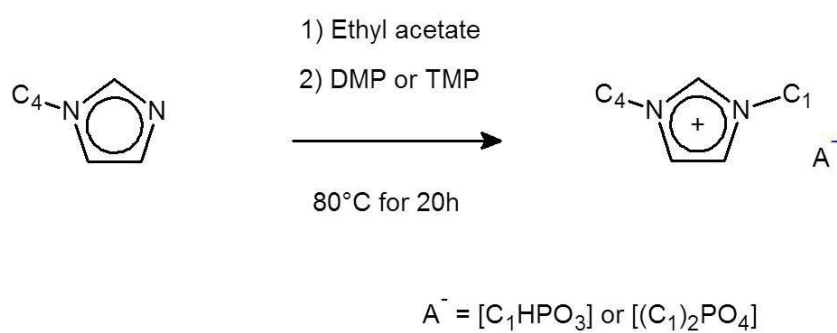
Table 2.1 - Representation, name, abbreviation of the ionic liquids synthesized by the one-step procedure

Cation	Anion	Name	Abbreviation
		1-butyl-3-methylimidazolium methylsulfate	$[\text{C}_1\text{C}_4\text{Im}][\text{C}_1\text{SO}_4]$
		1-butyl-3-methylimidazolium methylphosphite	$[\text{C}_1\text{C}_4\text{Im}][\text{C}_1\text{HPO}_3]$
		1-butyl-3-methylimidazolium dimethylphosphate	$[\text{C}_1\text{C}_4\text{Im}][(\text{C}_1)_2\text{PO}_4]$

A drop wise addition of the dimethylsulfate (DMS) on the butylimidazole affords  $[\text{C}_1\text{C}_4\text{Im}][\text{C}_1\text{SO}_4]$  (scheme 2.2). Since the reagents are water soluble, the addition of water followed by repeated washing of this phase with toluene afford pure  $[\text{C}_1\text{C}_4\text{Im}][(\text{CH}_3\text{O})\text{SO}_3]$  as a colorless liquid. The ionic liquid was dried under vacuum. A similar procedure, but at a higher reaction temperature and with longer reaction time, is applied for the synthesis of  $[\text{C}_1\text{C}_4\text{Im}][\text{C}_1\text{HPO}_3]$  and  $[\text{C}_1\text{C}_4\text{Im}][(\text{C}_1)_2\text{PO}_4]$ , as depicted in scheme 2.3. The reagents used were the trimethylphosphate (TMP) and dimethylphosphate (DMP), respectively. The purification of these ILs is done through a liquid-liquid (water-toluene) extraction, for 16h, affording colorless liquids. The aqueous phase was isolated, the water was removed and the ionic liquid dried under vacuum to completion at 120°C.



**Scheme 2.2** - Synthesis of  $[C_1C_4Im][C_1SO_4]$



**Scheme 2.3** - Synthesis of  $[C_1C_4Im][C_1HPO_3]$  and  $[C_1C_4Im][(C_1)_2PO_4]$

## 2.2 Two-step synthesis of ionic liquids

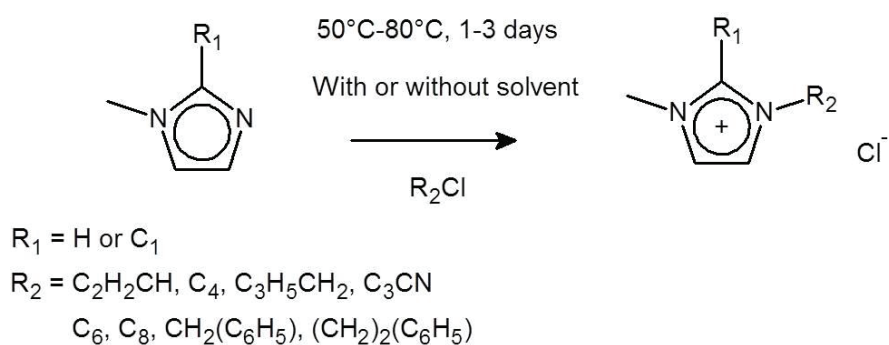
The two step synthesis performed consisted first in the quaternization of the amine with an alkylating agent containing a halogen (chloride or bromide) as a leaving group, and second in the change of the obtained chloride/bromide anion, by metathesis or addition of a Lewis acid, for the desired anion.

A series of ionic liquid precursors were obtained through the quaternization step, using similar procedures. The precursors obtained are listed and described in table 2.2.

Table 2.2 - Precursors of the ionic liquids synthesized by the two-step synthesis, along with abbreviations

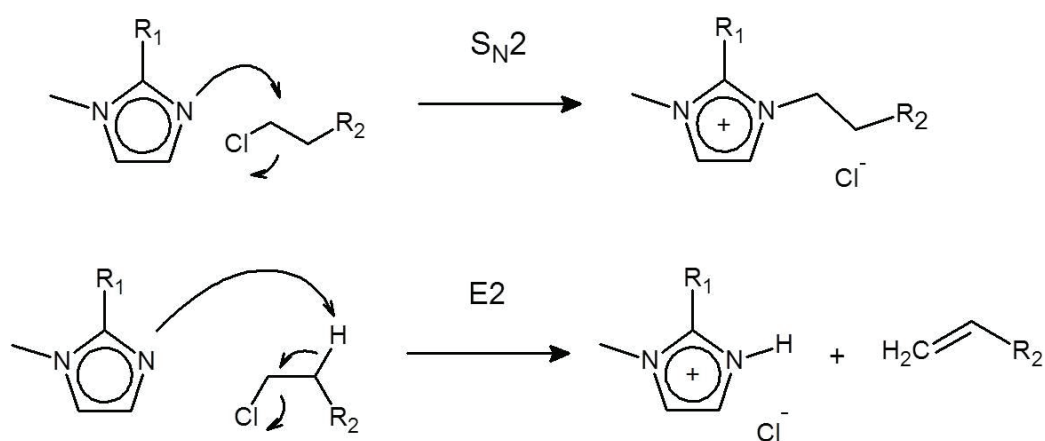
Ionic liquid precursor	Abbreviation
1-methyl-3-(propyn-3-yl)imidazolium chloride	$[\text{C}_1(\text{C}_2\text{H}_2\text{CH})\text{Im}][\text{Cl}]$
1-butyl-3-methylimidazolium chloride	$[\text{C}_1\text{C}_4\text{Im}][\text{Cl}]$
1-(buten-3-yl)-3-methylimidazolium bromide	$[\text{C}_1(\text{C}_3\text{H}_5\text{CH}_2)\text{Im}][\text{Br}]$
1-butyl-2,3-dimethylimidazolium chloride	$[\text{C}_1\text{C}_1\text{C}_4\text{Im}][\text{Cl}]$
1-(3-cyanopropyl)-3-methylimidazolium chloride	$[\text{C}_1\text{C}_3\text{CNIm}][\text{Cl}]$
1-hexyl-3-methylimidazolium chloride	$[\text{C}_1\text{C}_6\text{Im}][\text{Cl}]$
1-benzyl-3-methylimidazolium chloride	$[\text{C}_1(\text{CH}_2\text{C}_6\text{H}_5)\text{Im}][\text{Cl}]$

The apparatus and the reagents were kept dry and under inert atmosphere. Scheme 2.3 depicts the procedure used for the quaternization step. The halogenated product is usually added drop wise to the imidazole in order to avoid a possible bi-molecular elimination reaction, E2, producing 1-alkene and 1-methylimidazolium. The mechanism for the E2 reaction is depicted in scheme 2.4.<sup>13</sup> The reagents are kept under strong stirring and inert atmosphere at a temperature between 50°C and 80°C under reflux for 1 to 3 days. The reaction can be performed without solvent or with toluene or acetonitrile as solvents.



Scheme 2.3 - Quaternization step for the synthesis of ionic liquids

The reagents undergo a bi-molecular nucleophilic substitution reaction, designated  $\text{S}_{\text{N}}2$ , for which the mechanism is depicted in scheme 2.4.



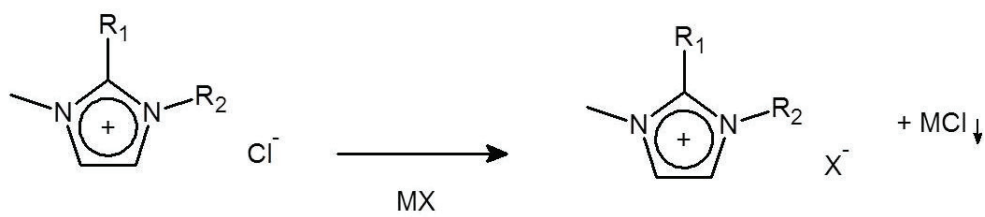
Scheme 2.4 - Mechanism for  $\text{S}_{\text{N}}2$  and E2 reaction

In the end of the 3-day reaction, the product is transferred into dry and cooled toluene or diethyl ether, causing the precipitation of the product.

The final product is filtered, washed with dry toluene and dried under high vacuum ( $10^{-8}$  bar) for at least 24h. Yield approximately 86%.

The metathesis step, depicted in Scheme 2.5, consists in adding the precursor obtained in the quaternization step to a salt of the desired final anion. The cation of the salt is selected to form an insoluble precipitate in the chosen reaction solvent, forcing the reaction in the direction of the desired products.

The ionic liquids synthesized using this method are listed in table 2.3.



$\text{R}_1 = \text{H}$  or  $\text{C}_1$

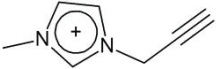
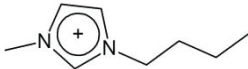
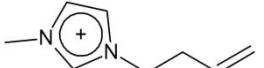
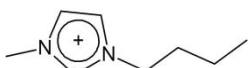
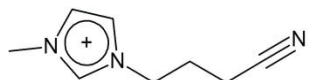
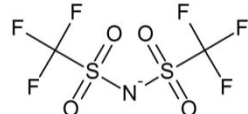
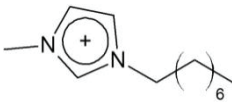
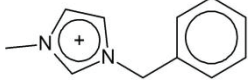
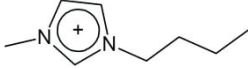
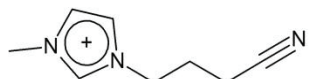
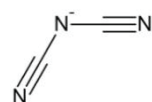
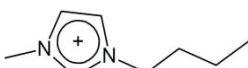
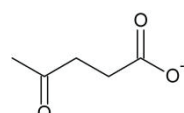
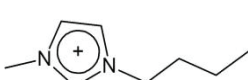
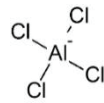
$\text{R}_2 = \text{C}_2\text{H}_2\text{CH}$ ,  $\text{C}_4$ ,  $\text{C}_3\text{H}_5\text{CH}_2$ ,  $\text{C}_3\text{CN}$

$\text{C}_6$ ,  $\text{C}_8$ ,  $\text{CH}_2(\text{C}_6\text{H}_5)$ ,  $(\text{CH}_2)_2(\text{C}_6\text{H}_5)$

$\text{MX} = \text{LiNTf}_2$ ,  $\text{NaDCA}$ ,  $\text{NaLev}$

Scheme 2.5 - Metathesis step for the synthesis of ionic liquids

Table 2.3 - Representation, name, abbreviation of the ionic liquids synthesized by the two-step procedure

Cation	Anion	Name	Abbreviation
		1-methyl-3-(propyn-3-yl)imidazolium bis(trifluoromethanesulfonyl)imide	[C <sub>1</sub> (C <sub>2</sub> H <sub>2</sub> CH)Im][NTf <sub>2</sub> ]*
		1-butyl-3-methylimidazolium bis(trifluoromethanesulfonyl)imide	[C <sub>1</sub> C <sub>4</sub> Im][NTf <sub>2</sub> ]
		1-(buten-3-yl)-3-methylimidazolium bis(trifluoromethanesulfonyl)imide	[C <sub>1</sub> (C <sub>3</sub> H <sub>5</sub> CH <sub>2</sub> )Im][NTf <sub>2</sub> ]
		1-butyl-2,3-dimethylimidazolium bis(trifluoromethanesulfonyl)imide	[C <sub>1</sub> C <sub>1</sub> C <sub>4</sub> Im][NTf <sub>2</sub> ]
		1-(3-cyanopropyl)-3-methylimidazolium bis(trifluoromethanesulfonyl)imide	[C <sub>1</sub> C <sub>3</sub> CNIIm][NTf <sub>2</sub> ]*
		1-hexyl-3-methylimidazolium bis(trifluoromethanesulfonyl)imide	[C <sub>1</sub> C <sub>6</sub> Im][NTf <sub>2</sub> ]
		1-methyl-3-octyl-imidazolium bis(trifluoromethanesulfonyl)imide	[C <sub>1</sub> C <sub>8</sub> Im][NTf <sub>2</sub> ]**
		1-benzyl-3-methylimidazolium bis(trifluoromethanesulfonyl)imide	[C <sub>1</sub> (CH <sub>2</sub> C <sub>6</sub> H <sub>5</sub> )Im][NTf <sub>2</sub> ]
		1-butyl-3-methylimidazolium dicyanamide	[C <sub>1</sub> C <sub>4</sub> Im][DCA]
		1-(3-cyanopropyl)-3-methylimidazolium dicyanamide	[C <sub>1</sub> C <sub>3</sub> CNIIm][DCA]*
		1-butyl-3-methylimidazolium levulinate	[C <sub>1</sub> C <sub>4</sub> Im][Lev]
		1-butyl-3-methylimidazolium tetrachloroaluminate	[C <sub>1</sub> C <sub>4</sub> Im][AlCl <sub>4</sub> ]

\* Kindly provided by Laboratory LC2P2 – Équipe Chimie Organométallique de Surface, Villeurbanne, France

\*\* Kindly provided by laboratory QUILL (Queen's University Ionic Liquid Laboratory), Belfast, Northern Ireland, UK

## 2.3 Materials and synthesis procedures

All operations were performed in the absence of oxygen and water under a purified argon atmosphere using glovebox (Jacomex or MBraun) or vacuum-line techniques.

The reagents used for the synthesis of ionic liquids are described in table 2.4. Methylimidazole, butylimidazole, and 1,2-dimethylimidazole were distilled prior to use. Dimethylsulfate, dimethylphosphite, trimethylphosphate, 1-chlorobutane, 4-bromo-1-butene, 4-chlorobutylnitrile, 1-chlorohexane, benzylchloride, 2-chloroethylbenzene, lithium bis(trifluoromethanesulfonyl)imide, sodium dicyanamide, sodium levulinate, silver nitrate, aluminium chloride, sodium propionate, sodium isobutyrate, levulinic acid, silver oxide and potassium hydroxide were not distilled or purified prior to use.

A commercial sample of [C<sub>1</sub>C<sub>4</sub>Im][DCA] with 98% purity provided by Solvionic was used in all posterior studies instead of the sample obtained by the method described in the patent<sup>14</sup>, due to patent sharing issues.

The ILs were characterized by <sup>1</sup>H, and <sup>13</sup>C NMR. The NMR spectra were performed in a Bruker Avance 400 MHz using CD<sub>2</sub>Cl<sub>2</sub> as solvent. High resolution mass spectroscopy (HRMS) was used to control the halide content. The high resolution mass spectra (MS QTOF) were recorded in a positive and negative ion mode on a hybrid quadrupole time-of-flight mass spectrometer (MicroTOFQ-II, Bruker Daltonics, Bremen) with an Electrospray Ionization (ESI) ion source. The gas flow of spray gas is 0.6 bar and the capillary voltage is +/-4.5 kV. The solutions are infused at 180 μL/h. The mass range of the analysis is 50-1000 m/z and the calibration was done with sodium formate. The original NMR and HRMS spectra can be found in appendix 2.

The metallic salt solubility in the ionic liquid was verified visually in a Leica DM 2500M Microscope coupled with a hot stage from Linkam LTS 420.

Table 2.4 - Reagents used in the synthesis of the ionic liquids, along with abbreviations, purity and supplier

Reagent	Abbreviation	Purity	Supplier
Butylimidazole	C <sub>4</sub> Im	98%	Sigma-Aldrich
Dimethylsulfate	DMS	>99%	Sigma-Aldrich
Dimethylphosphite	DMP	98%	Sigma-Aldrich
Trimethylphosphate	TMP	>99%	Sigma-Aldrich
Metylimidazole	C <sub>1</sub> Im	>99%	Aldrich
1,2-Dimethylimidazole	C <sub>1</sub> C <sub>1</sub> Im	98%	Sigma-Aldrich
3-Bromo-1-propyne	BrProp	80 wt. % in toluene	Sigma-Aldrich
1-Chlorobutane	ClBu	>99%	Aldrich
4-Bromo-1-butene	BrBud	>99%	Aldrich
4-Chlorobutyronitrile	ClBCN	>99%	Aldrich
1-Chlorohexane	ClHx	>99%	Aldrich
Benzylchloride	ClBz	99%	Sigma-Aldrich
Sodium dicyanamide	NaDCA	96%	Aldrich
Sodium levulinate	NaLev	-	LMOPS*
Silver nitrate	AgNO <sub>3</sub>	99.5%	Sigma-Aldrich
Aluminium chloride	AlCl <sub>3</sub>	99.9%	Sigma-Aldrich
Lithium bis(trifluoromethanesulfonyl)imide	LiNTf <sub>2</sub>	>99%	Solvionic
Nickel(II) bis(trifluoromethanesulfonyl)imide	Ni(NTf <sub>2</sub> ) <sub>2</sub>	99%	Solvionic
Copper(II) bis(trifluoromethanesulfonyl)imide	CU(NTf <sub>2</sub> ) <sub>2</sub>	99%	Solvionic

\*Kindly provided by the laboratory LMOPS, Lyon, France

All ionic liquids were degassed and dried using a multiple entry glass vacuum line, at approximately 8 Pa, for at least 48h prior to the measurement. The amount of water contained in each ionic liquid was determined with a coulometric Karl Fischer titrator (Mettler Toledo DL32) with a claimed precision of ±1 ppm. The amount of water in each ionic liquid is listed in table 2.5.

Table 2.5 - Amount of water, in ppm and molar fraction, present in the ionic liquid after at least 48 h under vacuum

Ionic Liquid	Amount of water /ppm	Mole fraction of water
[C <sub>1</sub> (C <sub>2</sub> H <sub>2</sub> CH)Im][NTf <sub>2</sub> ]	95	0.0021
[C <sub>1</sub> C <sub>4</sub> Im][NTf <sub>2</sub> ]	70	0.0016
[C <sub>1</sub> (C <sub>3</sub> H <sub>5</sub> CH <sub>2</sub> )Im][NTf <sub>2</sub> ]	100	0.0023
[C <sub>1</sub> C <sub>3</sub> CNIm][NTf <sub>2</sub> ]	43	0.0010
[C <sub>1</sub> C <sub>8</sub> Im][NTf <sub>2</sub> ]	63	0.0017
[C <sub>1</sub> (CH <sub>2</sub> C <sub>6</sub> H <sub>5</sub> )Im][NTf <sub>2</sub> ]	70	0.0018
[C <sub>1</sub> C <sub>4</sub> Im][DCA]	98	0.0011
[C <sub>1</sub> C <sub>3</sub> CNIm][DCA]	75	0.00090
[C <sub>1</sub> C <sub>4</sub> Im][C <sub>1</sub> HPO <sub>3</sub> ]	156	0.0020
[C <sub>1</sub> C <sub>4</sub> Im][Lev]	365	0.0051

### 1-Butyl-3-methylimidazolium methylsulfate, [C<sub>1</sub>C<sub>4</sub>Im][C<sub>1</sub>SO<sub>4</sub>]

83.96 g (676.1 mmol, 89 ml) of distilled butylimidazole was transferred into a 500 mL two-neck round bottomed flask with a large stirring bar. 100 ml of dry toluene were added and the flask was placed in an ice bath. 85.27 g (676.1 mmol, 64 mL) of dry dimethylsulfate was added drop wise. The mixture was stirred for 1 h at room temperature. The top phase was decanted and the lower phase was washed five times with 25 ml of toluene. The product, a colorless, viscous liquid, was dried under vacuum overnight. The yield was 121.2 g (484.1 mmol, 71.6%).

<sup>1</sup>H-NMR (400 MHz, CD<sub>2</sub>Cl<sub>2</sub>) δ (ppm): 9.40 (1H, s, N-CH-N), 7.49 (2H, m, N-CH-CH-N), 4.24 (2H, t, N-CH<sub>2</sub>), 3.99 (3H, s, N-CH<sub>3</sub>), 3.63 (3H, s, O-CH<sub>3</sub>), 1.88 (2H, m, N-CH<sub>2</sub>-CH<sub>2</sub>), 1.39 (2H, m, N-CH<sub>2</sub>-CH<sub>2</sub>-CH<sub>2</sub>), 0.97 (3H, t, N-CH<sub>2</sub>-CH<sub>2</sub>-CH<sub>2</sub>-CH<sub>3</sub>)

<sup>13</sup>C-NMR (400 MHz, CD<sub>2</sub>Cl<sub>2</sub>) δ (ppm): 137.4 (s, N-CH-N), 123.6 (s, N-CH-CH-N), 122.2 (s, N-CH-CH-N), 52.8 (s, O-CH<sub>3</sub>), 49.7 (s, N-CH<sub>2</sub>), 36.2 (s, N-CH<sub>3</sub>), 32.0 (s, N-CH<sub>2</sub>-CH<sub>2</sub>), 19.3 (s, N-CH<sub>2</sub>-CH<sub>2</sub>-CH<sub>2</sub>), 13.2 (s, N-CH<sub>2</sub>-CH<sub>2</sub>-CH<sub>2</sub>-CH<sub>3</sub>)

### **1-Butyl-3-methylimidazolium methylphosphite, [C<sub>1</sub>C<sub>4</sub>Im][C<sub>1</sub>HPO<sub>3</sub>]**

83.31 g (670.9 mmol, 88.16 mL) of distilled butylimidazole was mixed with 75 ml of ethyl acetate. 73.85 g (671.1 mmol, 61.5 mL) of dry dimethylphosphite was added drop wise. The mixture was stirred under nitrogen atmosphere at 80°C for 20 h. 40 ml of distilled water were added. The solution was placed in the continuous extractor and extracted with toluene for 16 h in order to remove excess reactants. The aqueous phase was isolated, the water was removed and the ionic liquid dried under vacuum at 80°C. The product was a clear, colorless, oily liquid. The yield was 116.4 g (497.1 mmol, 74.1%).

<sup>1</sup>H-NMR (400 MHz, CD<sub>2</sub>Cl<sub>2</sub>) δ (ppm): 9.98 (1H, s, N-CH-N), 7.64 (2H, m, N-CH-CH-N), 5.67 (1H, s, P-H), 4.22 (2H, t, N-CH<sub>2</sub>), 3.96 (3H, s, N-CH<sub>3</sub>), 3.41 (3H, d, O-CH<sub>3</sub>), 1.81 (2H, m, N-CH<sub>2</sub>-CH<sub>2</sub>), 1.31 (2H, m, N-CH<sub>2</sub>-CH<sub>2</sub>-CH<sub>2</sub>), 0.89 (3H, t, N-CH<sub>2</sub>-CH<sub>2</sub>-CH<sub>2</sub>-CH<sub>3</sub>)

<sup>13</sup>C-NMR (400 MHz, CD<sub>2</sub>Cl<sub>2</sub>) δ (ppm): 138.1 (s, N-CH-N), 123.8 (s, N-CH-CH-N), 122.1 (s, N-CH-CH-N), 50.0 (d, O-CH<sub>3</sub>), 49.3 (s, N-CH<sub>2</sub>), 36.1 (s, N-CH<sub>3</sub>), 32.1 (s, N-CH<sub>2</sub>-CH<sub>2</sub>), 19.3 (s, N-CH<sub>2</sub>-CH<sub>2</sub>-CH<sub>2</sub>), 13.2 (s, N-CH<sub>2</sub>-CH<sub>2</sub>-CH<sub>2</sub>-CH<sub>3</sub>)

<sup>31</sup>P-NMR (400 MHz, CD<sub>2</sub>Cl<sub>2</sub>) δ (ppm): - 4.55 (s, P)

### **1-Butyl-3-methylimidazolium dimethylphosphate, [C<sub>1</sub>C<sub>4</sub>Im][(C<sub>1</sub>)<sub>2</sub>PO<sub>4</sub>]**

55.1 g (444.1 mmol, 58.4 mL) of distilled 1-butylimidazole was mixed with 50 ml ethyl acetate. 62.2 g (444.4 mmol, 52 mL) of dry trimethyl phosphate was added dropwise. The mixture was stirred under nitrogen atmosphere at 80°C for 20 h. 25 ml of distilled water were added. The solution was placed in the continuous extractor and extracted with toluene for at least 16 h in order to remove excess reactants. The aqueous phase was isolated, the water was removed and the ionic liquid dried at 80°C under vacuum. The product was a clear, colorless, oily liquid. The yield was 91.3 g (345.5 mmol, 77.8%).

<sup>1</sup>H-NMR (400 MHz, CD<sub>2</sub>Cl<sub>2</sub>) δ (ppm): 10.50 (1H, s, N-CH-N), 7.71 (2H, m, N-CH-CH-N), 4.22 (2H, t, N-CH<sub>2</sub>), 3.97 (3H, s, N-CH<sub>3</sub>), 3.44 (6H, d, O-CH<sub>3</sub>), 1.81 (2H, m, N-CH<sub>2</sub>-CH<sub>2</sub>), 1.31 (2H, m, N-CH<sub>2</sub>-CH<sub>2</sub>-CH<sub>2</sub>), 0.89 (3H, t, N-CH<sub>2</sub>-CH<sub>2</sub>-CH<sub>2</sub>-CH<sub>3</sub>)

$^{13}\text{C}$ -NMR (400 MHz,  $\text{CD}_2\text{Cl}_2$ )  $\delta$  (ppm): 139.1 (s, N-**CH**-N), 123.7 (s, N-**CH**-CH-N), 122.1 (s, N-**CH**-CH-N), 52.9 (d, O-**CH**<sub>3</sub>), 49.2 (s, N-**CH**<sub>2</sub>), 35.8 (s, N-**CH**<sub>3</sub>), 32.1 (s, N-**CH**<sub>2</sub>-**CH**<sub>2</sub>), 19.3 (s, N-**CH**<sub>2</sub>-**CH**<sub>2</sub>-**CH**<sub>2</sub>), 13.1 (s, N-**CH**<sub>2</sub>-**CH**<sub>2</sub>-**CH**<sub>2</sub>-**CH**<sub>3</sub>)

$^{31}\text{P}$ -NMR (400 MHz,  $\text{CD}_2\text{Cl}_2$ )  $\delta$  (ppm): - 2.10 (s, **P**)

m/z (Fab+): 139 (100%)  $[\text{C}_4\text{C}_1\text{Im}]^+$ , 403  $[(\text{C}_1\text{C}_4\text{Im})_2(\text{CH}_3\text{O})_2\text{PO}_2]^+$

m/z (Fab-): 653 (100%)  $[(\text{C}_1\text{C}_4\text{Im})_2((\text{CH}_3\text{O})_2\text{PO}_2)_3]^-$

The synthesis of the  $\text{NTf}_2$ -based ionic liquids is performed by adding the desired imidazolium chloride/bromide precursor ionic liquid (table 2.2) and lithium bis(trifluoromethanesulfonyl)imide (in 0.1 molar excess) in water. A strong stirring and controlled room-temperature is maintained for 3-4 days. Dichloromethane or ethyl acetate and water are added and the mixture is thoroughly stirred. The organic phase will then contain the ionic liquid. This phase is washed several times with water. The washing continued until the presence of chloride in the aqueous phase was no further detected by the use of a solution of silver nitrate. Activated carbon and filtration through celite and alumina were used for further purification when the organic phase presented a slight yellow coloration. Yields from 87% to 97% for the first step and from 63% to 85% for the second step.

For simplicity, for the ionic liquids whose synthesis follows the same procedure as  $[\text{C}_1\text{C}_4\text{Im}][\text{Cl}]$  and  $[\text{C}_1\text{C}_4\text{Im}][\text{NTf}_2]$ , the procedure was omitted, but the characterization is described.

### **1-Methyl-3-(propyn-3-yl)imidazolium bromide, $[\text{C}_1(\text{C}_2\text{H}_2\text{CH})\text{Im}][\text{Br}]$**

Methylimidazole (10 g, 122 mmol) was dissolved in 40 mL of anhydrous acetonitrile. 3-bromo-1-propyne (6.7 g, 134 mmol) was added drop wise. The solution was stirred 2h at room temperature. The color of the solution changed to brown. The solution was then stirred at 50°C for 24h. The solvent was then removed via rotary evaporation, and diethylether (40 mL) was added, the solution was cooled at -18°C for 12h. The resulting brown solid was washed five times with 30 mL of diethylether. The product was dried in vacuum to afford compound as pale-yellow solid. The product yield was of 90%.

**1-Methyl-3-(propyn-3-yl)imidazolium bis(trifluoromethanesulfonyl)imide, [C<sub>1</sub>(C<sub>2</sub>H<sub>2</sub>CH)Im][NTf<sub>2</sub>]**

To a solution of 1-methyl-3-(propyn-3-yl)imidazolium bromide (50 g, 413 mmol) in distilled water (250 mL), lithium bis(trifluoromethanesulfonyl)imide, LiNTf<sub>2</sub>, (142 g, 495 mmol) was added at room temperature. The reaction mixture was stirred for 24 h. An oily liquid separated and the product was extracted into 50 mL of ethylacetate and the organic phase washed 3 times with 50 mL of distilled water, until no traces of chloride salt was detected in the washing water (tested with silver nitrate). The solvent was removed under vacuum, giving a clear pale-yellow liquid. The product yield is 63%.

<sup>1</sup>H-NMR (400 MHz, CD<sub>2</sub>Cl<sub>2</sub>) δ (ppm): 8.65 (1H, s, N-CH-N), 7.31 (H, d, N-CH-CH-N), 5.81 (2H, m, N-CH<sub>2</sub>-CH<sub>2</sub>-CH-CH<sub>2</sub>), 5.15 (1H, m, N-CH<sub>2</sub>-CH<sub>2</sub>-CH-CH<sub>2</sub>), 4.28 (2H, t, N-CH<sub>2</sub>-CH<sub>2</sub>-CH-CH<sub>2</sub>), 3.95 (3H, s, N-CH<sub>3</sub>), 2.65 (2H, m, N-CH<sub>2</sub>-CH<sub>2</sub>-CH-CH<sub>2</sub>)  
<sup>13</sup>C-NMR (400 MHz, CD<sub>2</sub>Cl<sub>2</sub>) δ (ppm): 135.9 (s, N-CH-N), 132.0 (s, N-CH<sub>2</sub>-CH<sub>2</sub>-CH-CH<sub>2</sub>), 123.6 (s, N-CH-CH-N), 122.4 (s, N-CH-CH-N), 119.5 (s, N-CH<sub>2</sub>-CH<sub>2</sub>-CH-CH<sub>2</sub>), 117.7 (q, CF<sub>3</sub>), 49.4 (s, N-CH<sub>2</sub>-CH<sub>2</sub>-CH-CH<sub>2</sub>), 36.4 (s, N-CH<sub>3</sub>), 34.1 (s, N-CH<sub>2</sub>-CH<sub>2</sub>-CH-CH<sub>2</sub>)

**1-Butyl-3-methylimidazolium chloride, [C<sub>1</sub>C<sub>4</sub>Im][Cl]**

1-Chlorobutane (106 mL, 1010 mmol) was added to freshly distilled methylimidazole (50 mL, 630 mmol). The mixture was stirred for 48 h at 65 °C. The hot solution was then transferred drop wise via a cannula into toluene (200 mL) at 0 °C under vigorous mechanical stirring. The white precipitate that formed was then filtered and washed repeatedly with toluene. The product was dried overnight under vacuum giving a white powder (95.6 g, 87 %).

<sup>1</sup>H-NMR (400 MHz, CD<sub>2</sub>Cl<sub>2</sub>) δ (ppm): 10.76 (1H, s, N-CH-N), 7.64 (2H, m, N-CH-CH-N), 4.31 (2H, t, N-CH<sub>2</sub>), 4.07 (3H, s, N-CH<sub>3</sub>), 1.88 (2H, m, N-CH<sub>2</sub>-CH<sub>2</sub>), 1.35 (2H, m, N-CH<sub>2</sub>-CH<sub>2</sub>-CH<sub>2</sub>), 0.95 (3H, t, N-CH<sub>2</sub>-CH<sub>2</sub>-CH<sub>2</sub>-CH<sub>3</sub>)  
<sup>13</sup>C-NMR (400 MHz, CD<sub>2</sub>Cl<sub>2</sub>) δ (ppm): 138.2 (s, N-CH-N), 123.4 (s, N-CH-CH-N), 121.9 (s, N-CH-CH-N), 49.5 (s, N-CH<sub>2</sub>), 36.3 (s, N-CH<sub>3</sub>), 32.0 (s, N-CH<sub>2</sub>-CH<sub>2</sub>), 19.4 (s, N-CH<sub>2</sub>-CH<sub>2</sub>-CH<sub>2</sub>), 13.2 (s, N-CH<sub>2</sub>-CH<sub>2</sub>-CH<sub>2</sub>-CH<sub>3</sub>)

### **1-Butyl-3-methylimidazolium bis(trifluoromethanesulfonyl)imide, [C<sub>1</sub>C<sub>4</sub>Im][NTf<sub>2</sub>]**

A solution of LiNTf<sub>2</sub> (50 g, 170 mmol) in water (50 mL) was added to a solution of [C<sub>1</sub>C<sub>4</sub>Im][Cl] (30.4 g, 170 mmol) in water (100 mL). The solution was stirred for 2 h at room temperature, then dichloromethane (50 mL) was added and the mixture transferred to a separating funnel. The lower phase was collected and washed repeatedly with water (8 × 100 mL) until no chloride traces remained in the washings (tested with silver nitrate solution). The ionic liquid in dichloromethane was purified through a short alumina column and the solvent removed in vacuum giving a colourless viscous liquid.

<sup>1</sup>H-NMR (400 MHz, CD<sub>2</sub>Cl<sub>2</sub>) δ (ppm): 8.63 (1H, s, N-CH-N), 7.34 (2H, m, N-CH-CH-N), 4.19 (2H, t, N-CH<sub>2</sub>), 3.94 (3H, s, N-CH<sub>3</sub>), 1.88 (2H, m, N-CH<sub>2</sub>-CH<sub>2</sub>), 1.41 (2H, m, N-CH<sub>2</sub>-CH<sub>2</sub>-CH<sub>2</sub>), 0.98 (3H, t, N-CH<sub>2</sub>-CH<sub>2</sub>-CH<sub>2</sub>-CH<sub>3</sub>)

<sup>13</sup>C-NMR (400 MHz, CD<sub>2</sub>Cl<sub>2</sub>) δ (ppm): 135.8 (s, N-CH-N), 126.3 (s, N-CH-CH-N), 124.1 (s, N-CH-CH-N), 117.8 (q, CF<sub>3</sub>), 50.0 (s, N-CH<sub>2</sub>), 36.4 (s, N-CH<sub>3</sub>), 31.7 (s, N-CH<sub>2</sub>-CH<sub>2</sub>), 19.4 (s, N-CH<sub>2</sub>-CH<sub>2</sub>-CH<sub>2</sub>), 12.8 (s, N-CH<sub>2</sub>-CH<sub>2</sub>-CH<sub>2</sub>-CH<sub>3</sub>)

### **1-(Buten-3-yl)-3-methylimidazolium chloride, [C<sub>1</sub>(C<sub>3</sub>H<sub>5</sub>CH<sub>2</sub>)Im][Br]**

1-Bromobutane (148 mmol) was added to freshly distilled methylimidazole (100 mmol). The mixture was stirred for 3 days under reflux at 80 °C. The slight orange oil was washed with toluene and dried under vacuum. (20.9 g, 96.7 mmol, 97 %).

### **1-(Buten-3-yl)-3-methylimidazolium bis(trifluoromethanesulfonyl)imide, [C<sub>1</sub>(C<sub>3</sub>H<sub>5</sub>CH<sub>2</sub>)Im][NTf<sub>2</sub>]**

A solution of LiNTf<sub>2</sub> (27.7 g, 96.7 mmol) in water was added to a solution of [C<sub>1</sub>(C<sub>3</sub>H<sub>5</sub>CH<sub>2</sub>)Im][Br] (20.9 g, 96.7 mmol) in water. The solution was stirred overnight at room temperature, then dichloromethane was added and the mixture transferred to a separating funnel. The lower phase was collected and washed repeatedly with water until no chloride traces remained in the washings (tested with silver nitrate solution). The ionic liquid in the dichloromethane was purified through a short alumina column and the solvent removed in vacuum giving a slight orange viscous liquid.

$^1\text{H-NMR}$  (400 MHz,  $\text{CD}_2\text{Cl}_2$ )  $\delta$  (ppm): 8.65 (1H, s, N-CH-N), 7.31 (H, d, N-CH-CH-N), 5.81 (2H, m, N-CH<sub>2</sub>-CH<sub>2</sub>-CH-CH<sub>2</sub>), 5.15 (1H, m, N-CH<sub>2</sub>-CH<sub>2</sub>-CH-CH<sub>2</sub>), 4.28 (2H, t, N-CH<sub>2</sub>-CH<sub>2</sub>-CH-CH<sub>2</sub>), 3.95 (3H, s, N-CH<sub>3</sub>), 2.65 (2H, m, N-CH<sub>2</sub>-CH<sub>2</sub>-CH-CH<sub>2</sub>)  
 $^{13}\text{C-NMR}$  (400 MHz,  $\text{CD}_2\text{Cl}_2$ )  $\delta$  (ppm): 135.9 (s, N-CH-N), 132.0 (s, N-CH<sub>2</sub>-CH<sub>2</sub>-CH-CH<sub>2</sub>), 123.6 (s, N-CH-CH-N), 122.4 (s, N-CH-CH-N), 119.5 (s, N-CH<sub>2</sub>-CH<sub>2</sub>-CH-CH<sub>2</sub>), 117.7 (q,  $\text{CF}_3$ ), 49.4 (s, N-CH<sub>2</sub>-CH<sub>2</sub>-CH-CH<sub>2</sub>), 36.4 (s, N-CH<sub>3</sub>), 34.1 (s, N-CH<sub>2</sub>-CH<sub>2</sub>-CH-CH<sub>2</sub>)

**1-Butyl-2,3-dimethylimidazolium bis(trifluoromethanesulfonyl)imide,  
[C<sub>1</sub>C<sub>1</sub>C<sub>4</sub>Im][NTf<sub>2</sub>]**

$^1\text{H-NMR}$  (400 MHz,  $\text{CD}_2\text{Cl}_2$ )  $\delta$  (ppm): 7.24 (2H, d, N-CH-CH-N), 4.07 (2H, t, N-CH<sub>2</sub>), 3.81 (3H, s, N-CH<sub>3</sub>), 2.61 (3H, s, N-C-CH<sub>3</sub>), 1.81 (2H, m, N-CH<sub>2</sub>-CH<sub>2</sub>), 1.42 (2H, m, N-CH<sub>2</sub>-CH<sub>2</sub>-CH<sub>2</sub>), 0.99 (3H, t, N-CH<sub>2</sub>-CH<sub>2</sub>-CH<sub>2</sub>-CH<sub>3</sub>)  
 $^{13}\text{C-NMR}$  (400 MHz,  $\text{CD}_2\text{Cl}_2$ )  $\delta$  (ppm): 143.8 (s, N-CH-N), 122.7 (s, N-CH-CH-N), 117.8 (s, N-CH-CH-N), 113.4 (q,  $\text{CF}_3$ ), 49.2 (s, N-CH<sub>2</sub>-CH<sub>2</sub>-CH<sub>2</sub>-CH<sub>3</sub>), 35.5 (s, N-CH<sub>3</sub>), 31.7 (s, N-CH<sub>2</sub>-CH<sub>2</sub>), 19.4 (s, N-CH<sub>2</sub>-CH<sub>2</sub>-CH<sub>2</sub>), 13.1 (s, N-CH<sub>2</sub>-CH<sub>2</sub>-CH<sub>2</sub>-CH<sub>3</sub>), 9.57 (s, N-C-CH<sub>3</sub>)

**1-(3-Cyanopropyl)-3-methylimidazolium chloride, [C<sub>1</sub>C<sub>3</sub>CNIIm][Cl]**

A mixture of methylimidazole (20 g, 244 mmol) and 4-chlorobutyronitrile (29.5 g, 293 mmol) was stirred at 80°C for 24h. Diethylether (40 mL) was added at room temperature to the oily liquid, the mixture was stirred for 2 h. The resulting pale yellow solid was washed 3 times with 30 mL of diethyl ether. The solvent was removed via rotary evaporation and the product was dried under vacuum to afford a white solid in quantitative yield.

**1-(3-Cyanopropyl)-3-methylimidazolium bis(trifluoromethanesulfonyl)imide,  
[C<sub>1</sub>C<sub>3</sub>CNIIm][NTf<sub>2</sub>]**

To a solution of [C<sub>1</sub>C<sub>3</sub>CNIIm][Cl] (20 g, 108 mmol) in distilled 70 mL of water, LiNTf<sub>2</sub> (34g, 119 mmol) was added at room temperature and an oily liquid immediately separated. The reaction mixture was stirred for 2 h, and the product was

extracted into 50 mL of ethylacetate. The organic phase was washed 3 times with 50 mL of water. The solvent was removed by rotary evaporation and the product was dried in vacuum to afford a pale-yellow liquid. The product yield was 65%.

$^1\text{H-NMR}$  (300 MHz,  $\text{DMSO-d}^6$ )  $\delta$  (ppm): 9.01 (1H, s, N-CH-N), 7.61 (2H, m, N-CH-CH-N), 4.19 (2H, t, N-CH<sub>2</sub>), 3.78 (3H, s, N-CH<sub>3</sub>), 2.48 (2H, m, N-CH<sub>2</sub>-CH<sub>2</sub>), 2.11 (2H, m, N-CH<sub>2</sub>-CH<sub>2</sub>-CH<sub>2</sub>)

$^{13}\text{C-NMR}$  (400 MHz,  $\text{CD}_2\text{Cl}_2$ )  $\delta$  (ppm): 137.1 (s, N-CH-N), 123.8 (s, CN), 119.2 (s, N-CH-CH-N), 119.3 (s, N-CH-CH-N), 113.4 (q, CF<sub>3</sub>), 48.3 (s, N-CH<sub>2</sub>), 36.2 (s, N-CH<sub>3</sub>), 25.5 (s, N-CH<sub>2</sub>-CH<sub>2</sub>), 13.8 (s, N-CH<sub>2</sub>-CH<sub>2</sub>-CH<sub>2</sub>)

m/z (Fab<sup>+</sup>): 580.1 (100%) [(C<sub>1</sub>C<sub>3</sub>CNIIm)<sub>2</sub>NTf<sub>2</sub>]<sup>+</sup>

**1-Hexyl-3-methylimidazolium bis(trifluoromethanesulfonyl)imide, [C<sub>1</sub>C<sub>6</sub>Im][NTf<sub>2</sub>]**

$^1\text{H-NMR}$  (400 MHz,  $\text{CD}_2\text{Cl}_2$ )  $\delta$  (ppm): 8.65 (1H, s, N-CH-N), 7.33 (2H, m, N-CH-CH-N), 4.19 (2H, t, N-CH<sub>2</sub>), 3.96 (3H, s, N-CH<sub>3</sub>), 1.89 (2H, m, N-CH<sub>2</sub>-CH<sub>2</sub>), 1.35 (6H, s, N-CH<sub>2</sub>-CH<sub>2</sub>-CH<sub>2</sub>-CH<sub>2</sub>-CH<sub>2</sub>), 0.92 (3H, t, N-CH<sub>2</sub>-CH<sub>2</sub>-CH<sub>2</sub>-CH<sub>2</sub>-CH<sub>2</sub>-CH<sub>3</sub>)

$^{13}\text{C-NMR}$  (400 MHz,  $\text{CD}_2\text{Cl}_2$ )  $\delta$  (ppm): 135.8 (s, N-CH-N), 123.7 (s, N-CH-CH-N), 122.3 (s, N-CH-CH-N), 117.7 (q, CF<sub>3</sub>), 50.3 (s, N-CH<sub>2</sub>), 36.3 (s, N-CH<sub>3</sub>), 30.9 (s, N-CH<sub>2</sub>-CH<sub>2</sub>), 29.9 (s, N-CH<sub>2</sub>-CH<sub>2</sub>-CH<sub>2</sub>), 25.7 (s, N-CH<sub>2</sub>-CH<sub>2</sub>-CH<sub>2</sub>-CH<sub>2</sub>), 22.3 (s, N-CH<sub>2</sub>-CH<sub>2</sub>-CH<sub>2</sub>-CH<sub>2</sub>-CH<sub>2</sub>), 13.6 (s, N-CH<sub>2</sub>-CH<sub>2</sub>-CH<sub>2</sub>-CH<sub>2</sub>-CH<sub>2</sub>-CH<sub>3</sub>)

**1-Benzyl-3-methylimidazolium chloride, [C<sub>1</sub>(CH<sub>2</sub>C<sub>6</sub>H<sub>5</sub>)Im][Cl]**

Benzylchloride (29.92 g, 236 mmol) was added dropwise to methylimidazole (19.41 g, 236 mmol) and stirred at 80°C for 3 days. A slightly yellow liquid was formed. The hot solution was then transferred drop wise via a cannula into 150 mL of toluene at 0 °C under vigorous mechanical stirring. The resulting white solid was washed several times with toluene. The product was dried under vacuum affording product in a quantitative yield.

### **1-Benzyl-3-methylimidazolium bis(trifluoromethanesulfonyl)imide, [C<sub>1</sub>(CH<sub>2</sub>C<sub>6</sub>H<sub>5</sub>)Im][NTf<sub>2</sub>]**

To a solution of [C<sub>1</sub>(CH<sub>2</sub>C<sub>6</sub>H<sub>5</sub>)Im][Cl] (4.6 g, 22 mmol) in distilled 20 mL of water, LiNTf<sub>2</sub> (6.9 g, 24 mmol) was added at room temperature. The reaction mixture was stirred for 3 days, and the product was extracted into 20 mL of dichloromethane. The organic phase was washed several times with water. The ionic liquid in the dichloromethane was purified with activated carbon and through an alumina column. The product was dried in vacuum to afford a pale-yellow liquid in quantitative yield.

<sup>1</sup>H-NMR (400 MHz, CD<sub>2</sub>Cl<sub>2</sub>) δ (ppm): 8.69 (1H, s, N-CH-N), 7.42 (5H, m, Ar-C<sub>6</sub>H<sub>5</sub>), 7.28 (2H, m, N-CH-CH-N), 3.94 (3H, s, N-CH<sub>3</sub>)

<sup>13</sup>C-NMR (400 MHz, CD<sub>2</sub>Cl<sub>2</sub>) δ (ppm): 135.8 (s, N-CH-N), 132.3 (s, Ar-C<sub>6</sub>H<sub>5</sub>), 129.5 (s, Ar-C<sub>6</sub>H<sub>5</sub>), 128.8 (s, Ar-C<sub>6</sub>H<sub>5</sub>), 123.9 (s, N-CH-CH-N), 122.3 (s, N-CH-CH-N), 36.4 (s, N-CH<sub>2</sub>-Ar)

m/z (Fab+): 173.1 (100%) [C<sub>1</sub>(C<sub>3</sub>H<sub>5</sub>CH<sub>2</sub>)Im]<sup>+</sup>, 626.1 (40%) [C<sub>1</sub>(C<sub>3</sub>H<sub>5</sub>CH<sub>2</sub>)Im]<sub>2</sub>[NTf<sub>2</sub>]<sup>+</sup>

### **1-Butyl-3-methylimidazolium dicyanamide, [C<sub>1</sub>C<sub>4</sub>Im][DCA]**

The synthesis of this ionic liquid was patented.<sup>14</sup> Sodium dicyanamide (1.12 g, 12.63 mmol) was added with a Bush tube into melted [C<sub>1</sub>C<sub>4</sub>Im][Cl] (2 g, 11.49 mmol) at 70°C and kept under stirring for 24 h. After cooling down at 25°C, 20 mL of THF were added. The white precipitate of NaCl was filtered, and the filtrate was kept at -5°C overnight to complete the precipitation of NaCl. The precipitate was filtered off. This work up was repeated until no more NaCl precipitate observed. Evaporation of THF afforded [C<sub>1</sub>C<sub>4</sub>Im][N(CN)<sub>2</sub>] as a slightly yellow oil. Yield of 85%.

<sup>1</sup>H-NMR (400 MHz, CD<sub>2</sub>Cl<sub>2</sub>) δ (ppm): 8.61 (1H, s, N-CH-N), 7.37 (2H, m, N-CH-CH-N), 4.10 (2H, t, N-CH<sub>2</sub>), 3.79 (3H, s, N-CH<sub>3</sub>), 1.78 (2H, m, N-CH<sub>2</sub>-CH<sub>2</sub>), 1.23 (2H, m, N-CH<sub>2</sub>-CH<sub>2</sub>-CH<sub>2</sub>), 0.83 (3H, t, N-CH<sub>2</sub>-CH<sub>2</sub>-CH<sub>2</sub>-CH<sub>3</sub>)

<sup>13</sup>C-NMR (400 MHz, CD<sub>2</sub>Cl<sub>2</sub>) δ (ppm): 136.2 (s, N-CH-N), 123.7 (s, N-CH-CH-N), 122.4 (s, N-CH-CH-N), 119.7 (s, CN), 49.5 (s, N-CH<sub>2</sub>), 35.9 (s, N-CH<sub>3</sub>), 31.6 (s, N-CH<sub>2</sub>-CH<sub>2</sub>), 19.2 (s, N-CH<sub>2</sub>-CH<sub>2</sub>-CH<sub>2</sub>), 13.1 (s, N-CH<sub>2</sub>-CH<sub>2</sub>-CH<sub>2</sub>-CH<sub>3</sub>)

m/z (Fab+): 139 (100%) [C<sub>4</sub>C<sub>1</sub>Im]<sup>+</sup>, 344 (20%) [(C<sub>4</sub>C<sub>1</sub>Im)<sub>2</sub>DCA]<sup>+</sup>

m/z (Fab-): 66 (100%) [DCA]<sup>-</sup>

### 1-(3-Cyanopropyl)-3-methylimidazolium dicyanamide, [C<sub>1</sub>C<sub>3</sub>CNIm][DCA]

To a solution of [C<sub>1</sub>C<sub>3</sub>CNIm][Cl] (20 g, 108 mmol) in 70 mL of distilled water, sodium dicyanamide (10.5 g, 119 mmol) was added at room temperature. The reaction mixture was stirred at 25°C for 24 h, then the water was evaporated. 50 mL of ethylacetate were added and the solution was cooled at -18°C for several hours. The sodium chloride precipitate was filtered and the solution was dried under vacuum. Yield was of 75%.

<sup>1</sup>H-NMR (300 MHz, DMSO-d<sup>6</sup>) δ (ppm): 9.11 (1H, s, N-CH-N), 7.73 (2H, m, N-CH-CH-N), 4.24 (2H, t, N-CH<sub>2</sub>), 3.84 (3H, s, N-CH<sub>3</sub>), 2.65 (2H, m, N-CH<sub>2</sub>-CH<sub>2</sub>), 2.20 (2H, m, N-CH<sub>2</sub>-CH<sub>2</sub>-CH<sub>2</sub>)

<sup>13</sup>C-NMR (400 MHz, CD<sub>2</sub>Cl<sub>2</sub>) δ (ppm): 137.2 (s, N-CH-N), 124.2 (s, N-CH-CH-N), 122.7 (s, N-CH-CH-N), 120.0 (s, CN), 48.1 (s, N-CH<sub>2</sub>), 35.9 (s, N-CH<sub>3</sub>), 26.3 (s, N-CH<sub>2</sub>-CH<sub>2</sub>), 13.7 (s, N-CH<sub>2</sub>-CH<sub>2</sub>-CH<sub>2</sub>)

### 1-Butyl-3-methylimidazolium levulinate, [C<sub>1</sub>C<sub>4</sub>Im][Lev]<sup>15</sup>

Sodium levulinate (32.9 g, 238 mmol) was dissolved in 50 mL of water and [C<sub>1</sub>C<sub>4</sub>Im][Cl] (34.4 g, 197 mmol) was dissolved in 170 mL of dichloromethane. The aqueous phase was added dropwise to the organic phase under strong stirring, at 30°C. The mixture was left stirring during 60-70h at 30°C. After separating the two phases and drying the aqueous one, a dark viscous fluid was obtained. Less than 4 mL of product were recovered. From the NMR and HRMS results we estimated a minimum 75% purity of the product.

<sup>1</sup>H-NMR (400 MHz, CD<sub>2</sub>Cl<sub>2</sub>) δ (ppm): 8.62 (1H, s, N-CH-N), 7.38 (2H, m, N-CH-CH-N), 4.09 (2H, t, N-CH<sub>2</sub>), 3.76 (3H, s, N-CH<sub>3</sub>), 2.67 (2H, t, CH<sub>3</sub>-CO-CH<sub>2</sub>-CH<sub>2</sub>-COO), 2.30 (2H, t, CH<sub>3</sub>-CO-CH<sub>2</sub>-CH<sub>2</sub>-COO), 2.11 (3H, s, CH<sub>3</sub>-CO-CH<sub>2</sub>-CH<sub>2</sub>-COO), 1.74 (2H, m, N-CH<sub>2</sub>-CH<sub>2</sub>), 1.22 (2H, m, N-CH<sub>2</sub>-CH<sub>2</sub>-CH<sub>2</sub>), 0.81 (3H, t, N-CH<sub>2</sub>-CH<sub>2</sub>-CH<sub>2</sub>-CH<sub>3</sub>)

<sup>13</sup>C-NMR (400 MHz, CD<sub>2</sub>Cl<sub>2</sub>) δ: 214.8 (s, CH<sub>3</sub>-CO-CH<sub>2</sub>-CH<sub>2</sub>-COO), 180.7 (s, CH<sub>3</sub>-CO-CH<sub>2</sub>-CH<sub>2</sub>-COO), 135.8 (s, N-CH-N), 123.5 (s, N-CH-CH-N), 122.2 (s, N-CH-CH-N), 49.3 (s, N-CH<sub>2</sub>), 39.4 (s, CH<sub>3</sub>-CO-CH<sub>2</sub>-CH<sub>2</sub>-COO), 35.7 (s, N-CH<sub>3</sub>), 31.2 (s, N-CH<sub>2</sub>-CH<sub>2</sub>), 31.0 (s, CH<sub>3</sub>-CO-CH<sub>2</sub>-CH<sub>2</sub>-COO), 29.3 (s, CH<sub>3</sub>-CO-CH<sub>2</sub>-CH<sub>2</sub>-COO), 18.8 (s, N-CH<sub>2</sub>-CH<sub>2</sub>-CH<sub>2</sub>-CH<sub>3</sub>), 12.7

(s, N-CH<sub>2</sub>-CH<sub>2</sub>-CH<sub>2</sub>-CH<sub>3</sub>)

m/z (Fab+): 139 (100%) [C<sub>4</sub>C<sub>1</sub>Im]<sup>+</sup>, 313 (25%) [(C<sub>4</sub>C<sub>1</sub>Im)<sub>2</sub>Cl]<sup>+</sup>, 393 (20%) [(C<sub>4</sub>C<sub>1</sub>Im)<sub>2</sub>Lev]<sup>+</sup>

### 1-Butyl-3-methylimidazolium tetrachloroaluminate, [C<sub>1</sub>C<sub>4</sub>Im][AlCl<sub>4</sub>]

The ionic liquid [C<sub>1</sub>C<sub>4</sub>Im][AlCl<sub>4</sub>] was produced by addition of the Lewis acid aluminium chloride, to equimolar amount of dry [C<sub>1</sub>C<sub>4</sub>Im][Cl], under inert atmosphere. The reaction is exothermic so the reagents should be added gently under strong stirring. The synthesis is straightforward, but requires great care in reagents purity and proportion for achieving a high purity product.

<sup>1</sup>H-NMR (400 MHz, CD<sub>2</sub>Cl<sub>2</sub>) δ (ppm): 10.76 (1H, s, N-CH-N), 7.64 (2H, m, N-CH-CH-N), 4.31 (2H, t, N-CH<sub>2</sub>), 4.07 (3H, s, N-CH<sub>3</sub>), 1.88 (2H, m, N-CH<sub>2</sub>-CH<sub>2</sub>), 1.35 (2H, m, N-CH<sub>2</sub>-CH<sub>2</sub>-CH<sub>2</sub>), 0.95 (3H, t, N-CH<sub>2</sub>-CH<sub>2</sub>-CH<sub>2</sub>-CH<sub>3</sub>)

<sup>13</sup>C-NMR (400 MHz, CD<sub>2</sub>Cl<sub>2</sub>) δ (ppm): 138.2 (s, N-CH-N), 123.4 (s, N-CH-CH-N), 121.9 (s, N-CH-CH-N), 49.5 (s, N-CH<sub>2</sub>), 36.3 (s, N-CH<sub>3</sub>), 32.0 (s, N-CH<sub>2</sub>-CH<sub>2</sub>), 19.4 (s, N-CH<sub>2</sub>-CH<sub>2</sub>-CH<sub>2</sub>), 13.2 (s, N-CH<sub>2</sub>-CH<sub>2</sub>-CH<sub>2</sub>-CH<sub>3</sub>)

<sup>27</sup>Al-NMR (400 MHz, CD<sub>2</sub>Cl<sub>2</sub>) δ (ppm): 103.9 (s, Al)

## Synthesis of carboxylate and dicyanamide-based ionic liquids

A series of syntheses was attempted in order to produce ionic liquids with the dicyanamide anion and anions constituted by a carboxylate derivative (table 2.6). Because these ionic liquids are hydrophilic, their synthesis tends to be more complicated, since it becomes harder to separate reagents and products.<sup>1</sup> For this reason a method using the silver salt of the desired anion is commonly used, in order to force the formation of the ionic liquid by precipitation of silver chloride.<sup>1</sup> However, the high price of the reagents along with the presence of silver in the products urged the search for new synthetic paths. It is important to mention the conditions and procedures that failed to produce a pure or quantitative amount of ionic liquid during this search. The reagents used for these syntheses are described in tables 2.4 and 2.7.

For some of the syntheses, a formation of a precipitate was observed after the drying of the ionic liquid, which confirmed that it contained impurities. In other cases, the <sup>1</sup>H, <sup>13</sup>C and/or HRMS results confirmed the presence of several products or halides.

Table 2.6 - Representation, name and abbreviation of the ionic liquids synthesized by an attempted two-step procedure

Cation	Anion	Name	Abbreviation
		1-butyl-3-methylimidazolium dicyanamide	[C <sub>1</sub> C <sub>4</sub> Im][DCA]
		1-butyl-3-methylimidazolium propionate	[C <sub>1</sub> C <sub>4</sub> Im][Pro]
		1-butyl-3-methylimidazolium isobutyrate	[C <sub>1</sub> C <sub>4</sub> Im][Iso]
		1-butyl-3-methylimidazolium levulinate	[C <sub>1</sub> C <sub>4</sub> Im][Lev]
		1-hexyl-3-methylimidazolium levulinate	[C <sub>1</sub> C <sub>6</sub> Im][Lev]

Table 2.7 - Reagents used in the metathesis step (except if already mentioned in table 2.4), for attempted synthesis, along with purity and supplier

Reagent	Purity	Supplier
Sodium propionate	-	LMOPS*
Sodium isobutyrate	-	LMOPS*
Levulinic acid	-	LMOPS*
Silver oxide	99%	Sigma-Aldrich
Potassium hydroxide	90%	Sigma-Aldrich

\*Kindly provided by the laboratory LMOPS, Lyon, France

### 1-Butyl-3-methylimidazolium dicyanamide, [C<sub>1</sub>C<sub>4</sub>Im][DCA]

The first attempt to synthesize [C<sub>1</sub>C<sub>4</sub>Im][DCA] consisted in using the same procedure as described for the synthesis of the NTf<sub>2</sub>-based ionic liquids, but using sodium dicyanamide. After the organic phase was dried, we observed a formation of a precipitate. The mixture was filtered and thoroughly purified using the two purification techniques described for the synthesis of NTf<sub>2</sub>-based ionic liquids. A small amount of lightly yellow liquid was obtained, and later a formation of a precipitate was observed.

The second attempt was based in the publication by Brandt *et al.*<sup>16</sup> It consists in forming silver dicyanamide by adding an aqueous solution of silver nitrate to an aqueous solution of sodium dicyanamide. The silver dicyanamide is then added to [C<sub>1</sub>C<sub>4</sub>Im][Cl], in order to form the desired product. The resulting mixture was filtered and the liquid phase purified by continuous extraction with dichloromethane for 3 days. The dichloromethane phase was isolated and the solvent removed under vacuum. A white solid was obtained and not the expected ionic liquid.

### 1-Butyl-3-methylimidazolium isobutyrate, [C<sub>1</sub>C<sub>4</sub>Im][Iso]

The first attempt to synthesize this ionic liquid consisted in dissolving [C<sub>1</sub>C<sub>4</sub>Im][Cl] in dry dichloromethane and slowly adding the sodium isobutyrate under

strong stirring for one week. Then, dichloromethane was added and the mixture was filtered. The liquid phase was dried and a dark yellow oily phase was obtained. Dry dichloromethane was added and a formation of two phases was observed. The solution was filtered through celite and dried. The resulting liquid contained a precipitate.

The second procedure adopted was the same as described for the synthesis of [C<sub>1</sub>C<sub>4</sub>Im][Lev], except the sodium isobutyrate was dissolved in water at 40°C and the reaction was left under stirring for 4 days. A 3 phase mixture was obtained. From the aqueous phase, an oily yellow liquid was obtained, containing a precipitate.

The third attempt consisted in using the same patented procedure<sup>14</sup> used for [C<sub>1</sub>C<sub>4</sub>Im][DCA], but the yield was not quantitative.

### **1-Butyl-3-methylimidazolium propionate, [C<sub>1</sub>C<sub>4</sub>Im][Pro]**

The synthesis was attempted using the same patented procedure<sup>14</sup> used for [C<sub>1</sub>C<sub>4</sub>Im][DCA], but the yield and purity were poor.

### **1-Butyl-3-methylimidazolium levulinate, [C<sub>1</sub>C<sub>4</sub>Im][Lev]**

The first synthesis attempt consisted in dissolving [C<sub>1</sub>C<sub>4</sub>Im][Cl] in dry dichloromethane and slowly add the sodium levulinate under strong stirring overnight. Water was then added to the mixture and separation by continuous extraction was performed during 4 days. The organic phase was dried, diluted in dry acetone and left stirring under inert atmosphere overnight. The solution was then filtrated through celite. After drying, an orange oily liquid was obtained.

The second attempt was based in the publication by Yokoseki *et al.*<sup>17</sup> It consisted in the *in situ* production of silver levulinate, to which a solution of [C<sub>1</sub>C<sub>4</sub>Im][Cl] is added. However, after purification, the yield was very low and the product was black, sign that there was still silver present.

In the third attempt the production of potassium levulinate was performed *in situ*, using levulinic acid and potassium hydroxide. Then a solution of [C<sub>1</sub>C<sub>4</sub>Im][Cl] is added and the mixture heated. The water was removed and an oily yellow liquid with precipitate was obtained, even after purification.

The fourth attempt consisted in using the same patented procedure<sup>14</sup> used for [C<sub>1</sub>C<sub>4</sub>Im][DCA], but the yield and purity were poor.

### **1-Hexyl-3-methylimidazolium levulinate, [C<sub>1</sub>C<sub>6</sub>Im][Lev]**

The synthesis was attempted using the same patented procedure<sup>14</sup> used for [C<sub>1</sub>C<sub>4</sub>Im][DCA], but the yield was not quantitative.

## 2.4 Ionic liquid and metallic salt solutions

Three metallic salt solutions were prepared using 1-benzyl-3-methylimidazolium bis(trifluoromethanesulfonyl)imide,  $[\text{C}_1(\text{CH}_2\text{C}_6\text{H}_5)\text{Im}][\text{NTf}_2]$  with lithium (I), nickel (II) and copper (II)  $\text{NTf}_2^-$  salts. The solutions were prepared by adding the salts to the previously dried ionic liquid, at room temperature. The resulting solutions were kept under vacuum and stirring overnight before use.

Several solutions were prepared for each metallic salt- $[\text{C}_1(\text{CH}_2\text{C}_6\text{H}_5)\text{Im}][\text{NTf}_2]$  combination:  $0.33 \text{ mol L}^{-1}$  (molar fraction 0.091) and  $2 \text{ mol L}^{-1}$  (molar fraction 0.38) solutions with  $\text{LiNTf}_2$ ;  $0.18 \text{ mol L}^{-1}$  (molar fraction 0.052),  $0.5 \text{ mol L}^{-1}$  (molar fraction 0.13) and  $2 \text{ mol L}^{-1}$  (molar fraction 0.38) solutions with  $\text{Ni}(\text{NTf}_2)_2$  and  $0.01 \text{ mol L}^{-1}$  (molar fraction 0.0030) and  $0.13 \text{ mol L}^{-1}$  (molar fraction 0.039) solutions with  $\text{Cu}(\text{NTf}_2)_2$ . The evolution of the solubility of the salts in the ionic liquid at several temperatures was analyzed and recorded with a microscope.

We concluded that the maximum solubility in the ionic liquid is higher than  $2 \text{ mol L}^{-1}$  for the lithium salt, between  $0.5 \text{ mol L}^{-1}$  and  $2 \text{ mol L}^{-1}$  for the nickel salt and lower than  $0.01 \text{ mol L}^{-1}$  for the copper salt, between 30 and  $90^\circ\text{C}$ , in  $[\text{C}_1(\text{CH}_2\text{C}_6\text{H}_5)\text{Im}][\text{NTf}_2]$ .

## B. Physicochemical characterization

We have measured the density and viscosity of several ionic liquids and ionic liquid solutions. Measurements of density variation with temperature are necessary for determination of the volume of ionic liquid in the solubility measurements and can also give indications on the purity of the sample. Viscosity is a measure of the internal fluid friction, *i.e.* the resistance to movement of one layer of liquid in relation to another layer. The greater the friction, the greater the force required to cause this movement, which is called shear. If the viscosity of the fluid is independent of the applied shear rate, the fluid is designated as Newtonian, if not it is called non-Newtonian. From an application point of view, viscosity is a key factor since it affects diffusion, pump costs and power requirements for stirring.<sup>18,19,20,38</sup>

## 2.5 Density measurement

Density measurements were performed using two models of U-shaped vibrating-tube densimeters from Anton Paar; DMA 512P and DMA 5000 M, operating in a static mode. The characteristic frequency of the vibrating tube that contains the sample will change according to the density of the sample. The density of the sample is determined by comparison of the period of oscillation of the tube and a reference oscillator.

The DMA 512P densimeter allows the measurement of densities from 263 K to 423 K and from atmospheric pressure up to 30 MPa. This densimeter was calibrated with 4 reference fluids in order to correlate vibration frequency with density. The fluids were chosen in order to obtain a density measurement range large enough to contain the densities of the ionic liquids, from 684.0 Kg m<sup>-3</sup> to 1493.6 Kg m<sup>-3</sup> at 293 K and 0.1 MPa. The chosen fluids were n-heptane (≥99.5% Fluka), tridistilled water, 2,5-dichlorotoluene (99%, Sigma-Aldrich) and bromobenzene (≥99.5%, Fluka).<sup>21,22</sup> Prior to measurements, the calibration fluids were submitted to at least 3 freeze-pump-thaw cycles for degasification. Before and after each measurement these constants are validated by measuring the density of freshly tridistilled degased water.

The temperature was maintained constant within ±0.01 K by means of a recirculating bath equipped with a PID temperature controller (Julabo FP40-HP). The temperature of the tube was measured by means of a 4 wire 100Ω PRT (TC direct Pt100) with a precision of ±0.02 K. The pressure was measured by means of a Druck precision pressure transmitter PTX 610 with ±0.08% full scale accuracy, working in a pressure range from 0 to 70 MPa. The interface Anton Paar mPDS translates the electric signal from the vibrating tube in an oscillation period and collects the signals from the thermometer and pressure transmitter. A computer acquires the oscillation period, temperature and pressure via an HP VEE program. The vibration period of the vibrating tube of the densimeter,  $\tau$ , is related to the density,  $\rho$ , by equation 2.1,

$$\rho = A(T, p)\tau^2 + B(T, p) \quad (2.1)$$

where  $A$  and  $B$  are the calibration constants that depend on the temperature and pressure. The DMA 512P densimeter performs with an estimated uncertainty in

density and temperature of  $\pm 0.1 \text{ Kg m}^{-3}$  and  $\pm 0.001 \text{ }^\circ\text{C}$ , respectively. For samples with viscosity values higher than  $15 \text{ mPa}\cdot\text{s}$  a correction is necessary due to take into account the damping of the oscillation of the tube due to the shear forces that occur in viscous liquids. Equation 2.2 is recommended by the manufacturer for the DMA 512P to calculate the correction factor,  $\Delta\rho$ .<sup>23</sup>

$$\frac{\Delta\rho}{\rho} = [-0.5 + 0.45\sqrt{\eta}]10^{-4} \quad (2.2)$$

where  $\Delta\rho$  is the difference between the density measurement obtained,  $\rho$ , and the corrected density due to the effect of viscosity and  $\eta$  is the dynamic viscosity of the sample in  $\text{mPa}\cdot\text{s}$ .

The densimeter Anton Paar, model DMA 5000 M allows the measurement of densities from 273 K to 368 K at atmospheric pressure and was used with the factory calibration, verified before and after each measurement with air and tridistilled degased water. The DMA 5000 densimeter performs with an estimated uncertainty in density and temperature of  $\pm 0.1 \text{ Kg m}^{-3}$  and  $\pm 0.001 \text{ }^\circ\text{C}$ , respectively. The device has a built-in correction for liquids with a viscosity up to  $700 \text{ mPa}\cdot\text{s}$ .

The obtained experimental values for density, along with correction factors for viscosity,  $\Delta\rho$  are reported in table 2.8. All measurements were performed at atmospheric pressure and at temperatures ranging from 283 K to 373 K.

The solutions in  $[\text{C}_1(\text{CH}_2\text{C}_6\text{H}_5)\text{Im}][\text{NTf}_2]$  had the following metallic salt concentrations  $0.33 \text{ mol L}^{-1}$  for  $\text{LiNTf}_2$ ;  $0.18 \text{ mol L}^{-1}$  for  $\text{Ni}(\text{NTf}_2)_2$  and less than  $0.01 \text{ mol L}^{-1}$  for  $\text{Cu}(\text{NTf}_2)_2$ .

Table 2.8 - Experimental values for corrected densities,  $\rho$ , of the studied ionic liquids and ionic liquid solutions, for temperatures between 283 K to 373 K and at atmospheric pressure, and correction factor,  $\Delta\rho$ , applied at each temperature

<b>[C<sub>1</sub>(C<sub>2</sub>H<sub>2</sub>CH)Im][NTf<sub>2</sub>]</b>			<b>[C<sub>1</sub>(C<sub>3</sub>H<sub>5</sub>CH<sub>2</sub>)Im][NTf<sub>2</sub>]</b>		
<b>T /K</b>	<b><math>\rho</math> /Kg · m<sup>-3</sup></b>	<b><math>\Delta\rho</math> /Kg · m<sup>-3</sup></b>	<b>T /K</b>	<b><math>\rho</math> /Kg · m<sup>-3</sup></b>	<b><math>\Delta\rho</math> /Kg · m<sup>-3</sup></b>
298.07	1537.8	0.5	283.59	1482.5	0.6
312.53	1524.2	0.3	293.19	1472.8	0.4
331.70	1505.3	0.2	302.90	1463.1	0.3
351.00	1486.6	0.1	293.12	1472.8	0.4
370.57	1468.6	0.1	303.14	1463.2	0.3
			313.17	1453.6	0.3
			323.15	1444.1	0.2
			333.19	1434.6	0.2
			343.18	1425.3	0.1
			353.16	1416.2	0.1
<b>[C<sub>1</sub>C<sub>3</sub>CNIIm][NTf<sub>2</sub>]</b>			<b>[C<sub>1</sub>(CH<sub>2</sub>C<sub>6</sub>H<sub>5</sub>)Im][NTf<sub>2</sub>]</b>		
<b>T /K</b>	<b><math>\rho</math> /Kg · m<sup>-3</sup></b>	<b><math>\Delta\rho</math> /Kg · m<sup>-3</sup></b>	<b>T /K</b>	<b><math>\rho</math> /Kg · m<sup>-3</sup></b>	<b><math>\Delta\rho</math> /Kg · m<sup>-3</sup></b>
293.15	1521.0	0.9	282.80	1502.5	1.4
303.15	1511.6	0.7	293.15	1492.1	0.9
313.15	1502.3	0.6	302.75	1483.2	0.6
323.15	1493.0	0.5	302.82	1482.8	0.6
333.15	1483.9	0.4	313.13	1473.0	0.5
343.15	1474.9	0.4	321.87	1464.6	0.4
353.15	1465.9	0.3	333.06	1454.0	0.3
			342.81	1444.9	0.2
			352.90	1435.8	0.2
			363.03	1426.7	0.2
			372.82	1418.1	0.1

<b>[C<sub>1</sub>C<sub>4</sub>Im][DCA]</b>			<b>[C<sub>1</sub>C<sub>3</sub>CNIIm][DCA]</b>		
<b>T /K</b>	<b><math>\rho / \text{Kg} \cdot \text{m}^{-3}</math></b>	<b><math>\Delta\rho / \text{Kg} \cdot \text{m}^{-3}</math></b>	<b>T /K</b>	<b><math>\rho / \text{Kg} \cdot \text{m}^{-3}</math></b>	<b><math>\Delta\rho / \text{Kg} \cdot \text{m}^{-3}</math></b>
293.18	1062.7	0.3	293.15	1155.3	0.6
303.14	1056.3	0.2	303.15	1148.8	0.5
313.14	1050.0	0.2	313.15	1142.4	0.4
323.14	1043.8	0.2	323.15	1136.1	0.4
333.14	1037.6	0.2	333.15	1129.8	0.3
343.14	1031.5	0.1	343.15	1123.6	0.3
353.14	1025.5	0.1	353.15	1117.5	0.2

<b>[C<sub>1</sub>C<sub>4</sub>Im][NTf<sub>2</sub>]</b>			<b>[C<sub>1</sub>C<sub>4</sub>Im][C<sub>1</sub>HPO<sub>3</sub>]</b>		
<b>T /K</b>	<b><math>\rho / \text{Kg} \cdot \text{m}^{-3}</math></b>	<b><math>\Delta\rho / \text{Kg} \cdot \text{m}^{-3}</math></b>	<b>T /K</b>	<b><math>\rho / \text{Kg} \cdot \text{m}^{-3}</math></b>	<b><math>\Delta\rho / \text{Kg} \cdot \text{m}^{-3}</math></b>
293.15	1440.3	0.5	293.15	1147.5	0.8
303.15	1430.7	0.4	303.15	1141.1	0.7
313.15	1421.1	0.3	313.15	1134.7	0.6
323.15	1411.7	0.3	323.15	1128.4	0.5
333.15	1402.3	0.2	333.15	1122.1	0.4
343.15	1392.9	0.2	343.15	1115.9	0.4
353.15	1383.7	0.2	353.15	1109.7	0.3

<b>[C<sub>1</sub>C<sub>4</sub>Im][Lev]</b>			<b>[C<sub>1</sub>(CH<sub>2</sub>C<sub>6</sub>H<sub>5</sub>)Im][NTf<sub>2</sub>]+ 0.33 mol L<sup>-1</sup> LiNTf<sub>2</sub></b>		
<b>T /K</b>	<b><math>\rho / \text{Kg} \cdot \text{m}^{-3}</math></b>	<b><math>\Delta\rho / \text{Kg} \cdot \text{m}^{-3}</math></b>	<b>T /K</b>	<b><math>\rho / \text{Kg} \cdot \text{m}^{-3}</math></b>	<b><math>\Delta\rho / \text{Kg} \cdot \text{m}^{-3}</math></b>
303.11	1094.5	1.8	283.58	1522.5	1.7
313.17	1089.1	1.2	293.22	1513.0	1.1
323.22	1083.4	0.8	302.85	1504.0	0.7
333.17	1077.4	0.6	312.48	1494.4	0.5
			322.30	1484.7	0.4
			331.92	1475.5	0.3
			343.13	1464.8	0.3
			353.19	1455.4	0.2
			362.56	1447.5	0.2
			372.60	1437.8	0.1

$[\text{C}_1(\text{CH}_2\text{C}_6\text{H}_5)\text{Im}][\text{NTf}_2] + 0.18 \text{ mol L}^{-1} \text{ Ni}(\text{NTf}_2)_2$			$[\text{C}_1(\text{CH}_2\text{C}_6\text{H}_5)\text{Im}][\text{NTf}_2] + < 0.01 \text{ mol L}^{-1} \text{ Cu}(\text{NTf}_2)_2$		
T /K	$\rho / \text{Kg} \cdot \text{m}^{-3}$	$\Delta\rho / \text{Kg} \cdot \text{m}^{-3}$	T /K	$\rho / \text{Kg} \cdot \text{m}^{-3}$	$\Delta\rho / \text{Kg} \cdot \text{m}^{-3}$
283.96	1531.8	1.7	282.80	1502.4	1.4
293.24	1522.3	1.1	293.15	1492.1	0.9
302.88	1512.8	0.8	302.75	1483.1	0.6
312.46	1503.4	0.6	302.82	1482.8	0.6
323.16	1492.9	0.4	313.13	1473.0	0.5
333.40	1483.0	0.3	321.87	1464.6	0.4
343.19	1473.6	0.3	333.06	1454.0	0.3
353.46	1464.0	0.2	342.81	1444.9	0.2
363.26	1454.8	0.2	352.90	1435.8	0.2
373.09	1445.7	0.1	363.03	1426.7	0.2
			372.82	1418.1	0.1

The corrected values of density for each ionic liquid were linearly fitted as a function of temperature according to equation 2.3,

$$\rho(\text{Kgm}^{-3}) = aT(\text{K}) + b \quad (2.3)$$

The results of the fitting are presented in table 2.9.

The variation with temperature of the corrected density of several ionic liquids and ionic liquid solutions is presented in figure 2.1.

The correction factors for viscosity cause a decrease in the density values between 0.02% to 0.07% at 293 K, except for  $[\text{C}_1\text{C}_4\text{Im}][\text{Lev}]$ , which presents a correction factor of 0.2% at 303 K. The correction decreases with the temperature, reaching 0.06% for  $[\text{C}_1\text{C}_4\text{Im}][\text{Lev}]$  at 333 K and between 0.007% and 0.03% at 353 K for all other ionic liquids. Similar density correction factors were found for built-in correction and the ones calculated using equation 2.2, for the same ionic liquid.

Table 2.9 - Parameters  $a$  and  $b$  of the fitting of corrected experimental densities of ionic liquids, along with the standard deviation of each fit between the temperatures of 293 K and 353 K at atmospheric pressure

Ionic Liquid	$a$	$b$	Dev (%)
[C <sub>1</sub> (C <sub>2</sub> H <sub>2</sub> CH)Im][NTf <sub>2</sub> ]	-0.95892	1823.6	0.02
[C <sub>1</sub> (C <sub>3</sub> H <sub>5</sub> CH <sub>2</sub> )Im][NTf <sub>2</sub> ]	-0.95119	1751.7	0.02
[C <sub>1</sub> C <sub>3</sub> CNIIm][NTf <sub>2</sub> ]	-0.91779	1789.8	0.01
[C <sub>1</sub> (CH <sub>2</sub> C <sub>6</sub> H <sub>5</sub> )Im][NTf <sub>2</sub> ]	-0.93788	1766.9	0.03
[C <sub>1</sub> C <sub>4</sub> Im][DCA]	-0.62028	1244.3	0.01
[C <sub>1</sub> C <sub>3</sub> CNIIm][DCA]	-0.62915	1339.5	0.01
[C <sub>1</sub> C <sub>4</sub> Im][NTf <sub>2</sub> ]	-0.91813	1692.9	0.01
[C <sub>1</sub> C <sub>4</sub> Im][C <sub>1</sub> HPO <sub>3</sub> ]	-0.62951	1331.9	0.01
[C <sub>1</sub> C <sub>4</sub> Im][Lev]	-0.57012	1267.5	0.02
[C <sub>1</sub> (CH <sub>2</sub> C <sub>6</sub> H <sub>5</sub> )Im][NTf <sub>2</sub> ] + 0.33 M LiNTf <sub>2</sub>	-0.95203	1792.0	0.03
[C <sub>1</sub> (CH <sub>2</sub> C <sub>6</sub> H <sub>5</sub> )Im][NTf <sub>2</sub> ] + 0.18 M Ni(NTf <sub>2</sub> ) <sub>2</sub>	-0.96526	1805.2	0.02
[C <sub>1</sub> (CH <sub>2</sub> C <sub>6</sub> H <sub>5</sub> )Im][NTf <sub>2</sub> ] + < 0.01 M Cu(NTf <sub>2</sub> ) <sub>2</sub>	-0.93770	1766.9	0.03

We observe that the ionic liquid with the highest density at 313 K is [C<sub>1</sub>(C<sub>2</sub>H<sub>2</sub>CH)Im][NTf<sub>2</sub>] > [C<sub>1</sub>C<sub>3</sub>CNIIm][NTf<sub>2</sub>] > [C<sub>1</sub>(CH<sub>2</sub>C<sub>6</sub>H<sub>5</sub>)Im][NTf<sub>2</sub>] > [C<sub>1</sub>(C<sub>3</sub>H<sub>5</sub>CH<sub>2</sub>)Im][NTf<sub>2</sub>] > [C<sub>1</sub>C<sub>4</sub>Im][NTf<sub>2</sub>] > [C<sub>1</sub>C<sub>6</sub>Im][NTf<sub>2</sub>] > [C<sub>1</sub>C<sub>8</sub>Im][NTf<sub>2</sub>] > [C<sub>1</sub>C<sub>3</sub>CNIIm][DCA] > [C<sub>1</sub>C<sub>4</sub>Im][C<sub>1</sub>HPO<sub>3</sub>] > [C<sub>1</sub>C<sub>4</sub>Im][Lev] > [C<sub>1</sub>C<sub>4</sub>Im][DCA].

As expected, we observe that the density of ionic liquids is closely related to its molar mass (ionic liquids with heavier atoms are found to be denser). Density is strongly influenced by the anion type and decreases with the increase of the alkyl side chain length.<sup>24</sup> For example, the density increases from [C<sub>1</sub>C<sub>4</sub>Im][NTf<sub>2</sub>] to [C<sub>1</sub>C<sub>3</sub>CNIIm][NTf<sub>2</sub>], from [C<sub>1</sub>C<sub>3</sub>CNIIm][DCA] to [C<sub>1</sub>C<sub>3</sub>CNIIm][NTf<sub>2</sub>] and from [C<sub>1</sub>C<sub>4</sub>Im][NTf<sub>2</sub>] to [C<sub>1</sub>C<sub>8</sub>Im][NTf<sub>2</sub>]. Adding metallic salts to an ionic causes an increase its density. The increase was up to 2% for the salt types and concentrations studied.

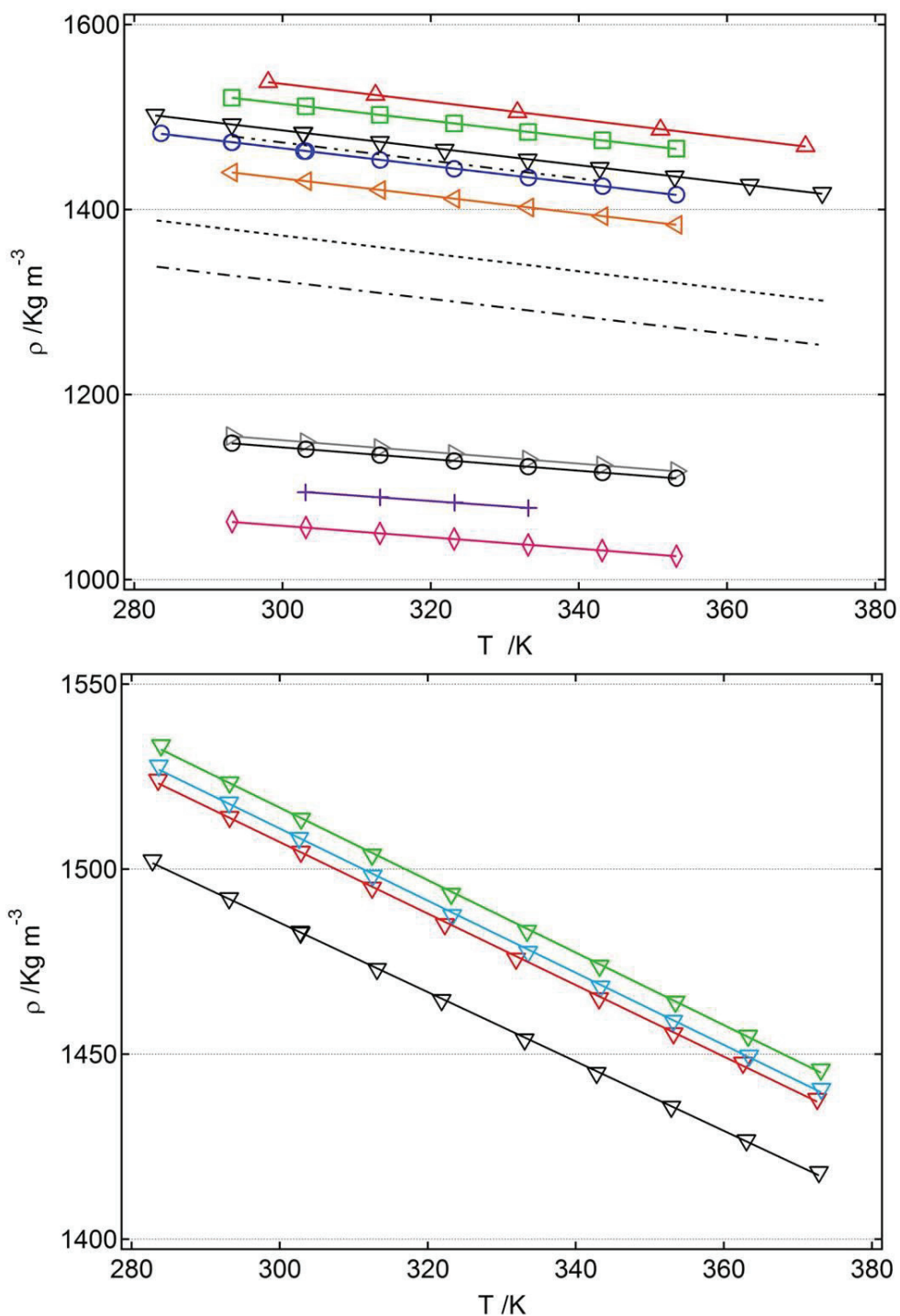


Figure 2.1 - Experimental density of ionic liquids (top) and ionic liquid solutions (bottom):  $\triangle$ ,  $[C_1(C_2H_2CH)Im][NTf_2]$ ;  $\square$ ,  $[C_1C_3CNIm][NTf_2]$ ;  $\nabla$ ,  $[C_1(CH_2C_6H_5)Im][NTf_2]$ ;  $\circ$ ,  $[C_1(C_3H_5CH_2)Im][NTf_2]$ ;  $\triangleleft$ ,  $[C_1C_4Im][NTf_2]$ ;  $\triangleright$ ,  $[C_1C_3CNIm][DCA]$ ;  $\circ$ ,  $[C_1C_4Im][C_1HPO_3]$ ;  $+$ ,  $[C_1C_4Im][Lev]$ ;  $\diamond$ ,  $[C_1C_4Im][DCA]$  with the temperature, corrected for viscosity.  $\dots\dots\dots$ ,  $[C_1C_3Im][NTf_2]$ <sup>25</sup>;  $-\cdot-\cdot-\cdot-$ ,  $[C_1C_6Im][NTf_2]$ <sup>26</sup>;  $-\cdot-\cdot-\cdot-$ ,  $[C_1C_8Im][NTf_2]$ <sup>26</sup>;  $\nabla$ ,  $[C_1(CH_2C_6H_5)Im][NTf_2] + 0.33 \text{ mol L}^{-1} \text{ LiNTf}_2$ ;  $\nabla$ ,  $[C_1(CH_2C_6H_5)Im][NTf_2] + 0.18 \text{ mol L}^{-1} \text{ Ni(NTf}_2)_2$  and  $\nabla$ ,  $[C_1(CH_2C_6H_5)Im][NTf_2] + < 0.01 \text{ mol L}^{-1} \text{ Cu(NTf}_2)_2$

Group contribution models have been developed for the prediction of the volumetric properties of ionic liquids.<sup>27,28,29</sup> The molar volume of an ionic liquid can be calculated as the sum of the effective molar volumes of the component anions, at a given temperature, as observed by Canongia Lopes *et al.*<sup>30</sup> Based on this observation, Jacquemin *et al.*<sup>27</sup> developed a group contribution model that uses the sum of the effective molar volume of the component ions to predict the molar volume of several ionic liquids, as a function of temperature, with a  $\pm 0.5\%$  uncertainty. The densities of the previously mentioned ionic liquids were calculated using this tool. The structure of the cation of the ionic liquid is decomposed in several simple groups, each having their contribution for the molar volume of the cation. For  $[\text{C}_1(\text{C}_3\text{H}_5\text{CH}_2)\text{Im}][\text{NTf}_2]$  we consider that the molar volume of the cation,  $V_{[\text{C}_1(\text{C}_3\text{H}_5\text{CH}_2)\text{Im}][\text{NTf}_2]}$ , is equal to:

$$V_{[\text{C}_1(\text{C}_3\text{H}_5\text{CH}_2)\text{Im}][\text{NTf}_2]} = V_{[\text{C}_1\text{C}_2\text{Im}]} + V_{-\text{CH}_=} + V_{=\text{CH}_2} \quad (2.4)$$

Where  $V_{[\text{C}_1\text{C}_2\text{Im}]}$ ,  $V_{-\text{CH}_=}$  and  $V_{=\text{CH}_2}$  are the contributions of the 1-ethyl-2-methylimidazolium cation and the  $-\text{CH}_2=$  and the terminal  $=\text{CH}_2$  groups of the alkyl chain of the cation, respectively. The molar volume of each group as a function of temperature is expressed by<sup>27</sup>:

$$V_{\text{group}}(T) = \sum_{i=0}^2 C_i (T - 298)^i \quad (2.5)$$

where the parameters  $C_i$  are determined from experimental densities.

Table 2.10 - Parameters  $C_i$  associated with equation 2.5, used to predict the variation with temperature of the molar volume contribution of an ion, at  $10^5$  Pa

Group	$C_0 / \text{cm}^3 \cdot \text{mol}^{-1}$	$10^3 C_1 / \text{cm}^3 \cdot \text{mol}^{-1} \cdot \text{K}^{-1}$	$10^6 C_2 / \text{cm}^3 \text{mol}^{-1} \cdot \text{K}^{-2}$
[C <sub>1</sub> C <sub>1</sub> Im]	84.12	1.516	490.3
[C <sub>1</sub> C <sub>2</sub> Im]	100.0	69.55	29.96
[C <sub>1</sub> C <sub>3</sub> Im]	117.2	42.54	1231
[C <sub>1</sub> C <sub>4</sub> Im]	134.3	88.90	43.04
[C <sub>1</sub> (CH <sub>2</sub> C <sub>6</sub> H <sub>5</sub> )Im]	146.7	146.9	675.9
[NTf <sub>2</sub> ]	157.6	104.3	50.52
[DCA]	59.39	-11.18	551.8
[C <sub>1</sub> (C <sub>2</sub> H <sub>2</sub> CH)Im] <sup>a</sup>	103.4	58.24	58.03
[C <sub>1</sub> (C <sub>3</sub> H <sub>5</sub> CH <sub>2</sub> )Im] <sup>a</sup>	126.7	79.72	75.20
[C <sub>1</sub> C <sub>3</sub> CNIm] <sup>a</sup>	126.2	67.38	58.69
[C <sub>1</sub> HPO <sub>3</sub> ] <sup>a</sup>	70.43	23.70	21.07
[Lev] <sup>a</sup>	97.46	31.45	21.18

<sup>a</sup> Determined in this work

It wasn't possible to predict the molar volume of [C<sub>1</sub>C<sub>4</sub>Im][C<sub>1</sub>HPO<sub>3</sub>], [C<sub>1</sub>(C<sub>2</sub>H<sub>2</sub>CH)Im][NTf<sub>2</sub>], [C<sub>1</sub>C<sub>3</sub>CNIm][NTf<sub>2</sub>], [C<sub>1</sub>(C<sub>3</sub>H<sub>5</sub>CH<sub>2</sub>)Im][NTf<sub>2</sub>], and [C<sub>1</sub>C<sub>4</sub>Im][Lev], due to lack of information on the molar volume contribution of the functional groups of the alkyl chain or on the levulinate or methylphosphite anions. In these cases, their contribution parameters were calculated and are reported in table 2.10.

It was possible to predict the molar volumes of [C<sub>1</sub>(CH<sub>2</sub>C<sub>6</sub>H<sub>5</sub>)Im][NTf<sub>2</sub>], [C<sub>1</sub>C<sub>4</sub>Im][DCA], [C<sub>1</sub>C<sub>3</sub>CNIm][DCA] and [C<sub>1</sub>C<sub>4</sub>Im][NTf<sub>2</sub>]. For [C<sub>1</sub>(CH<sub>2</sub>C<sub>6</sub>H<sub>5</sub>)Im][NTf<sub>2</sub>], the deviations from the predicted values starting from +0.37% at 283K to -2.33% at 373 K. For [C<sub>1</sub>C<sub>4</sub>Im][DCA], the deviation from the predicted values starts from +0.28% at 293 K to +1.53% at 353 K. In both cases, the deviations at lower temperatures are coherent with the 0.5% uncertainty claimed for this prediction method. At higher temperatures, the deviations increase but are still acceptable. These deviations are due to the few data available at higher temperatures for the construction of the model. For [C<sub>1</sub>C<sub>3</sub>CNIm][DCA], the data obtained for his NTf<sub>2</sub>-based counterpart were used to predict its molar volume. The values predicted agree with the measured ones within ±1.6% in the whole temperature range. For [C<sub>1</sub>C<sub>4</sub>Im][NTf<sub>2</sub>], a constant deviation of +0.1% is found for the whole temperature

range, well within the uncertainty of the model, as expected for an ionic liquid with a good amount of density data available.

The comparison between the density results obtained and the results from the literature will allow some insight about the accuracy of our results, experimental procedure and purity of the samples. The relative deviations between the experimental data and the data reported in the literature were calculated and are presented in figures 2.2 and 2.3.

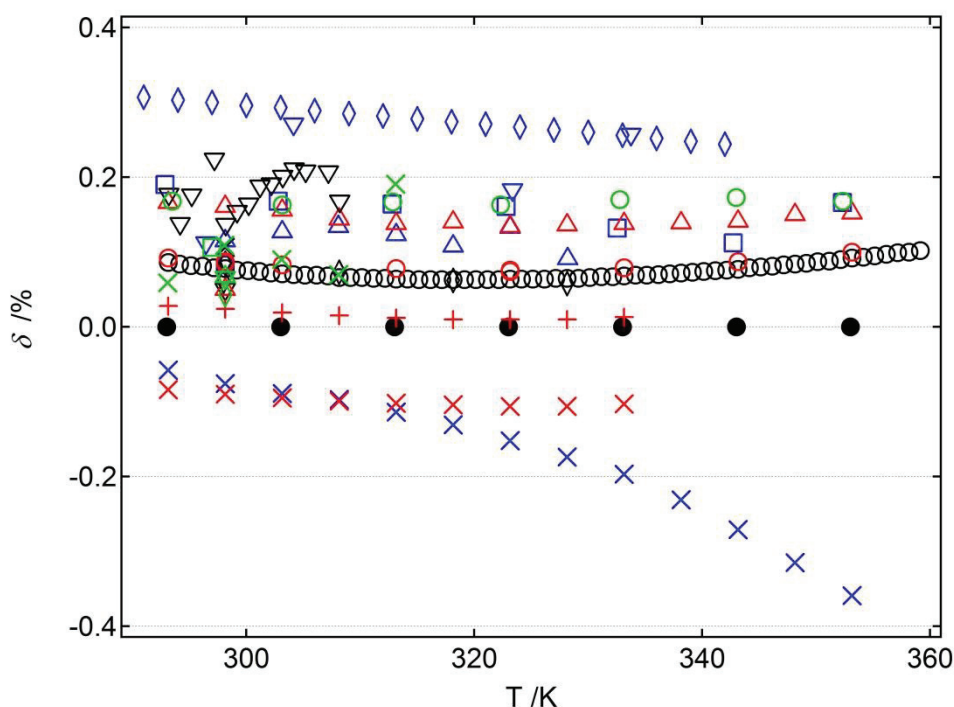


Figure 2.2 - Relative deviations between the experimental density of the ionic liquid  $[C_1C_4Im][NTf_2]$  in this work and data reported in the literature as a function of temperature. Measurement method, water, halide contents and purity of the ionic liquid are depicted in table 2.11. ●, this work, deviation of the experimental densities from the values obtained using equation 2.3. X, Oliveira *et al.*<sup>31</sup>; ▽, Corderi and González<sup>32</sup>; △, Seoane, González and González<sup>33</sup>; O, Castro *et al.*<sup>34</sup>; ◇, Wandschneider *et al.*<sup>35</sup>; △, Azevedo *et al.*<sup>36</sup>; ○, Andreatta<sup>37</sup>; □, Jacquemin *et al.*<sup>38</sup>; ◇, Jacquemin *et al.*<sup>39</sup>; X, Vranes *et al.*<sup>40</sup>; ○, Harris, Kanakubo and Woolf<sup>41</sup>; △, Krummen, Wasserscheid and Gmehling<sup>42</sup>; ▽, Katsuta *et al.*<sup>43</sup>; X, Troncoso *et al.*<sup>44</sup>; +, Troncoso *et al.*<sup>44</sup>; ○, Jacquemin *et al.*<sup>45</sup>; □, Shirota<sup>46</sup>; △, Domínguez<sup>47</sup>; ▽, Geppert-Rybczyńska<sup>48</sup>; X, Tokuda *et al.*<sup>49</sup>; ▽, Fredlake *et al.*<sup>50</sup> and ◇, McHale *et al.*<sup>52</sup>

The amount of halide and water in each  $[C_1C_4Im][NTf_2]$  ionic liquid sample are presented in table 2.11, along with the method used and corresponding measurement uncertainty.

Table 2.11 - Purity, halide and water amount in several [C<sub>1</sub>C<sub>4</sub>Im][NTf<sub>2</sub>] samples in the literature mentioned in figure 2.5, density measurement method used with corresponding uncertainty

Purity /%	Halide amount /ppm	Water amount /ppm	Method	Uncertainty /Kg m <sup>-3</sup>	Reference
99	-	70	vibrating-tube	±0.1	This work
99	-	235	vibrating-tube	±0.5	31
99	<90	10	vibrating-tube	±0.03	32
>99	<100	10	vibrating-tube	±0.03	33
-	200	<120	vibrating-tube	±6	34
-	chloride not detected by the silver nitrate test	<215	vibrating-tube	±0.1	35
-	chloride not detected by the silver nitrate test	<75	vibrating-tube	±0.3	36
-	bromide not detected by capillary electrophoresis	46.3	vibrating-tube	±0.03	37
>99	<50	<50	vibrating-tube	±6	38
>99	<50	<50	vibrating-tube	±1	39
99	-	1	vibrating-tube	±0.07	40
-	chloride not detected by the silver nitrate test	<19	vibrating-tube	±0.05	41
-	-	<100	vibrating-tube	-	42
-	2.3	8	vibrating-tube	±1	43
>99.8	130	-	vibrating-tube	±0.01	44
>99.5	20	-	vibrating-tube	±0.01	44
>99	<50	<50	vibrating-tube	±0.01	45
>99	-	176 to 256	vibrating-tube	±8	46
-	90	10	vibrating-tube	±0.03	47
-	-	39	vibrating-tube	±0.02	48
-	-	<40	vibrating-tube	±1	49
>99	-	460	pycnometer	±1	50
-	<5	96	vibrating-tube	-	52

The large majority of the density results for  $[\text{C}_1\text{C}_4\text{Im}][\text{NTf}_2]$  agree with ours within  $\pm 0.2\%$  and our sample is generally less dense. The density results from Wandschneider *et al.*,<sup>35</sup> Vranes *et al.*,<sup>40</sup> Tokuda *et al.*,<sup>49</sup> and Fredlake *et al.*<sup>50</sup> report densities that greatly deviate from our results when increasing the temperature, to half or twice as much than the initial deviation. This may indicate that the reported measurements present a poor temperature control. Taking into account the reported results that include the purity of the samples and that agree with ours within  $\pm 0.1\%$ , we can estimate that the amount of chloride in our sample between 5 ppm and 200 ppm.

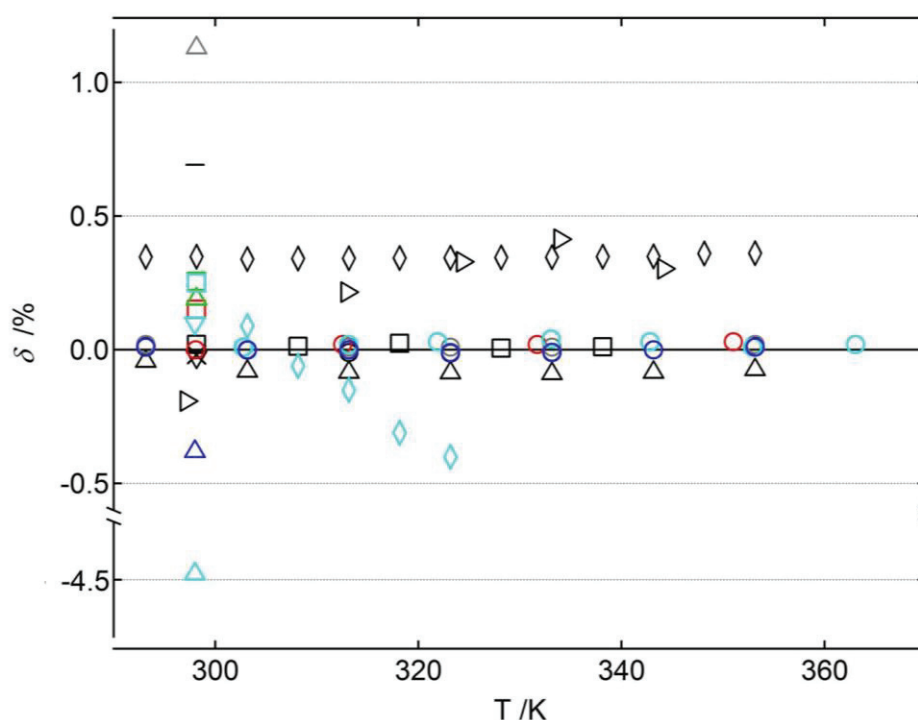


Figure 2.3 - Relative deviations between the experimental density of the ionic liquids  $[\text{C}_1\text{C}_4\text{Im}][\text{DCA}]$  (black symbols),  $[\text{C}_1(\text{C}_2\text{H}_2\text{CH})\text{Im}][\text{NTf}_2]$  (red symbols),  $[\text{C}_1\text{C}_3\text{CNIm}][\text{NTf}_2]$  (green symbols),  $[\text{C}_1\text{C}_3\text{CNIm}][\text{DCA}]$  (grey symbols),  $[\text{C}_1(\text{CH}_2\text{C}_6\text{H}_5)\text{Im}][\text{NTf}_2]$  (light blue symbols) and  $[\text{C}_1\text{C}_4\text{Im}][\text{C}_1\text{HPO}_3]$  (blue symbols) in this work and data reported in the literature as a function of temperature. Measurement method, water, halide contents and purity of the ionic liquids are depicted in table 2.12.  $\circ/\circ/\circ/\circ/\circ/\circ$ , this work, deviation of the experimental densities from the values obtained using equation 2.3.  $\triangleright$ , Fredlake *et al.*<sup>50</sup>;  $\times$ , Stoppa *et al.*<sup>51</sup>;  $\nabla$ , McHale *et al.*<sup>52</sup>;  $\triangle$ , Sánchez *et al.*<sup>53</sup>;  $\diamond$ , Carvalho *et al.*<sup>54</sup>;  $\square$ , Zech *et al.*<sup>55</sup>;  $-$ , Mahurin *et al.*<sup>56</sup>;  $\square$ , Carlisle *et al.*<sup>59</sup>;  $\square$ , Carlisle *et al.*<sup>59</sup>;  $\triangle$ , Zang *et al.*<sup>60</sup>;  $\triangle$ , Zang *et al.*<sup>60</sup>;  $\square$ , Ohlin *et al.*<sup>61</sup>;  $\diamond$ , Dzyuba *et al.*<sup>62</sup>;  $\nabla$ , Mandai *et al.*<sup>57</sup>;  $\triangle$ , Mahurin *et al.*<sup>58</sup> and  $\triangle$ , Zang *et al.*<sup>60</sup>

For the ionic liquids [C<sub>1</sub>C<sub>4</sub>Im][DCA], [C<sub>1</sub>(C<sub>2</sub>H<sub>2</sub>CH)Im][NTf<sub>2</sub>], [C<sub>1</sub>C<sub>3</sub>CNIIm][NTf<sub>2</sub>], [C<sub>1</sub>C<sub>3</sub>CNIIm][DCA], [C<sub>1</sub>(CH<sub>2</sub>C<sub>6</sub>H<sub>5</sub>)Im][NTf<sub>2</sub>] and [C<sub>1</sub>C<sub>4</sub>Im][C<sub>1</sub>HPO<sub>3</sub>], the deviations of the literature from our density results are presented in figure 2.6. The amount of halide and water in each ionic liquid sample are depicted in table 2.12, along with the method used and corresponding measurement uncertainty.

In the case of the ionic liquid [C<sub>1</sub>C<sub>4</sub>Im][DCA], we observe that the results reported by Fredlake *et al.*<sup>50</sup>, Stoppa *et al.*<sup>51</sup>, McHale *et al.*<sup>52</sup>, Sánchez *et al.*<sup>53</sup>, Carvalho *et al.*<sup>54</sup> and Zech *et al.*<sup>55</sup> agree with ours to within  $\pm 0.5\%$ . Fredlake's results present a deviation that increases with the temperature, probably due to a poor temperature control during the measurement. The deviations from Stoppa *et al.*<sup>51</sup>, McHale *et al.*<sup>52</sup>, Sánchez *et al.*<sup>53</sup> and Zech *et al.*<sup>55</sup> results are consistent with the difference in purity between our sample and the authors' samples. Sánchez *et al.*<sup>53</sup> and Zech *et al.*<sup>55</sup> results present a small and constant deviation throughout the temperature range. Carvalho *et al.*<sup>54</sup> data also present a constant deviation from our measurements, but of +0.35%. The result reported by Mahurin *et al.*<sup>56</sup> present the largest deviation, +0.7%. This deviation is hard to explain due to the lack of information about the method used or the purity of the sample. According to these results, we can estimate the amount of halide content in our sample to be around 2000 ppm.

For [C<sub>1</sub>(C<sub>2</sub>H<sub>2</sub>CH)Im][NTf<sub>2</sub>] and [C<sub>1</sub>C<sub>3</sub>CNIIm][NTf<sub>2</sub>] we observe respectively +0.15% and +0.25% deviations from the measurements performed by Carlisle *et al.*<sup>59</sup>, probably due to the low accuracy of the technique used by the authors. For [C<sub>1</sub>C<sub>3</sub>CNIIm][NTf<sub>2</sub>], a +0.19% deviation was obtained when comparing our measurements with the data from Zang *et al.*<sup>60</sup>. Zang *et al.*<sup>60</sup> also measured the density of [C<sub>1</sub>C<sub>3</sub>CNIIm][DCA], for which we obtain a +1.1% deviation from our measurements. These two deviations are harder to explain because the authors make no reference to the method accuracy or to impurities that might be present in the ionic liquid.

Table 2.12 - Purity, halide and water amount in several ionic liquids from this work and in the literature mentioned in figure 2.6, density measurement method used with corresponding uncertainty

Purity /%	Halide amount /ppm	Water amount /ppm	Method	Uncertainty /Kg m <sup>-3</sup>	Reference
<b>[C<sub>1</sub>C<sub>4</sub>Im][DCA]</b>					
98	-	98	vibrating-tube	±0.1	This work
-	<293	5150	pycnometer	±1	50
-	<5000	<50	vibrating-tube	±0.05	51
-	1830	256	vibrating-tube	-	52
>97	-	<680	vibrating-tube	±0.1	53
>99	<100	28	vibrating-tube	±0.5	54
-	2100	80	vibrating-tube	±0.05	55
-	-	-	-	-	56
<b>[C<sub>1</sub>(C<sub>2</sub>H<sub>2</sub>CH)Im][NTf<sub>2</sub>]</b>					
99	-	95	vibrating-tube	±0.1	This work
-	-	<300	volumetric	-	59
<b>[C<sub>1</sub>C<sub>3</sub>CNIm][NTf<sub>2</sub>]</b>					
99	-	45	vibrating-tube	±0.1	This work
-	-	<300	volumetric	-	59
-	-	-	vibrating-tube	-	60
<b>[C<sub>1</sub>C<sub>3</sub>CNIm][DCA]</b>					
99	-	75	vibrating-tube	±0.1	This work
-	-	-	vibrating-tube	-	60
<b>[C<sub>1</sub>(CH<sub>2</sub>C<sub>6</sub>H<sub>5</sub>)Im][NTf<sub>2</sub>]</b>					
99	-	70	vibrating-tube	±0.1	This work
-	-	-	-	-	61
-	-	-	vibrating-tube	-	62
-	-	-	vibrating-tube	-	57
-	-	-	-	±14	58
<b>[C<sub>1</sub>C<sub>4</sub>Im][C<sub>1</sub>HPO<sub>3</sub>]</b>					
99	-	156	vibrating-tube	±0.1	This work
-	-	300	pycnometer	±50	63

For  $[\text{C}_1(\text{CH}_2\text{C}_6\text{H}_5)\text{Im}][\text{NTf}_2]$ , our data were compared with the measurements of Mandai *et al.*,<sup>57</sup> Mahurin *et al.*,<sup>58</sup> Ohlin *et al.*<sup>61</sup> and Dzyuba *et al.*<sup>62</sup> With the exception of the measurements by Mahurin *et al.*<sup>58</sup>, the reported results agree with ours within  $\pm 0.3\%$ . The larger deviation is probably due to poor temperature control during the measurement. The data obtained here are more accurate than any of the measurement presented in the literature for this ionic liquid.

For  $[\text{C}_1\text{C}_4\text{Im}][\text{C}_1\text{HPO}_3]$ , the density results obtained are 0.4% higher than the one reported by Palgunadi *et al.*,<sup>63</sup> as can be expected because the authors used a much less precise method.

For density measurements performed with a vibrating tube element, a viscosity correction in density should be taken into account for highly viscous fluids. Such highly viscous liquid present shear forces that will cause a damping effect in the oscillation or rotation of the moving element. Only a few authors<sup>34,37,44,48,51,53</sup> discuss or take into account this effect, which has a contribution of up to +0.07% in the deviations observed.

## 2.6 Viscosity measurement

All the viscosity measurements were performed with an Anton Paar AMVn rolling ball viscometer at atmospheric pressure and at temperatures between 293.15 K and 373.15 K. The rolling ball technique consists of the measurement of a ball's rolling time in a diagonally mounted glass capillary filled with sample. The rolling time of the ball,  $t_1$ , is related to the viscosity of the fluid,  $\eta$ , by:

$$\eta = K_1(\rho_b - \rho_{IL})t_1 \quad (2.6)$$

where  $K_1$  is the calibration constant of the measuring system,  $\rho_b$  is the density of the ball and  $\rho_{IL}$  is the density of the ionic liquid sample. For each temperature, 3 inclination angles were used, with 12 repetitions each. The applied shear rate is influenced by changing the inclination angle of the capillary. The response of the sample to different shear rates allows to determine if the fluids are Newtonian or non-Newtonian.<sup>64</sup> The temperature was controlled to within 0.01 K and measured with accuracy better than 0.05 K. The falling time is measured within 0.001 sec and with a maximum accuracy of 0.002 sec. The measurements were performed using a 1.8 mm or a 3.0 mm diameter capillary tube that were calibrated as a function of temperature and angle of measurement using standard viscosity oils from Canon; N35, S60, N100 and N350, with approximate viscosity values of 56 mPa s, 105 mPa s, 203 mPa s, and 602 mPa s respectively, at 298.15 K. 2 to 3 mL of sample are necessary to fill the capillaries. The overall uncertainty on the viscosity was evaluated to be lower than 2%.

Table 2.13 - Experimental values for viscosities,  $\eta$ , of the studied ionic liquids, for temperatures between 293 K to 353 K and at atmospheric pressure

<b>[C<sub>1</sub>(C<sub>2</sub>H<sub>2</sub>CH)Im][NTf<sub>2</sub>]</b>		<b>[C<sub>1</sub>(C<sub>3</sub>H<sub>5</sub>CH<sub>2</sub>)Im][NTf<sub>2</sub>]</b>	
<b>T /K</b>	<b><math>\eta</math> / mPa · s</b>	<b>T /K</b>	<b><math>\eta</math> / mPa · s</b>
298.15	57.77	293.15	60.45
313.15	30.99	303.15	39.65
333.15	16.62	313.15	27.52
353.15	10.25	323.15	19.96
373.15	7.000	333.15	14.92
		343.15	11.56
		353.15	9.208

<b>[C<sub>1</sub>C<sub>3</sub>CNIIm][NTf<sub>2</sub>]</b>		<b>[C<sub>1</sub>(CH<sub>2</sub>C<sub>6</sub>H<sub>5</sub>)Im][NTf<sub>2</sub>]</b>	
<b>T /K</b>	<b><math>\eta</math> / mPa · s</b>	<b>T /K</b>	<b><math>\eta</math> / mPa · s</b>
298.15	215.3	293.15	197.8
303.15	161.9	303.15	104.6
313.15	95.20	313.15	62.33
323.15	60.88	323.15	40.34
333.15	41.30	333.15	27.95
353.15	21.78	343.15	20.15
		353.15	15.48

<b>[C<sub>1</sub>C<sub>4</sub>Im][DCA]</b>		<b>[C<sub>1</sub>C<sub>3</sub>CNIIm][DCA]</b>	
<b>T /K</b>	<b><math>\eta</math> / mPa · s</b>	<b>T /K</b>	<b><math>\eta</math> / mPa · s</b>
298.15	29.08	298.15	147.9
303.15	24.60	303.15	112.5
313.15	17.67	313.15	69.01
323.15	13.38	323.15	44.86
333.15	10.46	333.15	31.15
353.15	6.852	353.15	17.29

<b>[C<sub>1</sub>C<sub>4</sub>Im][Lev]</b>		<b>[C<sub>1</sub>C<sub>4</sub>Im][C<sub>1</sub>HPO<sub>3</sub>]</b>	
--------------------------------------------	--	---------------------------------------------------------------------	--

T /K	$\eta / \text{mPa} \cdot \text{s}$	T /K	$\eta / \text{mPa} \cdot \text{s}$
303.15	1441.0	298.15	99.68
313.15	619.6	303.15	72.46
323.15	300.2	313.15	44.32
333.15	165.0	323.15	29.50
		333.15	20.56
		353.15	11.37

$[\text{C}_1(\text{CH}_2\text{C}_6\text{H}_5)\text{Im}][\text{NTf}_2] + 0.33 \text{ mol L}^{-1} \text{ LiNTf}_2$		$[\text{C}_1(\text{CH}_2\text{C}_6\text{H}_5)\text{Im}][\text{NTf}_2] + 0.18 \text{ mol L}^{-1} \text{ Ni}(\text{NTf}_2)_2$	
T /K	$\eta / \text{mPa} \cdot \text{s}$	T /K	$\eta / \text{mPa} \cdot \text{s}$
298.15	200.4	298.15	212.3
303.15	146.8	303.15	154.4
313.15	79.46	313.15	87.40
323.15	51.77	323.15	54.30
333.15	34.69	333.15	36.32
353.15	18.36	353.15	19.26
373.15	11.36	373.15	11.58

$[\text{C}_1(\text{CH}_2\text{C}_6\text{H}_5)\text{Im}][\text{NTf}_2] + < 0.13 \text{ mol L}^{-1} \text{ Cu}(\text{NTf}_2)_2$	
T /K	$\eta / \text{mPa} \cdot \text{s}$
298.15	189.4
303.15	138.6
323.15	54.31
333.15	34.92
353.15	18.37
373.15	11.51

All the ionic liquids and ionic liquid solutions presented the same viscosity for each measurement angle, and are therefore considered to be Newtonian fluids.

The experimental data were fitted as a function of temperature to a Vogel-Fulcher-Tammann (VFT) equation<sup>65</sup>:

$$\eta = C \times T^{1/2} \exp\left(\frac{k}{T - T_0}\right) \quad (2.7)$$

where  $T_0$ ,  $C$  and  $k$  are adjustable parameters.  $T_0$  is sometimes designated as Vogel temperature or ideal glass transition temperature. It corresponds to the temperature at which the viscosity starts to diverge from an Arrhenius type equation and typically lies a few tens of degrees below the glass transition temperature,  $T_g$ .

The Arrhenius equation for viscosity has the form<sup>38</sup>:

$$\eta = \eta_\infty \exp\left(-\frac{E_a}{RT}\right) \quad (2.8)$$

where  $\eta_\infty$ ,  $E_a$  and  $R$  represent viscosity at infinite temperature, the activation energy and the gas constant, respectively. The VFT equation is an extension of the Arrhenius equation and was introduced since the latest could not account for the slight curvature of the  $\ln\eta$  vs  $1/T$  plot (Arrhenius plot of viscosity), typically observed for good glass-forming materials, such as ionic liquids. This departure from linearity of an Arrhenius plot of viscosity, at temperatures close to the glass transition temperature,  $T_g$ , is designated fragility. Fragility is a measure of the sensitivity of the liquid structure to changes in the temperature. Liquids with a VFT type of behavior are more fragile than the ones with an Arrhenius type of behavior. The fitting to the VFT type equation is usually done in a limited temperature range, resulting in the possibility of finding several sets of best fit parameters for the same experimental data. This should be taken into account when trying to extract fit parameters with physical meaning, and the viscosity obtained in the limit  $T \rightarrow T_g$  with the fit parameters should have a reasonable value.<sup>66,67,68,69</sup> However, since our goal was to find the parameters that would simply allow a correlation of the viscosity in the

temperature range, the physical meaning of the parameters was not taken into account. The parameters of the fits are reported in Table 2.14 and the experimental viscosity of several ionic liquids and ionic liquid solutions is presented as a function of the temperature in figures 2.4 and 2.5.

Table 2.14 - Vogel-Fulcher-Tammann equation parameters obtained for the measurements of viscosity,  $\eta$ , of ionic liquids for temperatures between 283 K and 373 K

Ionic liquid	$k(K)$	$C/10^{-3}(mPa \cdot s \cdot K^{-1/2})$	$T_0(K)$	AAD (%)
$[C_1(C_2H_2CH)Im][NTf_2]$	659	11.7	182	0.3
$[C_1(C_3H_5CH_2)Im][NTf_2]$	958	4.38	150	0.2
$[C_1C_3CNIm][NTf_2]$	998	4.70	172	0.7
$[C_1(CH_2C_6H_5)Im][NTf_2]$	644	12.8	199	0.3
$[C_1C_4Im][DCA]$	861	5.53	148	0.7
$[C_1C_3CNIm][DCA]$	906	5.78	174	0.4
$[C_1C_4Im][Lev]$	1196	2.10	190	0.5
$[C_1C_4Im][C_1HPO_3]$	390	12167	219	1.6
$[C_1(CH_2C_6H_5)Im][NTf_2] + 0.33 \text{ M LiNTf}_2$	547	7797	208	2.3
$[C_1(CH_2C_6H_5)Im][NTf_2] + 0.18 \text{ M Ni(NTf}_2)_2$	633	5609	200	0.6
$[C_1(CH_2C_6H_5)Im][NTf_2] + 0.13 \text{ M Cu(NTf}_2)_2$	672	5291	194	1.9

The viscosity of the ionic liquids decreases in the following order:  $[C_1C_4Im][Lev] > [C_1C_3CNIm][NTf_2] > [C_1C_3CNIm][DCA] > [C_1(CH_2C_6H_5)Im][NTf_2] > [C_1C_8Im][NTf_2] > [C_1C_4Im][C_1HPO_3] > [C_1C_6Im][NTf_2] > [C_1(C_2H_2CH)Im][NTf_2] > [C_1C_4Im][NTf_2] > [C_1(C_3H_5CH_2)Im][NTf_2] > [C_1C_4Im][DCA]$ . We observe that for ionic liquids sharing the same anion, the viscosity increases with the increase of the cation alkyl chain length. Taking  $[C_1C_4Im][NTf_2]$  as a reference we observe that changing the anion to  $DCA^-$  or to  $Lev^-$  results in a decrease in viscosity of 33% in the first case and in an increase of up to 36 times in the second, in the temperature range. Substituting the butyl group of  $[C_1C_4Im][NTf_2]$  by propynyl, butenyl, cyanopropyl or benzyl groups causes an average increase in viscosity of 12%, 1%, 2-4 times and 2-3 times, between 298 K and 353 K.

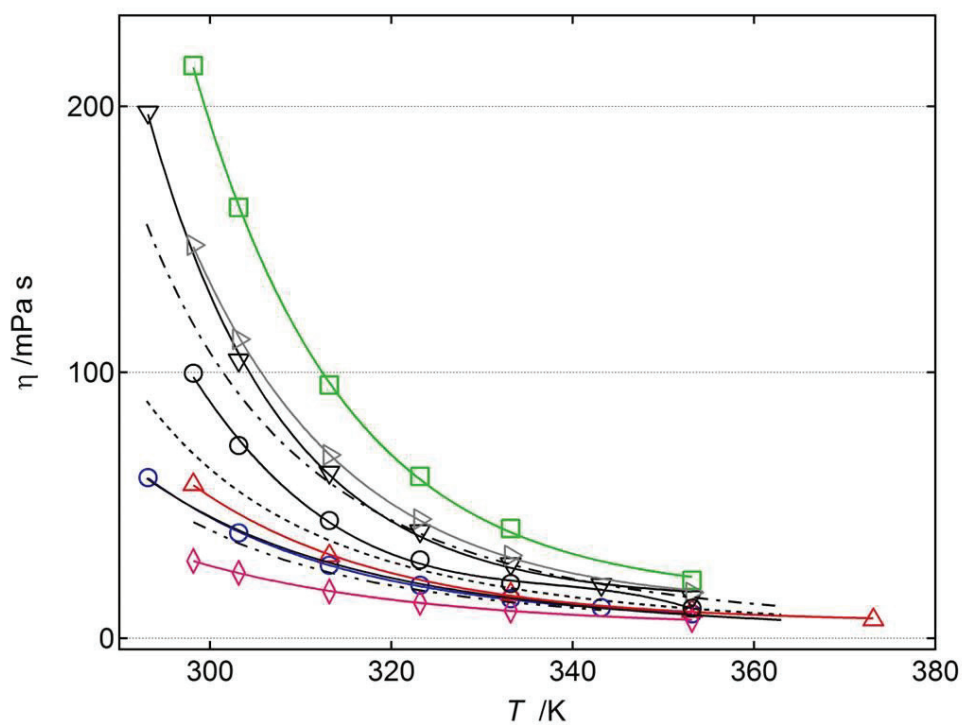
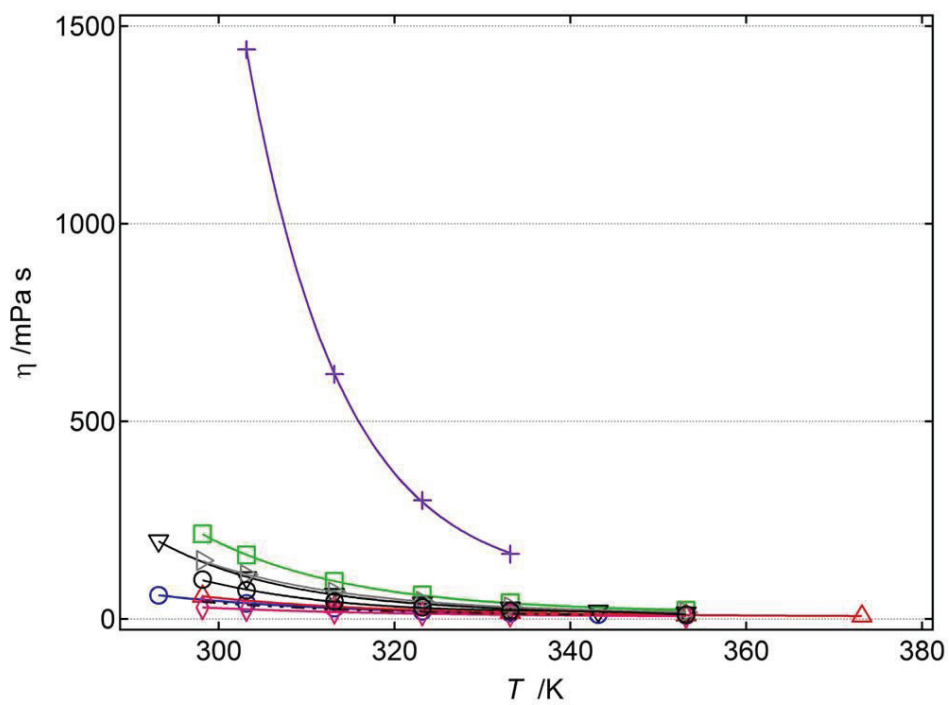


Figure 2.4 - Experimental viscosity of ionic liquids:  $\triangle$ ,  $[\text{C}_1(\text{C}_2\text{H}_2\text{CH})\text{Im}][\text{NTf}_2]$ ;  $\square$ ,  $[\text{C}_1\text{C}_3\text{CNIm}][\text{NTf}_2]$ ;  $\nabla$ ,  $[\text{C}_1(\text{CH}_2\text{C}_6\text{H}_5)\text{Im}][\text{NTf}_2]$ ;  $\circ$ ,  $[\text{C}_1(\text{C}_3\text{H}_5\text{CH}_2)\text{Im}][\text{NTf}_2]$ ;  $\triangleright$ ,  $[\text{C}_1\text{C}_3\text{CNIm}][\text{DCA}]$ ;  $+$ ,  $[\text{C}_1\text{C}_4\text{Im}][\text{Lev}]$ ;  $\circ$ ,  $[\text{C}_1\text{C}_4\text{Im}][\text{C}_1\text{HPO}_3]$ ;  $\diamond$ ,  $[\text{C}_1\text{C}_4\text{Im}][\text{DCA}]$  with the temperature.  $\cdots$ ,  $[\text{C}_1\text{C}_3\text{Im}][\text{NTf}_2]$ <sup>25</sup>;  $\text{---}$ ,  $[\text{C}_1\text{C}_4\text{Im}][\text{NTf}_2]$ <sup>70</sup>;  $\text{---}$ ,  $[\text{C}_1\text{C}_6\text{Im}][\text{NTf}_2]$ <sup>71</sup>;  $\text{---}$ ,  $[\text{C}_1\text{C}_8\text{Im}][\text{NTf}_2]$ <sup>72</sup>

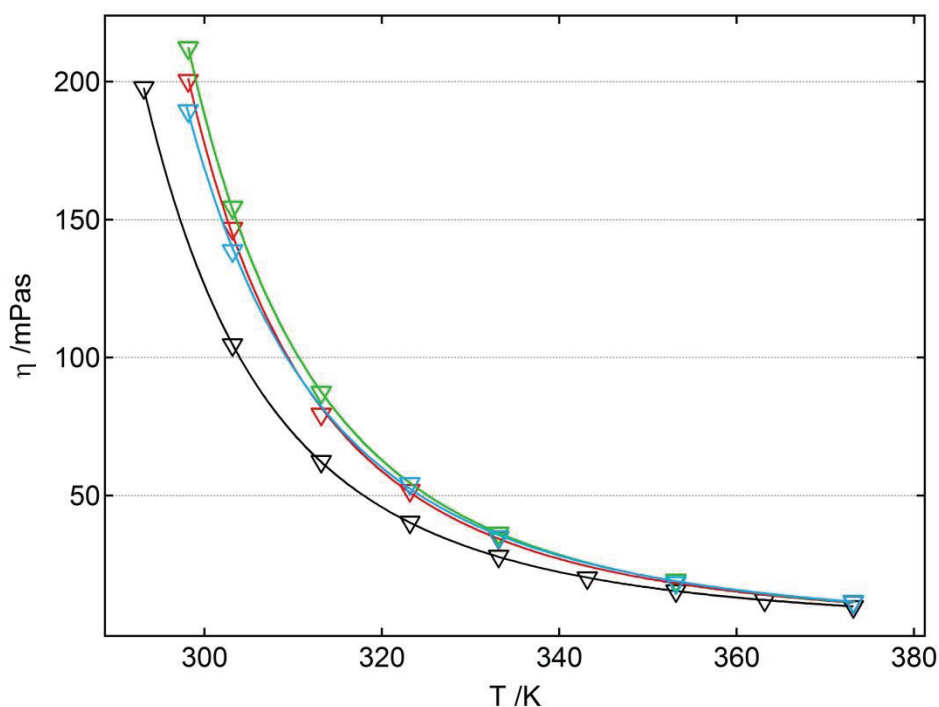


Figure 2.5 - Experimental viscosity of ionic liquids: ▽,  $[C_1(CH_2C_6H_5)Im][NTf_2]$ ; ▽,  $[C_1(CH_2C_6H_5)Im][NTf_2] + 0.33 \text{ mol L}^{-1} LiNTf_2$ ; ▽,  $[C_1(CH_2C_6H_5)Im][NTf_2] + 0.18 \text{ mol L}^{-1} Ni(NTf_2)_2$  and ▽,  $[C_1(CH_2C_6H_5)Im][NTf_2] + < 0.01 \text{ mol L}^{-1} Cu(NTf_2)_2$

Substituting the alkyl chain of the cation of  $[C_1C_8Im][NTf_2]$  from octyl to benzyl causes an increase of 10% in viscosity between the temperatures of 298 K and 353 K. Changing the phenyl substituent of  $[C_1(CH_2C_6H_5)Im][NTf_2]$  by a cyclohexyl leads to a 2 times increase in viscosity.<sup>73</sup> When the anion of the ionic liquid is the dicyanamide, adding a nitrile functional group to the end of the butyl chain causes an increase in viscosity of 3-5 times in the temperature range.

Adding metallic salts to an ionic causes an increase in the viscosity of  $[C_1(CH_2C_6H_5)Im][NTf_2]$ . The increase is up to 42%, 50% and 34% for the addition of  $0.33 \text{ mol L}^{-1}$  of lithium,  $0.18 \text{ mol L}^{-1}$  of nickel and for less than  $0.01 \text{ mol L}^{-1}$  of copper salts respectively and at 298 K, as can be observed in figure 2.5.

When possible, the results obtained were compared with the literature. Viscosity is very sensitive to the presence of impurities, and the comparison will allow some insight about the purity of the samples.

The relative deviations between the experimental data and the data reported in the literature were determined and the results of this analysis for  $[C_1C_4Im][DCA]$ ,

$[C_1(CH_2C_6H_5)Im][NTf_2]$ ,  $[C_1(C_3H_5CH_2)Im][NTf_2]$ ,  $[C_1C_3CNIm][NTf_2]$  and  $[C_1C_3CNIm][DCA]$  are presented in figure 2.6.

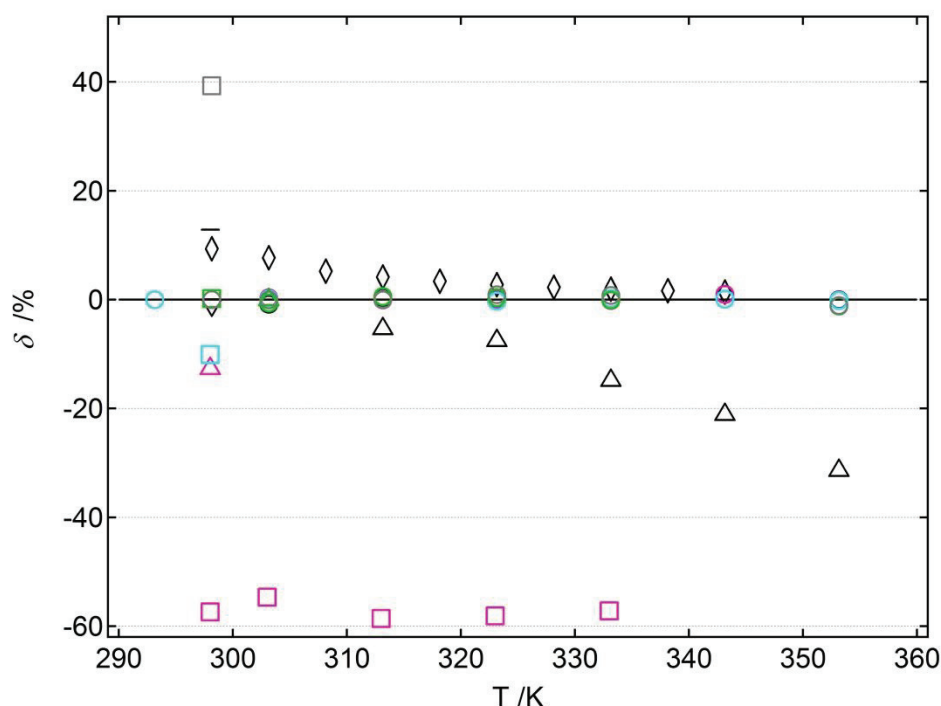


Figure 2.6 - Relative deviations between the experimental viscosity of the ionic liquids  $[C_1C_4Im][DCA]$  (black symbols),  $[C_1(CH_2C_6H_5)Im][NTf_2]$  (pink symbols),  $[C_1(C_3H_5CH_2)Im][NTf_2]$  (light blue symbols),  $[C_1C_3CNIm][NTf_2]$  (green symbols) and  $[C_1C_3CNIm][DCA]$  (grey symbols) in this work and data reported in the literature as a function of temperature. Water, halide contents and purity of the ionic liquid are reported in table 2.15.  $O/O/O/O/O$ , this work, deviation of the experimental viscosities from the values obtained using equation 2.5.  $\nabla$ , McHale *et al.*<sup>52</sup>;  $\Delta$ , Sánchez *et al.*<sup>53</sup>;  $\diamond$ , Carvalho *et al.*<sup>54</sup>;  $—$ , Mahurin *et al.*<sup>56</sup>;  $\square$ , Orita *et al.*<sup>74</sup>;  $\triangle$ , Mandai *et al.*<sup>57</sup>;  $\square$ , Mahurin *et al.*<sup>58</sup>;  $\square$ , Zang *et al.*<sup>60</sup>;  $\triangle$ , Xing *et al.*<sup>75</sup>; and  $\square$ , Zang *et al.*<sup>60</sup>

Carvalho *et al.*<sup>54</sup> data on  $[C_1C_4Im][DCA]$  present deviations that decrease with temperature, from +9.4% at 298.15 K to +1.4% at 343.15 K. This is probably due to the larger amount of impurities present in our sample. Because of the fast decrease in viscosity with the temperature, the effect of the impurities also decreases.<sup>38</sup> The +13% deviation between our measurements and those reported by Mahurin *et al.*<sup>56</sup> is hard to explain as the authors do not describe their sample or experimental method. Our viscosity data agree with that published by McHale *et al.*<sup>52</sup> to within  $\pm 1.0\%$  at 298.15 K, indicating that the amount of impurities in both samples is similar. Our data also agrees with those reported by McHale *et al.*<sup>52</sup> and Sánchez *et al.*<sup>53</sup> at lower

temperatures, but a deviation of -31% is observed at 353.15 K. This abrupt decrease in deviation can probably be explained by a poor temperature control.

For the ionic liquid  $[\text{C}_1(\text{CH}_2\text{C}_6\text{H}_5)\text{Im}][\text{NTf}_2]$  two references were found. Mandai *et al.*<sup>57</sup> results present 13% less viscosity than ours. Mahurin *et al.*<sup>58</sup> viscosity data present a constant deviation of -57% in the temperature range covered. Both deviations are hard to explain. In the first case, because the authors claim that their ionic liquid sample has a water content of less than 150 ppm, a value higher but sufficiently close to ours. In the second, there is a lack of information about the purity of the sample used by the authors, but the result is consistent with the presence of a higher amount of water.

For  $[\text{C}_1(\text{C}_3\text{H}_5\text{CH}_2)\text{Im}][\text{NTf}_2]$ , Orita *et al.*<sup>74</sup> obtained a viscosity 10% lower than ours at 298 K. The amount of water in the author's sample is consistent with ours; this may indicate that our sample contains a larger amount of halide impurities than the amount indicated by the authors, 150 ppm. The comparison of our viscosity results for  $[\text{C}_1\text{C}_3\text{CNIm}][\text{NTf}_2]$  and  $[\text{C}_1\text{C}_3\text{CNIm}][\text{DCA}]$  with the results from Zhang *et al.*<sup>60</sup> led to deviations of +0.15% and +39%, respectively. It is hard to discuss the reasons for these deviations due to lack of information about impurity amount in the author's samples. The results obtained by Xing *et al.*<sup>75</sup> for  $[\text{C}_1\text{C}_3\text{CNIm}][\text{NTf}_2]$  agree with ours within to  $\pm 0.04\%$ .

Table 2.15 - Purity, halide and water amount in several ionic liquid samples from this work and in the literature, viscosity measurement method used with corresponding uncertainty

Purity /%	Halide amount /ppm	Water amount /ppm	Method	Uncertainty /%	Reference
<b>[C<sub>1</sub>C<sub>4</sub>Im][DCA]</b>					
98	-	98	rolling ball	±2	This work
-	1830	256	rotating spindle	±1	52
>97	-	<680	Ubbelohde	±1	53
>99	<100	28	Stabinger	±0.35	54
-	-	-	-	-	56
<b>[C<sub>1</sub>(C<sub>3</sub>H<sub>5</sub>CH<sub>2</sub>)Im][NTf<sub>2</sub>]</b>					
99	-	95	rolling ball	±2	This work
-	<150	<100	-	-	74
<b>[C<sub>1</sub>C<sub>3</sub>CNIm][NTf<sub>2</sub>]</b>					
99	-	45	rolling ball	±2	This work
-	-	-	Stabinger	-	60
-	-	-	rotating cone/plate	-	75
<b>[C<sub>1</sub>C<sub>3</sub>CNIm][DCA]</b>					
99	-	75	rolling ball	±2	This work
-	-	-	Stabinger	-	60
<b>[C<sub>1</sub>(CH<sub>2</sub>C<sub>6</sub>H<sub>5</sub>)Im][NTf<sub>2</sub>]</b>					
99	-	70	rolling ball	±2	This work
-	-	<150	rolling ball	-	57
-	-	-	rotating cone/plate	-	58

## Conclusions

A series of imidazolium based ionic liquids were synthesized via a one-step or two-step synthesis path, with purities of at least 99%. The ionic liquids were characterized by proton and carbon NMR spectroscopy, high resolution mass spectroscopy and their density and viscosity were measured. Solutions of ionic liquid with metallic salts were also characterized in terms of their density and viscosity.

The ionic liquid with highest density is  $[C_1(C_2H_2CH)Im][NTf_2]$  and the one with the lowest is  $[C_1C_4Im][DCA]$ . The ionic liquid with highest viscosity is  $[C_1C_4Im][Lev]$  and the one with lowest is  $[C_1C_4Im][DCA]$ . The unsaturations can lead to viscosities up to 2 times greater than in ionic liquids with saturated side alkyl chains.

Density measurements are a popular and reliable ionic liquid characterization method. The method is sensitive to impurities, easy to perform, fast and inexpensive, which makes a good candidate to complement or verify the purity of a sample. In more recent years, more effort has been made into detailing the purity of the ionic liquid and the accuracy of the density method employed, making the assessment of purity easier.

The solubility, at 303 K, of the selected metallic salts in  $[C_1(CH_2C_6H_5)Im][NTf_2]$  roughly decreases with the size of the metallic cation for then salts studied. For the  $LiNTf_2$  salt the solubility in  $[C_1(CH_2C_6H_5)Im][NTf_2]$  is greater than 2 M, for  $Ni(NTf_2)_2$  the solubility is between 0.5 M and 2 M and for  $Cu(NTf_2)_2$  is lower than 0.01 M between 303 K and 363 K. Solutions of  $[C_1(CH_2C_6H_5)Im][NTf_2]$  with  $LiNTf_2$  with concentration of  $0.33 \text{ mol L}^{-1}$ ; with  $Ni(NTf_2)_2$  with  $0.18 \text{ mol L}^{-1}$  concentration and with  $Cu(NTf_2)_2$  at less than  $0.01 \text{ mol L}^{-1}$ . The addition of these metallic salts to the ionic liquid caused an increase its density of up to 2% for the salt types and concentrations studied. The addition of these metallic salts to the ionic liquid caused an increase in viscosity of 42%, 50% and 34% at 298 K for the lithium, nickel and copper salts respectively.

Due to the great impact of impurities in the physicochemical properties of the ionic liquids, it is critical to determine and report the purity of the sample and the synthetic route used to obtain it. In recent years, there has been an increasing effort in this sense and in finding synthetic routes avoiding the use of halogenated salts.

## References

---

- <sup>1</sup> Wasserscheid, P. and Welton, T. *Ionic Liquids in Synthesis*, Wiley-VCH, Weinheim, **2002**
- <sup>2</sup> Wasserscheid, P. and Keim, W. Ionic Liquids - New "Solutions" for Transition Metal Catalysis, *Angew. Chem. Int. Ed.* **2000**, 39, 3772-3789
- <sup>3</sup> Dupont, J.; Souza, R. F. and Suarez, P. A. Z. Ionic Liquid (Molten Salt) Phase Organometallic Catalysis, *Chem. Rev.* **2002**, 102, 3667-3691
- <sup>4</sup> Clare, B.; Sirwardana, A. and MacFarlane, D. R. Synthesis, Purification and Characterization of Ionic Liquids. In Kirchner, B. (Ed.) *Top. Curr. Chem.: Ionic Liquids*, Springer-Verlag, Berlin Heidelberg, **2009**
- <sup>5</sup> Himmler, S.; Hörmann, S.; van Hal, R.; Schulza, P. S. and Wasserscheid, P. Transesterification of Methylsulfate and Ethylsulfate Ionic Liquids - An Environmentally Benign Way to Synthesize Long-chain and Functionalized Alkylsulfate Ionic Liquids, *Green Chem.* **2006**, 8, 887-894
- <sup>6</sup> Holbrey, J. D., Reichert, W. M.; Swatloski, R. P.; Broker, G. A.; Pitner, W. R.; Seddon, K. R. and Rogers, R. D. Efficient, Halide Free Synthesis of New, Low Cost Ionic Liquids: 1,3-dialkylimidazolium Salts Containing Methyl- and Ethyl-sulfate Anions, *Green Chem.* **2002**, 4, 407-413
- <sup>7</sup> Del Sesto, R. E.; Corley, C.; Robertson, A. and Wilkes, J. S. Tetraalkylphosphonium-based Ionic Liquids, *J. Organomet. Chem.* **2005**, 690, 2536-2542
- <sup>8</sup> Kuhlmann, E.; Himmler, S.; Giebelhaus, H. and Wasserscheid, P. Imidazolium Dialkylphosphates - a Class of Versatile, Halogen-free and Hydrolytically Stable Ionic Liquids, *Green Chem.* **2007**, 9, 233-242
- <sup>9</sup> Holbrey, J. D.; Rogers, R. D.; Shukla, S. S. and Wilfred, C. D. Optimised Microwave-Assisted Synthesis of Methylcarbonate Salts: a Convenient Methodology to Prepare Intermediates for Ionic Liquid Libraries, *Green Chem.* **2010**, 12, 407-413
- <sup>10</sup> Earle, M. J. and Seddon, K. R. Preparation of Imidazole Carbenes and the Use Thereof for the Synthesis of Ionic Liquids, World Patent, WO 0177081 (**2001**)
- <sup>11</sup> Ferguson, J. L.; Holbrey, J. D.; Ng, S.; Plechkova, N. V.; Seddon, K. R.; Tomaszowska, A. A. and Wassell, D. F. A Greener, Halide-free Approach to Ionic Liquid Synthesis, *Pure Appl. Chem.* **2012**, 84, 723-744

- 
- <sup>12</sup> Brandt, A.; P. Hallett, J.; Leak, D. J.; Murphy, R. J. and Welton, T. The Effect of the Ionic Liquid Anion in the Pretreatment of Pine Wood Chips, *Green Chem.* **2010**, 12, 672-679
- <sup>13</sup> Solomons, T. W. G.; Fryhle, C. B. Organic Chemistry, John Wiley & Sons, Canada; 7<sup>th</sup> edition, **1999**
- <sup>14</sup> Srour, H., Santini, C., Rouault, H. and Moura, L. Method for Synthesizing Ionic Liquids, patent WO 2013 037923
- <sup>15</sup> Stevanovic, S.; Podgorsek, A.; Moura, L.; Santini, C. C.; Padua, A. A. H. and Costa Gomes, M. F. Absorption of Carbon Dioxide by Ionic Liquids With Carboxylate Anions, *Int. J. Greenh. Gas Con.* **2013**, 17, 78-88
- <sup>16</sup> Brandt, A.; P. Hallett, J.; Leak, D. J.; Murphy, R. J. and Welton, T. The Effect of the Ionic Liquid Anion in the Pretreatment of Pine Wood Chips, *Green Chem.* **2010**, 12, 672-679
- <sup>17</sup> Yokozeki, A.; Shiflett, M. B.; Junk, C. P.; Grieco, L. M. and Foo, T. Physical and Chemical Absorptions of Carbon Dioxide in Room-Temperature Ionic Liquids, *J. Phys. Chem. B* **2008**, 112, 16654-16663
- <sup>18</sup> Huddleston, J. G.; Visser, A. E.; Reichert, W. M.; Willauer, H. D.; Broker, G. A. and Rogers, R. D. Characterization and Comparison of Hydrophilic and Hydrophobic Room Temperature Ionic Liquids Incorporating the Imidazolium Cation, *Green Chem.* **2001**, 3, 156-164
- <sup>19</sup> Seddon, K. R.; Stark, A. and Torres, M. J. Influence of Chloride, Water, and Organic Solvents on the Physical Properties of Ionic Liquids, *Pure Appl. Chem.* **2000**, 72, 2275-2287
- <sup>20</sup> Ghatee, M. H.; Zare, M.; Moosavi, F. and Zolghadr, A. R. Temperature-Dependent Density and Viscosity of the Ionic Liquids 1-Alkyl-3-methylimidazolium Iodides: Experiment and Molecular Dynamics Simulation, *J. Chem. Eng. Data* **2010**, 55, 3084-3088
- <sup>21</sup> G. Schilling, G.; Kleinrahm, R. and Wagner, W. Measurement and Correlation of the ( $p$ ,  $\rho$ ,  $T$ ) Relation of Liquid N-heptane, N-nonane, 2, 4-dichlorotoluene, and Bromobenzene in the Temperature Range From (233.15 to 473.15) K at Pressures Up to 30 MPa For Use as Density Reference Liquids, *J. Chem. Thermodyn.* **2008**, 40, 1095-1105

- 
- <sup>22</sup> Wagner, W.; Cooper, J. R.; Dittmann, A.; Kijima, J.; Kretzschmar, H.-J.; Kruse, A.; Mareš, R.; Oguchi, K.; Sato, H.; Stöcker, I.; Šifner, O.; Takaishi, Y. Tanishita, I.; Trübenbach, J.; Willkommen, Th. The IAPWS Industrial Formulation 1997 for the Thermodynamic Properties of Water and Steam, *J. Eng. Gas Turb. Power* **2000**, 122, 150-182
- <sup>23</sup> Fandiño, O.; Pensado, A. S.; Lugo, L.; Comuñas, M. J. P. and Fernández, J. Compressed Liquid Densities of Squalane and Pentaerythritol Tetra(2-ethylhexanoate), *J. Chem. Eng. Data* **2005**, 50, 939-946
- <sup>24</sup> Rooney, D.; Jacquemin, J. and Gardas, R. Thermophysical Properties of Ionic Liquids. In Kirchner, B. (Ed.) *Top. Curr. Chem.: Ionic Liquids*, Springer-Verlag, Berlin Heidelberg, **2009**
- <sup>25</sup> Gómez, E.; Calvar, N.; Macedo, E. A. and Domínguez, A. Effect of the temperature on the physical properties of pure 1-propyl-3-methylimidazolium bis(trifluoromethylsulfonyl)imide and characterization of its binary mixtures with alcohols *J. Chem. Thermodyn.* **2012**, 45, 9-15
- <sup>26</sup> Costa Gomes, M. F.; Pison, L.; Pensado, A. S. and Pádua, A. A. H. Using Ethane and Butane as Probes to the Molecular Structure of 1-alkyl-3-methylimidazolium bis[(trifluoromethyl)sulfonyl]imide Ionic Liquids, *Faraday Discuss.* **2012**, 154, 41-52
- <sup>27</sup> Jacquemin, J.; Ge, R.; Nancarrow, P.; Rooney, D. W.; Costa Gomes, M. F.; Pádua, A. A. H. and Hardacre, C. Prediction of Ionic Liquid Properties. I. Volumetric Properties as a Function of Temperature at 0.1 MPa, *J. Chem. Eng. Data* **2008**, 53, 716-726,
- <sup>28</sup> Gardas, R. L.; Coutinho, J. A. P. Extension of the Ye and Shreeve Group Contribution Method for Density Estimation of Ionic Liquids in a Wide Range of Temperatures and Pressures, *Fluid Phase Equilib.* **2008**, 263, 26-32
- <sup>29</sup> Valderrama, J. O.; Reátegui, A. and Rojas, R. E. Density of Ionic Liquids Using Group Contribution and Artificial Neural Networks, *Ind. Eng. Chem. Res.* **2009**, 48, 3254-3259
- <sup>30</sup> Canongia Lopes, J. N.; Cordeiro, T. C.; Esperança, J. M. S. S., Guedes, H. J. R.; Huq, S.; Rebelo, L. P. N. and Seddon, K. R. Deviations from Ideality in Mixtures of Two Ionic Liquids Containing a Common Ion, *J. Phys. Chem. B* **2005**, 109, 3519-3525

- 
- <sup>31</sup> Oliveira, M. B.; Domínguez-Pérez, M.; Cabeza, O.; Silva, J. A. L.; Freire, M. G. and Coutinho, J. A. P. Surface Tensions of Binary Mixtures of Ionic Liquids with Bis(trifluoromethylsulfonyl)imide as the Common Anion. *J. Chem. Thermodyn.* **2013**, *64*, 22-27
- <sup>32</sup> Corderi, S. and Gonzalez, B. Ethanol Extraction From its Azeotropic Mixture with Hexane Employing Different Ionic Liquids as Solvents. *J. Chem. Thermodyn.* **2012**, 138-143
- <sup>33</sup> Seoane, R. G.; González, E. J. and González, B. 1-Alkyl-3-methylimidazolium Bis(trifluoromethylsulfonyl)imide Ionic Liquids as Solvents in the Separation of Azeotropic Mixtures. *J. Chem. Thermodyn.* **2012**, *53*, 152-157
- <sup>34</sup> Castro, C. A. N.; Langa, E.; Morais, A. L.; Lopes, M. L. M.; Lourenço, M. J. V.; Santos, F. J. V.; Santos, M. S. C. S.; Lopes, J. N. C.; Veiga, H. I. M.; Macatrão, M.; J. M. S. S. Esperança, J. M. S. S.; Marques, C. S.; Rebelo, L. P. N. and Afonso, C. A. M. Studies on the Density, Heat Capacity, Surface Tension and Infinite Dilution Diffusion with the Ionic Liquids [C<sub>4</sub>mim][NTf<sub>2</sub>], [C<sub>4</sub>mim][dca], [C<sub>2</sub>mim][EtOSO<sub>3</sub>] and [Aliquat][dca], *Fluid Phase Equilib.* **2010**, *294*, 157-179
- <sup>35</sup> Wandschneider, A.; Lehmann, J. K. and Heintz, A. Surface Tension and Density of Pure Ionic Liquids and Some Binary Mixtures with 1-Propanol and 1-Butanol, *J. Chem. Eng. Data* **2008**, *53*, 596-599
- <sup>36</sup> Azevedo, R. G.; Esperança, J. M. S. S.; Szydłowski, J.; Visak, Z. P.; Pires, P. F.; Guedes, H. J. R. and Rebelo, L. P. N. Thermophysical and Thermodynamic Properties of Ionic Liquids Over an Extended Pressure Range: [bmim][NTf<sub>2</sub>] and [hmim][NTf<sub>2</sub>]. *J. Chem. Thermodyn.* **2005**, *37*, 888-899
- <sup>37</sup> Andreatta, A. E.; Arce, A.; Rodil, E. and Soto, A. Physico-Chemical Properties of Binary and Ternary Mixtures of Ethyl Acetate + Ethanol + 1-Butyl-3-methyl-imidazolium bis(trifluoromethylsulfonyl)imide at 298.15 K and Atmospheric Pressure, *J. Solution Chem.* **2010**, *39*, 371-383
- <sup>38</sup> Jacquemin, J.; Husson, P.; Padua, A. A. H. and Majer, V. Density and Viscosity of Several Pure and Water-Saturated Ionic Liquids, *Green Chem.* **2006**, *8*, 172-180
- <sup>39</sup> Jacquemin, J.; Husson, P.; Majer, V. and Costa Gomes, M. F. Influence of the Cation on the Solubility of CO<sub>2</sub> and H<sub>2</sub> in Ionic Liquids Based on the Bis(trifluoromethylsulfonyl)imide Anion, *J. Solution Chem.* **2007**, *36*, 967-979

- 
- <sup>40</sup> Vranes, M.; Dozic, S.; Djeric, V. and Gadzuric, S. Physicochemical Characterization of 1-Butyl-3-methylimidazolium and 1-Butyl-1-methylpyrrolidinium Bis(trifluoromethylsulfonyl)imide, *J. Chem. Eng. Data* **2012**, 57, 1072-1077
- <sup>41</sup> Harris, K. R.; Kanakubo, M. and Woolf, L. A. Temperature and Pressure Dependence of the Viscosity of the Ionic Liquids 1-Hexyl-3-methylimidazolium Hexafluorophosphate and 1-Butyl-3-methylimidazolium Bis(trifluoromethylsulfonyl)imide, *J. Chem. Eng. Data* **2007**, 52, 1080-1085
- <sup>42</sup> Krummen, M.; Wasserscheid, P. and Gmehling, J. Measurement of Activity Coefficients at Infinite Dilution in Ionic Liquids Using the Dilutor Technique, *J. Chem. Eng. Data* **2002**, 47, 1411-1417
- <sup>43</sup> Katsuta, S.; Shiozawa, Y.; Imai, K.; Kudo, Y. and Takeda, Y. Stability of Ion Pairs of Bis(trifluoromethanesulfonyl)amide-Based Ionic Liquids in Dichloromethane, *J. Chem. Eng. Data* **2010**, 55, 1588-1593
- <sup>44</sup> Troncoso, J.; Cerdeirin, C. A.; Sanmamed, Y. A.; Romaní, L. and Rebelo, L. P. N. Thermodynamic Properties of Imidazolium-Based Ionic Liquids: Densities, Heat Capacities, and Enthalpies of Fusion of [bmim][PF<sub>6</sub>] and [bmim][NTf<sub>2</sub>]. *J. Chem. Eng. Data* **2006**, 51, 1856-1859
- <sup>45</sup> Jacquemin, J.; Husson, P.; Mayer, V. and Cibulka, I. High-Pressure Volumetric Properties of Imidazolium-Based Ionic Liquids: Effect of the Anion, *J. Chem. Eng. Data* **2007**, 52, 2204-2211
- <sup>46</sup> Shirota, H.; Mandai, T.; Fukazawa, H. and Kato, T. Comparison Between Dicationic and Monocationic Ionic Liquids: Liquid Density, Thermal Properties, Surface Tension, and Shear Viscosity, *J. Chem. Eng. Data* **2011**, 56, 2453-2459
- <sup>47</sup> Domínguez, I.; González, E. J.; González, R. and Domínguez, A. Extraction of Benzene from Aliphatic Compounds Using Commercial Ionic Liquids as Solvents: Study of the Liquid-Liquid Equilibrium at T=298.15 K, *J. Chem. Eng. Data* **2011**, 56, 3376-3383
- <sup>48</sup> Geppert-Rybczyńska, M.; Heintz, A.; Lehmann, J. K. and Golus, A. Volumetric Properties of Binary Mixtures Containing Ionic Liquids and Some Aprotic Solvents, *J. Chem. Eng. Data* **2010**, 55, 4114-4120
- <sup>49</sup> Tokuda, H.; Tsuzuki, S.; Susan, M. A. B. H.; Hayamizu, K. and Watanabe, M. How Ionic Are Room-Temperature Ionic Liquids? An Indicator of the Physicochemical Properties *J. Phys. Chem. B* **2006**, 110, 19593-19600

- 
- <sup>50</sup> Fredlake, C. P.; Crosthwaite, J. M.; Hert, D. G.; Aki, S. N. V. K. and Brennecke, J. F. Thermophysical Properties of Imidazolium-Based Ionic Liquids, *J. Chem. Eng. Data* **2004**, 49, 954-964
- <sup>51</sup> Stoppa, A.; Hunger, J. and Buchner, R. Conductivities of Binary Mixtures of Ionic Liquids with Polar Solvents, *J. Chem. Eng. Data* **2009**, 54, 472-479
- <sup>52</sup> McHale, G.; Hardacre, C.; Ge, R.; Doy, N.; Allen, R. W. K.; MacInnes, J. M.; Bown, M. R. and Newton, M. I. Density-Viscosity Product of Small-Volume Ionic Liquid Samples Using Quartz Crystal Impedance Analysis, *Anal. Chem.* **2008**, 80, 5806-5811
- <sup>53</sup> Sánchez, L. G.; Espel, J. R.; Onink, F.; Meindersma, G. W. and de Haan, A. B. Density, Viscosity, and Surface Tension of Synthesis Grade Imidazolium, Pyridinium, and Pyrrolidinium Based Room Temperature Ionic Liquids, *J. Chem. Eng. Data* **2009**, 54, 2803-2812
- <sup>54</sup> Carvalho, P. J.; Regueira, T.; Santos, L. M. N. B. F.; Fernandez, J. and Coutinho, J. A. P. Effect of Water on the Viscosities and Densities of 1-Butyl-3-methylimidazolium Dicyanamide and 1-Butyl-3-methylimidazolium Tricyanomethane at Atmospheric Pressure, *J. Chem. Eng. Data* **2010**, 55, 645-652
- <sup>55</sup> Zech, O.; Stoppa, A.; Buchner, R. and Kunz, W. The Conductivity of Imidazolium-Based Ionic Liquids from (248 to 468) K. B. Variation of the Anion, *J. Chem. Eng. Data* **2010**, 55, 1774-1778
- <sup>56</sup> Mahurin, S. M.; Lee, J. S.; Baker, G. A.; Luo, H.; Dai, S. Performance of nitrile-containing anions in task-specific ionic liquids for improved CO<sub>2</sub>/N<sub>2</sub> separation, *J. Membrane Sci.* **2010**, 353, 177-183
- <sup>57</sup> Mandai, T.; Matsumura, A.; Imanari, M. and Nishikawa, K. Effects of Cyclic-Hydrocarbon Substituents and Linker Length on Physicochemical Properties and Reorientational Dynamics of Imidazolium-Based Ionic Liquids, *J. Phys. Chem. B* **2012**, 116, 2090-2095
- <sup>58</sup> Mahurin, S. M.; Dai, T.; Yeary, J. S.; Luo, H. and Dai, S. Benzyl-Functionalized Room Temperature Ionic Liquids for CO<sub>2</sub>/N<sub>2</sub> Separation, *Ind. Eng. Chem. Res.* **2011**, 50, 14061-14069
- <sup>59</sup> Carlisle, T. K.; Bara, J. E.; Gabriel, C. J.; Noble, R. D. and Gin, D. L. Interpretation of CO<sub>2</sub> Solubility and Selectivity in Nitrile-Functionalized Room-Temperature Ionic

---

Liquids Using a Group Contribution Approach, *Ind. Eng. Chem. Res.* **2008**, 47, 7005-7012

<sup>60</sup> Zhang, Q.; Li, Z.; Zhang, J.; Zhang, S.; Zhu, L.; Yang, J.; Zhang, X. and Deng, Y. Physicochemical Properties of Nitrile-Functionalized Ionic Liquids, *J. Phys. Chem. B* **2007**, 111, 2864-2872

<sup>61</sup> Ohlin, C. A.; Dyson, P. J. and Laurenczy, G. Carbon Monoxide Solubility in Ionic Liquids: Determination, Prediction and Relevance to Hydroformylation, *Chem. Commun.* **2004**, 1070-1071

<sup>62</sup> Dzyuba, S. V. and Bartsch, R. A. Influence of Structural Variations in 1-Alkyl(aralkyl)-3-Methylimidazolium Hexafluorophosphates and Bis(trifluoromethylsulfonyl)imides on Physical Properties of the Ionic Liquids, *ChemPhysChem.* **2002**, 3, 161-166

<sup>63</sup> Palgunadi, J.; Hong, S. Y.; Lee, J. K.; Lee, H.; Lee, S. D.; Cheong, M. and Kim, H. S. Correlation Between Hydrogen Bond Basicity and Acetylene Solubility in Room Temperature Ionic Liquids, *J. Phys. Chem. B* **2011**, 115, 1067-1074

<sup>64</sup> AMVn Automated Microviscometer Instruction Manual, Anton Paar

<sup>65</sup> Mahiuddin S. and Ismail, K. Concentration Dependence of the Viscosity of Aqueous Electrolytes. A Probe into Higher Concentration, *J. Phys. Chem.* **1983**, 87, 5241-5244

<sup>66</sup> Ribeiro, M. C. C. Low-frequency Raman Spectra and Fragility of Imidazolium Ionic Liquids, *J. Chem. Phys.* **2010**, 133, 024503

<sup>67</sup> Vila, J.; Ginés, P.; Pico, J. M.; Franjo, C.; Jiménez, E.; Varela, L. M. and Cabeza, O. Temperature Dependence of the Electrical Conductivity in EMIM-based Ionic Liquids Evidence of Vogel-Tamman-Fulcher Behavior, *Fluid Phase Equilibr.* **2006**, 242, 141-146

<sup>68</sup> Chiappe, C.; Sanzone, A.; Mendola, D.; Castiglione, F.; Famulari, A.; Raos, G. and Mele, A. Pyrazolium-versus Imidazolium-Based Ionic Liquids: Structure, Dynamics and Physicochemical Properties, *J. Phys. Chem. B* **2013**, 117, 668-676

<sup>69</sup> Ikeda, M. and Aniya, M. Understanding the Vogel-Fulcher-Tammann Law in Terms of the Bond Strength-coordination Number Fluctuation Model, *J. Non-Cryst. Solids* **2013**, 371-372, 53-57

- 
- <sup>70</sup> Costa Gomes, M. F.; Pison, L.; Pensado, A. S. and Pádua, A. A. H. Using Ethane and Butane as Probes to the Molecular Structure of 1-alkyl-3-methylimidazolium bis[(trifluoromethyl)sulfonyl]imide Ionic Liquids, *Faraday Discuss.* **2012**, 154, 41-52
- <sup>71</sup> O. Fandiño, O.; Pensado, A. S.; Lugo, L.; Comuñas, M. J. P. and Fernández, J. Compressed Liquid Densities of Squalane and Pentaerythritol Tetra(2-ethylhexanoate), *J. Chem. Eng. Data* **2005**, 50, 939-946
- <sup>72</sup> Almantariotis, D.; Gefflaut, T.; Pádua, A. A. H.; Coxam, J.-Y. and Costa Gomes, M. F. Effect of Fluorination and Size of the Alkyl Side-Chain on the Solubility of Carbon Dioxide in 1-Alkyl-3-methylimidazolium Bis(trifluoromethylsulfonyl)amide Ionic Liquids, *J. Phys. Chem. B* **2010**, 114, 3608-3617
- <sup>73</sup> Mandai, T.; Matsumura, A.; Imanari, M.; and Nishikawa, K. Effects of Cyclic-Hydrocarbon Substituents and Linker Length on Physicochemical Properties and Reorientational Dynamics of Imidazolium-Based Ionic Liquids, *J. Phys. Chem. B* **2012**, 116, 2090-2095
- <sup>74</sup> Orita, A.; Kamijima, K. and Yoshida, M. Allyl-Functionalized Ionic Liquids as Electrolytes for Electric Double-Layer Capacitors, *J. Power Sources* **2010**, 195, 7471-7479
- <sup>75</sup> Xing, H.; Zhao, X.; Li, R.; Yang, Q.; Su, B.; Bao, Z.; Yang, Y. and Ren, Q. Improved Efficiency of Ethylene/Ethane Separation Using a Symmetrical Dual Nitrile-Functionalized Ionic Liquid, *ACS Sustainable Chem. Eng.* **2013**, 1, 1357-1363

# Chapter 3

---

Ethane and Ethene Solubility in Ionic Liquids



In this chapter the original experimental data of the solubility of ethane and ethene in selected imidazolium based ionic liquids will be presented.

The high solubility of unsaturated hydrocarbons in ionic liquids compared with their saturated counterparts has been explained by the favorable electrostatic interactions between the cation of the ionic liquid and the  $\pi$ -system of the solute.<sup>1,2</sup> Other interactions have been evoked to explain the solvation properties of hydrocarbons in ILs e.g. hydrogen bond between the gas and the anion, anion- $\pi$  interaction between the gas and the anion and/or  $\pi$ - $\pi$  interaction between the gas and the cation.<sup>3,9</sup> It has also been reported that, in the presence of a metal ion, a higher solubility for alkene gases versus alkanes, is observed due to a  $\pi$ -complex bond formation between olefins and some transition metal ions.<sup>4</sup>

Four groups of pure ionic liquids were selected in order to study the influence of different functional groups or anions in the solubility and ideal selectivity of ethane and ethene. The *first group* of ionic liquids was used as a reference and served as an indicator of the influence of the length of the alkyl side chain of the cation; 1-butyl-3-methylimidazolium bis(trifluoromethanesulfonyl)imide,  $[\text{C}_1\text{C}_4\text{Im}][\text{NTf}_2]$  and 1-methyl-3-octyl-imidazolium bis(trifluoromethanesulfonyl)imide,  $[\text{C}_1\text{C}_8\text{Im}][\text{NTf}_2]$ . A *second group* was used to test the influence of the presence of unsaturations in the alkyl side chain of the cation; 1-methyl-3-(propyn-3-yl)imidazolium bis(trifluoromethanesulfonyl)imide,  $[\text{C}_1(\text{C}_2\text{H}_2\text{CH})\text{Im}][\text{NTf}_2]$ ; 1-(buten-3-yl)-3-methylimidazolium bis(trifluoromethanesulfonyl)imide,  $[\text{C}_1(\text{C}_3\text{H}_5\text{CH}_2)\text{Im}][\text{NTf}_2]$ , 1-benzyl-3-methylimidazolium bis(trifluoromethanesulfonyl)imide,  $[\text{C}_1(\text{CH}_2\text{C}_6\text{H}_5)\text{Im}][\text{NTf}_2]$ . The *third group* consisted in a systematic study of the influence of the cyano groups, due to the apparent positive effect in the selective absorption of propene in propane/propene mixtures<sup>5</sup>; 1-butyl-3-methylimidazolium dicyanamide,  $[\text{C}_1\text{C}_4\text{Im}][\text{DCA}]$ ; 1-(3-cyanopropyl)-3-methylimidazolium bis(trifluoromethanesulfonyl)imide,  $[\text{C}_1\text{C}_3\text{CNIm}][\text{NTf}_2]$  and 1-(3-cyanopropyl)-3-methylimidazolium dicyanamide,  $[\text{C}_1\text{C}_3\text{CNIm}][\text{DCA}]$ . The *forth group* consists of an ionic liquid with a phosphite based anion, 1-butyl-3-methylimidazolium methylphosphite,  $[\text{C}_1\text{C}_4\text{Im}][\text{C}_1\text{HPO}_3]$ .

A study of the influence in ethene absorption of the presence metallic salts in 1-benzyl-3-methylimidazolium bis(trifluoromethanesulfonyl)imide,  $[\text{C}_1(\text{CH}_2\text{C}_6\text{H}_5)\text{Im}][\text{NTf}_2]$  was also performed. Three metallic salt-ionic liquid solutions

were prepared with the following concentrations: LiNTf<sub>2</sub> at 0.33 mol L<sup>-1</sup>, Ni(NTf<sub>2</sub>)<sub>2</sub> at 0.18 mol L<sup>-1</sup> and Cu(NTf<sub>2</sub>)<sub>2</sub> at less than 0.01 mol L<sup>-1</sup>.

Our first publications in international peer-reviewed journals can be found in appendix 3.

### 3. Gas Solubility in ionic liquids

The gas solubility measurements were performed using an isochoric saturation method that allows the determination of the solubility at pressures close to the atmospheric pressure and at different temperatures. In this method a known amount of gas is put in contact with a precisely determined quantity of degassed ionic liquid. The pressure at thermodynamic equilibrium allows the determination of the amount of gas absorbed by the ionic liquid. The experimental method is schematically represented in figure 3.1.<sup>28,25,26</sup>

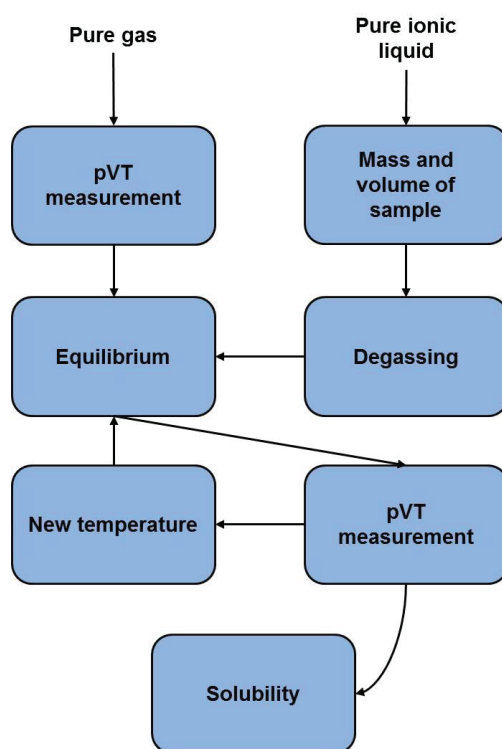


Figure 3.1 - Scheme of the experimental method for the measurement of solubility

The experimental device used is depicted in figure 3.2. The equilibrium cell (EC) is placed in a thermostated water bath (TB). The temperature is controlled through a PID controller (Hart Scientific model 2200, resolution  $\pm 0.01$  K) and is measured with a  $100 \Omega$  platinum resistance thermometer (Hart Scientific model 1502A with a NVLAP-accredited calibration probe, model 5615, accuracy of  $\pm 0.010$  K at 273.15 K). The equilibrium cell includes a manometer (M) (Druck RPT350S,

pressure range from 35 to 2620 mbar, accuracy of  $\pm 0.01\%$  full scale) and a glass bulb (GB) where the gas is kept.

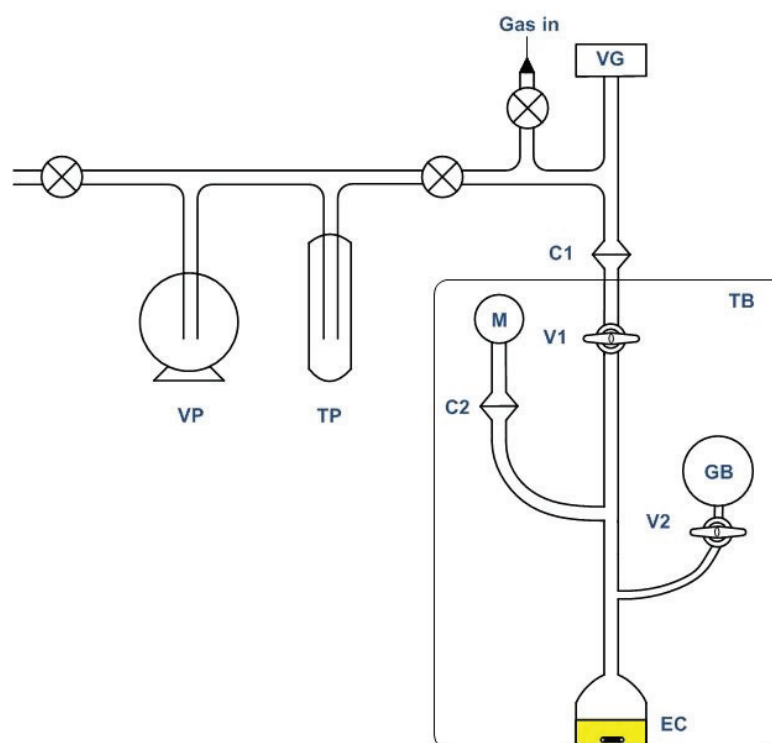


Figure 3.2 - Solubility apparatus used in this work: (VP) vacuum pump; (TP) cold trap; (VG) vacuum gauge; (GB) gas bulb; (M) precision manometer; (TB) thermostated bath; (EC) equilibrium cell; (V1, V2) constant volume glass valves; (C1, C2) vacuum o-ring connections.

Before the equilibrium cell is assembled, the volume of the glass bulb (GB) was calibrated with degassed distilled water at 2 temperatures. The total volume of the assembled cell is also calibrated at two temperatures by a gas expansion method.

The first step of the solubility measurement consists in filling and isolating the gas bulb with a known amount of gas at a known temperature, closing the V2 valve. Then, a precise amount of ionic liquid measured gravimetrically is introduced in the cell through the C2 connection. The study of variation of the density of the ionic liquid with the temperature at atmospheric pressure allows the determination of the volume it occupies in the cell at each temperature. This value is considered to be equal to the volume occupied by the solution after saturation with the gas. After degassing, the ionic liquid is put in contact with the gas, which was kept in the gas bulb. The contact

between them is optimized by stirring the liquid.\* The temperature and pressure of the cell are registered throughout the entire measurement. After thermodynamic equilibrium is attained, a new temperature is set. The gas solubility is typically measured at five temperatures between 303.15 K and 343.15 K. To ensure the accuracy of the results, at least 3 independent measurements are performed for the same system.

In the first  $pVT$  measurement, the amount of gas in the gas bulb,  $n_2^{tot}$ , can be determined:

$$n_2^{tot} = \frac{p_{ini}V_{ini}}{[Z_2(p_{ini}, T_{ini})RT_{ini}]} \quad (3.1)$$

where  $p_{ini}$ ,  $T_{ini}$  and  $V_{ini}$  are the initial pressure, temperature and volume of the gas bulb, respectively, before the insertion of the ionic liquid;  $R$  is the gas constant and  $Z_2$  is the compressibility factor of the pure gas (subscripts 1 and 2 represent solvent and solute, respectively). The compressibility factor is calculated by

$$Z_2(p_{ini}, T_{ini}) = 1 + \frac{p_{ini}B_{22}}{RT_{ini}} \quad (3.2)$$

where  $B_{22}$  is the second virial coefficient of the pure gas, obtained from the compilation of data by Dymond and Smith.<sup>6</sup> We consider that the ionic liquid presents a negligible vapor pressure in the range of temperatures covered, and so the total amount of liquid is equal to its amount in the liquid solution,  $n_1^{liq}$ , and that the only contribution for the equilibrium pressure is from the solute.

The second  $pVT$  measurement is performed when the thermodynamic equilibrium is attained, after the contact between the gas solute and the ionic liquid.

The amount of free gas in the cell,  $n_2^{vap}$ , is given by

$$n_2^{vap} = \frac{p_{eq}(V_{tot} - V_{liq})}{[Z_2(p_{eq}, T_{eq})RT_{eq}]} \quad (3.3)$$

---

\* A glass coated magnetic stirrer was used

where  $p_{eq}$  and  $T_{eq}$  are the pressure and temperature of the cell after the thermodynamic equilibrium is reached.  $V_{tot}$  and  $V_{liq}$  are the total volume of the cell and the volume occupied by the ionic liquid, respectively, at the equilibrium temperature. The amount of solute in the ionic liquid sample,  $n_2^{liq}$ , is given by

$$n_2^{liq} = n_2^{tot} - n_2^{vap} \quad (3.4)$$

The solubility can be expressed as the solute mole fraction,  $x_2$ ,

$$x_2(p, T) = \frac{n_2^{liq}}{n_2^{liq} + n_1^{liq}} \quad (3.5)$$

Value which can be used to calculate the Henry's law constant,

$$K_H = \lim_{x_2 \rightarrow 0} \frac{f_2^{liq}(p, T, x_2)}{x_2} \quad (3.6)$$

where  $x_2$  is mole fraction of the solute and  $f_2^{liq}$  is its fugacity in the liquid phase. At the thermodynamic equilibrium,  $f_2^{liq}$  is determined:

$$f_2^{liq} = f_2^{vap} = \phi_2(p_{eq}, T_{eq}, y_2) y_2 p_{eq} \quad (3.7)$$

with  $f_2^{vap}$  is the fugacity in the vapor phase,  $\phi_2$  is the fugacity coefficient of the solute and  $y_2$  is the mole fraction of the solute in the gas phase, in the present case is equal to one, due to the negligible vapor pressure of the ionic liquid. Therefore equation 3.7 becomes

$$f_2^{vap} = \phi_2(p_{eq}, T_{eq}) p_{eq} \quad (3.8)$$

And by substitution in equation 3.6,

$$K_H \cong \frac{\phi_2(p_{eq}, T_{eq})p_{eq}}{x_2} \quad (3.9)$$

The fugacity coefficient of the solute,  $\phi_2$ , can be determined by

$$\phi_2(p_{eq}, T_{eq}) = \exp\left[\frac{p_{eq}B_{22}(T_{eq})}{RT_{eq}}\right] = \exp[Z_2(p_{eq}, T_{eq}) - 1] \quad (3.10)$$

The Henry's law constants calculated from the experimental solubilities were fitted to a power series in T

$$\ln[K_H/10^5 Pa] = \sum_{i=0}^n A_i (T/K)^i \quad (3.11)$$

For the metallic salts-ionic liquid solutions, the absorption results can be expressed as solute mole fraction,  $x_2$ ,

$$x_2(p, T) = \frac{n_2^{liq}}{n_1^{liq} + n_2^{liq} + n_{metal}^{liq}} \quad (3.12)$$

or as the amount of solute per amount of metallic cation in the solution,  $x_2^{metal}$ ,

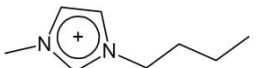
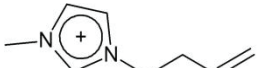
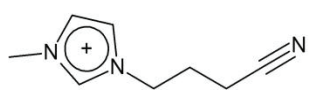
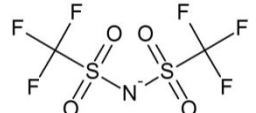
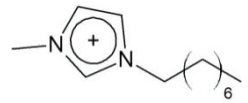
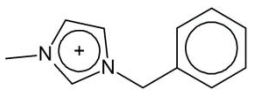
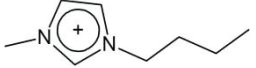
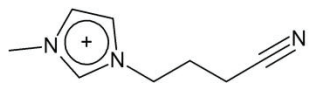
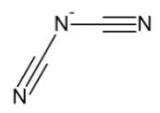
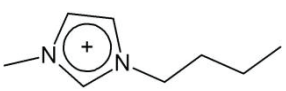
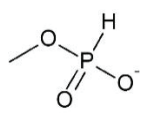
$$x_2^{metal}(p, T) = \frac{n_2^{liq}}{n_{metal}^{liq}} \quad (3.13)$$

where  $n_{metal}^{liq}$  represents the amount of metal salt,  $n_1^{liq}$  the amount of ionic liquid and  $n_2^{liq}$  the amount of gas solute in the metallic salt-ionic liquid solution.

### 3.1 Materials

Linde Gas supplied the gases used for this study: ethane 3.5, mole fraction purity of 0.9995 and ethene 2.8, mole fraction purity of 0.998. All gases were used as received from the manufacturer. The metallic salts  $\text{LiNTf}_2$ ,  $\text{Ni}(\text{NTf}_2)_2$  and  $\text{Cu}(\text{NTf}_2)_2$  have been used as received from Solvionic.

Table 3.1 - Representation, name, abbreviation of the ionic liquids used for the solubility measurements

Cation	Anion	Name	Abbreviation
		1-methyl-3-(propyn-3-yl)imidazolium bis(trifluoromethanesulfonyl)imide	$[\text{C}_1(\text{C}_2\text{H}_2\text{CH})\text{Im}][\text{NTf}_2]$
		1-butyl-3-methylimidazolium bis(trifluoromethanesulfonyl)imide	$[\text{C}_1\text{C}_4\text{Im}][\text{NTf}_2]$
		1-(buten-3-yl)-3-methylimidazolium bis(trifluoromethanesulfonyl)imide	$[\text{C}_1(\text{C}_3\text{H}_5\text{CH}_2)\text{Im}][\text{NTf}_2]$
		1-(3-cyanopropyl)-3-methylimidazolium bis(trifluoromethanesulfonyl)imide	$[\text{C}_1\text{C}_3\text{CNIm}][\text{NTf}_2]$
		1-methyl-3-octylimidazolium bis(trifluoromethanesulfonyl)imide	$[\text{C}_1\text{C}_8\text{Im}][\text{NTf}_2]$
		1-benzyl-3-methylimidazolium bis(trifluoromethanesulfonyl)imide	$[\text{C}_1(\text{CH}_2\text{C}_6\text{H}_5)\text{Im}][\text{NTf}_2]$
		1-butyl-3-methylimidazolium dicyanamide	$[\text{C}_1\text{C}_4\text{Im}][\text{DCA}]$
		1-(3-cyanopropyl)-3-methylimidazolium dicyanamide	$[\text{C}_1\text{C}_3\text{CNIm}][\text{DCA}]$
		1-butyl-3-methylimidazolium methylphosphite	$[\text{C}_1\text{C}_4\text{Im}][\text{C}_1\text{HPO}_3]$

The name and structures of the ionic liquids used are listed in table 3.1. To remove water, the ionic liquid samples were kept under primary vacuum at least 48 h prior to use. Before each measurement, the water content of the degassed ionic liquid was verified with a coulometric Karl Fischer titrator (Mettler Toledo DL32). The amount of water in each ionic liquid sample is presented in table 3.2.

Table 3.2 - Amount of water, in ppm, present in the ionic liquid after at least 48 h under primary vacuum

Ionic Liquid	Amount of water /ppm	Mole fraction of water
[C <sub>1</sub> (C <sub>2</sub> H <sub>2</sub> CH)Im][NTf <sub>2</sub> ]	95	0.0021
[C <sub>1</sub> C <sub>4</sub> Im][NTf <sub>2</sub> ]	70	0.0016
[C <sub>1</sub> (C <sub>3</sub> H <sub>5</sub> CH <sub>2</sub> )Im][NTf <sub>2</sub> ]	100	0.0023
[C <sub>1</sub> C <sub>3</sub> CNIm][NTf <sub>2</sub> ]	43	0.0010
[C <sub>1</sub> C <sub>8</sub> Im][NTf <sub>2</sub> ]	63	0.0017
[C <sub>1</sub> (CH <sub>2</sub> C <sub>6</sub> H <sub>5</sub> )Im][NTf <sub>2</sub> ]	70	0.0018
[C <sub>1</sub> C <sub>4</sub> Im][DCA]	98	0.0011
[C <sub>1</sub> C <sub>3</sub> CNIm][DCA]	75	0.00090
[C <sub>1</sub> C <sub>4</sub> Im][C <sub>1</sub> HPO <sub>3</sub> ]	156	0.0020

Three metallic salt-[C<sub>1</sub>(CH<sub>2</sub>C<sub>6</sub>H<sub>5</sub>)Im][NTf<sub>2</sub>] solutions were prepared with the following concentrations: LiNTf<sub>2</sub> at 0.33 mol L<sup>-1</sup>, Ni(NTf<sub>2</sub>)<sub>2</sub> at 0.18 mol L<sup>-1</sup> and Cu(NTf<sub>2</sub>)<sub>2</sub> at less than 0.01 mol L<sup>-1</sup>.

## 3.2 Ethane and ethene solubility

For each ionic liquid-gas pair, several solubility experimental data points were measured for temperatures between 303 K and 343 K in steps of approximately 10 K.

The experimental solubilities for ethane and ethene in the ionic liquids  $[\text{C}_1(\text{C}_2\text{H}_2\text{CH})\text{Im}][\text{NTf}_2]$ ,  $[\text{C}_1(\text{C}_3\text{H}_5\text{CH}_2)\text{Im}][\text{NTf}_2]$ ,  $[\text{C}_1(\text{CH}_2\text{C}_6\text{H}_5)\text{Im}][\text{NTf}_2]$ ,  $[\text{C}_1\text{C}_4\text{Im}][\text{DCA}]$ ,  $[\text{C}_1\text{C}_3\text{CNIm}][\text{NTf}_2]$  and  $[\text{C}_1\text{C}_3\text{CNIm}][\text{DCA}]$  and  $[\text{C}_1\text{C}_4\text{Im}][\text{C}_1\text{HPO}_3]$ , and for ethene in  $[\text{C}_1\text{C}_4\text{Im}][\text{NTf}_2]$  and  $[\text{C}_1\text{C}_8\text{Im}][\text{NTf}_2]$  are reported in table 3.3 and figures 3.3 to 3.8.

Table 3.3 - Henry's law constants,  $K_H$  of ethane,  $\text{C}_2\text{H}_6$ , and ethene,  $\text{C}_2\text{H}_4$  in pure ionic liquids, along with their solubility as gas mole fraction,  $x_2$ , corrected for a partial pressure of solute of 0.1 MPa<sup>a</sup>

$[\text{C}_1\text{C}_4\text{Im}][\text{NTf}_2] + \text{C}_2\text{H}_4$					$[\text{C}_1\text{C}_8\text{Im}][\text{NTf}_2] + \text{C}_2\text{H}_4$				
$\frac{T}{K}$	$\frac{p}{10^2 Pa}$	$\frac{K_H}{10^5 Pa}$	$\frac{x_2}{10^{-3}}$	%dev	$\frac{T}{K}$	$\frac{p}{10^2 Pa}$	$\frac{K_H}{10^5 Pa}$	$\frac{x_2}{10^{-3}}$	%dev
283.67	803.0	54.62	18.19	+0.2	303.17	647.9	54.03	18.41	-0.7
293.76	833.8	63.91	15.56	+0.1	303.57	893.2	52.52	18.94	+2.8
303.57	872.4	75.11	13.24	-1.3	303.57	878.4	55.14	18.04	-2.1
303.57	863.3	73.67	13.50	+0.6	313.17	671.4	62.12	16.02	-1.3
313.59	903.0	86.32	11.53	-0.8	313.58	924.4	60.44	16.47	+2.0
323.61	923.2	96.64	10.30	+1.9	323.16	694.7	70.93	14.04	-1.2
323.61	933.3	98.55	10.10	-0.1	323.59	940.1	72.15	13.80	-2.3
333.63	963.6	112.6	8.847	+0.0	323.59	955.4	69.09	14.41	+2.1
343.65	993.9	128.9	7.732	-0.5	333.16	717.7	80.57	12.36	-0.6
					333.59	986.4	79.21	12.58	+1.7
					343.16	740.7	91.35	10.91	+0.1
					343.59	1001	93.45	10.66	-1.6
					343.60	1017	90.95	10.95	+1.1

[C <sub>1</sub> (C <sub>2</sub> H <sub>2</sub> CH)Im][NTf <sub>2</sub> ] + C <sub>2</sub> H <sub>6</sub>					[C <sub>1</sub> (C <sub>2</sub> H <sub>2</sub> CH)Im][NTf <sub>2</sub> ] + C <sub>2</sub> H <sub>4</sub>				
$\frac{T}{K}$	$\frac{p}{10^2 Pa}$	$\frac{K_H}{10^5 Pa}$	$\frac{x_2}{10^{-3}}$	%dev	$\frac{T}{K}$	$\frac{p}{10^2 Pa}$	$\frac{K_H}{10^5 Pa}$	$\frac{x_2}{10^{-3}}$	%dev
303.56	663.6	174.9	5.692	-0.2	303.16	658.4	113.4	8.787	-2.0
303.57	654.7	175.4	5.674	-0.5	303.16	659.3	111.4	8.947	-0.2
303.57	910.4	172.5	5.760	+1.2	303.57	653.0	109.3	9.119	+2.3
313.56	686.1	204.6	4.865	-1.9	313.16	681.0	127.7	7.804	-1.2
313.58	676.8	201.8	4.933	-0.6	313.16	681.9	126.4	7.885	-0.1
313.59	941.2	197.6	5.029	+1.6	313.58	675.6	125.2	7.963	+1.4
323.54	708.3	234.4	4.248	-1.3	323.11	703.5	145.3	6.860	-2.0
323.60	698.9	233.6	4.263	-0.9	323.16	704.4	141.4	7.050	+0.7
323.62	972.1	227.6	4.368	+1.8	323.59	697.9	141.7	7.037	+1.1
333.50	730.3	265.6	3.751	+0.6	333.08	725.7	161.9	6.159	-1.4
333.61	720.8	267.0	3.731	+0.3	333.15	726.7	158.5	6.293	+0.8
333.64	1003.0	265.6	3.745	+0.8	333.59	720.1	159.5	6.252	+0.7
343.41	752.5	316.2	3.151	-2.3	343.05	747.8	179.0	5.573	-0.5
343.63	742.7	303.7	3.281	+2.0	343.14	749.0	176.9	5.638	+0.8
343.70	1034.0	311.8	3.191	-0.5	343.60	742.3	179.8	5.548	-0.4
[C <sub>1</sub> (C <sub>3</sub> H <sub>5</sub> CH <sub>2</sub> )Im][NTf <sub>2</sub> ] + C <sub>2</sub> H <sub>6</sub>					[C <sub>1</sub> (C <sub>3</sub> H <sub>5</sub> CH <sub>2</sub> )Im][NTf <sub>2</sub> ] + C <sub>2</sub> H <sub>4</sub>				
$\frac{T}{K}$	$\frac{p}{10^2 Pa}$	$\frac{K_H}{10^5 Pa}$	$\frac{x_2}{10^{-3}}$	%dev	$\frac{T}{K}$	$\frac{p}{10^2 Pa}$	$\frac{K_H}{10^5 Pa}$	$\frac{x_2}{10^{-3}}$	%dev
303.56	680.4	110.8	8.981	+0.7	303.12	646.5	87.30	11.42	-0.4
303.57	685.3	111.9	8.894	-0.3	303.12	639.2	86.57	11.51	+0.6
313.57	703.6	126.9	7.845	-0.5	303.16	626.6	86.96	11.46	+0.2
313.58	708.7	127.2	7.827	-0.7	313.09	648.4	99.47	10.02	-0.6
323.59	726.4	141.6	7.034	-0.5	313.12	668.9	99.33	10.04	-0.4
323.60	731.5	138.6	7.182	+1.6	313.12	661.5	98.88	10.08	+0.0
333.60	749.0	154.9	6.430	+0.2	323.00	670.0	112.8	8.841	-0.7
333.62	754.6	155.5	6.406	-0.2	323.09	683.6	112.3	8.876	-0.2
343.61	771.7	172.9	5.762	-2.2	323.11	690.9	111.2	8.965	+0.8
343.64	777.1	165.7	6.011	+2.1	332.91	691.3	126.2	7.902	+0.3
					333.09	713.0	125.5	7.945	+1.1
					342.78	712.8	144.4	6.906	-1.1

					342.94	727.3	144.3	6.911	-0.9
					343.02	734.8	141.3	7.056	+1.3
$[C_1(CH_2C_6H_5)Im][NTf_2] + C_2H_6$					$[C_1(CH_2C_6H_5)Im][NTf_2] + C_2H_4$				
$\frac{T}{K}$	$\frac{p}{10^2 Pa}$	$\frac{K_H}{10^5 Pa}$	$\frac{x_2}{10^{-3}}$	%dev	$\frac{T}{K}$	$\frac{p}{10^2 Pa}$	$\frac{K_H}{10^5 Pa}$	$\frac{x_2}{10^{-3}}$	%dev
303.25	656.7	134.4	7.408	-0.6	303.55	675.0	94.91	10.50	-1.6
303.55	881.6	135.9	7.315	-1.3	303.58	680.7	92.09	10.82	+1.5
303.57	670.8	131.4	7.574	+2.1	313.53	698.2	107.9	9.241	-1.5
313.29	679.6	152.5	6.530	-1.1	313.60	704.3	104.2	9.560	+2.0
313.53	911.5	151.4	6.565	-0.1	323.49	721.3	123.4	8.079	-2.8
313.57	693.8	150.1	6.633	+0.8	323.63	727.7	118.1	8.443	+1.7
323.35	702.4	172.8	5.762	-1.6	333.42	743.9	136.0	7.331	-1.2
323.56	716.7	169.6	5.871	+0.5	333.67	751.0	131.7	7.572	+2.3
323.61	941.6	167.7	5.931	+1.7	343.35	766.4	150.2	6.640	-0.5
333.38	725.0	192.8	5.167	-0.7	343.67	774.3	149.8	6.659	+0.1
333.56	739.4	190.8	5.220	+0.5					
343.38	747.9	223.7	4.454	-3.9					
343.51	761.9	213.0	4.677	+1.1					
343.65	1002	209.8	4.744	+2.8					
$[C_1C_4Im][DCA] + C_2H_6$					$[C_1C_4Im][DCA] + C_2H_4$				
$\frac{T}{K}$	$\frac{p}{10^2 Pa}$	$\frac{K_H}{10^5 Pa}$	$\frac{x_2}{10^{-3}}$	%dev	$\frac{T}{K}$	$\frac{p}{10^2 Pa}$	$\frac{K_H}{10^5 Pa}$	$\frac{x_2}{10^{-3}}$	%dev
303.57	867.1	296.9	3.344	+0.7	303.56	685.2	178.5	5.571	-1.1
303.57	886.5	297.1	3.342	+0.6	303.56	667.7	176.7	5.630	+1.5
304.16	665.3	303.0	3.277	-0.7	303.58	683.6	180.1	5.523	-0.4
313.58	896.1	346.4	2.868	-1.5	313.56	690.2	202.8	4.908	-0.6
323.60	925.1	401.7	2.475	+0.6	313.60	707.0	206.3	4.823	-2.2
333.61	954.2	489.0	2.034	+0.9	323.50	731.3	233.4	4.267	-1.4
343.61	983.4	620.9	1.603	-0.6	323.56	712.5	226.1	4.403	+1.9
					323.62	730.2	233.7	4.261	-1.3
					333.53	734.8	257.8	3.864	+3.3
					333.63	753.3	263.5	3.780	+1.2
					343.19	776.0	319.6	3.117	-3.2

					343.44	777.4	314.3	3.170	-1.2
					343.46	757.1	303.8	3.280	+2.2
[C <sub>1</sub> C <sub>3</sub> CNI <sub>m</sub> ][NTf <sub>2</sub> ] + C <sub>2</sub> H <sub>6</sub>					[C <sub>1</sub> C <sub>3</sub> CNI <sub>m</sub> ][NTf <sub>2</sub> ] + C <sub>2</sub> H <sub>4</sub>				
$\frac{T}{K}$	$\frac{p}{10^2 Pa}$	$\frac{K_H}{10^5 Pa}$	$\frac{x_2}{10^{-3}}$	%dev	$\frac{T}{K}$	$\frac{p}{10^2 Pa}$	$\frac{K_H}{10^5 Pa}$	$\frac{x_2}{10^{-3}}$	%dev
303.57	873.3	195.7	5.075	+0.1	303.16	659.5	131.2	7.580	+0.1
313.59	902.6	225.0	4.415	-0.2	313.13	681.2	150.2	6.627	-0.2
323.60	931.8	259.6	3.830	-0.1	323.10	702.8	172.2	5.782	+0.2
333.62	961.0	300.1	3.315	+0.3	333.06	724.4	200.1	4.979	-0.1
343.63	990.2	350.5	2.840	-0.1	343.06	746.0	232.9	4.279	+0.0
[C <sub>1</sub> C <sub>3</sub> CNI <sub>m</sub> ][DCA] + C <sub>2</sub> H <sub>6</sub>					[C <sub>1</sub> C <sub>3</sub> CNI <sub>m</sub> ][DCA] + C <sub>2</sub> H <sub>4</sub>				
$\frac{T}{K}$	$\frac{p}{10^2 Pa}$	$\frac{K_H}{10^5 Pa}$	$\frac{x_2}{10^{-3}}$	%dev	$\frac{T}{K}$	$\frac{p}{10^2 Pa}$	$\frac{K_H}{10^5 Pa}$	$\frac{x_2}{10^{-3}}$	%dev
303.17	700.1	672.6	1.476	-0.8	303.15	664.4	317.1	3.137	+0.1
303.17	682.9	665.7	1.492	+0.2	313.13	686.1	356.9	2.788	-0.2
313.16	722.9	766.7	1.296	-0.4	323.10	707.8	403.4	2.468	-0.4
313.16	705.1	746.8	1.330	+2.2	333.08	729.4	452.5	2.201	+0.7
323.16	745.7	876.5	1.134	-0.3	343.02	751.0	519.8	1.917	-0.3
323.16	727.4	882.7	1.126	-1.0					
333.15	768.4	1013	0.9817	-1.4					
333.17	749.5	985.9	1.009	+1.3					
343.15	791.0	1158	0.8594	-1.5					
343.16	771.6	1120	0.8886	+1.8					

[C <sub>1</sub> C <sub>4</sub> Im][C <sub>1</sub> HPO <sub>3</sub> ] + C <sub>2</sub> H <sub>6</sub>					[C <sub>1</sub> C <sub>4</sub> Im][C <sub>1</sub> HPO <sub>3</sub> ] + C <sub>2</sub> H <sub>4</sub>				
$\frac{T}{K}$	$\frac{p}{10^2 Pa}$	$\frac{K_H}{10^5 Pa}$	$\frac{x_2}{10^{-3}}$	%dev	$\frac{T}{K}$	$\frac{p}{10^2 Pa}$	$\frac{K_H}{10^5 Pa}$	$\frac{x_2}{10^{-3}}$	%dev
303.58	898.6	235.8	4.211	+0.2	303.57	884.1	162.8	6.110	-0.1
313.59	929.0	275.4	3.608	-0.4	313.59	914.1	183.9	5.410	+0.2
323.61	959.3	325.2	3.057	-0.0	323.61	944.2	210.5	4.730	-0.2

333.62	989.7	389.9	2.551	+0.5	333.62	974.1	240.4	4.143	+0.1
343.64	1020	479.1	2.077	-0.2					

<sup>a</sup> $p$  is the experimental equilibrium pressure and the percent deviation is relative to the correlations of the data reported in table 3.3

Table 3.4 - Henry's law constants,  $K_H$  of ethene,  $C_2H_4$ , in metallic salts-ionic liquid solutions, along with their absorption as gas mole fraction,  $x_2$ , corrected for a partial pressure of solute of 0.1 MPa<sup>a</sup> and amount of solute per amount of metallic cation in the solution at the equilibrium pressure,  $x_2^{metal}$

$[C_1(CH_2C_6H_5)Im][NTf_2]-0.33 \text{ mol L}^{-1} LiNTf_2+C_2H_4$						$[C_1(CH_2C_6H_5)Im][NTf_2]-0.18 \text{ mol L}^{-1} Ni(NTf_2)_2+C_2H_4$					
$\frac{T}{K}$	$\frac{p}{10^2 Pa}$	$\frac{K_H}{10^5 Pa}$	$\frac{x_2}{10^{-3}}$	$\frac{x_2^{metal}}{10^{-2}}$	%dev	$\frac{T}{K}$	$\frac{p}{10^2 Pa}$	$\frac{K_H}{10^5 Pa}$	$\frac{x_2}{10^{-3}}$	$\frac{x_2^{metal}}{10^{-2}}$	%dev
303.17	656.3	99.28	10.02	7.307	+0.3	303.27	655.2	91.89	10.82	13.81	-1.1
313.17	679.4	112.7	8.829	6.660	-0.7	313.17	677.4	102.8	9.681	12.76	+1.5
323.16	701.9	124.3	8.012	6.240	+0.1	332.79	721.6	131.6	7.571	10.62	-0.4
333.13	724.2	136.0	7.322	5.880	+0.6						
343.05	746.4	149.6	6.662	5.512	-0.3						
$[C_1(CH_2C_6H_5)Im][NTf_2]- < 0.01 \text{ mol L}^{-1} Cu(NTf_2)_2+C_2H_4$											
$\frac{T}{K}$	$\frac{p}{10^2 Pa}$	$\frac{K_H}{10^5 Pa}$	$\frac{x_2}{10^{-3}}$	$\frac{x_2^{metal}}{10^{-2}}$	%dev						
303.99	644.9	-	21.26	35.52	-						

<sup>a</sup> $p$  is the experimental equilibrium pressure and the percent deviation is relative to the correlations of the data reported in table 3.3

The experimental solubilities obtained for ethane and ethene in the ionic liquids  $[C_1(C_3H_5CH_2)Im][NTf_2]$ , and  $[C_1(CH_2C_6H_5)Im][NTf_2]$  and for ethene in  $[C_1C_4Im][NTf_2]$  have been published by us.<sup>7</sup> Reported experimental solubility results for ethane in  $[C_1C_4Im][NTf_2]$ <sup>8</sup> and  $[C_1C_8Im][NTf_2]$ <sup>8</sup> were added in figures 3.1 to 3.5 for comparison.

The experimental absorptions obtained for ethene in the ionic liquid solutions  $[C_1(CH_2C_6H_5)Im][NTf_2]-0.33 \text{ M } LiNTf_2$ ,  $[C_1(CH_2C_6H_5)Im][NTf_2]-0.18 \text{ M } Ni(NTf_2)_2$  and  $[C_1(CH_2C_6H_5)Im][NTf_2]-0.13 \text{ M } Cu(NTf_2)_2$  are reported in table 3.4 and figures 3.9 and 3.10.

The coefficients  $A_i$ , obtained from the fitting of the results to equation 3.12 are listed in table 3.5.

From the variation of the Henry's law constants with temperature, it is possible to calculate the thermodynamic properties of solvation, as previously described, using equations 3.11, 3.13 and 3.14. The values obtained, at the temperature of 323 K, are listed in table 3.6.  $K_H / 10^5$  Pa.

The solubility of ethane in  $[C_1C_3CNIm][NTf_2]$  was previously measured by Xing *et al.*<sup>20</sup> and an +11% deviation, at 303K was found between our results and the ones reported by the authors. The solubility of ethene was also measured in the same ionic liquid by Xing *et al.*<sup>20</sup> and Deng *et al.*<sup>22,23</sup>. In the first case, our results agree within  $\pm 3\%$  at 303 K. However, in the second case the deviations are as high as +49% at 303 K down to +25% at 323 K. The solubility of ethene in  $[C_1C_4Im][NTf_2]$  has been measured by Xing *et al.*<sup>20</sup>, Anthony *et al.*<sup>21</sup>, Palgunadi *et al.*<sup>24</sup> and is also reported in two publications from Deng *et al.*<sup>22,23</sup>. Our values agree with the ones from Anthony *et al.* within  $\pm 0.6\%$  at 323 K, but deviations increase to +13% at 283 K. Our values agree within  $\pm 2.7\%$  with the one reported by Palgunadi *et al.* at 313 K and within  $\pm 1.8\%$  with the one from Xing *et al.* The highest deviations were found from Deng *et al.*, from +17% at 303 K to +11% at 323 K. Similar deviations are attributed by the authors to the difference in the measuring methods, in that case, gravimetric microbalance and gas chromatography.<sup>22</sup>

Table 3.5 - Parameters of equation 3.12 used to smooth the experimental results on  $K_H$  from table 3.1 and 3.2 along with the percent average absolute deviation of the fit, AAD

<b>C<sub>2</sub>H<sub>6</sub></b>				
<b>Ionic Liquid</b>	<b>A<sub>0</sub></b>	<b>A<sub>1</sub></b>	<b>A<sub>2</sub></b>	<b>% AAD</b>
[C <sub>1</sub> (C <sub>2</sub> H <sub>2</sub> CH)Im][NTf <sub>2</sub> ]	+2.024	+6.805 × 10 <sup>-3</sup>	+1.163 × 10 <sup>-5</sup>	0.3
[C <sub>1</sub> (C <sub>3</sub> H <sub>5</sub> CH <sub>2</sub> )Im][NTf <sub>2</sub> ]	-4.782	+4.977 × 10 <sup>-2</sup>	-6.089 × 10 <sup>-5</sup>	0.3
[C <sub>1</sub> (CH <sub>2</sub> C <sub>6</sub> H <sub>5</sub> )Im][NTf <sub>2</sub> ]	+0.5989	+1.620 × 10 <sup>-2</sup>	-6.699 × 10 <sup>-6</sup>	0.4
[C <sub>1</sub> C <sub>4</sub> Im][DCA]	+16.45	-8.276 × 10 <sup>-2</sup>	+1.559 × 10 <sup>-4</sup>	0.2
[C <sub>1</sub> C <sub>3</sub> CNIIm][NTf <sub>2</sub> ]	+3.318	-6.691 × 10 <sup>-4</sup>	+2.346 × 10 <sup>-5</sup>	0.0
[C <sub>1</sub> C <sub>3</sub> CNIIm][DCA]	+1.844	+1.708 × 10 <sup>-2</sup>	-5.663 × 10 <sup>-6</sup>	0.2
[C <sub>1</sub> C <sub>4</sub> Im][C <sub>1</sub> HPO <sub>3</sub> ]	+8.814	-3.636 × 10 <sup>-2</sup>	+8.341 × 10 <sup>-5</sup>	0.0
<b>C<sub>2</sub>H<sub>4</sub></b>				
<b>Ionic Liquid</b>	<b>A<sub>0</sub></b>	<b>A<sub>1</sub></b>	<b>A<sub>2</sub></b>	<b>% AAD</b>
[C <sub>1</sub> C <sub>4</sub> Im][NTf <sub>2</sub> ]	-2.386	+2.941 × 10 <sup>-2</sup>	-2.428 × 10 <sup>-5</sup>	0.2
[C <sub>1</sub> C <sub>8</sub> Im][NTf <sub>2</sub> ]	-0.1976	+1.420 × 10 <sup>-2</sup>	-1.349 × 10 <sup>-6</sup>	0.4
[C <sub>1</sub> (C <sub>2</sub> H <sub>2</sub> CH)Im][NTf <sub>2</sub> ]	-1.902	+3.066 × 10 <sup>-2</sup>	-2.917 × 10 <sup>-5</sup>	0.3
[C <sub>1</sub> (C <sub>3</sub> H <sub>5</sub> CH <sub>2</sub> )Im][NTf <sub>2</sub> ]	-0.1297	+1.755 × 10 <sup>-2</sup>	-7.863 × 10 <sup>-6</sup>	0.2
[C <sub>1</sub> (CH <sub>2</sub> C <sub>6</sub> H <sub>5</sub> )Im][NTf <sub>2</sub> ]	-2.750	+3.480 × 10 <sup>-2</sup>	-3.566 × 10 <sup>-5</sup>	0.4
[C <sub>1</sub> C <sub>4</sub> Im][DCA]	+7.813	-2.848 × 10 <sup>-2</sup>	+6.534 × 10 <sup>-5</sup>	0.4
[C <sub>1</sub> C <sub>3</sub> CNIIm][NTf <sub>2</sub> ]	+3.975	-7.106 × 10 <sup>-3</sup>	+3.325 × 10 <sup>-5</sup>	0.1
[C <sub>1</sub> C <sub>3</sub> CNIIm][DCA]	+4.594	-3.619 × 10 <sup>-3</sup>	+2.463 × 10 <sup>-5</sup>	0.1
[C <sub>1</sub> C <sub>4</sub> Im][C <sub>1</sub> HPO <sub>3</sub> ]	+3.876	-4.203 × 10 <sup>-3</sup>	+2.704 × 10 <sup>-5</sup>	0.1
[C <sub>1</sub> (CH <sub>2</sub> C <sub>6</sub> H <sub>5</sub> )Im][NTf <sub>2</sub> ] + 0.33 mol L <sup>-1</sup> LiNTf <sub>2</sub>	-3.669	+4.245 × 10 <sup>-2</sup>	-5.005 × 10 <sup>-5</sup>	0.2
[C <sub>1</sub> (CH <sub>2</sub> C <sub>6</sub> H <sub>5</sub> )Im][NTf <sub>2</sub> ] + 0.18 mol L <sup>-1</sup> Ni(NTf <sub>2</sub> ) <sub>2</sub>	+0.7622	+1.221 × 10 <sup>-2</sup>	-	0.1

Table 3.6 - Thermodynamic properties of solvation of ethane, C<sub>2</sub>H<sub>6</sub>, and ethene, C<sub>2</sub>H<sub>4</sub>, at 323 K, in the ionic liquids and ionic liquid solutions used

<b>C<sub>2</sub>H<sub>6</sub></b>		
<b>Ionic Liquid</b>	<b><math>-\Delta_{solv}H^{\infty}/\text{kJ mol}^{-1}</math></b>	<b><math>-T\Delta_{solv}S^{\infty}/\text{kJ mol}^{-1}\text{K}^{-1}</math></b>
[C <sub>1</sub> C <sub>4</sub> Im][NTf <sub>2</sub> ]*	13 ± 1	26 ± 1
[C <sub>1</sub> C <sub>8</sub> Im][NTf <sub>2</sub> ]*	13 ± 1	25 ± 3
[C <sub>1</sub> (C <sub>2</sub> H <sub>2</sub> CH)Im][NTf <sub>2</sub> ]	12 ± 2	27 ± 3
[C <sub>1</sub> (C <sub>3</sub> H <sub>5</sub> CH <sub>2</sub> )Im][NTf <sub>2</sub> ]	9 ± 1	22 ± 1
[C <sub>1</sub> (CH <sub>2</sub> C <sub>6</sub> H <sub>5</sub> )Im][NTf <sub>2</sub> ]	10 ± 1	24 ± 2
[C <sub>1</sub> C <sub>4</sub> Im][DCA]	16 ± 6	32 ± 7
[C <sub>1</sub> C <sub>3</sub> CNIm][NTf <sub>2</sub> ]	13 ± 2	28 ± 3
[C <sub>1</sub> C <sub>3</sub> CNIm][DCA]	12 ± 1	30 ± 2
[C <sub>1</sub> C <sub>4</sub> Im][C <sub>1</sub> HPO <sub>3</sub> ]	15 ± 4	31 ± 5
<b>C<sub>2</sub>H<sub>4</sub></b>		
<b>Ionic Liquid</b>	<b><math>-\Delta_{solv}H^{\infty}/\text{kJ mol}^{-1}</math></b>	<b><math>-T\Delta_{solv}S^{\infty}/\text{kJ mol}^{-1}\text{K}^{-1}</math></b>
[C <sub>1</sub> C <sub>4</sub> Im][NTf <sub>2</sub> ]	12 ± 1	24 ± 1
[C <sub>1</sub> C <sub>8</sub> Im][NTf <sub>2</sub> ]	12 ± 1	23 ± 2
[C <sub>1</sub> (C <sub>2</sub> H <sub>2</sub> CH)Im][NTf <sub>2</sub> ]	10 ± 1	24 ± 1
[C <sub>1</sub> (C <sub>3</sub> H <sub>5</sub> CH <sub>2</sub> )Im][NTf <sub>2</sub> ]	11 ± 1	24 ± 2
[C <sub>1</sub> (CH <sub>2</sub> C <sub>6</sub> H <sub>5</sub> )Im][NTf <sub>2</sub> ]	10 ± 1	23 ± 1
[C <sub>1</sub> C <sub>4</sub> Im][DCA]	12 ± 3	27 ± 4
[C <sub>1</sub> C <sub>3</sub> CNIm][NTf <sub>2</sub> ]	13 ± 2	26 ± 3
[C <sub>1</sub> C <sub>3</sub> CNIm][DCA]	11 ± 2	27 ± 3
[C <sub>1</sub> C <sub>4</sub> Im][C <sub>1</sub> HPO <sub>3</sub> ]	12 ± 2	26 ± 3
[C <sub>1</sub> (CH <sub>2</sub> C <sub>6</sub> H <sub>5</sub> )Im][NTf <sub>2</sub> ] + 0.33 mol L <sup>-1</sup> LiNTf <sub>2</sub>	9 ± 1	22 ± 1
[C <sub>1</sub> (CH <sub>2</sub> C <sub>6</sub> H <sub>5</sub> )Im][NTf <sub>2</sub> ] + 0.18 mol L <sup>-1</sup> Ni(NTf <sub>2</sub> ) <sub>2</sub>	11 ± 1	23 ± 2

\* From reference 8

Deng *et al.*<sup>22,23</sup> also measured the solubility of ethene in  $[\text{C}_1\text{C}_3\text{CNIm}][\text{DCA}]$  and we found deviations as high as +72% at 303 to +58% at 323 K.

The solubility of ethene in  $[\text{C}_1\text{C}_4\text{Im}][\text{C}_1\text{HPO}_3]$  was measured by Palgunadi *et al.*<sup>9,24</sup> and our results agree within  $\pm 1\%$  at 313 K.

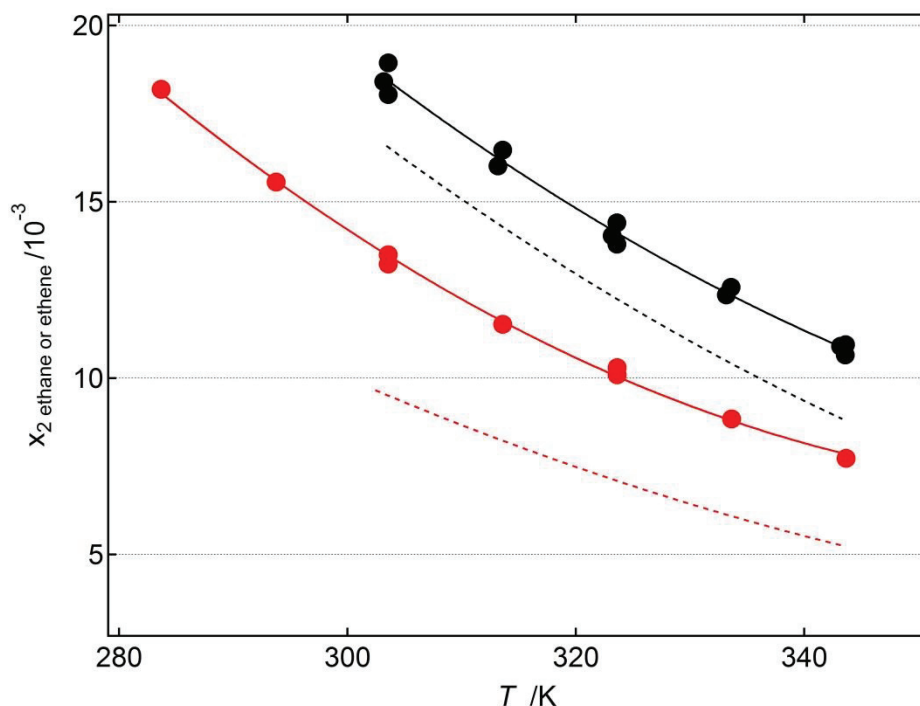


Figure 3.3 - Mole fraction solubilities of ethane and ethene at 0.1 MPa partial pressure and as a function of the temperature in the following ionic liquids: ●,  $[\text{C}_1\text{C}_8\text{Im}][\text{NTf}_2]$ ; ●,  $[\text{C}_1\text{C}_4\text{Im}][\text{NTf}_2]$ . Full lines represent the smoothed data and the dashed lines corresponds to the previously reported values of the solubility of ethane in  $[\text{C}_1\text{C}_4\text{Im}][\text{NTf}_2]$  (red) and  $[\text{C}_1\text{C}_8\text{Im}][\text{NTf}_2]$  (black) from reference 8.

For all ionic liquids studied, ethene is more soluble than ethane. For  $[\text{C}_1\text{C}_4\text{Im}][\text{NTf}_2]$ ,  $[\text{C}_1\text{C}_8\text{Im}][\text{NTf}_2]$ ,  $[\text{C}_1(\text{C}_2\text{H}_2\text{CH})\text{Im}][\text{NTf}_2]$ ,  $[\text{C}_1(\text{CH}_2\text{C}_6\text{H}_5)\text{Im}][\text{NTf}_2]$ ,  $[\text{C}_1\text{C}_4\text{Im}][\text{DCA}]$ ,  $[\text{C}_1\text{C}_3\text{CNIm}][\text{NTf}_2]$ ,  $[\text{C}_1\text{C}_3\text{CNIm}][\text{DCA}]$ ,  $[\text{C}_1\text{C}_4\text{Im}][\text{C}_1\text{HPO}_3]$  the higher ethene solubility is explained by more favorable entropies of solvation. For  $[\text{C}_1(\text{C}_3\text{H}_5\text{CH}_2)\text{Im}][\text{NTf}_2]$  the higher ethene solubility is due to more favorable gas-ionic liquid interactions, as expressed by a more negative enthalpy of solvation for  $\text{C}_2\text{H}_4$  than for  $\text{C}_2\text{H}_6$ .

The highest ethane and ethene solubility was found for the ionic liquid  $[\text{C}_1\text{C}_8\text{Im}][\text{NTf}_2]$ . No clear explanation is obtained from the analysis of the thermodynamic properties of solvation for these high solubilities. Both gases are

dissolved in the apolar part of the IL that is larger in  $[\text{C}_1\text{C}_8\text{Im}][\text{NTf}_2]$ , as observed in simulation results.<sup>7,8</sup>

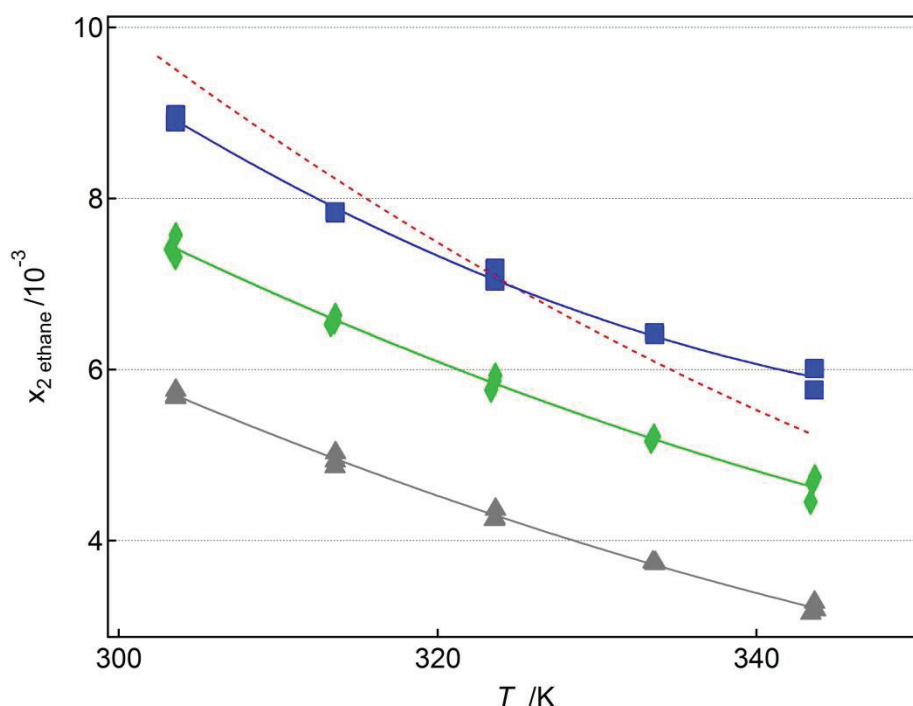


Figure 3.4 - Mole fraction solubilities of ethane at 0.1 MPa partial pressure and as a function of the temperature in the following ionic liquids: ▲,  $[\text{C}_1(\text{C}_2\text{H}_2\text{CH})\text{Im}][\text{NTf}_2]$ ; ■,  $[\text{C}_1(\text{C}_3\text{H}_5\text{CH}_2)\text{Im}][\text{NTf}_2]$ ; and ◆,  $[\text{C}_1(\text{CH}_2\text{C}_6\text{H}_5)\text{Im}][\text{NTf}_2]$ . Full lines represent the smoothed data and the dashed line corresponds to the previously reported values of the solubility of ethane in  $[\text{C}_1\text{C}_4\text{Im}][\text{NTf}_2]$  from reference 8.

The ionic liquids  $[\text{C}_1\text{C}_4\text{Im}][\text{NTf}_2]$  and  $[\text{C}_1\text{C}_8\text{Im}][\text{NTf}_2]$  will be used as reference for comparisons and as an indicator of the influence of the length of the alkyl side chain of the cation on the solubility of ethane and ethene. The solubility of ethane and ethene increases with the size of the alkyl side chain of the cation, due to more favorable entropies of solvation for the ionic liquid with a larger alkyl side chain. Due to the increase in the alkyl chain of the cation the solubility of ethane increased 42% and the solubility of ethene increased 28%. These values are in agreement to what is described in the literature (see chapter 1).

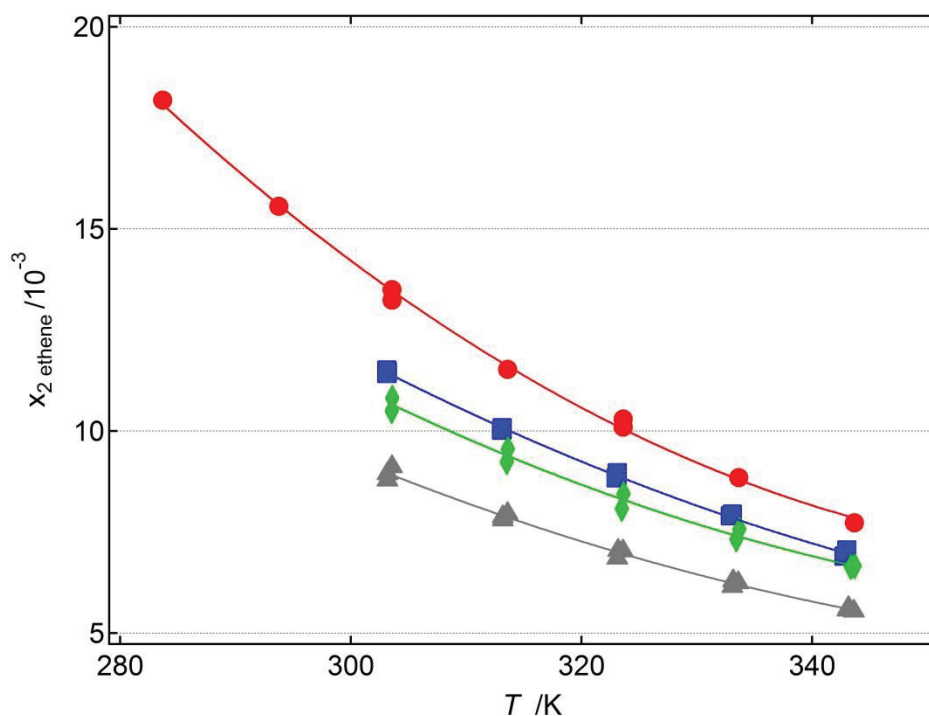


Figure 3.5 - Mole fraction solubilities of ethene at 0.1 MPa partial pressure and as a function of the temperature in the following ionic liquids: ●, [C<sub>1</sub>C<sub>4</sub>Im][NTf<sub>2</sub>]; ▲, [C<sub>1</sub>(C<sub>2</sub>H<sub>2</sub>CH)Im][NTf<sub>2</sub>]; ■, [C<sub>1</sub>(C<sub>3</sub>H<sub>5</sub>CH<sub>2</sub>)Im][NTf<sub>2</sub>]; and ◆, [C<sub>1</sub>(CH<sub>2</sub>C<sub>6</sub>H<sub>5</sub>)Im][NTf<sub>2</sub>]. Full lines represent the smoothed data.

The analysis of the solubility of the gases in [C<sub>1</sub>(C<sub>2</sub>H<sub>2</sub>CH)Im][NTf<sub>2</sub>], [C<sub>1</sub>(C<sub>3</sub>H<sub>5</sub>CH<sub>2</sub>)Im][NTf<sub>2</sub>] and [C<sub>1</sub>(CH<sub>2</sub>C<sub>6</sub>H<sub>5</sub>)Im][NTf<sub>2</sub>] will allow us to determine the influence of the presence of unsaturations in the alkyl side chain of the cation on the solubility of ethane and ethene. The order of the solubility of each gas is [C<sub>1</sub>(C<sub>3</sub>H<sub>5</sub>CH<sub>2</sub>)Im][NTf<sub>2</sub>] > [C<sub>1</sub>(CH<sub>2</sub>C<sub>6</sub>H<sub>5</sub>)Im][NTf<sub>2</sub>] > [C<sub>1</sub>(C<sub>2</sub>H<sub>2</sub>CH)Im][NTf<sub>2</sub>]. For ethane this order is due to gradually more unfavorable entropies of solvation, although countered by increasingly more favorable gas-ionic liquid interactions. In the case of ethene, the solubility order is justified by a more favorable interaction between the gas and [C<sub>1</sub>(C<sub>3</sub>H<sub>5</sub>CH<sub>2</sub>)Im][NTf<sub>2</sub>] than with [C<sub>1</sub>(CH<sub>2</sub>C<sub>6</sub>H<sub>5</sub>)Im][NTf<sub>2</sub>] or [C<sub>1</sub>(C<sub>2</sub>H<sub>2</sub>CH)Im][NTf<sub>2</sub>].

The solubility of ethane and ethene decreases with the presence of unsaturations in the alkyl side chain of the cation of the ionic liquid. The higher solubility of ethane and ethene in [C<sub>1</sub>C<sub>4</sub>Im][NTf<sub>2</sub>] than in all three ionic liquids presenting unsaturations is due to more favorable gas-ionic liquid interactions of the gases with [C<sub>1</sub>C<sub>4</sub>Im][NTf<sub>2</sub>].

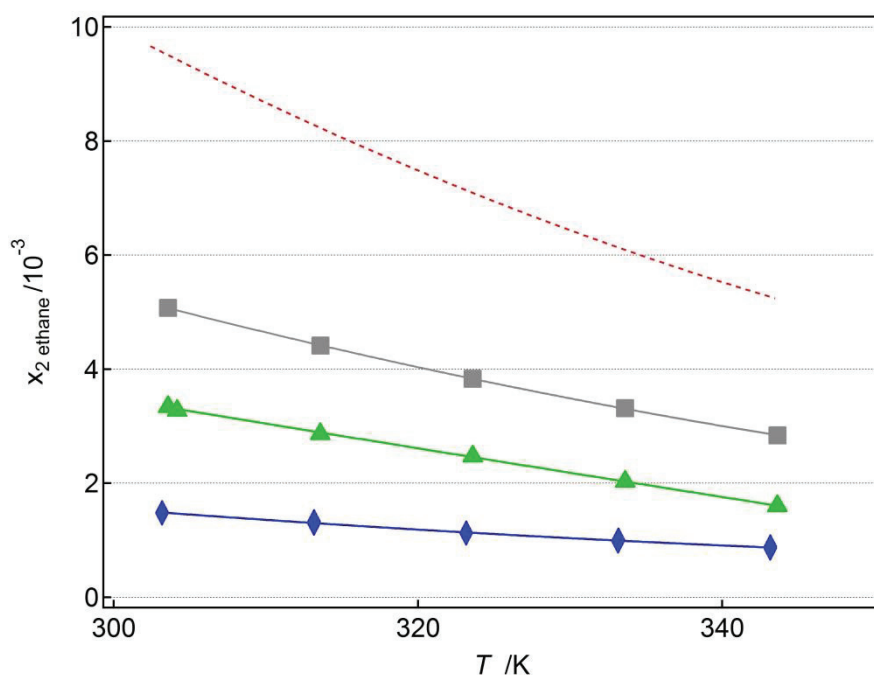


Figure 3.6 - Mole fraction solubilities of ethane at 0.1 MPa partial pressure and as a function of the temperature in the following ionic liquids: [C<sub>1</sub>C<sub>4</sub>Im][NTf<sub>2</sub>] (red curve); ▲, [C<sub>1</sub>C<sub>4</sub>Im][DCA]; ■, [C<sub>1</sub>C<sub>3</sub>CNIm][NTf<sub>2</sub>]; and ◆, [C<sub>1</sub>C<sub>3</sub>CNIm][DCA]. Full lines represent the smoothed data and the dashed lines corresponds to the previously reported values of the solubility of ethane in [C<sub>1</sub>C<sub>4</sub>Im][NTf<sub>2</sub>] from reference 8.

The ionic liquids [C<sub>1</sub>C<sub>4</sub>Im][DCA], [C<sub>1</sub>C<sub>3</sub>CNIm][NTf<sub>2</sub>] and [C<sub>1</sub>C<sub>3</sub>CNIm][DCA] allow the study of the influence of the cyano group in the solubility of ethane and ethene.

The solubility order of the two gases in the selected ionic liquids is [C<sub>1</sub>C<sub>3</sub>CNIm][NTf<sub>2</sub>] > [C<sub>1</sub>C<sub>4</sub>Im][DCA] > [C<sub>1</sub>C<sub>3</sub>CNIm][DCA]. Ethane is more soluble in [C<sub>1</sub>C<sub>3</sub>CNIm][NTf<sub>2</sub>] than in [C<sub>1</sub>C<sub>4</sub>Im][DCA] due a more favorable entropy of solvation in the first, in spite of the more favorable ethane-[C<sub>1</sub>C<sub>4</sub>Im][DCA] interaction. For ethene, it is the more favorable gas-ionic liquid interaction that justifies the higher solubility of the gas in [C<sub>1</sub>C<sub>3</sub>CNIm][NTf<sub>2</sub>]. The reason why both gases are more soluble in [C<sub>1</sub>C<sub>4</sub>Im][DCA] than [C<sub>1</sub>C<sub>3</sub>CNIm][DCA] is the same, a more favorable enthalpy of solvation for [C<sub>1</sub>C<sub>4</sub>Im][DCA].

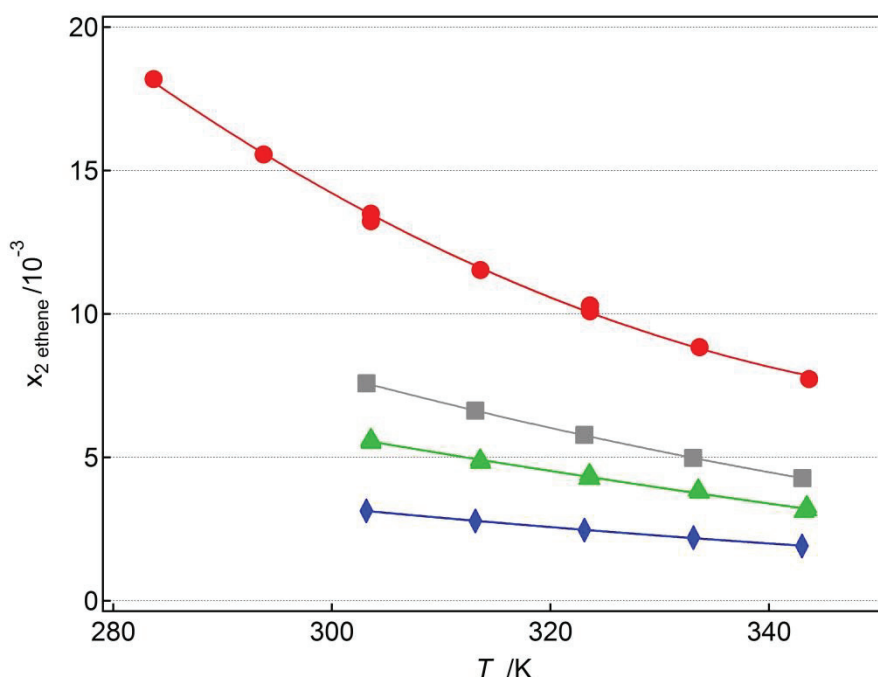


Figure 3.7 - Mole fraction solubilities of ethene at 0.1 MPa partial pressure and as a function of the temperature in the following ionic liquids: ●, [C<sub>1</sub>C<sub>4</sub>Im][NTf<sub>2</sub>]; ▲, [C<sub>1</sub>C<sub>4</sub>Im][DCA], ■, [C<sub>1</sub>C<sub>3</sub>CNIm][NTf<sub>2</sub>]; and ◆, [C<sub>1</sub>C<sub>3</sub>CNIm][DCA]. Full lines represent the smoothed data.

The presence of the cyano group in the alkyl side chain of the cation of the ionic liquid or in the form of the DCA<sup>-</sup> anion caused a decrease in the solubility of both ethane and ethene, when compared to the reference ionic liquid, [C<sub>1</sub>C<sub>4</sub>Im][NTf<sub>2</sub>]. The ethane and ethene solubility decrease was of 85% and 77%, respectively for [C<sub>1</sub>C<sub>3</sub>CNIm][NTf<sub>2</sub>]; 3 times and 2 times for [C<sub>1</sub>C<sub>4</sub>Im][DCA] and 6 times and 4 times for [C<sub>1</sub>C<sub>3</sub>CNIm][DCA]. In all three cases, the ethane solubility decreases more than the ethene solubility.

The reasons for the decrease are different in each case. For [C<sub>1</sub>C<sub>3</sub>CNIm][NTf<sub>2</sub>] and [C<sub>1</sub>C<sub>3</sub>CNIm][DCA], the ethane solubility decreases because the gas-solvent interactions are more favorable in the reference ionic liquid. For [C<sub>1</sub>C<sub>4</sub>Im][DCA] the reason behind the decrease is different, since gas-ionic liquid interactions are more favorable with this ionic liquid, but the entropic factors favor [C<sub>1</sub>C<sub>4</sub>Im][NTf<sub>2</sub>]. The reason why ethene is less soluble in [C<sub>1</sub>C<sub>3</sub>CNIm][NTf<sub>2</sub>] or [C<sub>1</sub>C<sub>4</sub>Im][DCA] than [C<sub>1</sub>C<sub>4</sub>Im][NTf<sub>2</sub>] is the same, the entropy of solvation of this gas in [C<sub>1</sub>C<sub>4</sub>Im][NTf<sub>2</sub>] is more favorable. Both the enthalpic and entropic factors favor a higher solubility of ethene in [C<sub>1</sub>C<sub>4</sub>Im][NTf<sub>2</sub>] when compared with [C<sub>1</sub>C<sub>3</sub>CNIm][DCA].

The study of the solubility of ethane and ethene in  $[\text{C}_1\text{C}_4\text{Im}][\text{C}_1\text{HPO}_3]$  will allow to determine the influence of a phosphite based anion in the solubility of these gases. In figures 3.8 and 3.10 we observe that the change of anion from  $[\text{C}_1\text{C}_4\text{Im}][\text{NTf}_2]$  to  $[\text{C}_1\text{C}_4\text{Im}][\text{C}_1\text{HPO}_3]$  leads to a decrease in both ethane and ethene solubility. This decrease is of 2.4 times for ethane and 2.2 times for ethene. As in the previous case, the solubility of ethane is more affected by changes in the ionic liquid than ethene. For ethane, the solubility decrease is due to a more favorable entropy of solvation in  $[\text{C}_1\text{C}_4\text{Im}][\text{NTf}_2]$  than in  $[\text{C}_1\text{C}_4\text{Im}][\text{C}_1\text{HPO}_3]$ , although the enthalpy of solvation is more favorable in the reference ionic liquid. For ethene, both the enthalpic and entropic terms contribute to a higher solubility in  $[\text{C}_1\text{C}_4\text{Im}][\text{NTf}_2]$  than in  $[\text{C}_1\text{C}_4\text{Im}][\text{C}_1\text{HPO}_3]$ . The solubility decrease when changing the anion from  $\text{C}_1\text{HPO}_3^-$  to  $\text{DCA}^-$  in a ionic liquid containing the  $\text{C}_1\text{C}_4\text{Im}^+$  cation is of 26% for ethane and 10% for ethene. Both gases are more soluble in  $[\text{C}_1\text{C}_4\text{Im}][\text{C}_1\text{HPO}_3]$ , due to a more favorable entropy of solvation.

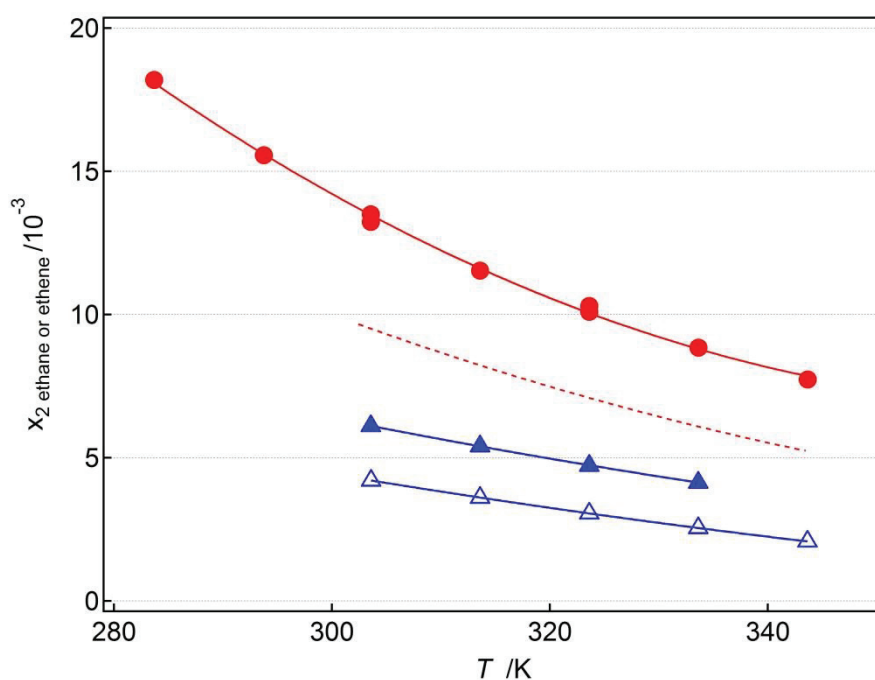


Figure 3.8 - Mole fraction solubilities of ethane (empty symbols) and ethene (full symbols) at 0.1 MPa partial pressure and as a function of the temperature in the following ionic liquids: ●,  $[\text{C}_1\text{C}_4\text{Im}][\text{NTf}_2]$ ; ▲/△,  $[\text{C}_1\text{C}_4\text{Im}][\text{C}_1\text{HPO}_3]$ . Full lines represent the smoothed data and the dashed lines corresponds to the previously reported values of the solubility of ethane in  $[\text{C}_1\text{C}_4\text{Im}][\text{NTf}_2]$  from reference 8.

To determine the influence of the type of unsaturation ( $\text{C}=\text{C}$  or  $\text{C}\equiv\text{N}$ ) on the cation alkyl side chain on ethane and ethene solubility we can compare the results for the ionic liquids  $[\text{C}_1\text{C}_3\text{CNIm}][\text{NTf}_2]$  and  $[\text{C}_1(\text{C}_3\text{H}_5\text{CH}_2)\text{Im}][\text{NTf}_2]$ . We observe that the

highest ethane and ethene solubility is obtained for  $[C_1(C_3H_5CH_2)Im][NTf_2]$ , due to a more favorable entropy of solvation, in spite of the more favorable ethane or ethene interaction with  $[C_1C_3CNIm][NTf_2]$ .

As can be observed in figure 3.9, the mole fraction absorption of ethene does not change significantly with the addition of lithium or nickel salts, but it almost doubles in the presence of the copper salt. There was no significant variation of the thermodynamic properties of solvation for ethene upon addition of lithium and nickel salts. The mole absorption of ethene slightly increases with size of metallic cation, but in the case of  $Li^+$  or  $Ni^{2+}$  is not due to coordination of ethene, as proven by the linear relationship between mole solubility and pressure, in figure 3.9 (on the bottom). The mole absorption of ethene in the copper solution is compatible with the values reported in the literature for other metallic cations.<sup>10,11</sup>

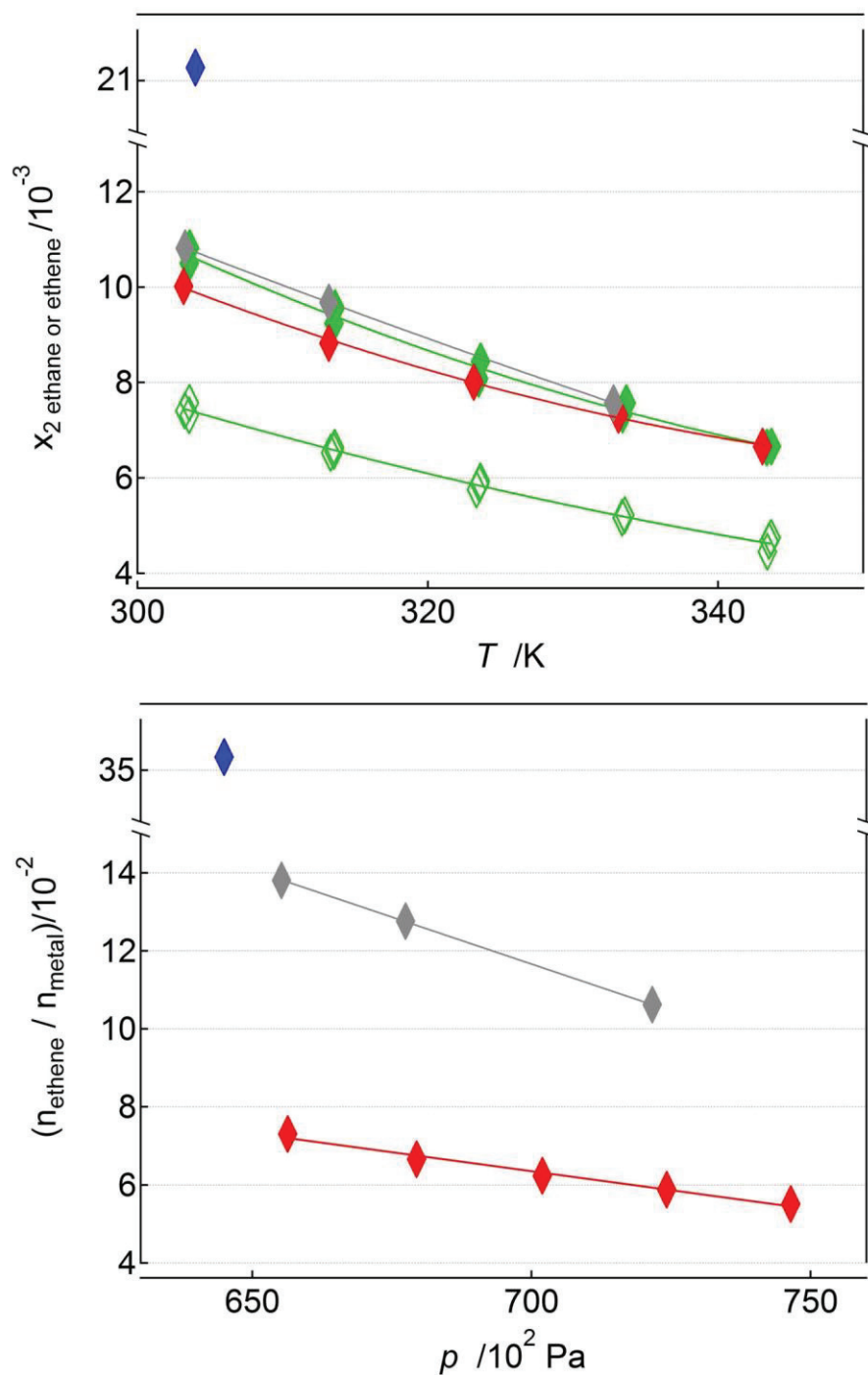


Figure 3.9 - Mole fraction absorption of ethane (empty symbols) and ethene (full symbols) at 0.1 MPa partial pressure and as a function of the temperature (on top) and amount of ethene *per* amount of metallic cation as a function of the equilibrium pressure (on bottom), in the following ionic liquids:  $\diamond$ ,  $[C_1(CH_2C_6H_5)Im][NTf_2]$ ;  $\blacklozenge$ ,  $[C_1(CH_2C_6H_5)Im][NTf_2] + 0.33 \text{ M LiNTf}_2$ ;  $\blacklozenge$ ,  $[C_1(CH_2C_6H_5)Im][NTf_2] + 0.18 \text{ M Ni}(NTf_2)_2$  and  $\blacklozenge$ ,  $[C_1(CH_2C_6H_5)Im][NTf_2] + < 0.01 \text{ mol L}^{-1} \text{ Cu}(NTf_2)_2$ . Full lines represent the smoothed data.

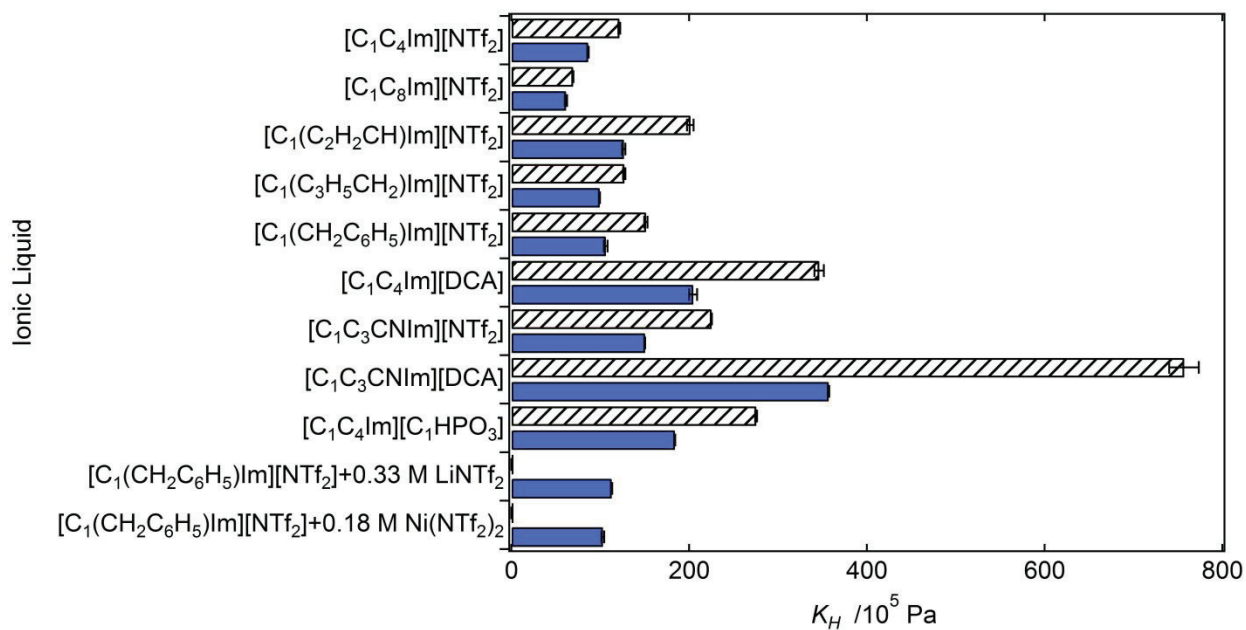


Figure 3.10 - Henry's law constant,  $K_H$ , for ethane, dashed bars, and ethene, full bars, in the ionic liquids and ionic liquid solutions used, at 313 K. Measurements for ethane in  $[\text{C}_1\text{C}_4\text{Im}][\text{NTf}_2]$  and  $[\text{C}_1\text{C}_8\text{Im}][\text{NTf}_2]$  from reference 8.

### 3.3 Ethane and ethene separation selectivity

The ideal selectivity,  $\alpha$ , was calculated for the separation of ethane and ethene in the selected ionic liquids. The ideal gas selectivity is not very different from the real mixed gas selectivity as both gases present relatively low absorptions and so their activity coefficients in the liquid phase are close to unity.

In figure 3.11, the selectivity is represented as a function of the respective Henry's law constant for ethene. A trend is observed, where the ionic liquids with higher ethene selectivity present lower ethene capacity.

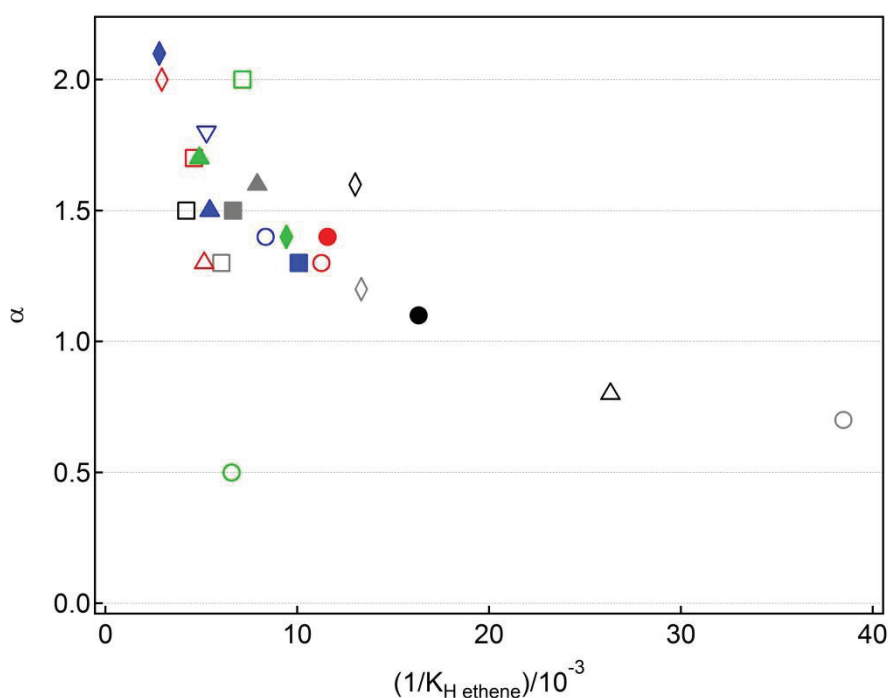


Figure 3.11 - Ethane/ethene ideal selectivity versus Henry's constant,  $K_H$ , of ethene in the ionic liquids,  $\circ$ ,  $[\text{C}_1\text{C}_2\text{Im}][\text{NTf}_2]$ <sup>12,13,14,15,16,17,18</sup>;  $\blacktriangle$ ,  $[\text{C}_1(\text{C}_2\text{H}_2\text{CH})\text{Im}][\text{NTf}_2]$ ;  $\bullet/\circ$ ,  $[\text{C}_1\text{C}_4\text{Im}][\text{NTf}_2]$ <sup>8,19,20,21,22,23,24</sup>;  $\circ$ ,  $[\text{C}_1\text{C}_6\text{Im}][\text{NTf}_2]$ <sup>\*,16,17,25</sup>;  $\bullet$ ,  $[\text{C}_1\text{C}_8\text{Im}][\text{NTf}_2]$ ;  $\blacksquare$ ,  $[\text{C}_1(\text{C}_3\text{H}_5\text{CH}_2)\text{Im}][\text{NTf}_2]$ ;  $\blacklozenge$ ,  $[\text{C}_1(\text{CH}_2\text{C}_6\text{H}_5)\text{Im}][\text{NTf}_2]$ ;  $\blacksquare/\square$ ,  $[\text{C}_1\text{C}_3\text{CNIm}][\text{NTf}_2]$ <sup>\*,20,22,23</sup>;  $\blacklozenge$ ,  $[\text{C}_1\text{C}_3\text{CNIm}][\text{DCA}]$ ;  $\square$ ,  $[(\text{C}_3\text{CN})_2\text{Im}][\text{NTf}_2]$ <sup>\*,20</sup>;  $\nabla$ ,  $[\text{C}_1\text{C}_2\text{Im}][\text{PF}_6]$ <sup>14</sup>;  $\triangle$ ,  $[\text{C}_1\text{C}_4\text{Im}][\text{PF}_6]$ <sup>\*,15,16,21,26</sup>;  $\blacktriangle$ ,  $[\text{C}_1\text{C}_4\text{Im}][\text{C}_1\text{HPO}_3]$ ;  $\blacklozenge$ ,  $[\text{C}_1\text{C}_2\text{Im}][\text{DCA}]$ <sup>14</sup>;  $\blacktriangle$ ,  $[\text{C}_1\text{C}_4\text{Im}][\text{DCA}]$ ;  $\square$ ,  $[\text{C}_1\text{C}_4\text{Im}][\text{BF}_4]$ <sup>22,24,27</sup>;  $\square$ ,  $[\text{C}_1\text{C}_2\text{Im}][\text{CF}_3\text{SO}_3]$ <sup>14</sup>;  $\triangle$ ,  $[\text{P}_{4444}][\text{TMPP}]$ <sup>13</sup>;  $\circ$ ,  $[\text{P}_{(14)666}][\text{TMPP}]$ <sup>28</sup>;  $\blacklozenge$ ,  $[\text{C}_1\text{C}_4\text{Pyr}][\text{NTf}_2]$ <sup>12,24</sup> and  $\blacklozenge$ ,  $[\text{C}_1\text{C}_6\text{Pyr}][\text{NTf}_2]$ <sup>29</sup> at 313 K. \* at 303 K. Full symbols represent our data and empty ones represent previously published values.

The largest selectivity was observed for  $[\text{C}_1\text{C}_3\text{CNIm}][\text{DCA}]$  which also presents the smallest ethene solubility. The largest ethene absorption was reported by Liu *et*

*al.*<sup>28</sup> for  $[P_{(14)666}][TMPP]$ , a very viscous ionic liquid designed to absorb more ethane than ethene, and so presenting a ethene selectivity smaller than 1.

## Conclusions

From the study of the absorption of ethane and ethene in different ionic liquids as a function of temperature, it was possible to determine the influence of several factors on the solubility of the two gases: the increase of the alkyl side chain of the cation of the ionic liquid; the presence of unsaturated bonds on the cation of the ionic liquid; the presence of cyano groups in the cation or anion of the ionic liquid or both and finally the influence of the a phosphite based anion in the ionic liquid.

We observed that small changes in the structure of the ionic liquid can have large effects in the ethane and ethene solubility and selectivity of the ionic liquid. Adding unsaturations in the alkyl chain of the cation of the ionic liquid, cyano groups in the alkyl chain of the cation or anion and changing the anion of the ionic liquid from an  $\text{NTf}_2^-$  to a  $\text{C}_1\text{HPO}_3^-$  or  $\text{DCA}^-$ , lead to decreases in the solubility of ethane and ethene, when compared to a reference ionic liquid,  $[\text{C}_1\text{C}_4\text{Im}][\text{NTf}_2]$ . The only exception is for  $[\text{C}_1(\text{C}_3\text{H}_5\text{CH}_2)\text{Im}][\text{NTf}_2]$ , where ethane solubility is not greatly affected. However, the introduction of these groups in the ionic liquid leads to an increase in the ethene selectivity.

For the ionic liquids tested, the difference in solubility of the two gases in each ionic liquid is due to entropic factors, meaning that the solubility is controlled by non-specific interactions.

The solubility of ethane is more affected by changes in the ionic liquid than ethene. The only exceptions from all the ionic liquids studied are for the ionic liquid  $[\text{C}_1(\text{C}_3\text{H}_5\text{CH}_2)\text{Im}][\text{NTf}_2]$  (where the solubility of ethane is similar and the solubility of ethene decreases 14%) and  $[\text{C}_1(\text{CH}_2\text{C}_6\text{H}_5)\text{Im}][\text{NTf}_2]$  (where the solubility of both gases decreases in a similar way).

The addition of copper salts almost doubles the absorption capacity of ethene in the ionic liquid  $[\text{C}_1(\text{CH}_2\text{C}_6\text{H}_5)\text{Im}][\text{NTf}_2]$ . We observe that metallic cations such as lithium and nickel slightly affect the absorption of ethene, and not through coordination of the unsaturated gas. The observed solubility results with the lithium salt are compatible with the known fact that this metallic cation, when present in a  $\text{NTf}_2^-$  containing ionic liquid, is surrounded by an average of 3-4 anions.<sup>30</sup>

## References

---

- <sup>1</sup> Gutel, T.; Santini, C. C.; Pádua, A. A. H.; Fenet, B.; Chauvin, Y.; Canongia Lopes, J. N.; Bayard, F.; Costa Gomes, M. F. and Pensado, A. S. Interaction between the  $\pi$ -System of Toluene and the Imidazolium Ring of Ionic Liquids: A Combined NMR and Molecular Simulation Study. *J. Phys. Chem. B* **2009**, 113, 170-177
- <sup>2</sup> Jacquemin, J.; Costa Gomes, M. F.; Husson, P.; Majer, V. and Pádua, A. A. H. Thermophysical Properties, Low Pressure Solubilities and Thermodynamics of Solvation of Carbon Dioxide and Hydrogen in Two Ionic Liquids Based on the Alkylsulfate Anion. *Green Chem.* **2008**, 10, 944-950
- <sup>3</sup> Kim, D.; Hu, S.; Tarakeshwar, P. and Kim, K. S. Cation- $\pi$  Interactions: A Theoretical Investigation of the Interaction of Metallic and Organic Cations with Alkenes, Arenes, and Heteroarenes, *J. Phys. Chem. A* **2003**, 107, 1228-1238
- <sup>4</sup> Ortiz, A.; Ruiz, A.; Gorri, D.; Ortiz, I. Room Temperature Ionic Liquid with Silver Salt as Efficient Reaction Media for Propene/Propane Separation: Absorption Equilibrium. *Sep. Purif. Technol.* **2008**, 63, 311-318
- <sup>5</sup> Mokrushin, V.; Assenbaum, D.; Paape, N.; Gerhard, D.; Mokrushina, L.; Wasserscheid, P.; Arlt, W.; Kistenmacher, H.; Neuendorf, S. and Göke, V. Ionic Liquids for Propene-Propane Separation. *Chem. Eng. Technol.* **2010**, 33, 63-73
- <sup>6</sup> Dymond, J. H.; Marsh, K. N.; Wilhoit, R. C.; Wong, K. C. The Virial Coefficients of Pure Gases and Mixtures, Landolt-Börnstein: Numerical Data and Functional Relationships in Science and Technology New Series, Subseries Physical Chemistry; Springer: New York, **2003**; 21B.
- <sup>7</sup> Moura, L.; Mishra, M.; Bernales, V. ; Fuentealba, P. ; Padua, A. A. H. ; Santini, C. C. and Costa Gomes, M. F. Effect of Unsaturation on the Absorption of Ethane and Ethylene in Imidazolium-Based Ionic Liquids, *J. Phys. Chem. B* **2013**, 117, 7416-7425
- <sup>8</sup> Costa Gomes, M. F.; Pison, L.; Pensado, A. S. and Pádua, A. A. H. Using Ethane and Butane as Probes to the Molecular Structure of 1-Alkyl-3-methylimidazolium bis[(trifluoromethyl)sulfonyl]imide Ionic Liquids, *Faraday Discuss.* **2012**, 154, 41-52
- <sup>9</sup> Lee, J. M.; Palgunadi, J.; Kim, J. H.; Jung, S.; Choi, Y.; Cheong, M. and Kim, H. S. Selective Removal of Acetylenes from Olefin Mixtures Through Specific Physicochemical Interactions of Ionic Liquids with Acetylenes, *Phys. Chem. Chem. Phys.* **2010**, 12, 1812-1816

- 
- <sup>10</sup> Sánchez, L. M. G.; Meindersma, G. W. and Haan, A. B. Potential of Silver-Based Room-Temperature Ionic Liquids for Ethene/Ethane Separation, *Ind. Eng. Chem. Res.* **2009**, *48*, 10650-10656
- <sup>11</sup> Mortaheb, H. R., Mafi, M.; Mokhtarani, B.; Sharifi, A.; Mirzaei, M.; Khodapanah, N. and Ghaemmaghami, F. Experimental Kinetic Analysis of Ethene Absorption in Ionic Liquid [Bmim]NO<sub>3</sub> with Dissolved AgNO<sub>3</sub> by a Semi-Continuous Process, *Chem. Eng. J.* **2010**, *158*, 384-392
- <sup>12</sup> Honga, G.; Jacquemin, J.; Deetlefs, M.; Hardacre, C.; Husson, P. and Costa Gomes, M. F. Solubility of Carbon Dioxide and Ethane in Three Ionic Liquids Based on the Bis{(trifluoromethyl)sulfonyl}imide Anion, *Fluid Phase Equilibr.* **2007**, *257*, 27-34
- <sup>13</sup> Liu, X.; Afzal, W. and Prausnitz, J. M. Solubilities of Small Hydrocarbons in Tetrabutylphosphonium Bis(2,4,4-trimethylpentyl) Phosphinate and in 1-Ethyl-3-methylimidazolium Bis(trifluoromethylsulfonyl)imide, *Ind. Eng. Chem. Res.* **2013**, *52*, 14975-14978
- <sup>14</sup> Camper, D.; Becker, C.; Koval, C. and Noble, R. Low Pressure Hydrocarbon Solubility in Room Temperature Ionic Liquids Containing Imidazolium Rings Interpreted Using Regular Solution Theory, *Ind. Eng. Chem. Res.* **2005**, *44*, 1928-1933
- <sup>15</sup> Camper, D.; Scovazzo, P.; Koval, C. and Noble, R. Gas Solubilities in Room-Temperature Ionic Liquids, *Ind. Eng. Chem. Res.* **2004**, *43*, 3049-3054
- <sup>16</sup> Kilaru, P. K. and Scovazzo, P. Correlations of Low-Pressure Carbon Dioxide and Hydrocarbon Solubilities in Imidazolium-, Phosphonium-, and Ammonium-Based Room-Temperature Ionic Liquids. Part 2. Using Activation Energy of Viscosity, *Ind. Eng. Chem. Res.* **2008**, *47*, 910-919
- <sup>17</sup> Kilaru, P. K.; Condemarin, R. A. and Scovazzo, P. Correlations of Low-Pressure Carbon Dioxide and Hydrocarbon Solubilities in Imidazolium-, Phosphonium-, and Ammonium-Based Room-Temperature Ionic Liquids. Part 1. Using Surface Tension, *Ind. Eng. Chem. Res.* **2008**, *47*, 900-909
- <sup>18</sup> Morgan, D.; Ferguson, L. and Scovazzo, P. Diffusivities of Gases in Room-Temperature Ionic Liquids: Data and Correlations Obtained Using a Lag-Time Technique, *Ind. Eng. Chem. Res.* **2005**, *44*, 4815-4823

- 
- <sup>19</sup> Gan, Q.; Zou, Y.; Rooney, D.; Nancarrow, P.; Thompson, J.; Liang, L.; Lewis, M. Theoretical and Experimental Correlations of Gas Dissolution, Diffusion, and Thermodynamic Properties in Determination of Gas Permeability and Selectivity in Supported Ionic Liquid Membranes, *Adv. Colloid Interfac.* **2011**, 164, 45-55
- <sup>20</sup> Xing, H.; Zhao, X.; Li, R.; Yang, Q.; Su, B.; Bao, Z.; Yang, Y. and Ren, Q. Improved Efficiency of Ethylene/Ethane Separation Using a Symmetrical Dual Nitrile-Functionalized Ionic Liquid, *ACS Sustainable Chem. Eng.* **2013**, 1, 1357-1363
- <sup>21</sup> Anthony, J. L.; Anderson, J. L.; Maginn, E. J. and Brennecke, J. F. Anion Effects on Gas Solubility in Ionic Liquids, *J. Phys. Chem. B* **2005**, 109, 6366-6374
- <sup>22</sup> Zhang, J.; Zhang, Q.; Qiao, B. and Deng, Y. Solubilities of the Gaseous and Liquid Solutes and Their Thermodynamics of Solubilization in the Novel Room-Temperature Ionic Liquids at Infinite Dilution by Gas Chromatography, *J. Chem. Eng. Data* **2007**, 52, 2277-2283
- <sup>23</sup> Zhang, Q.; Li, Z.; Zhang, J.; Zhang, S.; Zhu, L. ; Yang, J.; Zhang, X. and Deng, Y. Physicochemical Properties of Nitrile-Functionalized Ionic Liquids, *J. Phys. Chem. B* **2007**, 111, 2864-2872
- <sup>24</sup> Palgunadi, J.; Kim, H. S.; Lee, J. M.; Jung, S. Ionic Liquids for Acetylene and Ethylene Separation: Material Selection and Solubility Investigation, *Chem. Eng. Process.* **2010**, 49, 192-198
- <sup>25</sup> Costa Gomes, M. F. Low-Pressure Solubility and Thermodynamics of Solvation of Carbon Dioxide, Ethane, and Hydrogen in 1-Hexyl-3-methylimidazolium Bis(trifluoromethylsulfonyl)amide between Temperatures of 283 K and 343 K, *J. Chem. Eng. Data* **2007**, 52, 472-475
- <sup>26</sup> Jacquemin, J.; Husson, P.; Majer, V. and Costa Gomes, M. F. Low-Pressure Solubilities and Thermodynamics of Solvation of Eight Gases in 1-Butyl-3-methylimidazolium Hexafluorophosphate, *Fluid Phase Equilib.* **2006**, 240, 87-95
- <sup>27</sup> Jacquemin, J.; Costa Gomes, M. F.; Husson, P. and Majer, V. Solubility of Carbon Dioxide, Ethane, Methane, Oxygen, Nitrogen, Hydrogen, Argon, and Carbon Monoxide in 1-Butyl-3-methylimidazolium Tetrafluoroborate Between Temperatures 283 K and 343 K and at Pressures Close to Atmospheric, *J. Chem. Thermodyn.* **2006**, 38, 490-502

- 
- <sup>28</sup> Liu, X.; Afzal, W.; Yu, G.; He, M. and Prausnitz, J. M. High Solubilities of Small Hydrocarbons in Trihexyl Tetradecylphosphonium Bis(2,4,4-trimethylpentyl) Phosphinate, *J. Phys. Chem. B* **2013**, 117, 10534-10539
- <sup>29</sup> Anderson, J. L.; Dixon, J. K. and Brennecke, J. F. Solubility of CO<sub>2</sub>, CH<sub>4</sub>, C<sub>2</sub>H<sub>6</sub>, C<sub>2</sub>H<sub>4</sub>, O<sub>2</sub>, and N<sub>2</sub> in 1-Hexyl-3-methylpyridinium Bis(trifluoromethylsulfonyl)imide: Comparison to Other Ionic Liquids, *Acc. Chem. Res.* **2007**, 40, 1208-1216
- <sup>30</sup> Borodin, O.; Smith, G. D. and Henderson, W. Li<sup>+</sup> Cation Environment, Transport, and Mechanical Properties of the LiTFSI Doped N-Methyl-N-alkylpyrrolidinium<sup>+</sup>TFSI<sup>-</sup> Ionic Liquids, *J. Phys. Chem. B* **2006**, 110, 16879-16886

# Chapter 4

---

Conclusions and Perspectives



The goal of this project was to determine the potential of a selection of ionic liquids for the separation of ethane from ethene. This selection of ionic liquids was designed to escape the tendencies observed in the literature for the solubility of ethane and ethene in order to increase both the selectivity and absorption capacity for the unsaturated gas in ionic liquids.

Contrary to what is suggested in the literature, the solubility of unsaturated gases, such as ethene and propene is not always higher than of their saturated counterparts, ethane and propane. In fact, their solubilities range overlap. Ethyne and propyne present the highest mole fraction solubilities, in imidazolium and/or pyrrolidinium based ionic liquids. Ethyne and propyne are followed by propane and propene with solubilities of the same order of magnitude for phosphonium based ionic liquids (larger molecular weights). Ethane and ethene are one order of magnitude less soluble than ethyne in the same phosphonium based ionic liquids. For a low molecular weight ionic liquid such as  $[C_1C_2Im][NTf_2]$  propyne is the most soluble gas, followed by ethyne and propene (3-5 times less soluble), propane and ethene (at least one order of magnitude less soluble than propyne and 3-4 times less soluble than ethyne and propene) and ethane (20 times less soluble than propyne, 4-7 times less soluble than propene and ethyne and 2 times less soluble than propane and ethene). The tendencies observed for ethane, ethene, propane and propene are similar. The solubility of these gases increases with the size of the non-polar domains of the cation or anion of the ionic liquid, suggesting that the solubility of these gases in the group of ionic liquids studied is ruled by nonspecific interactions. The solubility order in terms of cations is  $P_{nmpq}^+ > N_{nmpq}^+ > C_nPyr^+ > C_nC_mPyr^+ > C_nC_mIm^+$ . In comparison, the solubility dependency in terms of the nature of the anion is much smaller, for the same gases. The tendencies found for ethyne are the opposite. The influence of the cation size is much less important than the influence of the nature of the anion. The highest ethyne solubilities are found in ionic liquids containing anions with a Lewis base character, such as alkylphosphates, alkylphosphites and alkylsulphates. This is probably due to the presence of a relatively acidic proton in ethyne. The order of solubility of ethyne relative to anions for imidazolium and pyrrolidinium-based cations is:  $C_nC_mPO_4^- > OAc^- > C_nHPO_3^- > C_nSO_4^- > TFA^- > BF_4^- > PF_6^- \approx NTf_2^-$ . Ideal selectivities of 40 and 15 and mole fraction solubilities of 0.1 and 0.2 can be obtained for ethene/ethyne and propene/propyne separations, respectively.

Completing the solubility data on ethane, ethene, ethyne and propyne (tables 4.1 and 4.2) would provide a good start on a database in light hydrocarbon solubility in ILs. This information could also be used as a good basis for the development of a model that would allow the prediction of the solubility of these gases in other ionic liquids.

For this project, a selected group of ionic liquids were used to test the influence of structural modifications in the ionic liquid on the absorption of ethane and ethene. The presence of: an increasing alkyl side-chain on the cation of the ionic liquid; unsaturations on the alkyl side-chain on the cation of the ionic liquid; cyano groups in the cation or anion of the ionic liquid or both and a phosphite based anion in the ionic liquid were tested for their influence on the density and viscosity of the ionic liquid and in the solubility of ethane and ethene. The selected ionic liquids were synthesized via a one-step or two-step synthesis path, with purities of at least 99%. The ionic liquids were characterized by proton and carbon NMR spectroscopy, high resolution mass spectroscopy, and density and viscosity measurements. Solutions of ionic liquid with metallic salts of lithium (I), nickel (II) and copper (II) were also characterized in terms of density and viscosity.

The ionic liquid with the highest density is  $[\text{C}_1(\text{C}_2\text{H}_2\text{CH})\text{Im}][\text{NTf}_2]$  and the one with the lowest is  $[\text{C}_1\text{C}_4\text{Im}][\text{DCA}]$ . The ionic liquid with highest viscosity is  $[\text{C}_1\text{C}_4\text{Im}][\text{Lev}]$  and the one with the lowest is  $[\text{C}_1\text{C}_4\text{Im}][\text{DCA}]$ . The presence of unsaturations in the alkyl chain of the cation can lead to viscosities up to 2 times greater than in ionic liquids with saturated side alkyl chains.

Small changes in the structure of the ionic liquid can have large effects in the ethane and ethene solubility and ethane/ethene separation selectivity of the ionic liquid. Adding unsaturations in the alkyl chain of the cation of the ionic liquid, cyano groups in the alkyl chain of the cation or anion and changing the anion of the ionic liquid from an  $\text{NTf}_2^-$  to a  $\text{C}_1\text{HPO}_3^-$  or DCA, lead to decreases in the solubility of ethane and ethylene, when compared to a reference ionic liquid,  $[\text{C}_1\text{C}_4\text{Im}][\text{NTf}_2]$ . The only exception is for  $[\text{C}_1(\text{C}_3\text{H}_5\text{CH}_2)\text{Im}][\text{NTf}_2]$ , where ethane solubility is not greatly affected. The introduction of these groups in the ionic liquid also leads to increases in the ethene selectivity. The solubility of ethane is more affected by changes in the ionic liquid than ethene. For example, increasing the alkyl side chain of the cation from  $[\text{C}_1\text{C}_4\text{Im}][\text{NTf}_2]$  to  $[\text{C}_1\text{C}_8\text{Im}][\text{NTf}_2]$  leads to an increase in ethane and ethene solubility but the increase was larger for the saturated gas. The only exceptions are for the

ionic liquid containing a double bond (where the solubility of ethane is similar and the solubility of ethene decreases 14%) and containing a benzyl group (where the solubility of both gases decreases in a similar way).

For the group of ionic liquids tested, the difference in solubility of the two gases in each ionic liquid is due to entropic factors, which means that the solubility is still controlled by non-specific interactions, in the same way as it was observed in the literature analysis. The interactions between the selected group of ionic liquids and ethene were not strong or specific enough to gain against what is lost due to entropy. This was further confirmed by observing that for the group of ionic liquids selected for this study, the ones that present higher ethene absorption capacity and lower ideal selectivity are the ones with highest molar volume and vice-versa, as can be observed in figure 4.1.

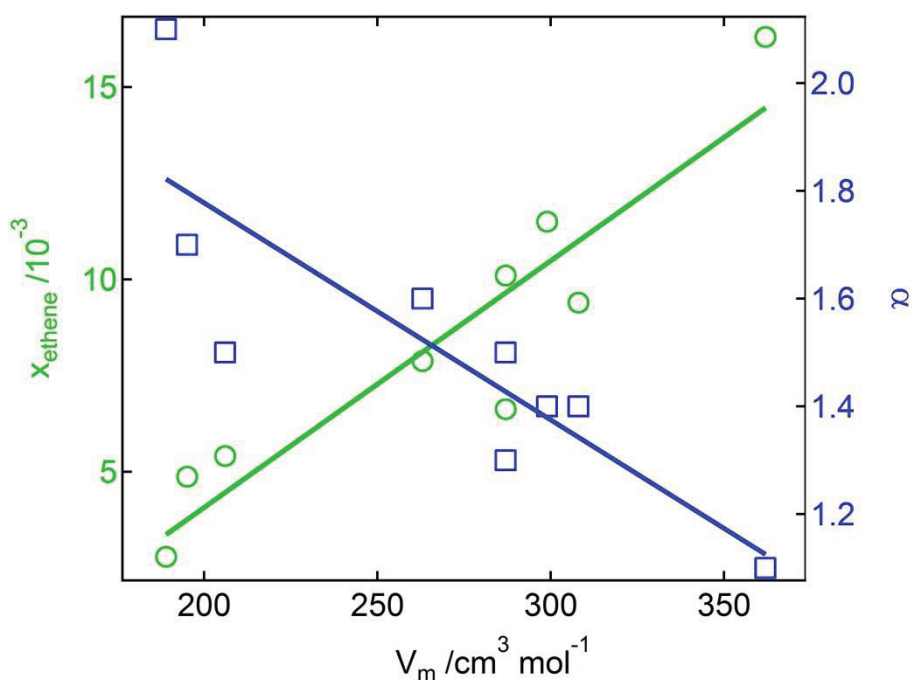


Figure 4.1 – Molar volume of the ionic liquids, in  $\text{cm}^3 \text{ mol}^{-1}$ , versus the molar fraction absorption capacity of each ionic liquid for ethene and versus the ionic liquids ideal selectivities

For the group of ionic liquids tested the one possessing the largest ethene capacity and lowest ideal selectivity corresponds to the one containing the largest alkyl chain in the cation,  $[\text{C}_1\text{C}_8\text{Im}][\text{NTf}_2]$ . The ionic liquid family that presents the best selectivity and smallest absorption capacity for ethene is the one containing cyano groups;  $[\text{C}_1\text{C}_3\text{CNIm}][\text{NTf}_2]$ ,  $[\text{C}_1\text{C}_4\text{Im}][\text{DCA}]$  and  $[\text{C}_1\text{C}_3\text{CNIm}][\text{DCA}]$ .

The influence in ethene solubility of the presence of three different metallic cations, lithium (I), nickel (II) and copper (II) in an ionic liquid was also studied. The presence of copper was found to cause a large increase in the solubility of ethene. The solubility, at 303 K, of the metallic salts in  $[C_1(CH_2C_6H_5)Im][NTf_2]$  decreases with the size of the metallic cation. The addition of these metallic salts to the ionic liquid caused an increase its density of up to 2% for the salt types and concentrations studied and an increase in viscosity of 42%, 50% and 34% upon addition of the lithium, nickel and copper salts respectively and at 298 K. The addition of copper salts almost doubles the absorption capacity of ethene in the ionic liquid  $[C_1(CH_2C_6H_5)Im][NTf_2]$ . We observe that metallic cations such as lithium and nickel slightly affect the solubility of ethene, and not through coordination of the unsaturated gas.

It would be of great interest to develop ionic liquids containing functionalizations or anions (such as  $AlCl_4^-$ ) that could promote a specific interaction with ethene. Another promising possibility is to develop ionic liquids containing metal ions in their structure.<sup>1</sup> However, the more specific are the interactions between the gas and the ionic liquid, the harder the recycling of the absorbent will be, and a balancing effect between specificity and recovery it should be taken into account into developing an ionic liquid for separation purposes.

Table 4.2 - Solubility of ethane, ethene, ethyne, propane, propene and propyne in several ionic liquids, expressed in Henry's law constant,  $K_H$ , the majority at 313 K

Ionic liquid	Gas						Solubility range	
	Ethane	Ethene	Ethyne	Propane	Propene	Propyne	$K_H / 10^{-5} \text{ Pa}$	color
[C <sub>1</sub> C <sub>2</sub> Im][NTf <sub>2</sub> ]	light yellow	yellow	dark red	orange	red		no data	
[C <sub>1</sub> (C <sub>2</sub> H <sub>2</sub> CH)Im][NTf <sub>2</sub> ]*	light green	yellow					0-10	dark brown
[C <sub>1</sub> C <sub>4</sub> Im][NTf <sub>2</sub> ]*	yellow	orange	dark red	orange	red		11-20	dark brown
[C <sub>1</sub> (C <sub>3</sub> H <sub>5</sub> CH <sub>2</sub> )Im][NTf <sub>2</sub> ]*	yellow	orange					21-30	dark red
[C <sub>1</sub> C <sub>6</sub> Im][NTf <sub>2</sub> ]	orange	light yellow			red		31-40	red
[C <sub>1</sub> (CH <sub>2</sub> C <sub>6</sub> H <sub>5</sub> )Im][NTf <sub>2</sub> ]*	light yellow	yellow					41-50	orange-red
[C <sub>1</sub> C <sub>8</sub> Im][NTf <sub>2</sub> ]*	orange	orange					51-100	orange
[C <sub>1</sub> C <sub>10</sub> Im][NTf <sub>2</sub> ]	orange						101-150	yellow
[C <sub>1</sub> C <sub>3</sub> CNIIm][NTf <sub>2</sub> ]*	light green	yellow					151-200	light yellow
[(C <sub>3</sub> CN) <sub>2</sub> Im][NTf <sub>2</sub> ]	light yellow	yellow					201-300	light green
[C <sub>1</sub> C <sub>1</sub> C <sub>3</sub> CNIIm][NTf <sub>2</sub> ]		yellow					301-400	green
[C <sub>1</sub> C <sub>1</sub> COOC <sub>5</sub> Im][NTf <sub>2</sub> ]	orange						401-500	green
[C <sub>1</sub> C <sub>1</sub> COOC <sub>2</sub> OC <sub>2</sub> Im][NTf <sub>2</sub> ]	orange						501-600	dark green
[C <sub>1</sub> C <sub>1</sub> COOC <sub>2</sub> OC <sub>2</sub> OC <sub>4</sub> Im][NTf <sub>2</sub> ]	orange						over 600	dark green
[C <sub>1</sub> C <sub>4</sub> Im][BETI]		orange			red			
[C <sub>1</sub> C <sub>4</sub> Im][FAP]	orange							
[C <sub>1</sub> C <sub>6</sub> Im][FAP]	orange							
[C <sub>1</sub> C <sub>2</sub> Im][DCA]	dark green	green		green	yellow			
[C <sub>1</sub> C <sub>4</sub> Im][DCA]*	green	light green						
[C <sub>1</sub> C <sub>3</sub> CNIIm][DCA]*	dark green	green						
[C <sub>1</sub> C <sub>1</sub> C <sub>3</sub> CNIIm][DCA]		green						
[C <sub>1</sub> C <sub>4</sub> Im][OAc]		yellow	dark brown					
[C <sub>1</sub> C <sub>4</sub> Im][n-C <sub>15</sub> H <sub>31</sub> COO]		orange						
[C <sub>1</sub> C <sub>4</sub> Im][n-C <sub>17</sub> H <sub>35</sub> COO]		orange						
[C <sub>1</sub> C <sub>2</sub> Im][PF <sub>6</sub> ]	green	light yellow		light yellow	orange			
[C <sub>1</sub> C <sub>4</sub> Im][PF <sub>6</sub> ]	green	light yellow	dark red		orange			
[C <sub>1</sub> C <sub>2</sub> Im][BF <sub>4</sub> ]			dark red					
[C <sub>1</sub> C <sub>4</sub> Im][BF <sub>4</sub> ]	green	light green	dark brown	light green	orange			
[C <sub>1</sub> C <sub>8</sub> Im][BF <sub>4</sub> ]		yellow						
[C <sub>1</sub> C <sub>4</sub> Im][TFA]		yellow	dark brown					
[C <sub>1</sub> C <sub>1</sub> Im][C <sub>1</sub> HPO <sub>3</sub> ]		green	dark brown			dark brown		
[C <sub>1</sub> C <sub>2</sub> Im][C <sub>1</sub> HPO <sub>3</sub> ]			dark brown					
[C <sub>1</sub> C <sub>2</sub> Im][C <sub>2</sub> HPO <sub>3</sub> ]		light green	dark brown		orange	dark brown		
[C <sub>1</sub> C <sub>4</sub> Im][C <sub>1</sub> HPO <sub>3</sub> ]*	light green	light yellow	dark brown			dark brown		
[C <sub>1</sub> C <sub>4</sub> Im][C <sub>4</sub> HPO <sub>3</sub> ]		yellow	dark brown		red	dark brown		
[C <sub>2</sub> C <sub>4</sub> Im][C <sub>2</sub> HPO <sub>3</sub> ]		yellow	dark brown		red	dark brown		
[C <sub>1</sub> C <sub>1</sub> Im][(C <sub>1</sub> ) <sub>2</sub> PO <sub>4</sub> ]		light green	dark brown					
[C <sub>1</sub> C <sub>2</sub> Im][(C <sub>1</sub> ) <sub>2</sub> PO <sub>4</sub> ]			dark brown					
[C <sub>1</sub> C <sub>2</sub> Im][(C <sub>2</sub> ) <sub>2</sub> PO <sub>4</sub> ]								
[C <sub>1</sub> C <sub>4</sub> Im][(C <sub>1</sub> ) <sub>2</sub> PO <sub>4</sub> ]		yellow	dark brown					
[C <sub>1</sub> C <sub>4</sub> Im][(C <sub>4</sub> ) <sub>2</sub> PO <sub>4</sub> ]								
[C <sub>1</sub> C <sub>1</sub> Im][C <sub>1</sub> SO <sub>4</sub> ]			dark brown					

\*measurements performed in the context of this work

Table 4.3 - Solubility of ethane, ethene, ethyne, propane, propene and propyne in several ionic liquids, expressed in Henry's law constant,  $K_H$ , the majority at 313 K

Gas

Ionic liquid

	Ethane	Ethene	Ethyne	Propane	Propene	Propyne
[C <sub>1</sub> C <sub>2</sub> Im][C <sub>1</sub> SO <sub>4</sub> ]						
[C <sub>1</sub> C <sub>2</sub> Im][C <sub>2</sub> SO <sub>4</sub> ]						
[C <sub>1</sub> C <sub>4</sub> Im][C <sub>1</sub> SO <sub>4</sub> ]						
[C <sub>1</sub> C <sub>1</sub> COOC <sub>5</sub> Im][C <sub>8</sub> SO <sub>4</sub> ]						
[C <sub>1</sub> C <sub>2</sub> Im][CF <sub>3</sub> SO <sub>3</sub> ]						
[(C <sub>2</sub> SO <sub>2</sub> C <sub>2</sub> )C <sub>1</sub> Im][CF <sub>3</sub> SO <sub>3</sub> ]						
[C <sub>1</sub> C <sub>6</sub> Pyrr][NTf <sub>2</sub> ]						
[C <sub>1</sub> C <sub>4</sub> Pyrr][NTf <sub>2</sub> ]						
[C <sub>1</sub> C <sub>4</sub> Pyrr][FAP]						
[C <sub>1</sub> C <sub>4</sub> Pyrr][DCA]						
[C <sub>1</sub> C <sub>4</sub> Pyrr][OAc]						
[C <sub>1</sub> C <sub>4</sub> Pyrr][TFA]						
[C <sub>1</sub> C <sub>1</sub> Pyrr][C <sub>1</sub> HPO <sub>3</sub> ]						
[C <sub>1</sub> C <sub>2</sub> Pyrr][C <sub>2</sub> HPO <sub>3</sub> ]						
[C <sub>1</sub> C <sub>4</sub> Pyrr][C <sub>4</sub> HPO <sub>3</sub> ]						
[N <sub>(1)444</sub> ][NTf <sub>2</sub> ]						
[N <sub>(4)111</sub> ][NTf <sub>2</sub> ]						
[N <sub>(4)113</sub> ][NTf <sub>2</sub> ]						
[N <sub>(6)111</sub> ][NTf <sub>2</sub> ]						
[N <sub>(6)113</sub> ][NTf <sub>2</sub> ]						
[N <sub>(10)111</sub> ][NTf <sub>2</sub> ]						
[N <sub>(6)222</sub> ][NTf <sub>2</sub> ]						
[N <sub>(10)113</sub> ][NTf <sub>2</sub> ]						
[N <sub>(1)888</sub> ][NTf <sub>2</sub> ]						
[N <sub>1132-OH</sub> ][NTf <sub>2</sub> ]						
[P <sub>(14)666</sub> ][NTf <sub>2</sub> ]						
[P <sub>(14)666</sub> ][Cl]						
[P <sub>(14)666</sub> ][FAP]						
[P <sub>(14)666</sub> ][DCA]						
[P <sub>(2)444</sub> ][(C <sub>2</sub> ) <sub>2</sub> PO <sub>4</sub> ]						
[P <sub>4444</sub> ][TMPP]						
[P <sub>(14)666</sub> ][TMPP]						
[P <sub>(14)444</sub> ][DBS]						

Solubility range

K <sub>H</sub> /10 <sup>-5</sup> Pa	color
no data	
0-10	
11-20	
21-30	
31-40	
41-50	
51-100	
101-150	
151-200	
201-300	
301-400	
401-500	
501-600	
over 600	

---

<sup>1</sup> Lin, I. J. B.; Vasam, C. S. Metal-Containing Ionic Liquids and Ionic Liquid Crystals Based on Imidazolium Moiety, *J. Organomet. Chem.* **2005**, 690, 3498-3512

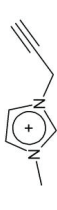
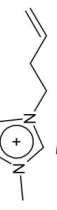
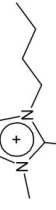
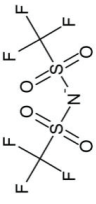
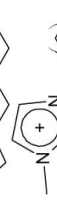
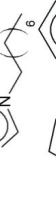
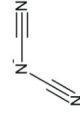
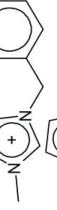
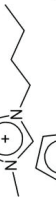
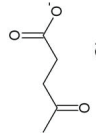
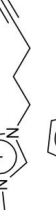


# Appendix 1

---



Table A.1 - Representation, name, abbreviation and CAS number of the ionic liquids synthesized

Cation	Anion	Name	Abbreviation	CAS
		1-butyl-3-methylimidazolium methylsulfate	[C <sub>1</sub> C <sub>4</sub> Im][(CH <sub>3</sub> O)SO <sub>3</sub> ]	401788-98-5
		1-butyl-3-methylimidazolium methylphosphonate	[C <sub>1</sub> C <sub>4</sub> Im][(CH <sub>3</sub> O)HPO <sub>2</sub> ]	-
		1-butyl-3-methylimidazolium dimethylphosphate	[C <sub>1</sub> C <sub>4</sub> Im][(CH <sub>3</sub> O) <sub>2</sub> PO <sub>2</sub> ]	-
		1-methyl-3-(propyn-3-yl)imidazolium bis(trifluoromethanesulfonyl)imide	[C <sub>1</sub> (C <sub>2</sub> H <sub>2</sub> CH)Im][NTf <sub>2</sub> ]*	-
		1-butyl-3-methylimidazolium bis(trifluoromethanesulfonyl)imide	[C <sub>1</sub> C <sub>4</sub> Im][NTf <sub>2</sub> ]	174899-83-3
		1-(buten-3-yl)-3-methylimidazolium bis(trifluoromethanesulfonyl)imide	[C <sub>1</sub> (C <sub>3</sub> H <sub>5</sub> CH <sub>2</sub> )Im][NTf <sub>2</sub> ]	-
		1-butyl-2,3-dimethylimidazolium bis(trifluoromethanesulfonyl)imide	[C <sub>1</sub> C <sub>1</sub> C <sub>4</sub> Im][NTf <sub>2</sub> ]	350493-08-2
		1-(3-cyanopropyl)-3-methylimidazolium bis(trifluoromethanesulfonyl)imide	[C <sub>1</sub> C <sub>3</sub> CNIIm][NTf <sub>2</sub> ]*	778593-18-3
		1-hexyl-3-methylimidazolium bis(trifluoromethanesulfonyl)imide	[C <sub>1</sub> C <sub>6</sub> Im][NTf <sub>2</sub> ]	382150-50-7
		1-methyl-3-octyl-imidazolium bis(trifluoromethanesulfonyl)imide	[C <sub>1</sub> C <sub>8</sub> Im][NTf <sub>2</sub> ]**	178631-04-4
		1-benzyl-3-methylimidazolium bis(trifluoromethanesulfonyl)imide	[C <sub>1</sub> (CH <sub>2</sub> C <sub>6</sub> H <sub>5</sub> )Im][NTf <sub>2</sub> ]	-
		1-butyl-3-methylimidazolium dicyanamide	[C <sub>1</sub> C <sub>4</sub> Im][DCA]	448245-52-1
		1-(3-cyanopropyl)-3-methylimidazolium dicyanamide	[C <sub>1</sub> C <sub>3</sub> CNIIm][DCA]*	879866-74-7
		1-butyl-3-methylimidazolium levulinate	[C <sub>1</sub> C <sub>4</sub> Im][Lev]	-
		1-butyl-3-methylimidazolium tetrachloroaluminate	[C <sub>1</sub> C <sub>4</sub> Im][AlCl <sub>4</sub> ]	80432-09-3

\* Kindly provided by Laboratory C2P2 - Equipe Organometallique de Surface, Villeurbanne, France

\*\* Kindly provided by laboratory QUILL - Queen's University Ionic Liquid Laboratory, Belfast, Northern Ireland, UK



# Appendix 2

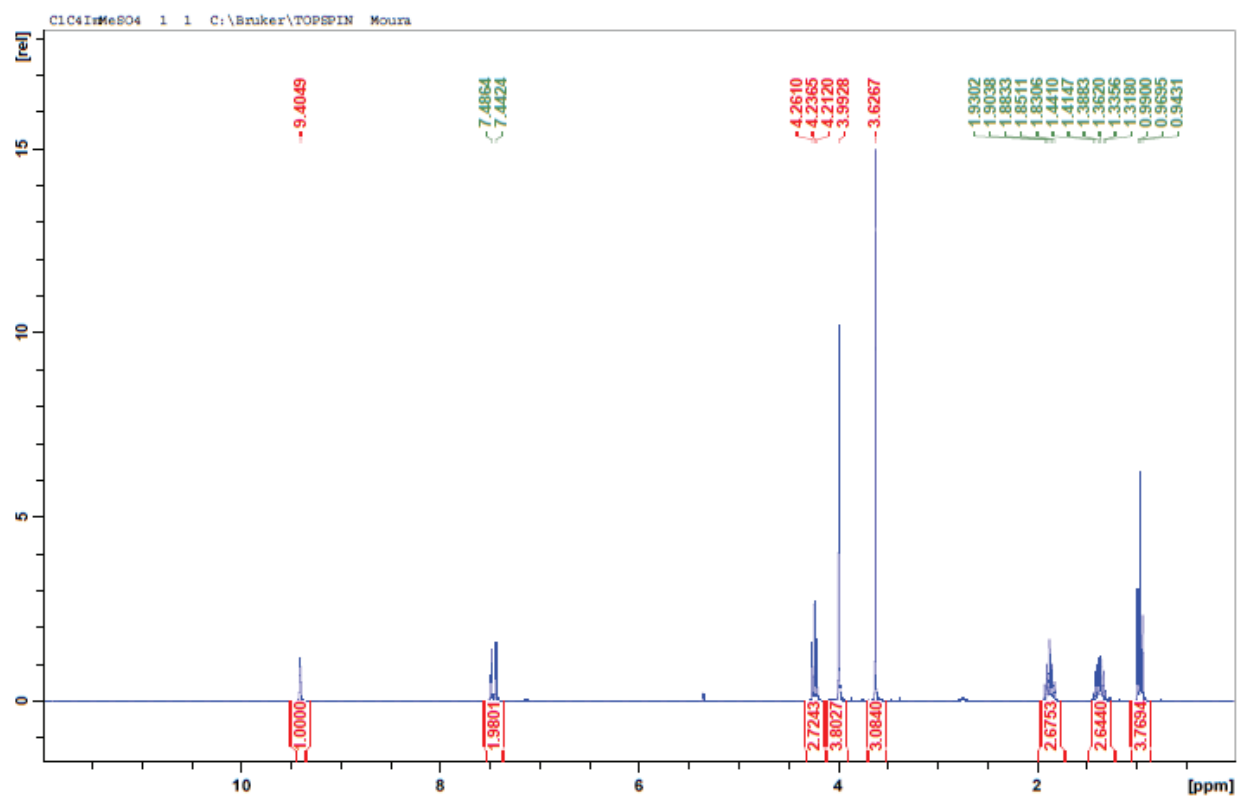
---

NMR and HRMS spectra of the Ionic Liquids

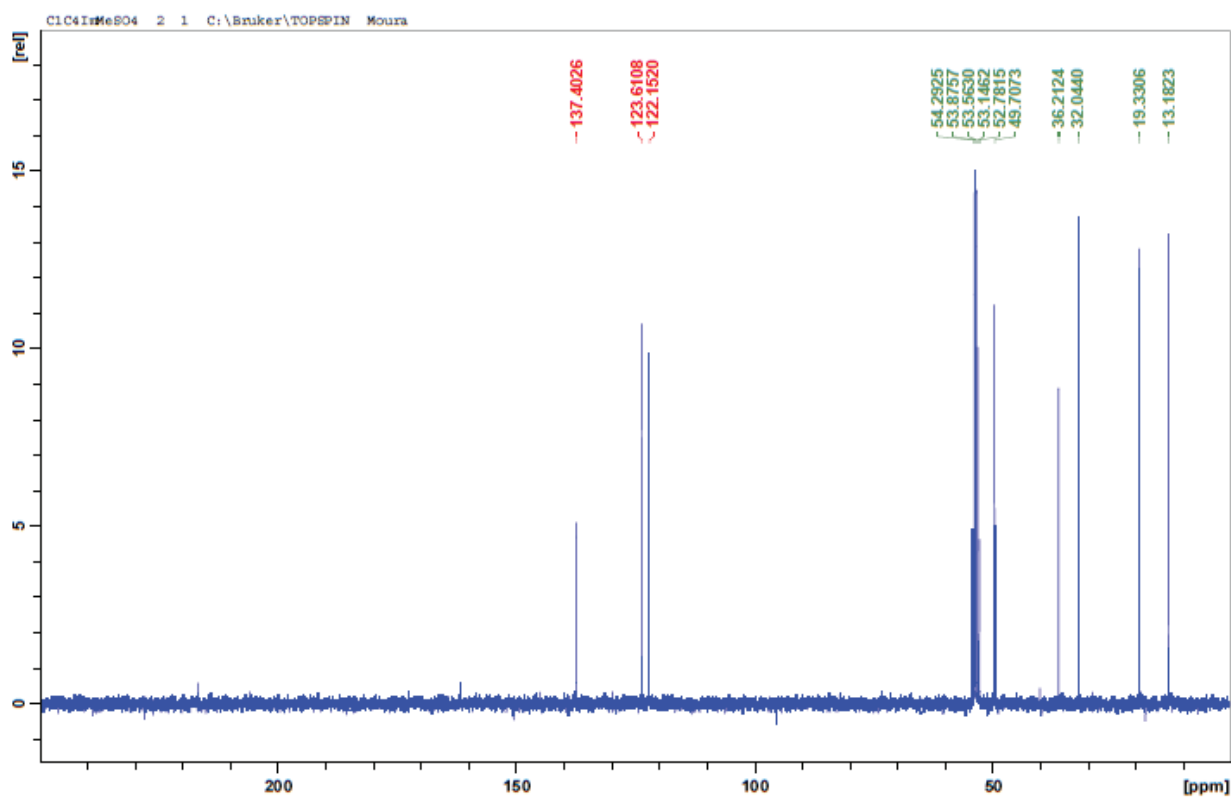


1-Butyl-3-methylimidazolium methylsulfate, [C<sub>1</sub>C<sub>4</sub>Im][(CH<sub>3</sub>O)SO<sub>3</sub>]

<sup>1</sup>H-NMR

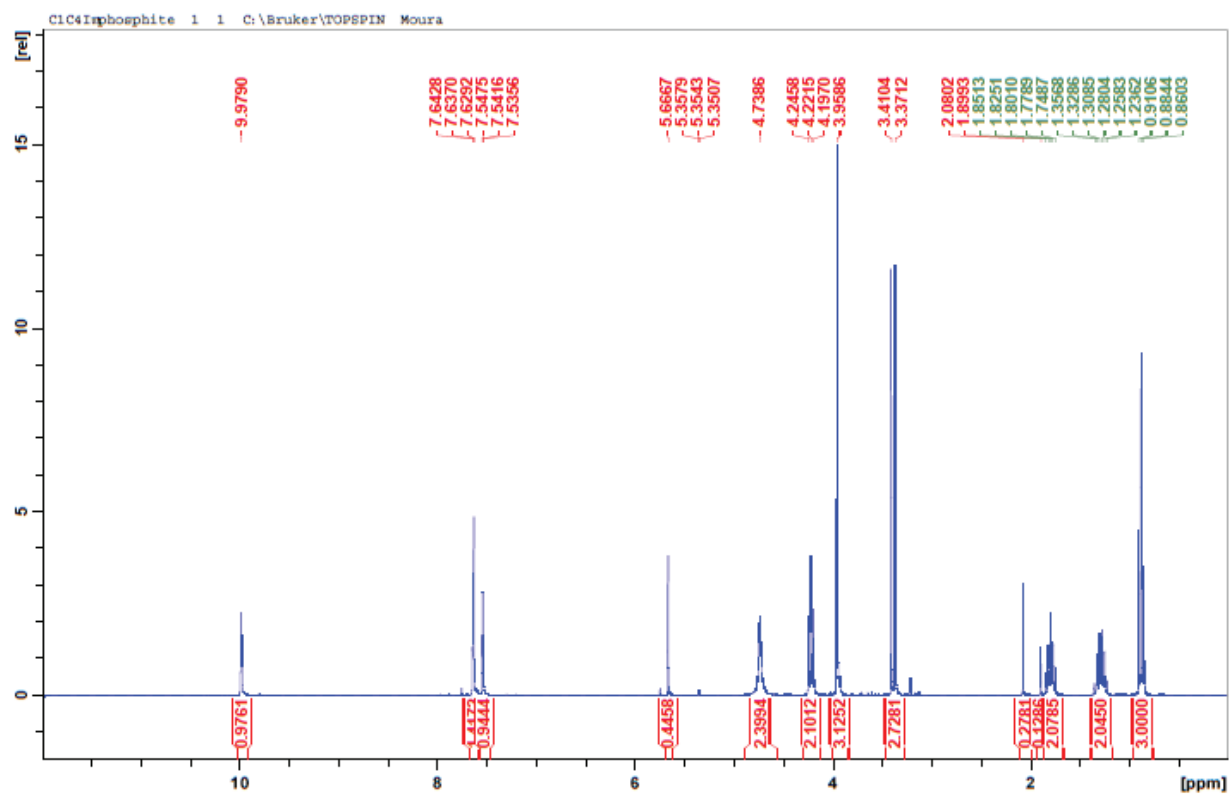


<sup>13</sup>C-NMR

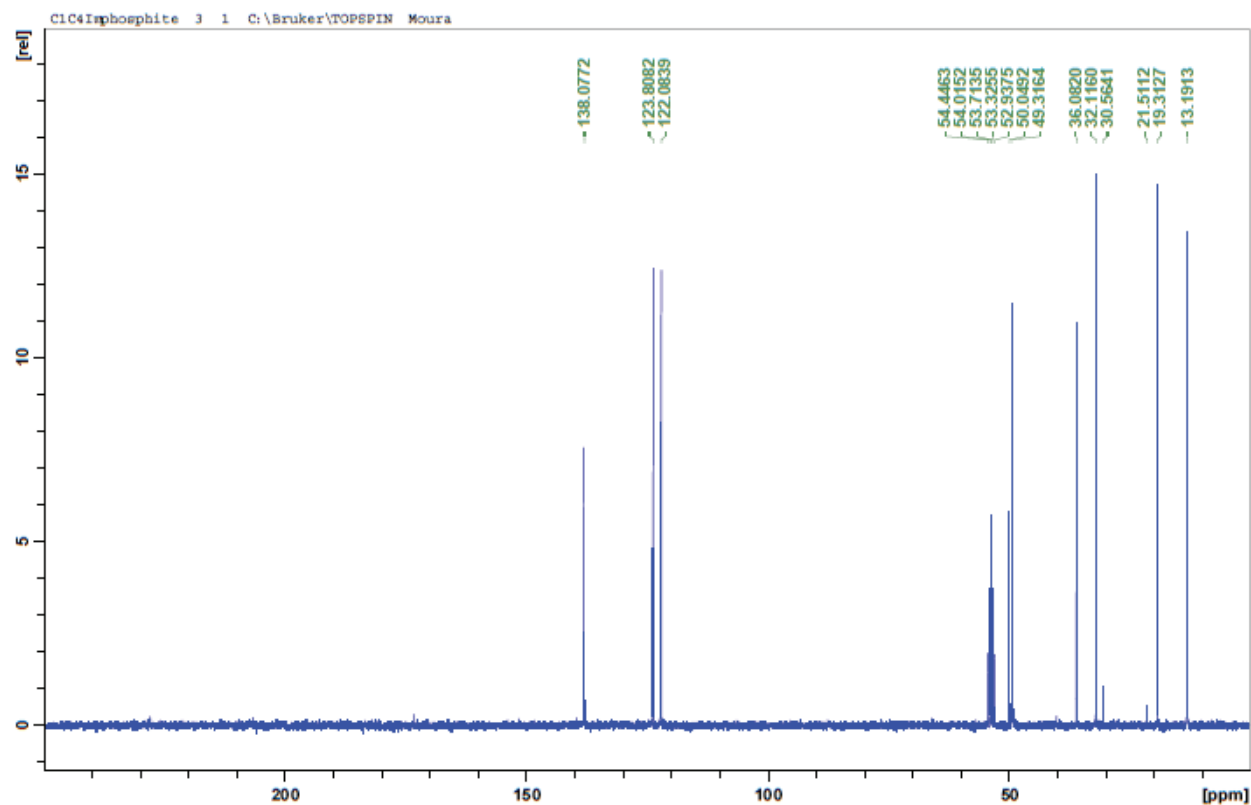


1-Butyl-3-methylimidazolium methylphosphonate, [C<sub>1</sub>C<sub>4</sub>Im][(CH<sub>3</sub>O)HPO<sub>2</sub>]

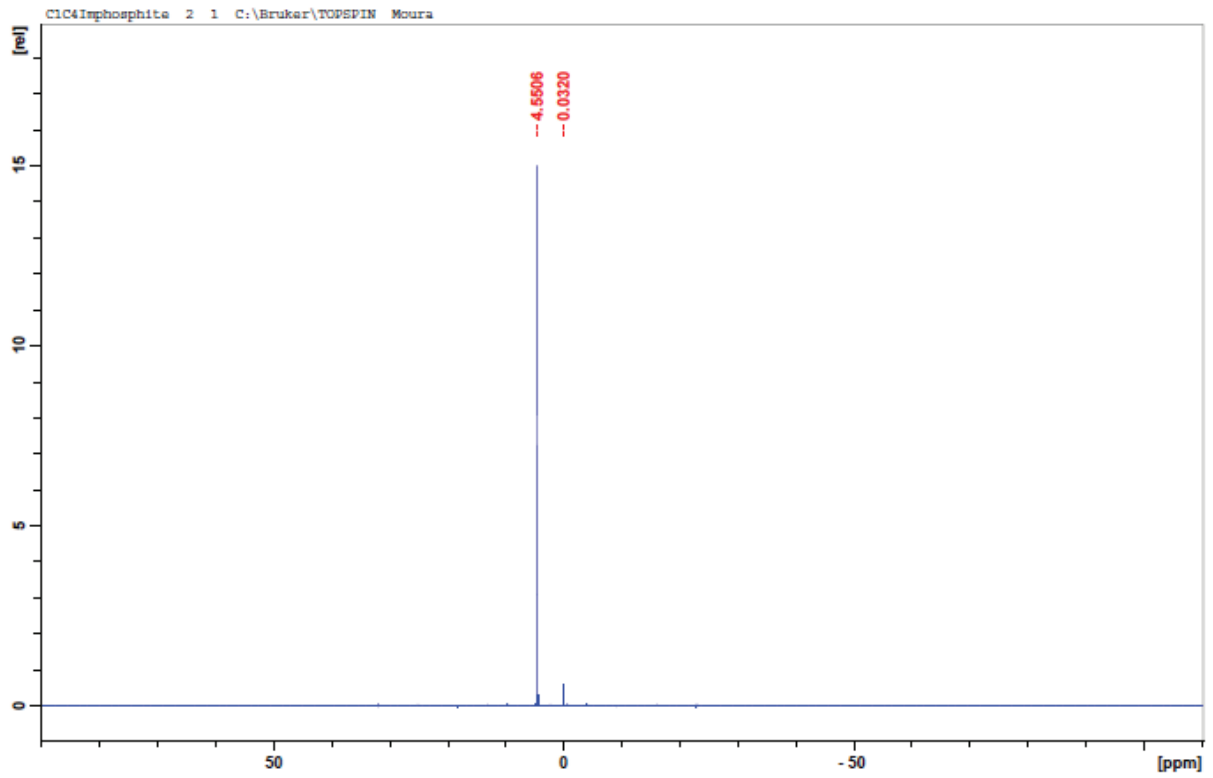
<sup>1</sup>H-NMR



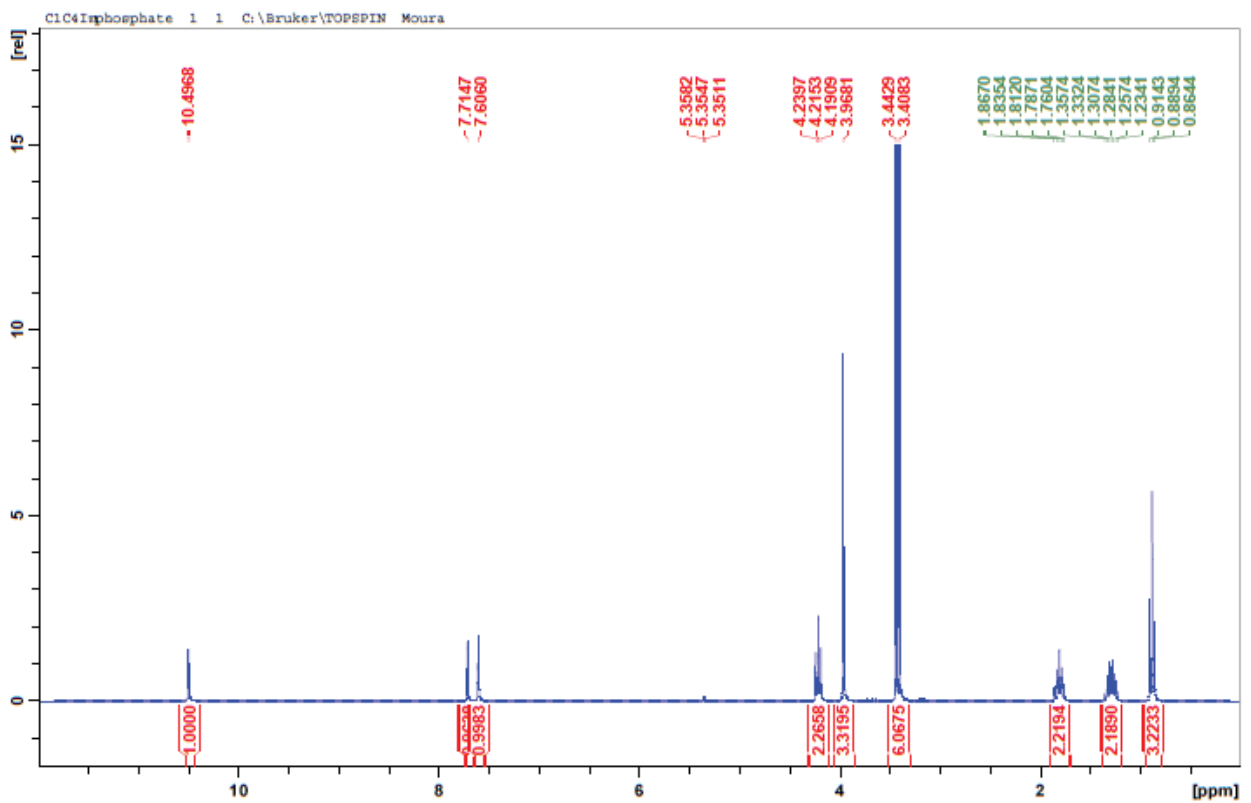
<sup>13</sup>C-NMR



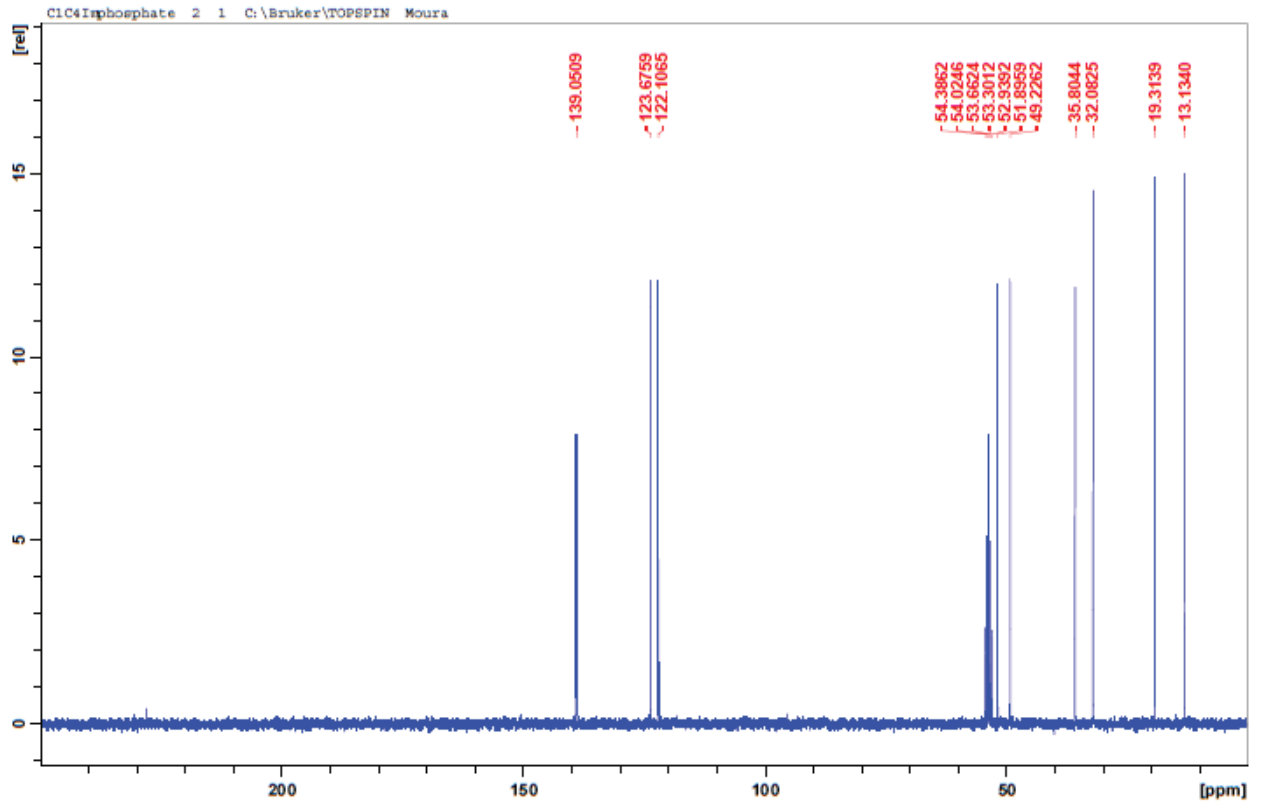
<sup>31</sup>P-NMR



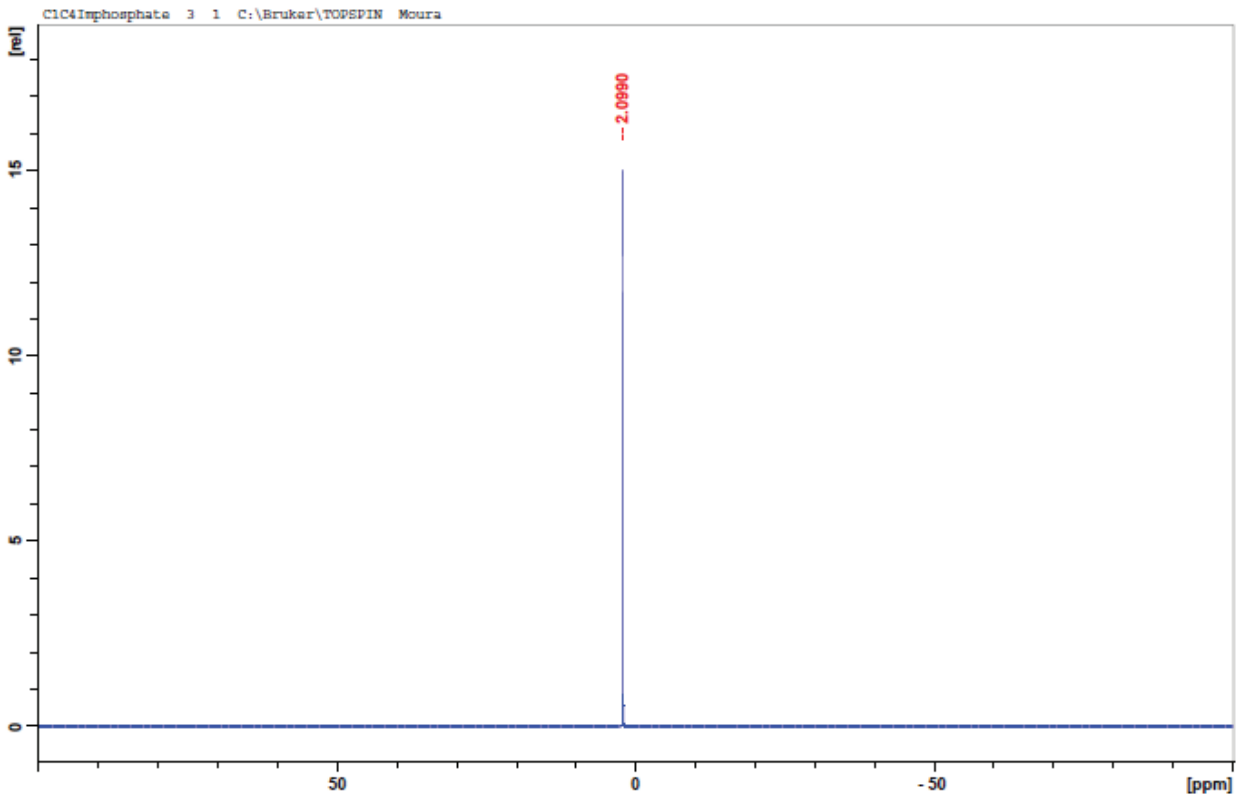
**1-Butyl-3-methylimidazolium dimethylphosphate, [C<sub>1</sub>C<sub>4</sub>Im][[(CH<sub>3</sub>O)<sub>2</sub>PO<sub>2</sub>]**  
<sup>1</sup>H-NMR



<sup>13</sup>C-NMR

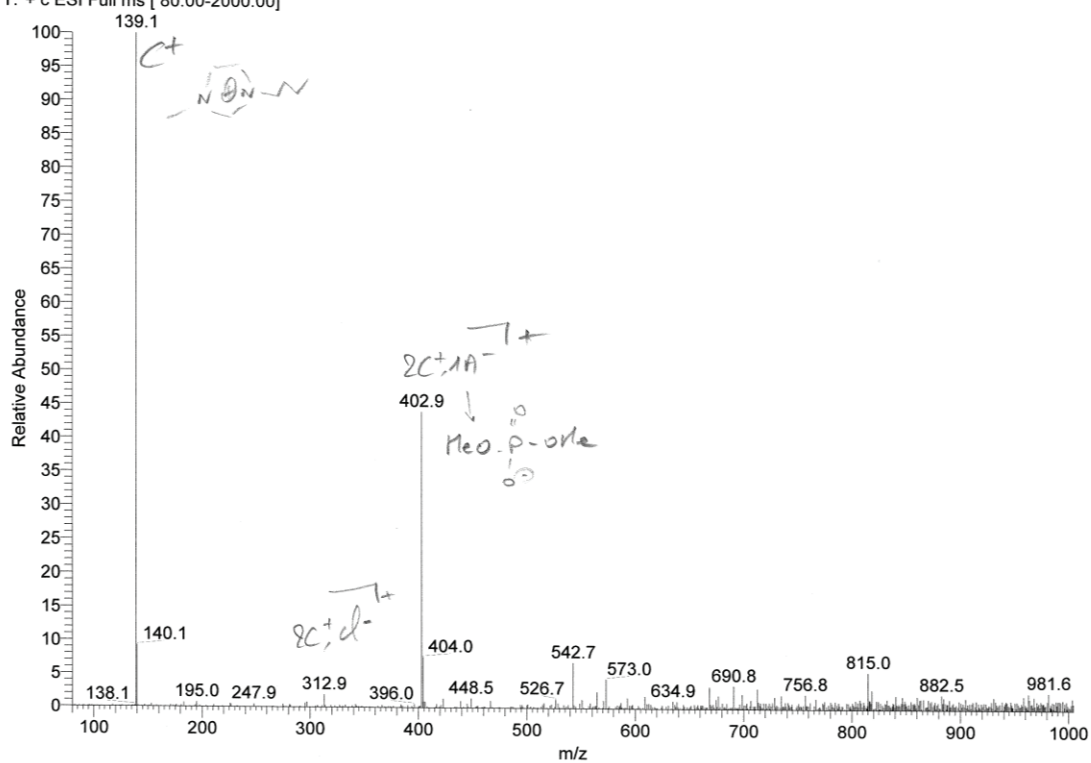


<sup>31</sup>P-NMR



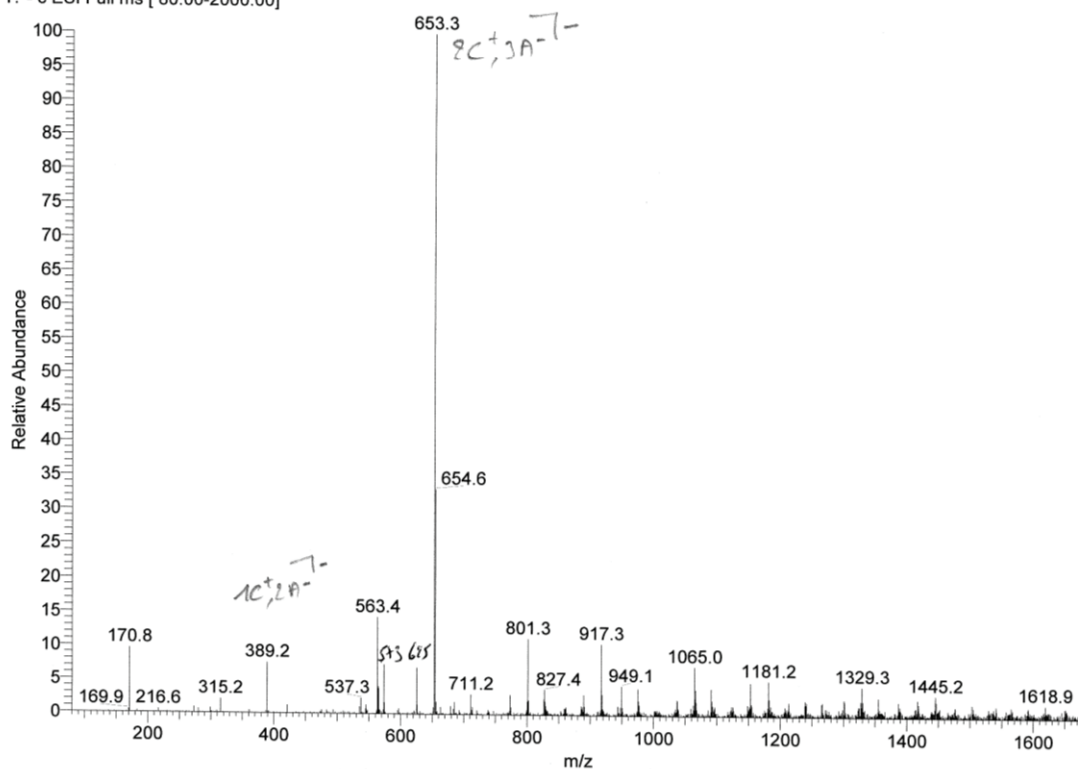
m/z (Fab+)

LCQ110225.04 #44-50 RT: 1.35-1.54 AV: 7 SB: 14 0.23-0.64 NL: 4.17E6  
T: + c ESI Full ms [ 80.00-2000.00]

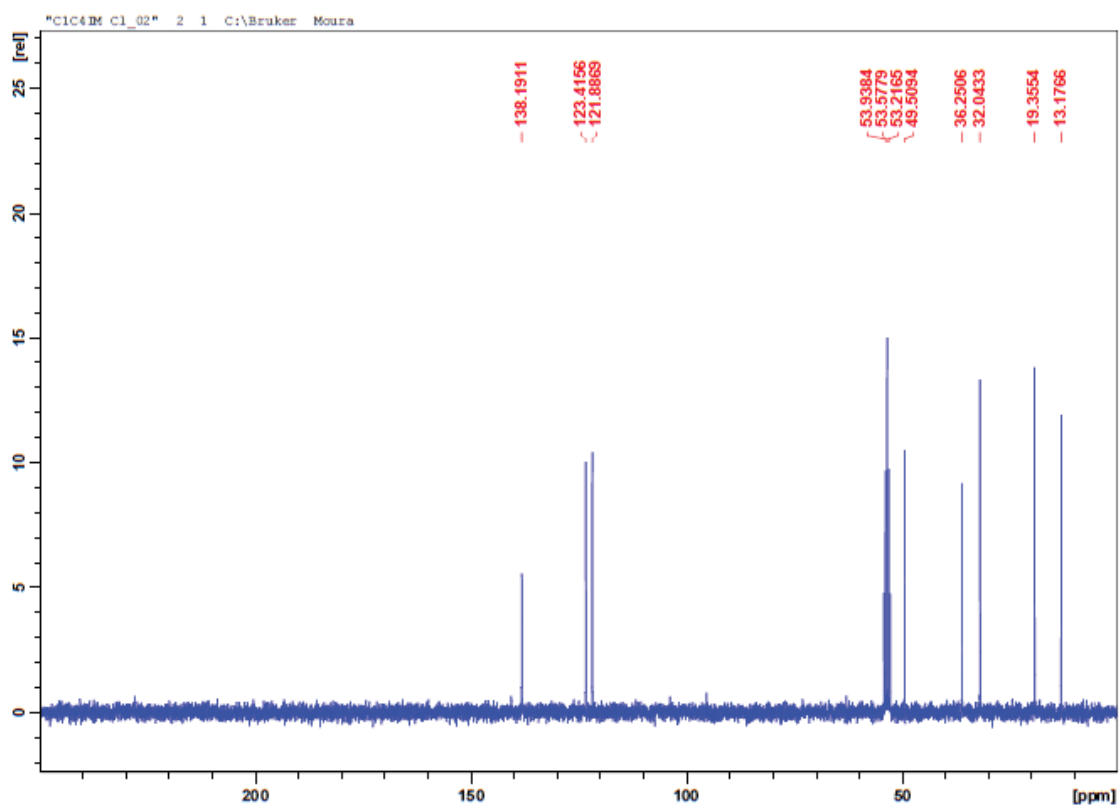
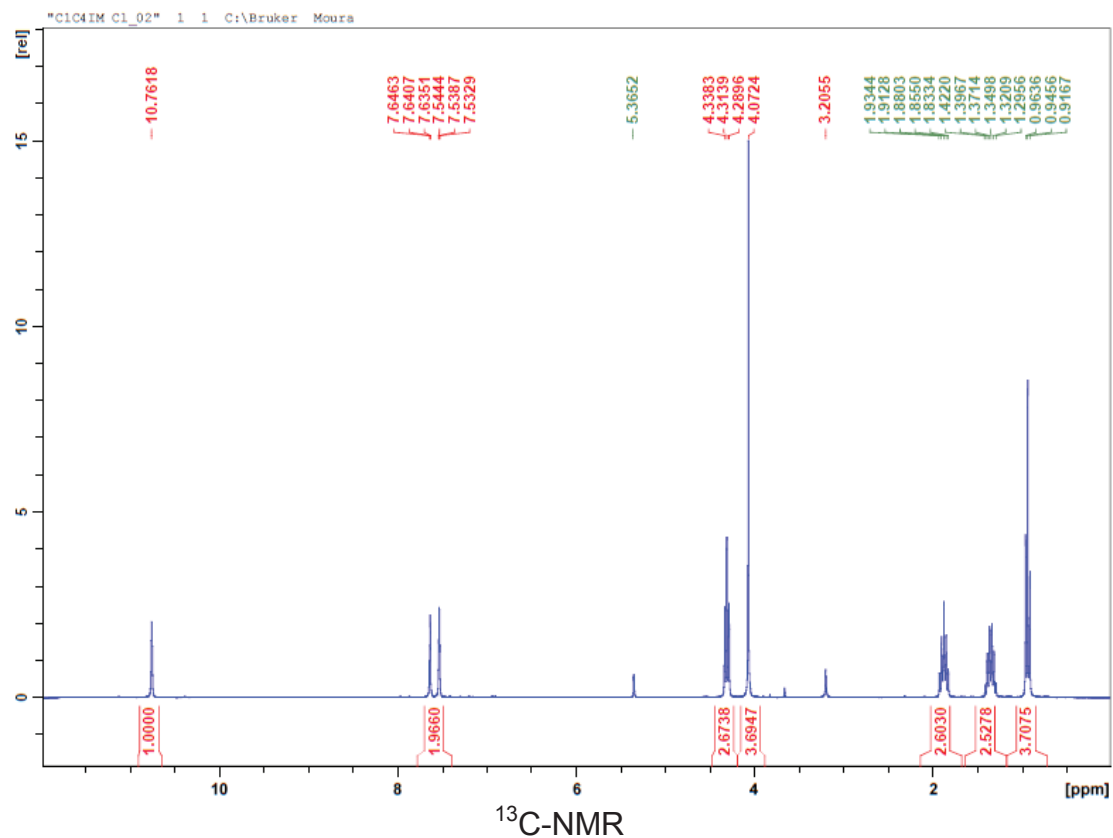


m/z (Fab<sup>-</sup>)

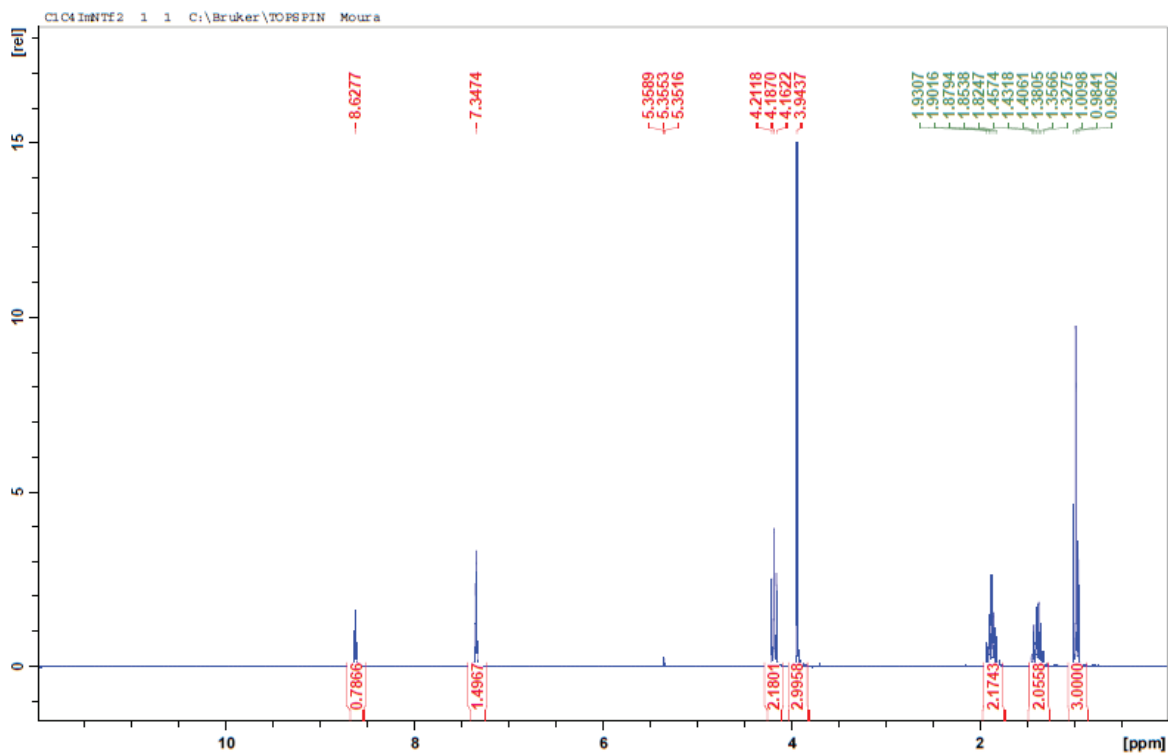
LCQ110225.05 #49-54 RT: 1.50-1.65 AV: 6 SB: 8 0.14-0.35 NL: 8.25E5  
T: - c ESI Full ms [ 80.00-2000.00]



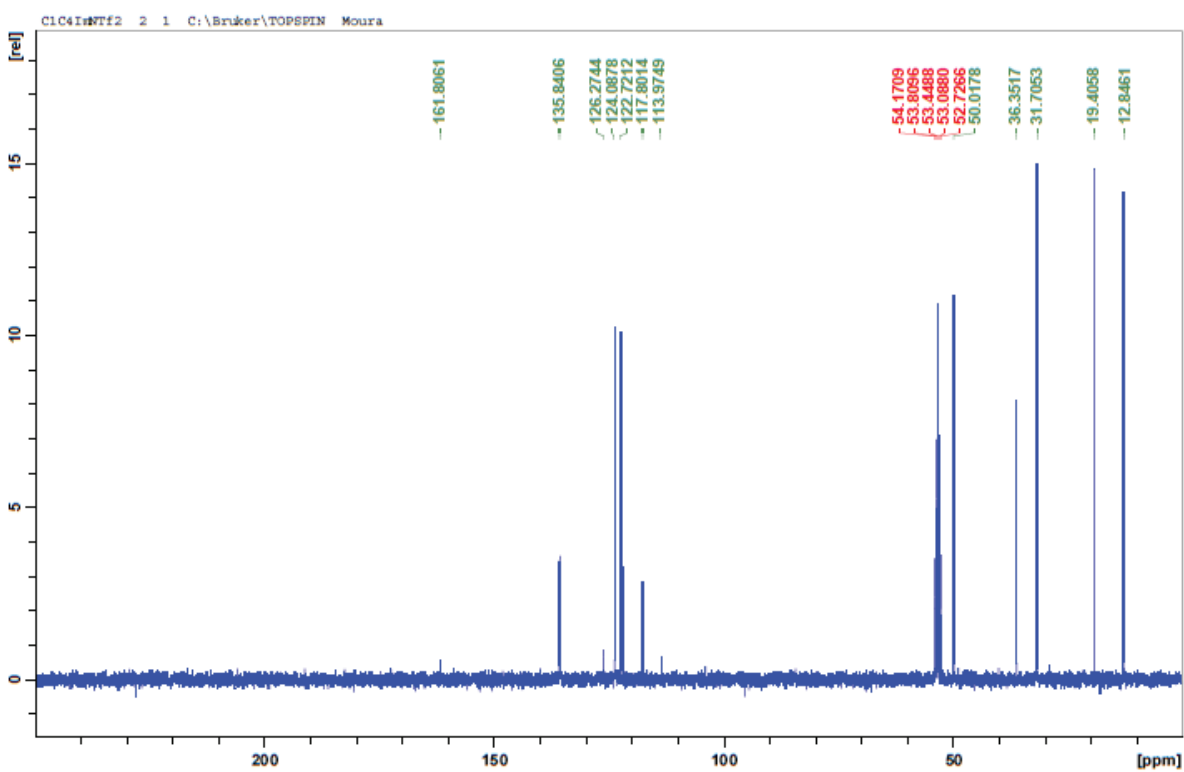
1-Butyl-3-methylimidazolium chloride, [C<sub>1</sub>C<sub>4</sub>Im][Cl]  
<sup>1</sup>H-NMR



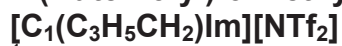
1-Butyl-3-methylimidazolium bis(trifluoromethanesulfonyl)imide,  $[\text{C}_1\text{C}_4\text{Im}][\text{NTf}_2]$



<sup>13</sup>C-NMR

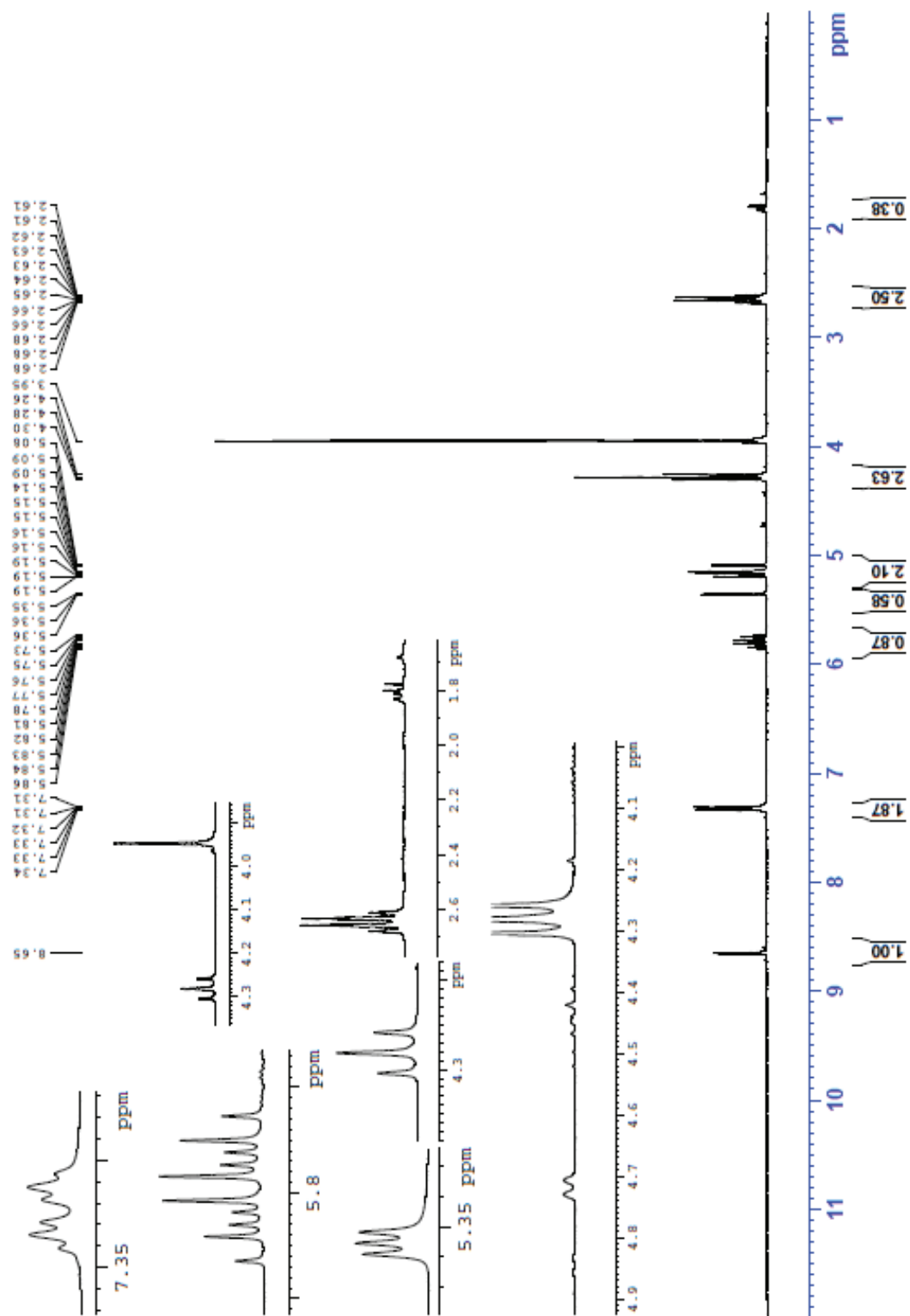


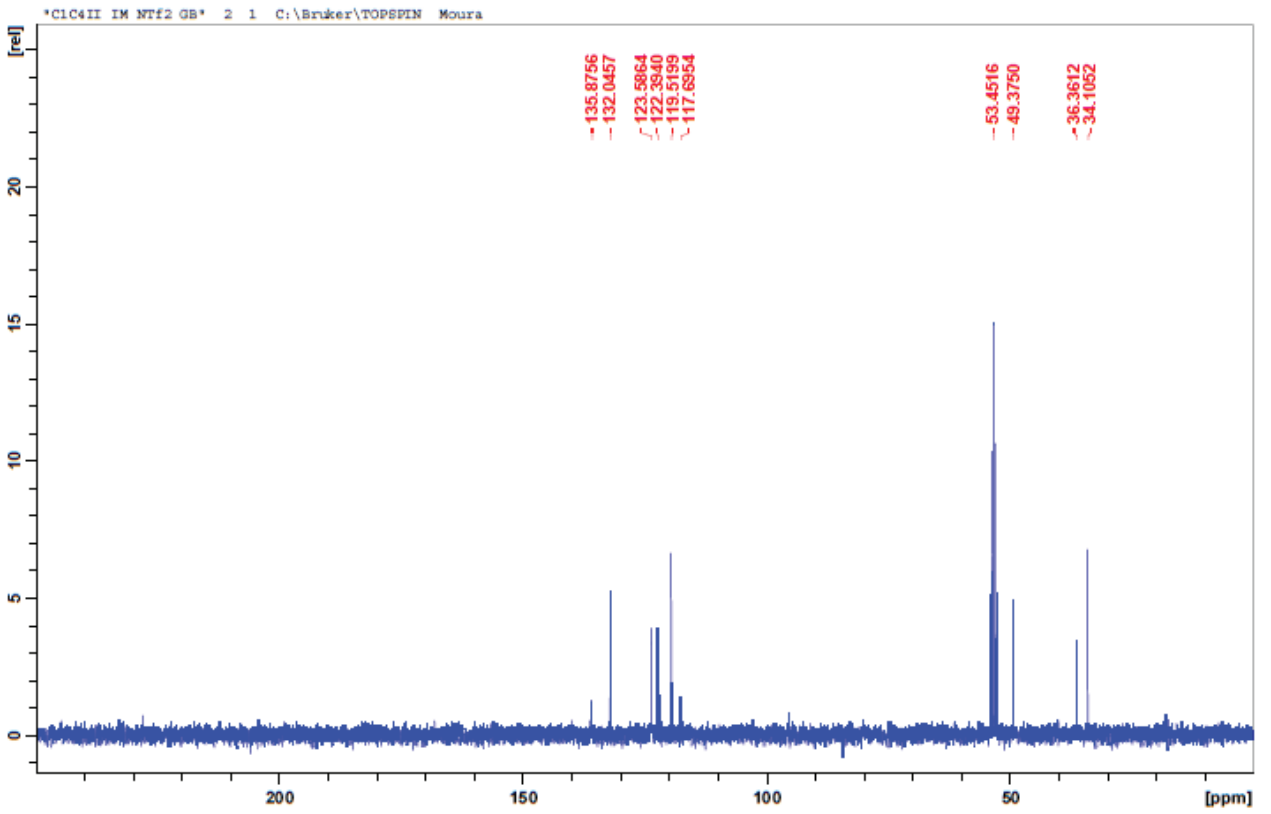
1-(Buten-3-yl)-3-methylimidazolium bis(trifluoromethanesulfonyl)imide



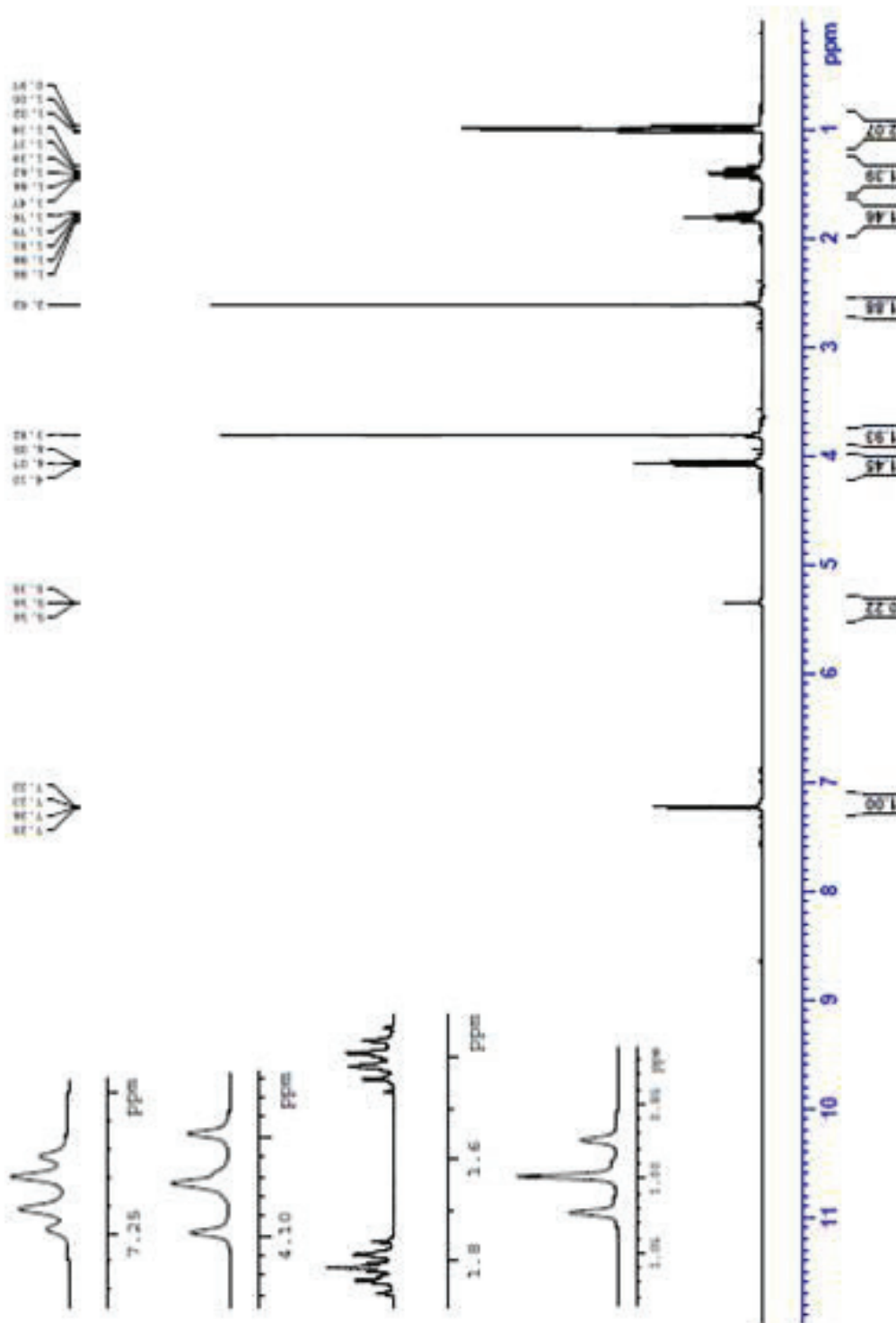
<sup>1</sup>H-NMR

$^{13}\text{C}$ -NMR

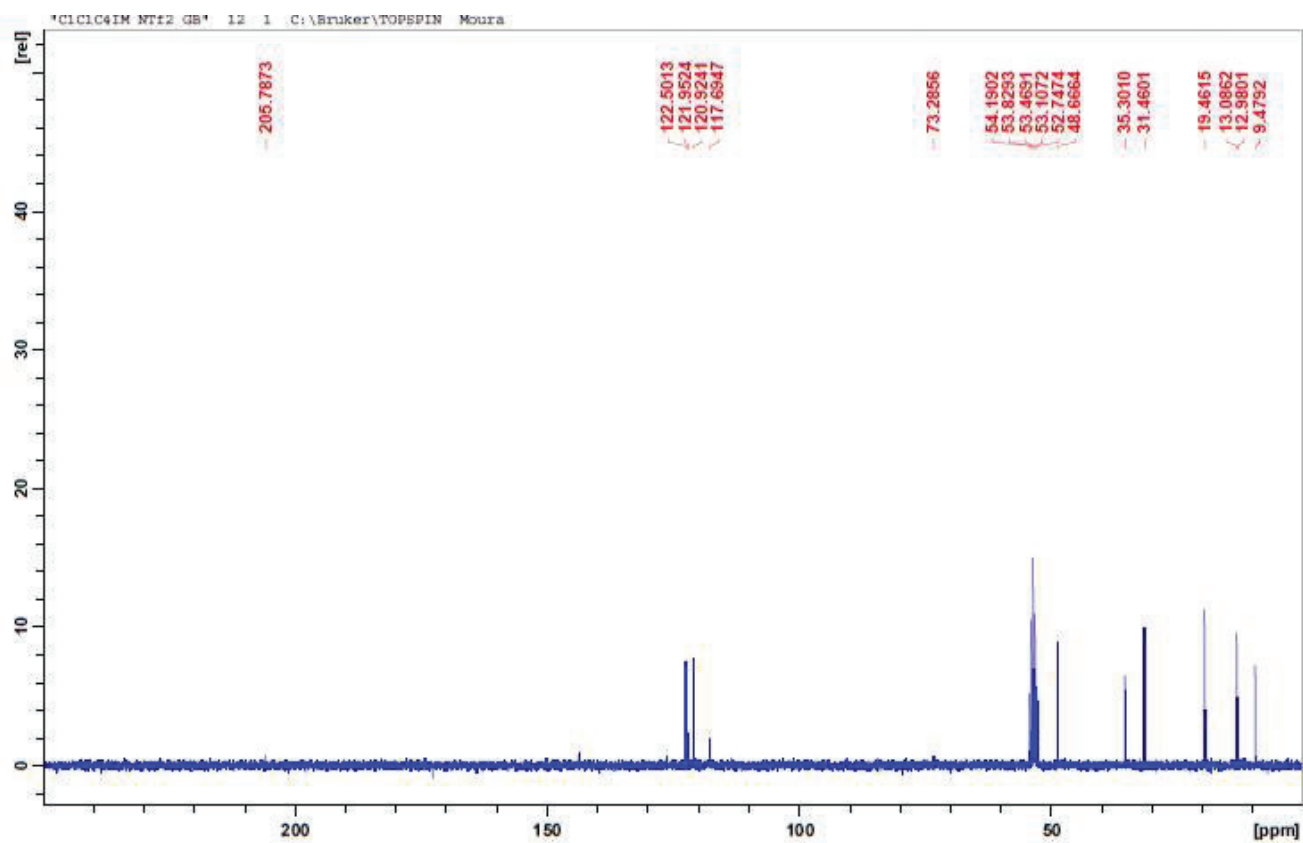




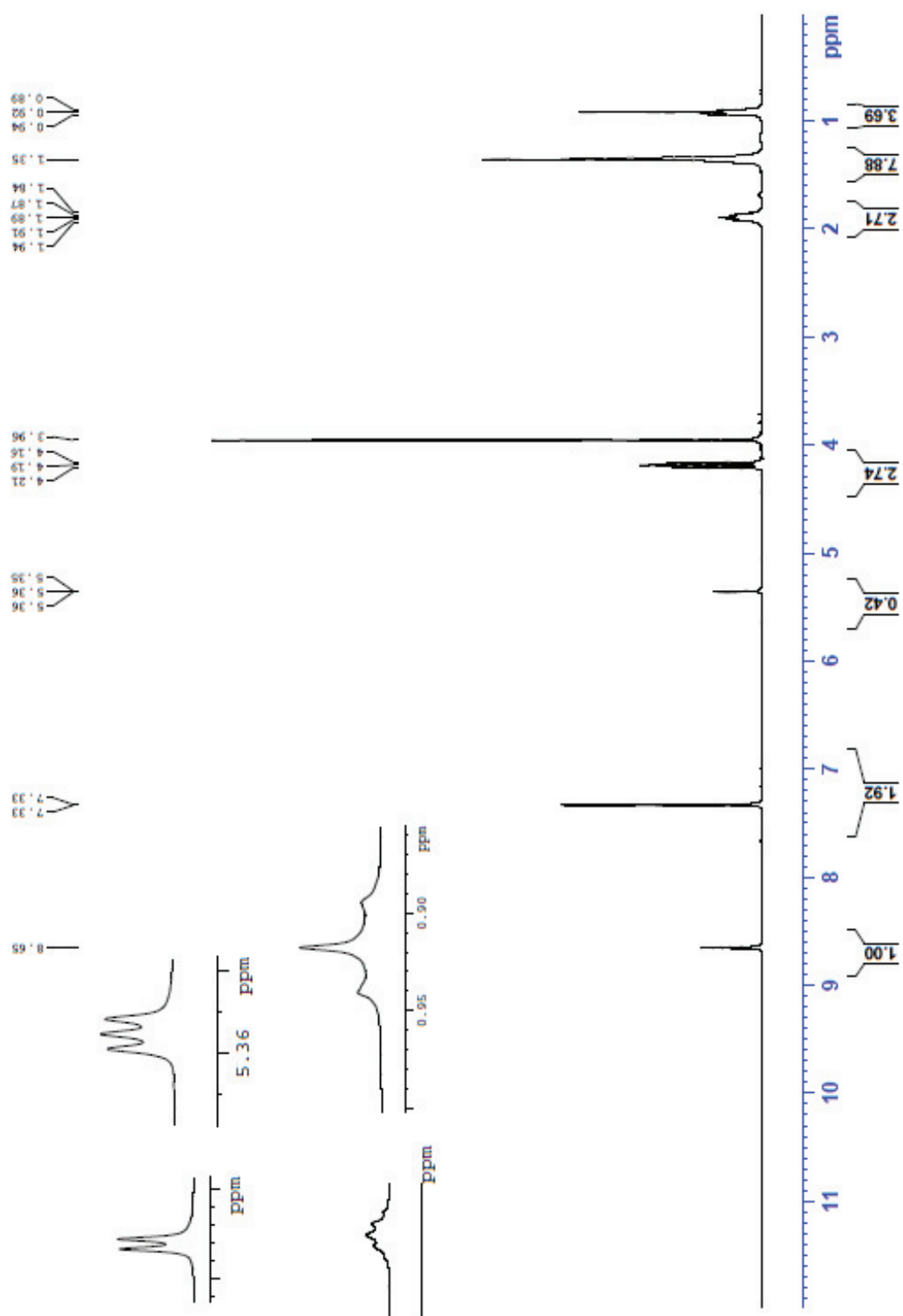
1-Butyl-2,3-dimethylimidazolium bis(trifluoromethanesulfonyl)imide,  
[C<sub>1</sub>C<sub>1</sub>C<sub>4</sub>Im][NTf<sub>2</sub>]  
<sup>1</sup>H-NMR



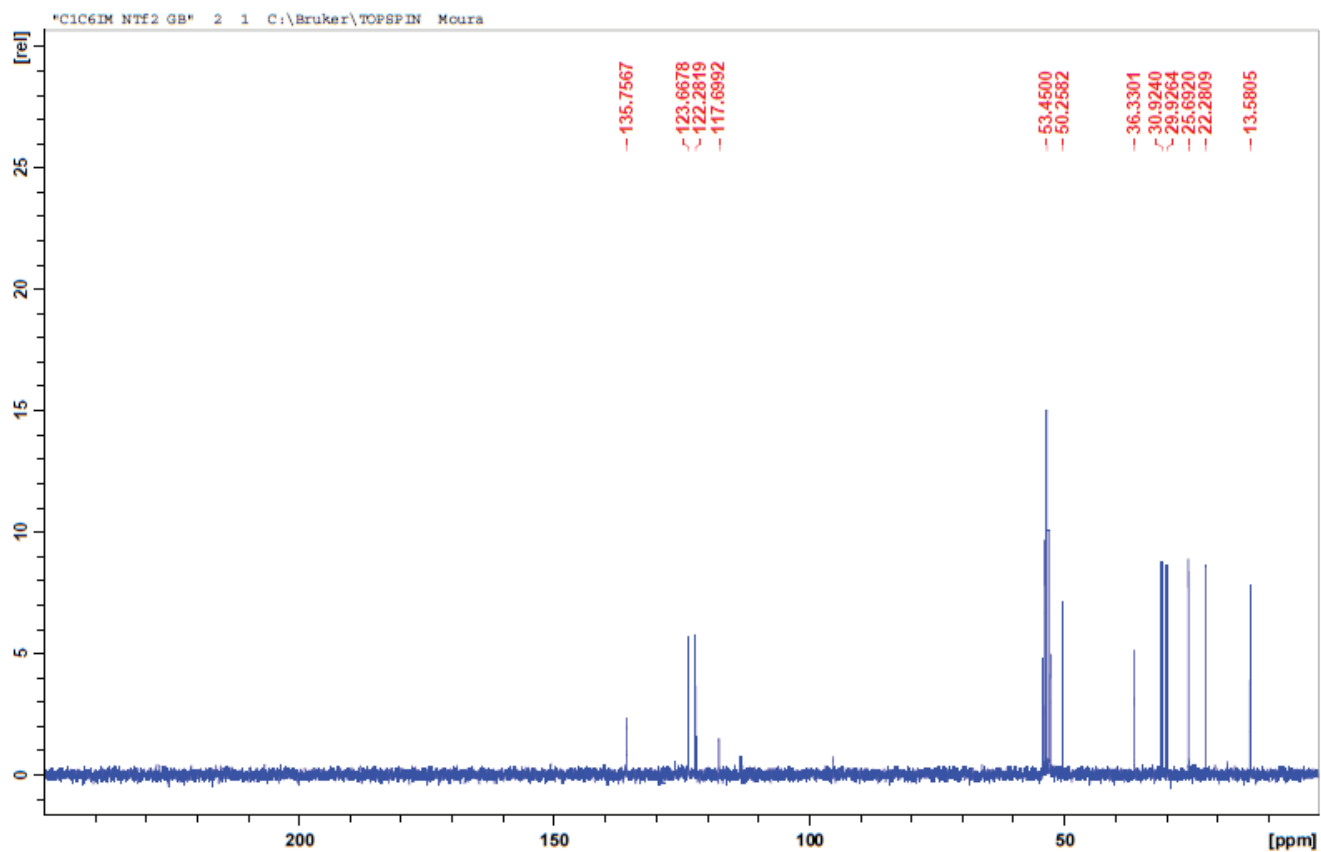
<sup>13</sup>C-NMR



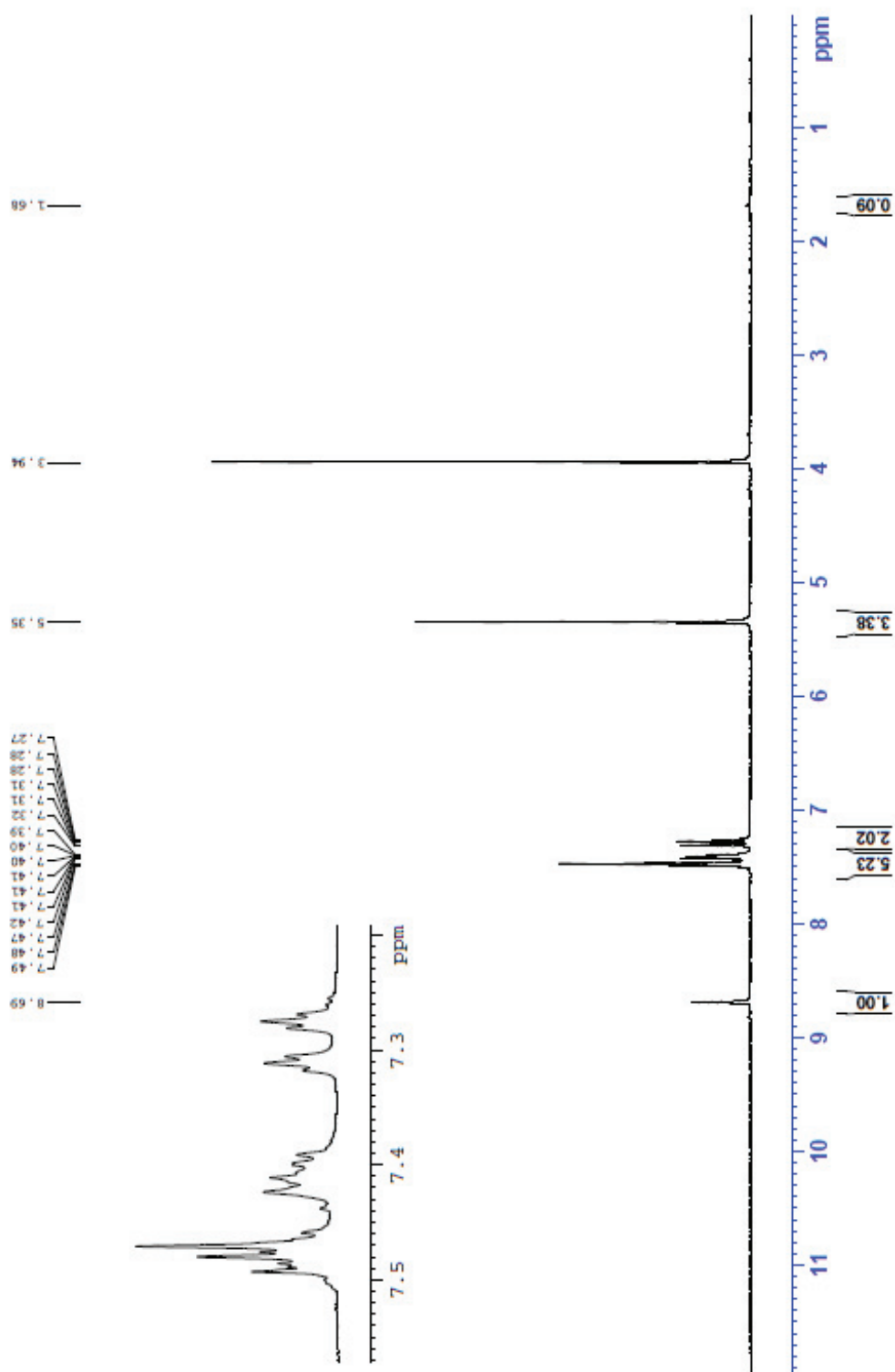
1-Hexyl-3-methylimidazolium bis(trifluoromethanesulfonyl)imide,  
 [C<sub>1</sub>C<sub>6</sub>Im][NTf<sub>2</sub>]  
<sup>1</sup>H-NMR



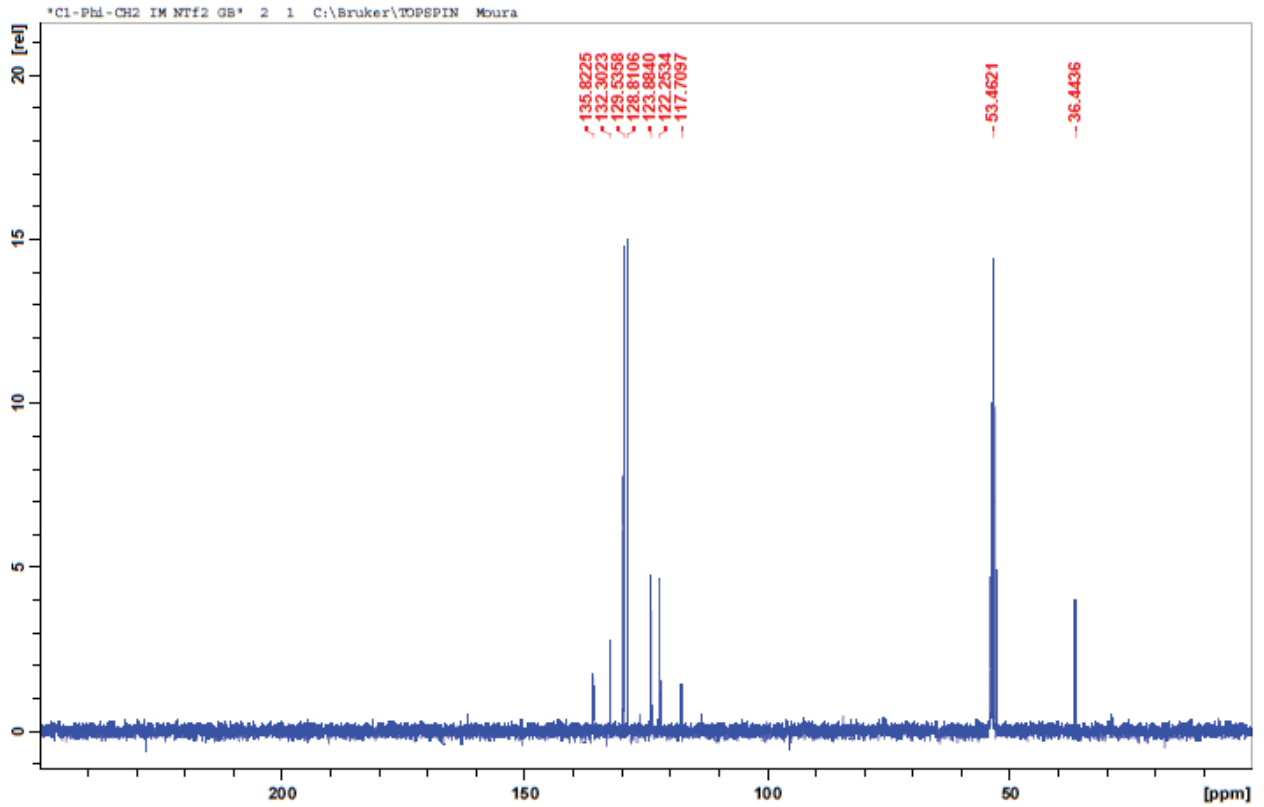
# <sup>13</sup>C-NMR



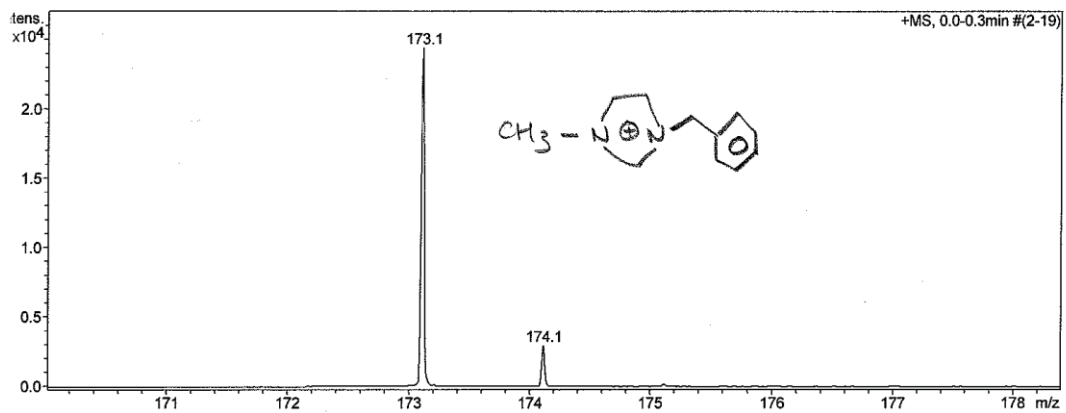
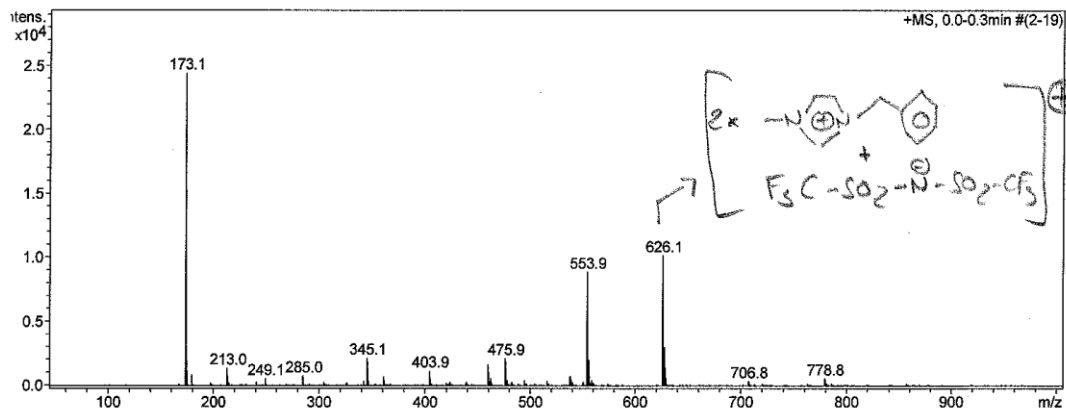
1-Benzyl-3-methylimidazolium bis(trifluoromethanesulfonyl)imide,  
[C<sub>1</sub>(CH<sub>2</sub>C<sub>6</sub>H<sub>5</sub>)Im][NTf<sub>2</sub>]  
<sup>1</sup>H-NMR



# <sup>13</sup>C-NMR

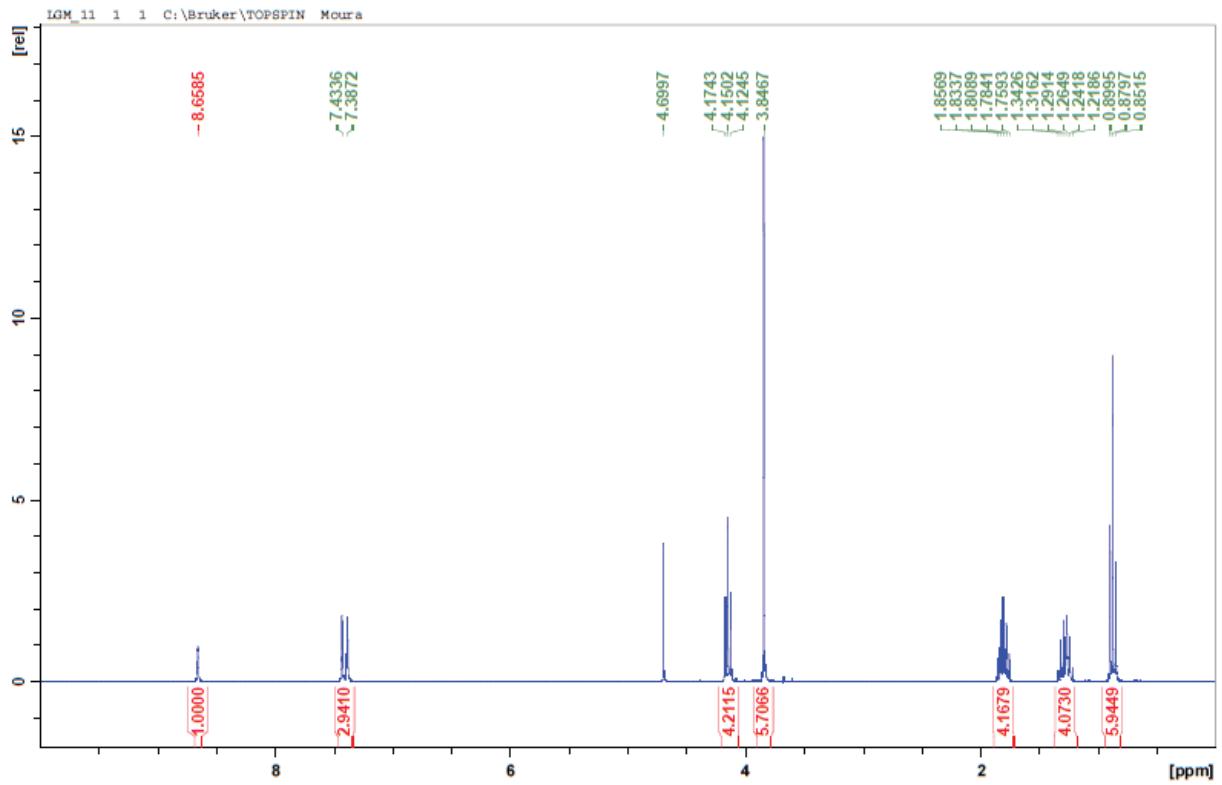


# m/z (Fab+)

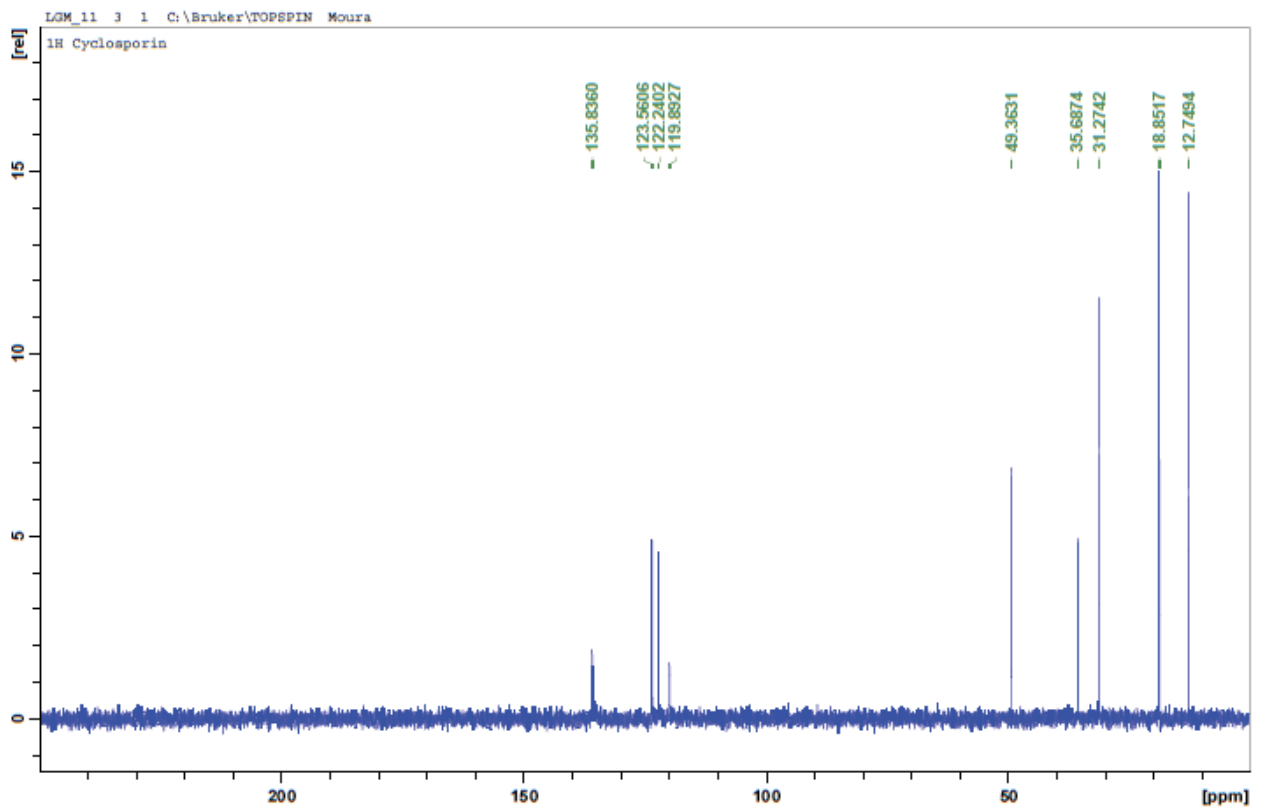


# 1-Butyl-3-methylimidazolium dicyanamide, [C<sub>1</sub>C<sub>4</sub>Im][DCA]

# <sup>1</sup>H-NMR

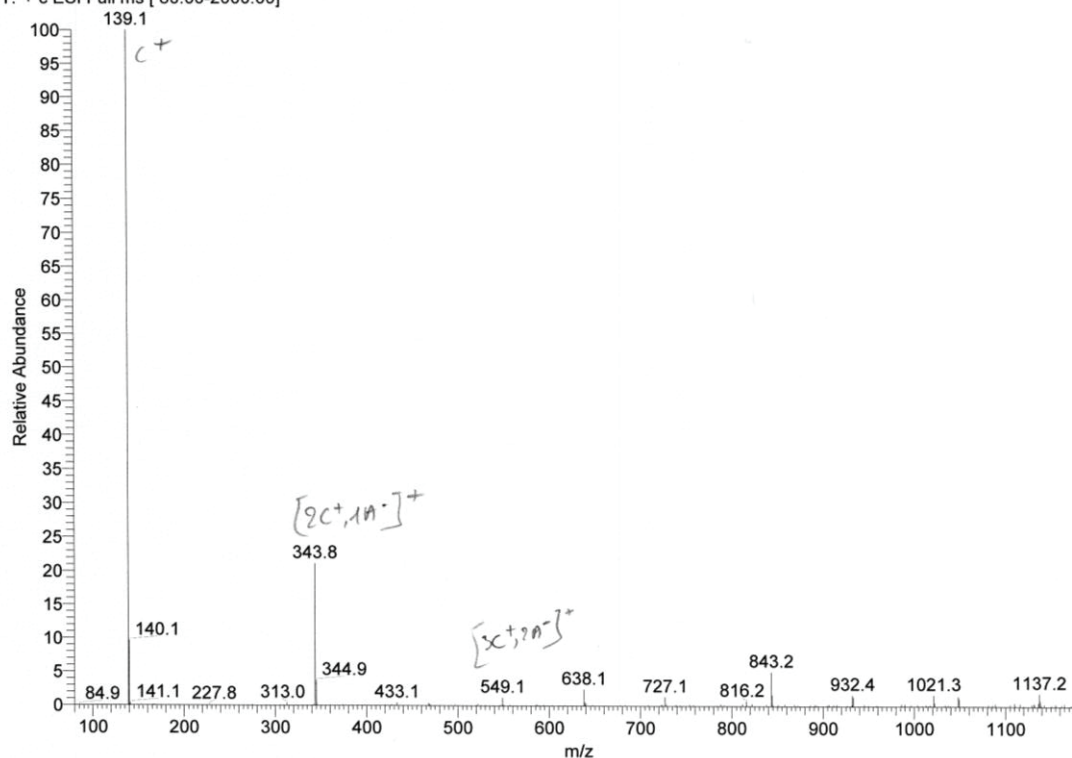


<sup>13</sup>C-NMR



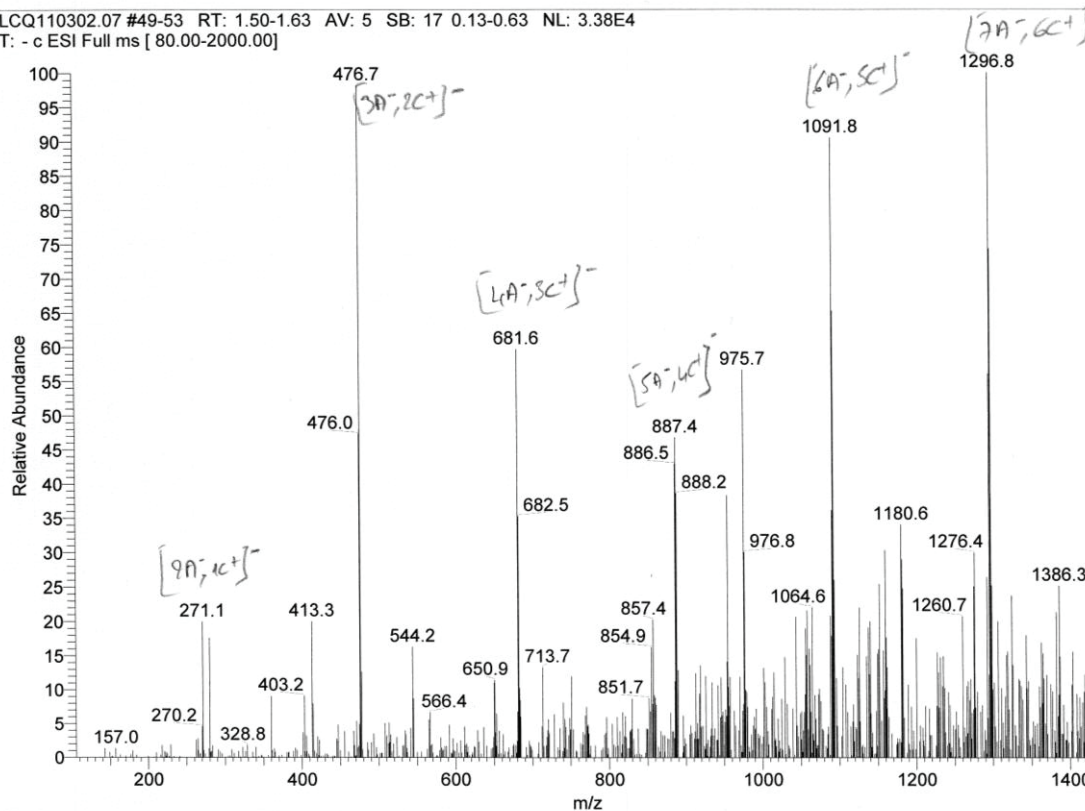
m/z (Fab+)

LCQ110302.06 #48-51 RT: 1.46-1.56 AV: 4 SB: 15 0.19-0.63 NL: 6.43E6  
T: + c ESI Full ms [ 80.00-2000.00]

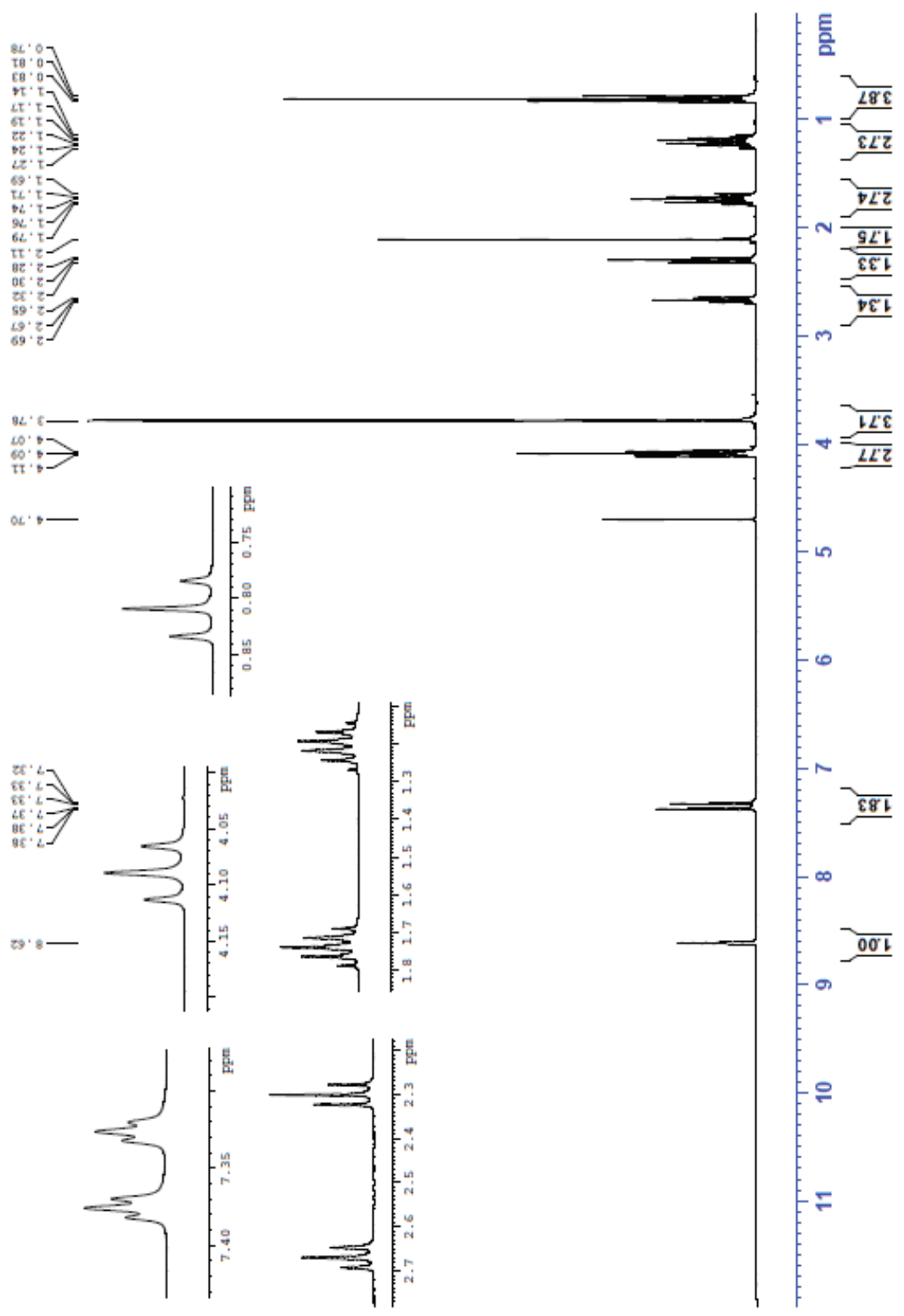


m/z (Fab-)

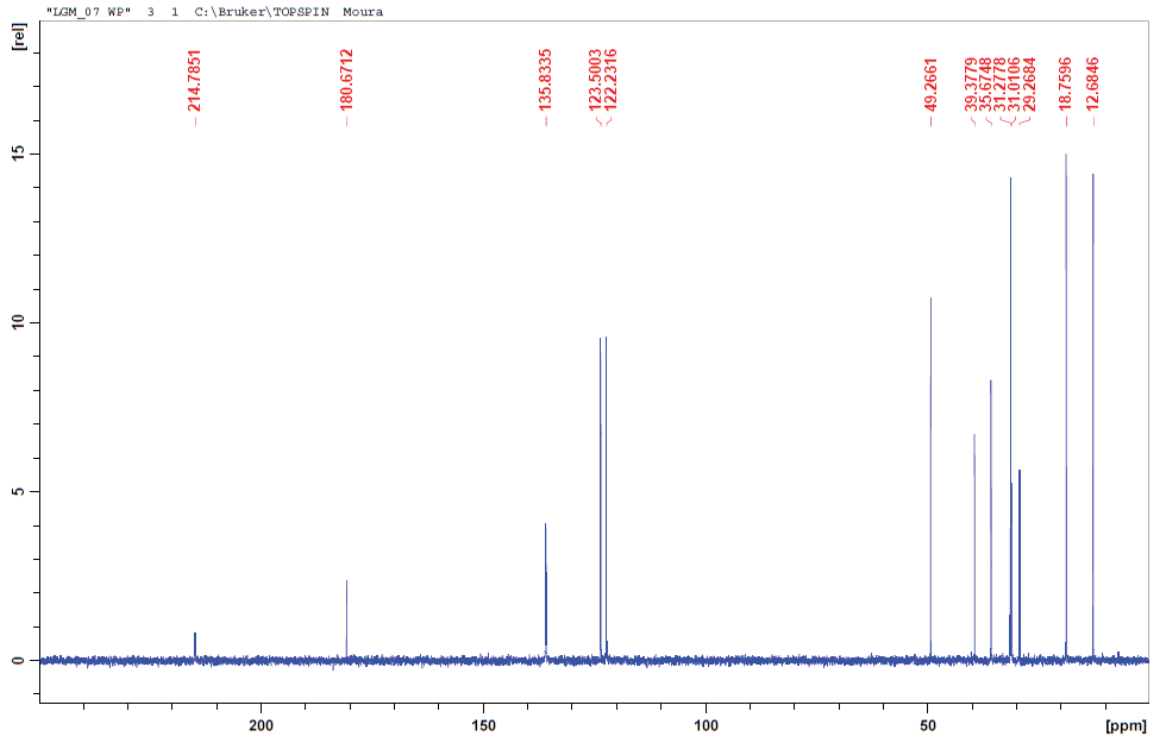
LCQ110302.07 #49-53 RT: 1.50-1.63 AV: 5 SB: 17 0.13-0.63 NL: 3.38E4  
T: - c ESI Full ms [ 80.00-2000.00]



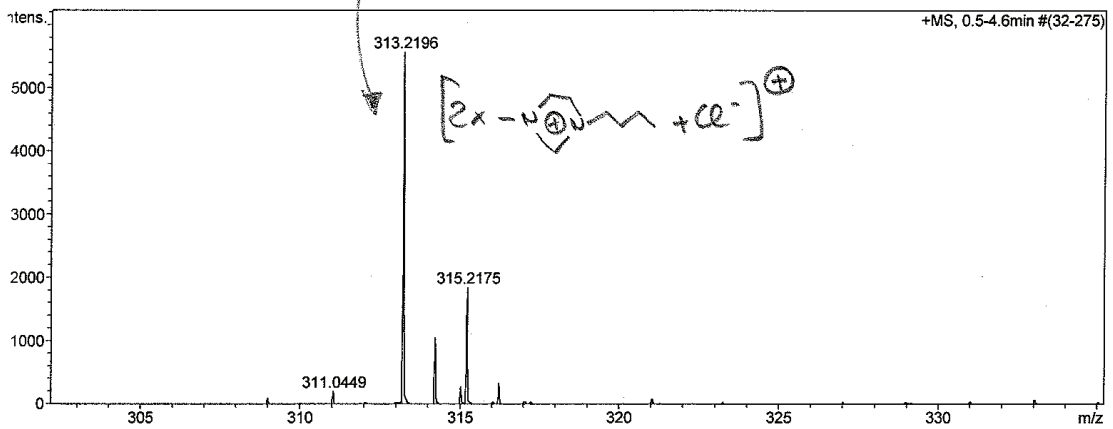
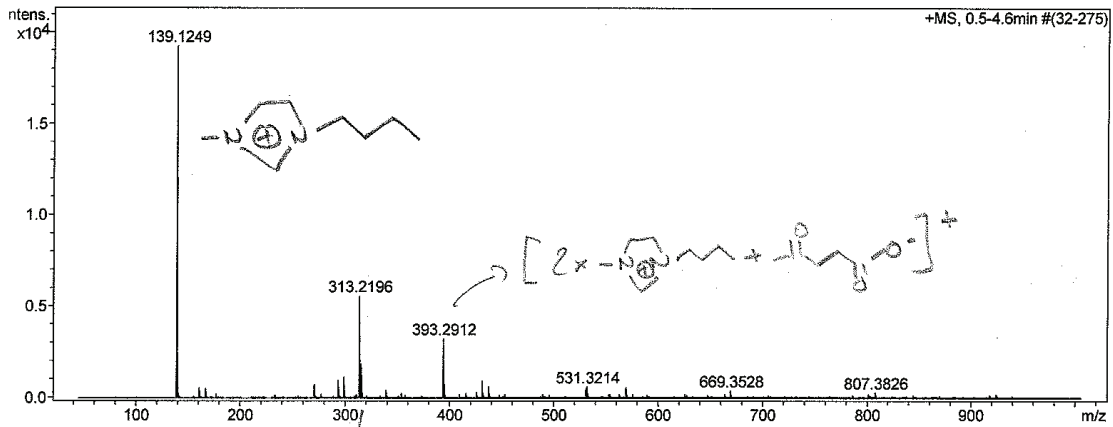
1-Butyl-3-methylimidazolium levulinate, [C<sub>1</sub>C<sub>4</sub>Im][Lev]  
<sup>1</sup>H-NMR



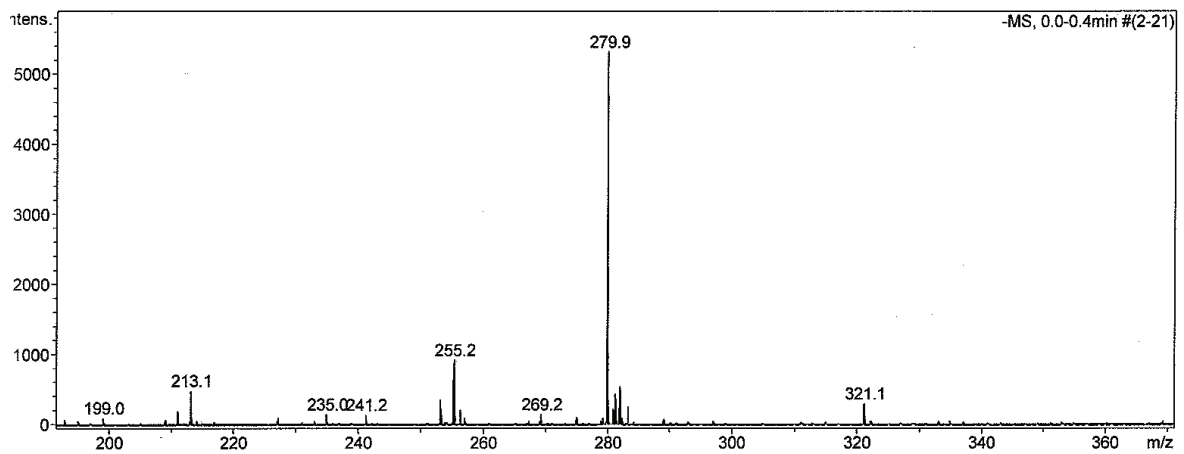
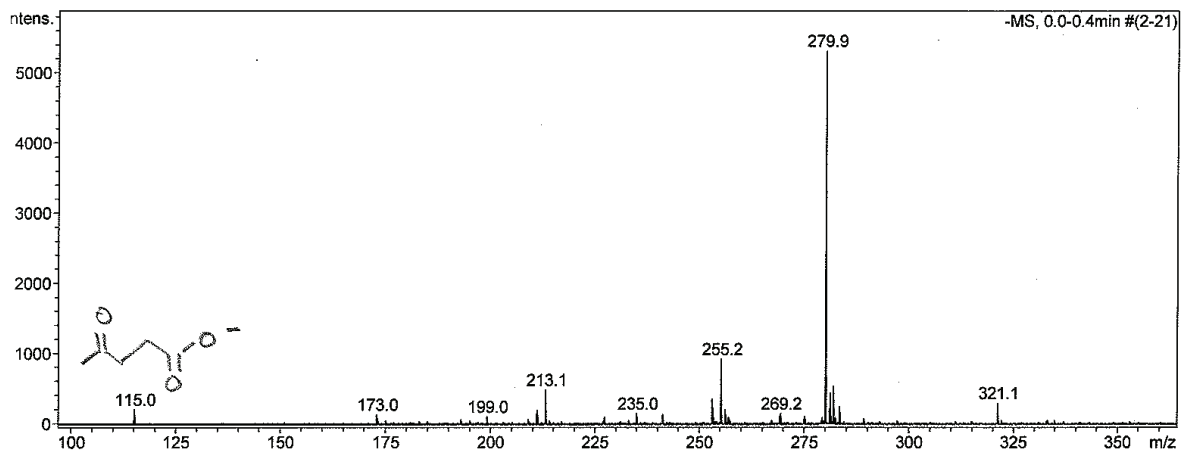
<sup>13</sup>C-NMR



m/z (Fab+)

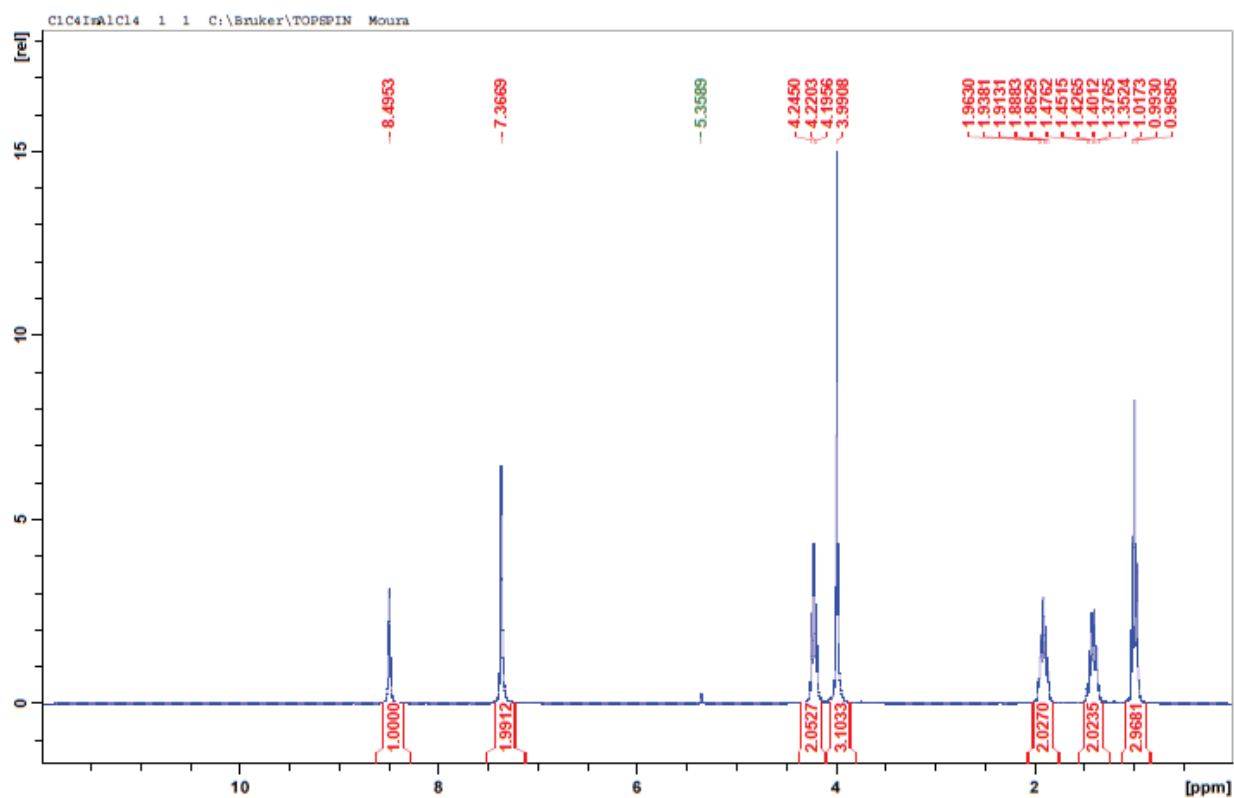


m/z (Fab-)

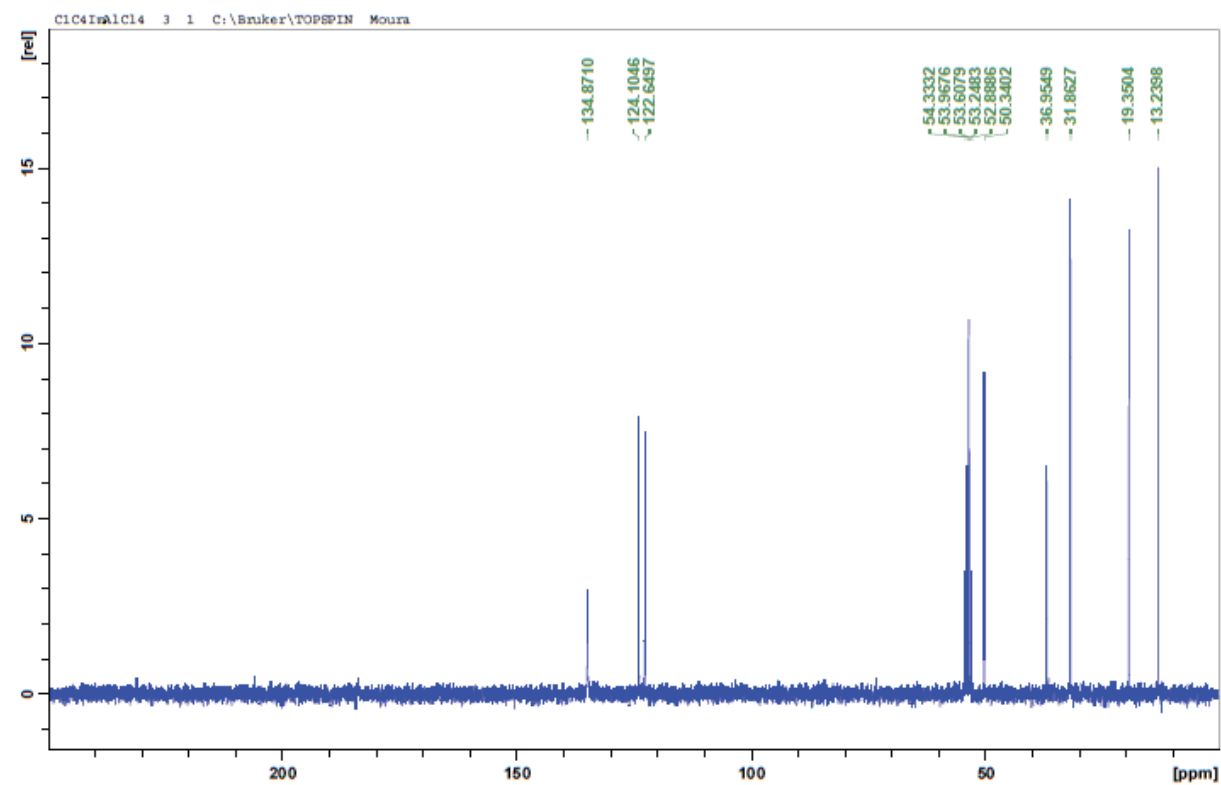


# 1-Butyl-3-methylimidazolium tetrachloroaluminate, [C<sub>1</sub>C<sub>4</sub>Im][AlCl<sub>4</sub>]

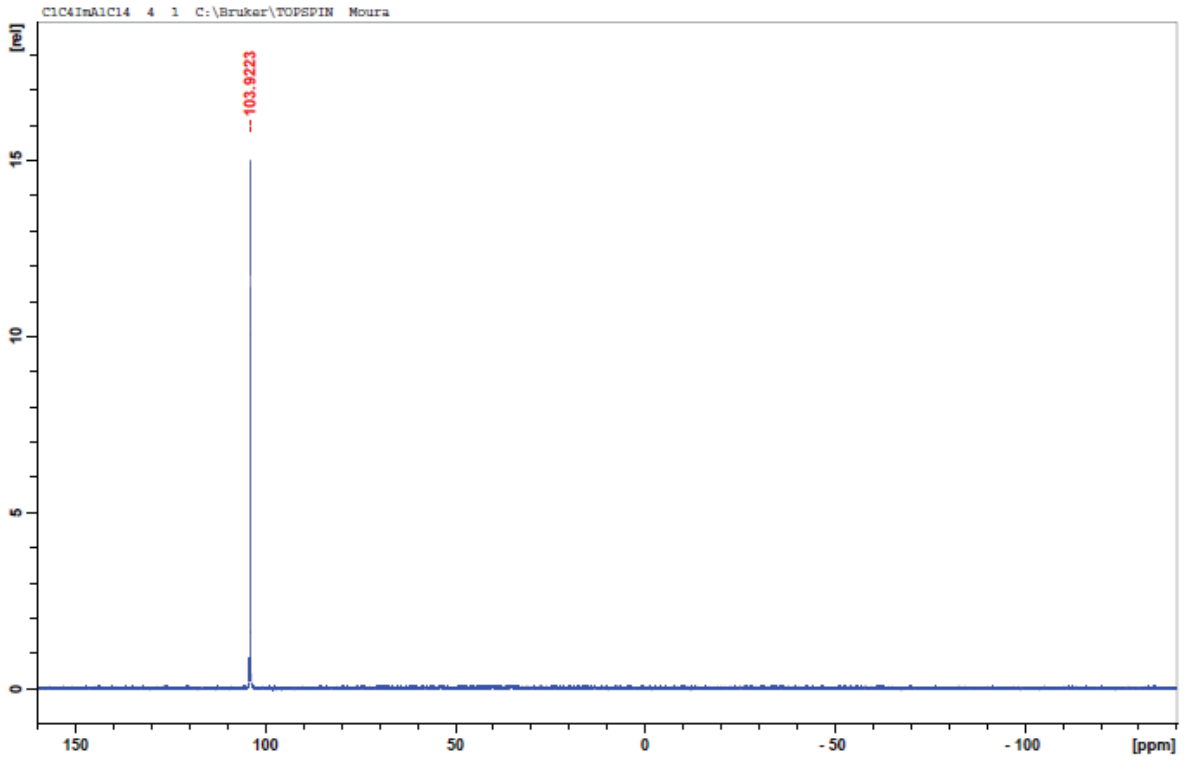
## <sup>1</sup>H-NMR



## <sup>13</sup>C-NMR



## <sup>27</sup>Al-NMR



# Appendix 3

---

Collection of Publications



## Effect of Unsaturation on the Absorption of Ethane and Ethylene in Imidazolium-Based Ionic Liquids

Leila Moura,<sup>†,||</sup> Manas Mishra,<sup>†</sup> Varinia Bernales,<sup>†,‡</sup> Patricio Fuentealba,<sup>§</sup> Agilio A.H. Padua,<sup>†</sup> Catherine C. Santini,<sup>||</sup> and Margarida F. Costa Gomes<sup>†,\*</sup>

<sup>†</sup>Clermont Université, Université Blaise Pascal, Institut de Chimie de Clermont-Ferrand, UMR 6296 CNRS, équipe Thermodynamique et Interactions Moléculaires, ICCF-TIM, BP 80026, F-63171 Aubière, France

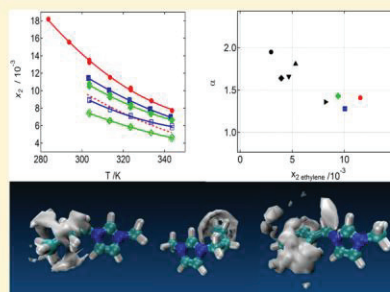
<sup>‡</sup>Departamento de Química, Facultad de Ciencias, Universidad de Chile, Las Palmeras #3425, Ñuñoa, Casilla 653-SCL, Santiago, Chile

<sup>§</sup>Departamento de Física, Facultad de Ciencias, Universidad de Chile, Las Palmeras #3425, Ñuñoa, Casilla 653-SCL, Santiago, Chile

<sup>||</sup>Université de Lyon, Institut de Chimie de Lyon, UMR 5265 CNRS, Université de Lyon 1-ESCE Lyon, LC2P2, Équipe Chimie Organométallique de Surface, 69616 Villeurbanne, France

### Supporting Information

**ABSTRACT:** The influence of the presence of imidazolium side chain unsaturation on the solubility of ethane and ethylene was studied in three ionic liquids: 1-butyl-3-methylimidazolium bis(trifluoromethanesulfonyl)amide—saturated alkyl side-chain in the cation; 1-methyl-3-(buten-3-yl)imidazolium bis(trifluorosulfonyl)imide—double bond in the side-chain of the cation; and 1-methyl-3-benzylimidazolium bis(trifluorosulfonyl)imide—benzyl group in the side-chain of the cation. The solubility of both gases decreases when the side-chain of the cations is functionalized with an unsaturated group. This can be explained by a less favorable enthalpy of solvation. The difference of solubility between ethane and ethylene can be explained from a balance of enthalpic and entropic factors: for the ionic liquid with the saturated alkyl side-chain and the benzyl-substituted side-chain, it is the favorable entropy of solvation that explains the larger ethylene solubility, whereas in the case of the saturated side-chain, it is the more favorable enthalpy of solvation. Molecular simulation allowed the identification of the mechanisms of solvation and the preferential solvation sites for each gas in the different ionic liquids. Simulations have shown that the entropy of solvation is more favorable when the presence of the gas weakens the cation–anion interactions or when the gas can be solvated near different sites of the ionic liquid.



## INTRODUCTION

Light olefins and paraffins are commonly separated by cryogenic distillation. Although reliable and still unchallenged in this application, this procedure implies high capital and operating costs. Thus the high demand for an alternative energy-saving separation process.<sup>1–4</sup>

Alternative processes for separating gaseous olefins from paraffins include ion exchanging resins,<sup>5</sup> adsorption on high-surface-area SiO<sub>2</sub>,<sup>6</sup> on alumina,<sup>7</sup> on zeolites<sup>8</sup> and molecular sieves,<sup>9</sup> or on metallic organic frameworks,<sup>10</sup> and the use of several types of membranes.<sup>3,11,12</sup> Most of the alternatives proposed involve liquid or solid selective absorbents containing transition metals such as copper or silver, which are believed to form a complex with the unsaturated gas molecule.<sup>1–3,13,14</sup> These alternatives have not been applied to an industrial scale due to several drawbacks linked to the synthesis, the efficacy, the reliability or the contamination of the different materials and also related to economical obstacles.<sup>1,2,15</sup>

The molecular diversity of cations and anions that can form an ionic liquid and the general attractive properties of these

fluids, including high thermal stability, negligible vapor pressure, and nonflammability, makes them good candidates as absorbents for gas separation.<sup>16,17</sup> Most of the published studies concerning the solubility of gases in ionic liquids involve the absorption of carbon dioxide, and much less report the solubility of light hydrocarbon gases in ionic liquids.<sup>4</sup> It has, nevertheless, been observed that unsaturated hydrocarbons, such as alkenes, are significantly more soluble in ionic liquids than their saturated counterpart<sup>4,17</sup> this fact being the basis for considering ionic liquids as possible absorbents to be used for hydrocarbon gas separation.<sup>18,19</sup>

The molecular mechanisms involved in the solvation of light hydrocarbon gases in ionic liquids are not yet well identified.<sup>17</sup> Several types of specific interactions between the unsaturated gases and the solvents have been suggested to explain their high solubilities such as  $\pi$ – $\pi$ ,  $\pi$ –cation,  $\pi$ –anion, and hydrogen

Received: March 28, 2013

Revised: May 27, 2013

Published: May 28, 2013

bonding.<sup>4,17,18,43</sup> A deeper understanding of the solution's molecular structure and gas-solvent interactions is still necessary both for the design of an optimized ionic liquid and for the development of a potential separation process.

In the present study, we have designed a series of ionic liquids thought to favor the selective absorption of gaseous alkenes. We describe experimental solubilities of ethane and ethylene in these ionic liquids. Gas solubilities were measured as a function of temperature and at pressures close to atmospheric, using an isochoric saturation method. The knowledge of the variation with temperature of the solubility allows the calculation of the thermodynamic properties of solvation. Those can be related with molecular simulation calculations of the microscopic structure and molecular interactions in the gas-ionic liquid solutions in order to assess the mechanisms involved in the solvation of the different gaseous solutes.<sup>20</sup>

## EXPERIMENTAL SECTION

**Materials.** Linde Gas supplied the gases used for this study: ethane 3.5, mole fraction purity of 0.9995 and ethylene 2.8, mole fraction purity of 0.998. All gases were used as received from the manufacturer.

1-Methylimidazole (>99%) (Aldrich), chlorobutane, benzyl chloride, 4-chloro-1-butene (>99%, Aldrich), and 3-chloro-1-propene (>99%, Aldrich) were distilled prior to use. Bis(trifluoromethanesulfonyl)imide lithium salt (Solvionic) was used without further purification.

The ionic liquids used in this work, 1-butyl-3-methylimidazolium bis(trifluorosulfonyl)imide,  $[C_1C_4\text{Im}][\text{NTf}_2]$ , 1-methyl-3-(buten-3-yl)imidazolium bis(trifluorosulfonyl)imide,  $[C_1(C_3H_5CH_2)\text{Im}][\text{NTf}_2]$ , and 1-methyl-3-benzylimidazolium bis(trifluorosulfonyl)imide,  $[C_1(\text{CH}_2\text{C}_6\text{H}_5)\text{Im}][\text{NTf}_2]$ , were synthesized as previously reported and as described in the Supporting Information, SI.<sup>21–23</sup> Their structures are represented Figure 1.

The purity of the ionic liquid samples (>99%) was checked by <sup>1</sup>H and <sup>13</sup>C NMR (Bruker Avance 400 MHz using CD<sub>2</sub>Cl<sub>2</sub> as solvent) and mass spectroscopy (see the SI). The high-resolution mass spectra (MS QTOF) were recorded in a

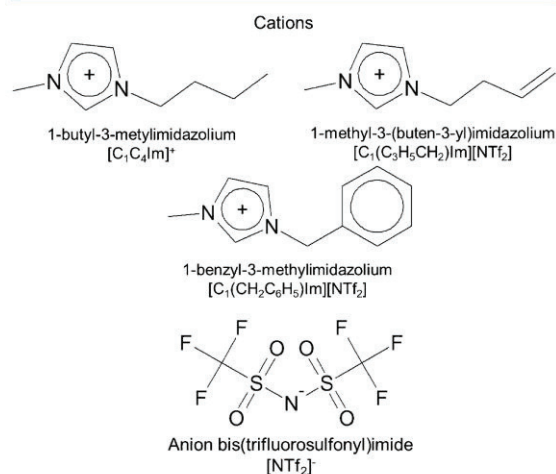


**Figure 1.** The structures and nomenclature system of the ionic liquids studied.

positive and negative ion mode on a hybrid quadrupole time-of-flight mass spectrometer (MicroTOFQ-II, Bruker Daltonics, Bremen) with an Electrospray Ionization (ESI) ion source. The gas flow of spray gas is  $6 \times 10^{-4}$  Pa, and the capillary voltage is  $\pm 4.5$  kV. The solutions are infused at 180  $\mu\text{L}/\text{h}$ . The mass range of the analysis is 50–1000  $m/z$  and the calibration was done with sodium formate.

To remove water, the ionic liquid samples were kept under primary vacuum at least 24 h prior to use. Before each measurement, the water content of the degassed ionic liquid was verified with a coulometric Karl Fischer titrator (Mettler Toledo DL32). It was found to be lower than 100 ppm for  $[C_1(C_3H_5CH_2)\text{Im}][\text{NTf}_2]$  and 70 ppm for  $[C_1(\text{CH}_2\text{C}_6\text{H}_5)\text{Im}][\text{NTf}_2]$ . The decomposition temperatures ( $T_{\text{start}}/T_{\text{onset}}$ ) of the same ionic liquids were 482 K/579 and 564 K/599 K, respectively, determined using a DSC 2920 from TA Instruments.

**Density Measurements.** Density measurements were performed using a U-shaped vibrating-tube densimeter (Anton Paar, model DMA 512P) operating in a static mode. All measurements were performed at atmospheric pressure and at temperatures ranging from 283 to 353 K following a procedure described in previous publications.<sup>24</sup> The temperature was maintained constant within  $\pm 0.01$  K by means of a recirculating bath equipped with a PID temperature controller (Julabo FP40-HP). The uncertainty of the density measurements is estimated as  $\pm 0.1$  kg  $\text{m}^{-3}$ .

**Viscosity Measurements.** All of the viscosity measurements were performed with an Anton Paar AMVn rolling ball viscosimeter at atmospheric pressure and at temperatures between 293.15 and 373.15 K. The temperature was controlled to within 0.01 K and measured with accuracy better than 0.05 K. The measurements were performed using a 1.8 mm and a 3.0 mm diameter capillary tube that were calibrated as a function of temperature and angle of measurement using standard viscosity oils from Cannon (N35, S60, and N100). The overall uncertainty on the viscosity is estimated as  $\pm 1.5\%$ .

**Solubility Measurements.** The solubility measurements were made using an isochoric saturation technique described in previous publications.<sup>25–27</sup>

In this technique, a known amount of gaseous solute is put in contact with a precisely determined amount of degassed ionic liquid, at constant temperature. At thermodynamic equilibrium, the pressure above the condensed phase is constant and directly related to the solubility of the gas in the fluid sample. The measurements were performed at temperatures between 303 and 343 K for  $[C_1(C_3H_5CH_2)\text{Im}][\text{NTf}_2]$  and  $[C_1(\text{CH}_2\text{C}_6\text{H}_5)\text{Im}][\text{NTf}_2]$  and between 283 and 343 K for  $[C_1C_4\text{Im}][\text{NTf}_2]$ .

The amount of ionic liquid sample is determined gravimetrically and the volume it occupies in the measuring cell,  $V_{\text{liq}}$ , is evaluated by the independent determination of the density at atmospheric pressure and as a function of temperature. This value is considered to be equal to the volume occupied by the solution after saturation with the gas. Since the ionic liquid does not present a measurable vapor pressure in the range of temperatures covered, the total amount of liquid is equal to its amount in the liquid solution,  $n_1^{\text{liq}}$  (subscripts 1 and 2 represent solvent and solute, respectively). The amount of solute in the liquid solution is obtained from the comparison between two  $pVT$  measurements: first when the gas is introduced in the cell and second when the thermodynamic equilibrium is attained:

$$n_2^{\text{liq}} = \frac{p_{\text{ini}} V_{\text{B}}}{[Z_2(p_{\text{ini}}, T_{\text{ini}})RT_{\text{ini}}]} - \frac{p_{\text{eq}}(V_{\text{tot}} - V_{\text{liq}})}{[Z_2(p_{\text{eq}}, T_{\text{eq}})RT_{\text{eq}}]} \quad (1)$$

where  $p_{\text{ini}}$  and  $T_{\text{ini}}$  are the pressure and temperature in the first  $pVT$  measurement and  $p_{\text{eq}}$  and  $V_{\text{eq}}$  correspond to the pressure and temperature after the system reaches the thermodynamic equilibrium, and  $V_{\text{B}}$  is the volume of the gas bulb.  $V_{\text{tot}}$  is the total volume of the equilibration cell, and  $Z_2$  designates the compression factor for the pure gas.

The solubility results, expressed in mole fraction of the gas, are used to calculate the Henry's law constant,  $K_{\text{H}}$ :

$$K_{\text{H}} = \lim_{x_2 \rightarrow 0} \frac{f_2(p, T, x_2)}{x_2} \approx \frac{\phi_2(p_{\text{eq}}, T_{\text{eq}})p_{\text{eq}}}{x_2} \quad (2)$$

where  $f_2$  is the fugacity of the solute, and  $\phi_2$  corresponds to the fugacity coefficient, calculated using the second virial coefficient of the gas.

**Molecular Simulations.** Ionic liquids were represented by an all-atom force field, which is based on the AMBER/OPLS-AA framework<sup>28,29</sup> with parameters developed specifically for the cations considered here.<sup>30–32</sup> For the  $[\text{C}_1(\text{C}_3\text{H}_5\text{CH}_2)\text{Im}]$  cation, the force field parameters were determined in this work and are listed in the SI. The gases were modeled using OPLS-AA force fields.<sup>28,33</sup>

The ionic liquids were simulated in periodic cubic boxes containing 246 ion pairs, using the molecular dynamics method implemented in the DL\_POLY package.<sup>27</sup> Initial low-density configurations, with ions placed at random in periodic cubic boxes, were equilibrated to attain liquid-like densities and structures at 373 K and 1 bar. Temperature and pressure were maintained using a Nosé-Hoover thermostat and barostat, respectively. Once the equilibrium density was attained, simulations runs of 400 ps were performed, with an explicit cutoff distance of 16 Å for nonbonded interactions, from which 5000 configurations were stored. Structural quantities such as radial and spatial distribution functions were calculated from configurations generated during the production runs. Additionally, simulation boxes containing 8 molecules of ethane and 8 molecules of ethylene separately were prepared in the same manner, to calculate solute–solvent radial distribution functions between the gas and the ionic liquid and the cation–anion interaction energy in the presence of the solute molecules.

The total energy of the simulated systems containing solute and ionic liquid was decomposed into contributions from different pairs of species, in order to quantify the predominant interactions. For that, the energy of each configuration (same atomic coordinates) was recalculated, taking into account only the relevant pairs of species, in turn. Also, the total energy was decomposed into intramolecular terms, short-range (Lennard–Jones) and electrostatic. In this manner, a detailed picture of the energetics of the system can be obtained.

## RESULTS AND DISCUSSION

The experimentally measured densities of the ionic liquids  $[\text{C}_1(\text{C}_3\text{H}_5\text{CH}_2)\text{Im}][\text{NTf}_2]$ , and  $[\text{C}_1(\text{CH}_2\text{C}_6\text{H}_5)\text{Im}][\text{NTf}_2]$  are reported in Table 1. Because the ionic liquids studied are relatively viscous, the experimental values of density were corrected, as recommended by the manufacturer, for the densimeter model used, by means of the equation:<sup>34</sup>

**Table 1.** Experimental Values for Densities,  $\rho$ , of the Studied Ionic Liquids, for Temperatures between 283 to 373 K and at Atmospheric Pressure, after Applying Correction factor,  $\Delta\rho$

$\rho$ (kg m <sup>-3</sup> )			
$T$ (K)	$[\text{C}_1(\text{C}_3\text{H}_5\text{CH}_2)\text{Im}][\text{NTf}_2]$	$T$ (K)	$[\text{C}_1(\text{CH}_2\text{C}_6\text{H}_5)\text{Im}][\text{NTf}_2]$
283.59	1482.5	282.80	1502.4
293.12	1472.8	293.15	1492.1
293.19	1463.1	302.75	1483.1
302.90	1472.8	302.82	1482.8
303.14	1463.2	313.13	1473.0
313.17	1453.6	321.87	1464.6
323.15	1444.1	333.06	1454.0
333.19	1434.6	342.81	1444.9
343.18	1425.3	352.90	1435.8
353.16	1416.2	363.03	1426.7
		372.82	1418.1

$$\frac{\Delta\rho}{\rho} = [-0.5 + 0.45\sqrt{n}]10^{-4} \quad (3)$$

The values found for  $\Delta\rho$  vary between 0.09 kgm<sup>-3</sup> at approximately 283 K to 0.009 kgm<sup>-3</sup> at 373 K for  $[\text{C}_1(\text{CH}_2\text{C}_6\text{H}_5)\text{Im}][\text{NTf}_2]$ . The corrections are much lower to  $[\text{C}_1(\text{C}_3\text{H}_5\text{CH}_2)\text{Im}][\text{NTf}_2]$ , for which a maximum value of 0.03 kgm<sup>-3</sup> was found for  $\Delta\rho$  at 293 K.

The values of density were fitted to linear functions of temperature, the standard deviation of the fits being always better than 0.05%:

$$\rho_{[\text{C}_1(\text{C}_3\text{H}_5\text{CH}_2)\text{Im}][\text{NTf}_2]}/\text{kgm}^{-3} = 1751.7 - 0.95120 \times (T/\text{K}) \quad (4)$$

$$\rho_{[\text{C}_1(\text{CH}_2\text{C}_6\text{H}_5)\text{Im}][\text{NTf}_2]}/\text{kgm}^{-3} = 1766.9 - 0.93770 \times (T/\text{K}) \quad (5)$$

The densities of the two ionic liquids have been previously reported at 298 K by Mahurin et al.<sup>35</sup> (only for  $[\text{C}_1(\text{CH}_2\text{C}_6\text{H}_5)\text{Im}][\text{NTf}_2]$ ) and by Mandai et al.<sup>36</sup> The value reported by Mahurin et al. has a lower precision than the ones reported herein and is significantly lower, a result compatible with the higher (and noncontrolled) amount of water of the ionic liquid used by the authors. The density values measured at 298 K by Mandai et al. agree with the ones measured here to within 0.1%.

The experimentally measured viscosities of the ionic liquids  $[\text{C}_1(\text{C}_3\text{H}_5\text{CH}_2)\text{Im}][\text{NTf}_2]$  and  $[\text{C}_1(\text{CH}_2\text{C}_6\text{H}_5)\text{Im}][\text{NTf}_2]$  are reported in Table 2. The experimental data were fitted as a function of temperature to a Vogel–Fulcher–Tammann (VFT) equation:

$$\eta = A \times T^{1/2} \exp\left(\frac{k}{T - T_0}\right) \quad (6)$$

the parameters of the fits are reported in Table 3.

It can be observed that  $[\text{C}_1(\text{CH}_2\text{C}_6\text{H}_5)\text{Im}][\text{NTf}_2]$  is much more viscous than  $[\text{C}_1(\text{C}_3\text{H}_5\text{CH}_2)\text{Im}][\text{NTf}_2]$ , especially at the lower temperatures where the differences in viscosity are as high as 70% (or 137.4 mPa·s at 293 K). The difference in viscosity between the two liquids is much lower at the higher temperatures studied being of only of 40% at 353 K (or 6.27 mPa s).

**Table 2.** Experimental Values for the Viscosities the Studied Ionic Liquids, For Temperatures between 283 and 373 K

$\eta$ (mPa·s)			
$T$ (K)	$[\text{C}_1(\text{C}_3\text{H}_5\text{CH}_2)\text{Im}][\text{NTf}_2]$	$T$ (K)	$[\text{C}_1(\text{CH}_2\text{C}_6\text{H}_5)\text{Im}][\text{NTf}_2]$
293.15	60.45	293.15	197.8
303.15	39.65	303.15	104.6
313.15	27.52	313.15	62.33
323.15	19.96	323.15	40.34
333.15	14.92	333.15	27.95
343.15	11.56	343.15	20.15
353.15	9.208	353.15	15.48
		363.15	12.05
		373.15	9.745

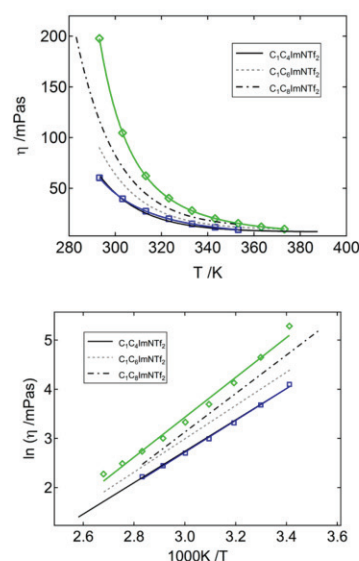
**Table 3.** Vogel–Fulcher–Tammann Equation Parameters Obtained for the Measurements of Viscosity,  $\eta$ , of  $[\text{C}_1(\text{C}_3\text{H}_5\text{CH}_2)\text{Im}][\text{NTf}_2]$  and  $[\text{C}_1(\text{CH}_2\text{C}_6\text{H}_5)\text{Im}][\text{NTf}_2]$  Ionic Liquids, For Temperatures between 283 and 373 K

$\eta$ (mPa·s)				
	$k$ (K)	$A/10^{-3}$ (mPa·s·K <sup>-1/2</sup> )	$T_0$ (K)	AAD (%)
$[\text{C}_1(\text{C}_3\text{H}_5\text{CH}_2)\text{Im}][\text{NTf}_2]$	947	4.50	151	0.7
$[\text{C}_1(\text{CH}_2\text{C}_6\text{H}_5)\text{Im}][\text{NTf}_2]$	643	12.8	199	0.4

Orita et al.<sup>37</sup> have determined the viscosity of the ionic liquid  $[\text{C}_1(\text{C}_3\text{H}_5\text{CH}_2)\text{Im}][\text{NTf}_2]$  at 298 K. Their value agrees with our measurements to within 3%. Mahurin et al.<sup>34</sup> and Mandai et al.<sup>35</sup> studied the viscosity of  $[\text{C}_1(\text{CH}_2\text{C}_6\text{H}_5)\text{Im}][\text{NTf}_2]$  between 298 and 333 K and at 298 K, respectively. The present values are much higher than those reported in ref 34, the deviation of 57% being constant in the whole temperature range and compatible with the presence of a relatively large amount of water in the ionic liquid used. The value at 298 K reported in ref 35 is 13% lower than the one reported here, a difference more difficult to explain as the authors claim that their ionic liquid sample has a water content of less than 150 ppm, a value higher but sufficiently close to ours.

As depicted in Figure 2, the viscosity of  $[\text{C}_1(\text{C}_3\text{H}_5\text{CH}_2)\text{Im}][\text{NTf}_2]$  is very similar to that of  $[\text{C}_1\text{C}_4\text{Im}][\text{NTf}_2]$ <sup>38</sup> (a difference of less than 3% in the whole temperature range), proving that the presence of a double bond on the side chain of the cation does not significantly affect the viscosity of imidazolium based ionic liquids. The same is not observed for  $[\text{C}_1(\text{CH}_2\text{C}_6\text{H}_5)\text{Im}][\text{NTf}_2]$ , even when its viscosity is compared with that of  $[\text{C}_1\text{C}_8\text{Im}][\text{NTf}_2]$ <sup>39</sup> (that has the same number of carbon atoms in the side-chain of the cation), for which a much higher viscosity was measured in the temperature range studied. We have also compared the viscosity of  $[\text{C}_1(\text{CH}_2\text{C}_6\text{H}_5)\text{Im}][\text{NTf}_2]$  with that of 1-methyl-3-methylcyclohexylimidazolium bis(trifluorosulfonyl)imide,  $[\text{C}_1(\text{CH}_2\text{C}_6\text{H}_{11})\text{Im}][\text{NTf}_2]$ , reported by Mandai et al.<sup>35</sup> at 298 K. We have found that the viscosity of  $[\text{C}_1(\text{CH}_2\text{C}_6\text{H}_{11})\text{Im}][\text{NTf}_2]$  is more than 100% higher than that of the ionic liquid containing the benzyl group in the side chain of the cation.

For each ionic liquid–gas pair, several solubility experimental data points were obtained for temperatures between 303 and 343 K in steps of approximately 10 K. The experimental solubilities obtained for ethane and ethylene in the ionic liquids  $[\text{C}_1(\text{C}_3\text{H}_5\text{CH}_2)\text{Im}][\text{NTf}_2]$ , and  $[\text{C}_1(\text{CH}_2\text{C}_6\text{H}_5)\text{Im}][\text{NTf}_2]$  and

**Figure 2.** Viscosities of the studied ionic liquids: blue  $\square$ ,  $[\text{C}_1(\text{C}_3\text{H}_5\text{CH}_2)\text{Im}][\text{NTf}_2]$ , and green  $\diamond$ ,  $[\text{C}_1(\text{CH}_2\text{C}_6\text{H}_5)\text{Im}][\text{NTf}_2]$  for temperatures between 283 and 373 K. Viscosity of  $[\text{C}_1\text{C}_4\text{Im}][\text{NTf}_2]$ ,<sup>38</sup>  $[\text{C}_1\text{C}_6\text{Im}][\text{NTf}_2]$ ,<sup>45</sup> and  $[\text{C}_1\text{C}_8\text{Im}][\text{NTf}_2]$ <sup>39</sup> added for comparison. The lines in the experimental data represent the VFT equation fitting using the parameters of Table 3.

for ethylene in  $[\text{C}_1\text{C}_4\text{Im}][\text{NTf}_2]$  are reported in Table 4 and depicted in Figure 3, together with experimental results already published for ethane<sup>26</sup> in  $[\text{C}_1\text{C}_4\text{Im}][\text{NTf}_2]$ . For the calculation of the Henry's law constants, the compressibility factor,  $Z_2$ , and the fugacity coefficient,  $\phi_2$ , were calculated from the second virial coefficient, obtained from the data compiled by Dymond and Smith.<sup>40</sup> The volume of ionic liquid in the equilibrium cell,  $V_{\text{liq}}$ , was obtained from the experimental density of the pure ionic liquid, as reported in Table 1.

The calculated Henry's law constants were fitted to a power series in  $T$ :

$$\ln[K_{\text{H}}/10^5\text{Pa}] = \sum_{i=0}^n A_i(T/K)^i \quad (7)$$

The coefficients  $A_i$ , being listed in Table 5. From the variation of the Henry's law constants with temperature, it is possible to calculate the thermodynamic properties of solvation as previously described.<sup>26,41,42</sup> The values obtained, at the temperature of 323 K, are listed in Table 6.

The solubility of ethylene in  $[\text{C}_1\text{C}_4\text{Im}][\text{NTf}_2]$  has been previously measured by Anderson et al.<sup>43</sup> from 283 to 323 K. Our values of the Henry's law constant agree to within 0.6% at 323 K, the deviations increasing at lower temperatures to reach 13% at 283 K.

The solubility of the two studied gases is larger for  $[\text{C}_1\text{C}_4\text{Im}][\text{NTf}_2]$  than for the two other liquids. This difference can be attributed to more negative enthalpies of solvation for both gases in  $[\text{C}_1\text{C}_4\text{Im}][\text{NTf}_2]$ .

For the three ionic liquids studied, ethylene is always more soluble than ethane in the temperature range covered. The higher solubility of ethylene can be explained, for  $[\text{C}_1(\text{C}_3\text{H}_5\text{CH}_2)\text{Im}][\text{NTf}_2]$ , by more favorable gas–ionic liquid interactions, as expressed by a more negative enthalpy of

**Table 4.** Experimental Values for the Solubility of Ethane, C<sub>2</sub>H<sub>6</sub>, and Ethylene, C<sub>2</sub>H<sub>4</sub>, in [C<sub>1</sub>(C<sub>3</sub>H<sub>5</sub>CH<sub>2</sub>)Im][NTf<sub>2</sub>] and [C<sub>1</sub>(CH<sub>2</sub>C<sub>6</sub>H<sub>5</sub>)Im][NTf<sub>2</sub>] Pure Ionic Liquids, and for ethylene, C<sub>2</sub>H<sub>4</sub>, in [C<sub>1</sub>C<sub>4</sub>Im][NTf<sub>2</sub>] Expressed Both As Henry's Law Constants, K<sub>H</sub>, and as Gas Mole Fraction, X<sub>2</sub>, Corrected for a Partial Pressure of Solute of 0.1 MPa<sup>a</sup>

T (K)	p (10 <sup>2</sup> Pa)	K <sub>H</sub> (10 <sup>5</sup> Pa)	X <sub>2</sub> (10 <sup>-3</sup> )	%dev	T (K)	p (10 <sup>2</sup> Pa)	K <sub>H</sub> (10 <sup>5</sup> Pa)	X <sub>2</sub> (10 <sup>-3</sup> )	%dev
C <sub>2</sub> H <sub>6</sub> + [C <sub>1</sub> (C <sub>3</sub> H <sub>5</sub> CH <sub>2</sub> )Im][NTf <sub>2</sub> ]					C <sub>2</sub> H <sub>4</sub> + [C <sub>1</sub> (C <sub>3</sub> H <sub>5</sub> CH <sub>2</sub> )Im][NTf <sub>2</sub> ]				
303.56	680.4	111.9	8.895	+ 0.7	303.12	639.2	87.30	11.42	- 0.4%
303.57	685.3	110.8	8.983	- 1.3	303.12	646.5	86.57	11.51	+ 0.0%
313.56	703.6	126.9	7.847	- 0.9	303.16	626.6	86.96	11.46	- 0.4%
313.58	708.7	127.2	7.829	- 1.1	313.09	648.4	99.47	10.02	- 0.3%
323.59	726.4	141.5	7.035	- 1.1	313.12	661.5	99.33	10.04	- 0.1%
323.60	731.5	138.6	7.184	+ 1.0	313.12	668.9	98.88	10.08	+ 0.4%
333.60	749.0	154.9	6.431	+ 0.1	323.00	670.0	112.8	8.841	- 0.1%
333.62	754.6	155.4	6.407	- 0.4	323.09	683.6	112.3	8.876	+ 0.4%
343.61	771.7	172.9	5.763	- 1.6	323.11	690.9	111.2	8.965	+ 1.4%
343.64	777.1	165.7	6.013	+ 2.7	332.91	691.3	126.2	7.902	+ 0.6%
303.56	680.4	111.9	8.895	+ 0.7	333.09	713.0	125.5	7.945	+ 1.4%
303.57	685.3	110.8	8.983	- 1.3	342.78	712.8	144.4	6.906	- 1.7%
313.57	703.6	126.9	7.847	- 0.9	342.94	727.3	144.3	6.911	- 1.4%
313.58	708.7	127.2	7.829	- 1.1	343.02	734.8	141.3	7.056	+ 0.7%
C <sub>2</sub> H <sub>6</sub> + [C <sub>1</sub> (CH <sub>2</sub> C <sub>6</sub> H <sub>5</sub> )Im][NTf <sub>2</sub> ]					C <sub>2</sub> H <sub>4</sub> + [C <sub>1</sub> (CH <sub>2</sub> C <sub>6</sub> H <sub>5</sub> )Im][NTf <sub>2</sub> ]				
303.25	656.7	134.4	7.408	- 1.2	303.55	675.0	94.91	10.50	- 1.6
303.55	881.6	135.9	7.315	- 1.9	303.58	680.7	92.09	10.82	+ 1.5
303.57	670.8	131.4	7.574	+ 1.5	313.53	698.2	107.9	9.241	- 1.5
313.29	679.6	152.5	6.530	- 0.8	313.60	704.3	104.2	9.560	+ 2.1
313.53	911.5	151.4	6.565	+ 0.2	323.49	721.3	123.4	8.079	- 2.8
313.57	693.8	150.1	6.633	+ 1.2	323.63	727.7	118.1	8.443	+ 1.7
323.35	702.4	172.8	5.762	- 1.0	333.42	743.9	136.0	7.331	- 1.2
323.56	716.7	169.6	5.871	+ 1.1	333.67	751.0	131.7	7.572	+ 2.3
323.61	941.6	167.7	5.931	+ 2.3	343.35	766.4	150.2	6.640	- 0.5
333.38	725.0	192.8	5.167	- 0.4	343.67	774.3	149.8	6.659	+ 0.1
333.56	739.4	190.8	5.220	+ 0.8					
343.38	747.9	223.7	4.454	- 4.4					
343.51	761.9	213.0	4.677	+ 0.5					
343.65	1002	209.8	4.744	+ 2.2					
C <sub>2</sub> H <sub>4</sub> + [C <sub>1</sub> C <sub>4</sub> Im][NTf <sub>2</sub> ]									
283.67	803.0	54.62	18.19	+ 0.2					
293.76	833.8	63.91	15.56	+ 0.1					
303.57	872.4	75.11	13.24	- 1.3					
303.57	863.3	73.67	13.50	+ 0.6					
313.59	903.0	86.32	11.53	- 0.8					
323.61	923.2	96.64	10.30	+ 1.9					
323.61	933.3	98.55	10.10	- 0.1					
333.63	963.6	112.6	8.847	+ 0.0					
343.65	993.9	128.9	7.732	- 0.5					

<sup>a</sup>p is the experimental equilibrium pressure and the percent deviation is relative to the correlations of the data reported in Table 5.

solvation for C<sub>2</sub>H<sub>4</sub> than for C<sub>2</sub>H<sub>6</sub> (Table 6). For [C<sub>1</sub>(CH<sub>2</sub>C<sub>6</sub>H<sub>5</sub>)Im][NTf<sub>2</sub>] and [C<sub>1</sub>C<sub>4</sub>Im][NTf<sub>2</sub>], the higher solubility of ethylene is explained by more favorable entropies of solvation, an effect more pronounced in the case of [C<sub>1</sub>C<sub>4</sub>Im][NTf<sub>2</sub>] even if the difference in the ethane and ethylene solubility is larger for [C<sub>1</sub>(CH<sub>2</sub>C<sub>6</sub>H<sub>5</sub>)Im][NTf<sub>2</sub>] than for the two other ionic liquids.

Together with the amount of each gas that can be absorbed by the ionic liquid, the difference in solubilities is important for the design of gas separation processes and is normally quantified as the ideal selectivity of the separation,  $\alpha$ , herein defined as follows:

$$\alpha = \frac{1}{\frac{K_{H\text{ethylene}}}{1}} \frac{1}{K_{H\text{ethane}}} \quad (8)$$

This ideal gas selectivity is not very different from the real mixed gas selectivity as both gases present relatively low absorptions and so their activity coefficients in the liquid phase are close to unity.

In the upper plot of Figure 4, the selectivity is represented as a function of temperature for the ionic liquids studied (for ethane in [C<sub>1</sub>C<sub>4</sub>Im][NTf<sub>2</sub>] the data from Costa Gomes et al.<sup>27</sup> was used in the calculation). It is observed that the selectivity for [C<sub>1</sub>C<sub>4</sub>Im][NTf<sub>2</sub>] is similar to that for [C<sub>1</sub>(CH<sub>2</sub>C<sub>6</sub>H<sub>5</sub>)Im][NTf<sub>2</sub>] and constant over the temperature range covered. The selectivity for [C<sub>1</sub>(C<sub>3</sub>H<sub>5</sub>CH<sub>2</sub>)Im][NTf<sub>2</sub>] is slightly lower and decreases with increasing temperatures (as expected as the difference in solubilities is entropically controlled). In the lower plot of Figure 4, the performance plot is represented for ethylene (selectivity as a function of mole fraction solubility) of different ionic liquids. The larger selectivity was observed by

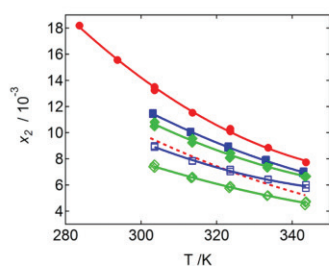


**Figure 3.** Mole fraction solubilities of ethane (empty symbols) and ethylene (full symbols) at 0.1 MPa partial pressure and as a function of the temperature in the following ionic liquids: red ●,  $[C_1C_4Im][NTf_2]$ ; blue ■/□,  $[C_1(C_3H_5CH_2)Im][NTf_2]$ ; and green ◆/◇,  $[C_1(CH_2C_6H_5)Im][NTf_2]$ . Full lines represent the smoothed data using the parameters in Table 5 and the dashed line corresponds to the previously reported values of the solubility of ethane in  $[C_1C_4Im][NTf_2]$ .<sup>27</sup>

**Table 5.** Parameters of Eq 7 Used to Smooth the Experimental Results on  $K_H$  from Table 4 along with the Percent Average Absolute Deviation of the Fit, AAD

ionic liquid	$A_0$	$A_1$	$A_2$	% AAD
		$C_2H_6$		
$[C_1(C_3H_5CH_2)Im][NTf_2]$	- 4.782	$49.77 \times 10^{-3}$	$- 6.089 \times 10^{-5}$	0.9
$[C_1(CH_2C_6H_5)Im][NTf_2]$	+ 0.5989	$16.20 \times 10^{-3}$	$- 6.699 \times 10^{-6}$	1.4
		$C_2H_4$		
$[C_1(C_3H_5CH_2)Im][NTf_2]$	- 0.1297	$17.55 \times 10^{-3}$	$- 7.863 \times 10^{-6}$	0.5
$[C_1(CH_2C_6H_5)Im][NTf_2]$	- 2.750	$34.80 \times 10^{-3}$	$- 3.566 \times 10^{-5}$	1.5
$[C_1C_4Im][NTf_2]$	- 2.386	$29.41 \times 10^{-3}$	$- 2.428 \times 10^{-5}$	0.6

**Table 6.** Thermodynamic Properties of Solvation of Ethane and Ethylene, at 323 K, in  $[C_1(C_3H_5CH_2)Im][NTf_2]$ ,  $[C_1(CH_2C_6H_5)Im][NTf_2]$ , and  $[C_1C_4Im][NTf_2]$

ionic liquid	$\Delta_{sol}H^{oo}$ (kJmol <sup>-1</sup> )	$T\Delta_{sol}S^{oo}$ (kJmol <sup>-1</sup> K <sup>-1</sup> )
	$C_2H_6$	
$[C_1(C_3H_5CH_2)Im][NTf_2]$	$- 8.90 \pm 0.1$	$- 22.2 \pm 0.7$
$[C_1(CH_2C_6H_5)Im][NTf_2]$	$- 10.1 \pm 0.1$	$- 23.9 \pm 0.7$
$[C_1C_4Im][NTf_2]^a$	$- 13.0 \pm 0.1$	$- 26.3 \pm 0.8$
	$C_2H_4$	
$[C_1(C_3H_5CH_2)Im][NTf_2]$	$- 11.1 \pm 0.2$	$- 23.6 \pm 0.7$
$[C_1(CH_2C_6H_5)Im][NTf_2]$	$- 9.52 \pm 0.1$	$- 22.3 \pm 0.5$
$[C_1C_4Im][NTf_2]$	$- 11.9 \pm 0.1$	$- 24.2 \pm 0.7$

<sup>a</sup>Value from ref 27.

Camper et al.<sup>44</sup> for 1-ethyl-3-methylimidazolium dicyanamide, the larger ethylene absorption being reported herein for  $[C_1C_4Im][NTf_2]$ .

In order to get an insight on the molecular mechanisms responsible for the behaviors observed, we have analyzed the structure of the gas-ionic liquid solutions by calculating all the site-site solute-solvent radial distribution functions (RDFs) for all the solutions of gas in ionic liquid. As can be seen in Figure 5, where some of the most significant solute-solvent RDFs are plotted, the most striking differences on the structure of the solutions of the two gases are observed for the ionic liquid with the benzyl group in the cation (Figure 5c). In this

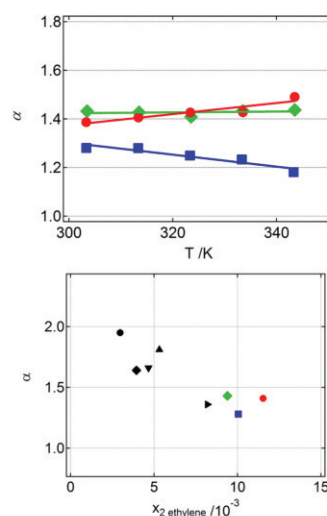


**Figure 4.** Upper plot: variation of the selectivity,  $\alpha$ , as defined in eq 8 for the ethane/ethylene separation, with the temperature for the ionic liquids: red ●,  $[C_1C_4Im][NTf_2]$ ; blue ■,  $[C_1(C_3H_5CH_2)Im][NTf_2]$ ; green ◆,  $[C_1(CH_2C_6H_5)Im][NTf_2]$ . Lines represent the linear fitting of the data. Lower plot: variation of the selectivity as a function of the mole fraction solubility of ethylene, usually called performance plot, for ethylene at 313 K. ■ 1-hexyl-3-methylpyridinium bis(trifluoromethylsulfonyl)imide ( $[C_1C_6py][NTf_2]$ );<sup>45</sup> ● 1-ethyl-3-methylimidazolium dicyanamide ( $[C_1C_2Im][DCA]$ );<sup>44</sup> ◆ 1-butyl-3-methylimidazolium tetrafluoroborate ( $[C_1C_4Im][BF_4]$ );<sup>44</sup> ▲ 1-butyl-3-methylimidazolium hexafluorophosphate ( $[C_1C_4Im][PF_6]$ );<sup>44</sup> ► 1-ethyl-3-methylimidazolium bis(trifluoromethylsulfonyl)imide ( $[C_1C_2Im][NTf_2]$ );<sup>44</sup> ▼ 1-ethyl-3-methylimidazolium trifluoromethanesulfonate ( $[C_1C_2Im][CF_3SO_3]$ ).<sup>44</sup>

case, ethane has a larger probability of being found near the anion of the ionic liquid while ethylene interacts with a larger probability with the benzyl ring of the cation, an evidence of the preferential  $\pi$ - $\pi$  interaction between ethylene and the cation of the ionic liquid. A more detailed view is given by the spatial distribution functions represented in Figure 6, where it can be seen that ethane is preferentially solvated near the equatorial hydrogen atoms of the benzyl group and ethylene rests planar to the aromatic ring on the side chain of the cation. Also represented in Figure 6 is the probability of finding the gases solvated near the imidazolium ring of the cation—once again there is evidence that the ethylene molecule rests planar to the imidazolium ring, while ethane is solvated near the equatorial hydrogen atoms.

We have also decomposed the overall system configuration energy calculated by molecular simulation to the energy between each pair of species, as represented in Figure 7. The cation-anion interaction energy is more negative for  $[C_1(CH_2C_6H_5)Im][NTf_2]$  in the presence of ethane than in presence of ethylene, an observation compatible with the higher entropy of solvation for ethylene that was observed experimentally. This difference on the total potential energy is due to a change on the electrostatic contribution, a fact that reinforces the conclusion that, in presence of ethane, the cation-anion interaction in the ionic liquid is stronger than in presence of ethylene.

Important differences can also be observed in Figure 5, parts a and b, for the two gaseous solutes in the other two ionic

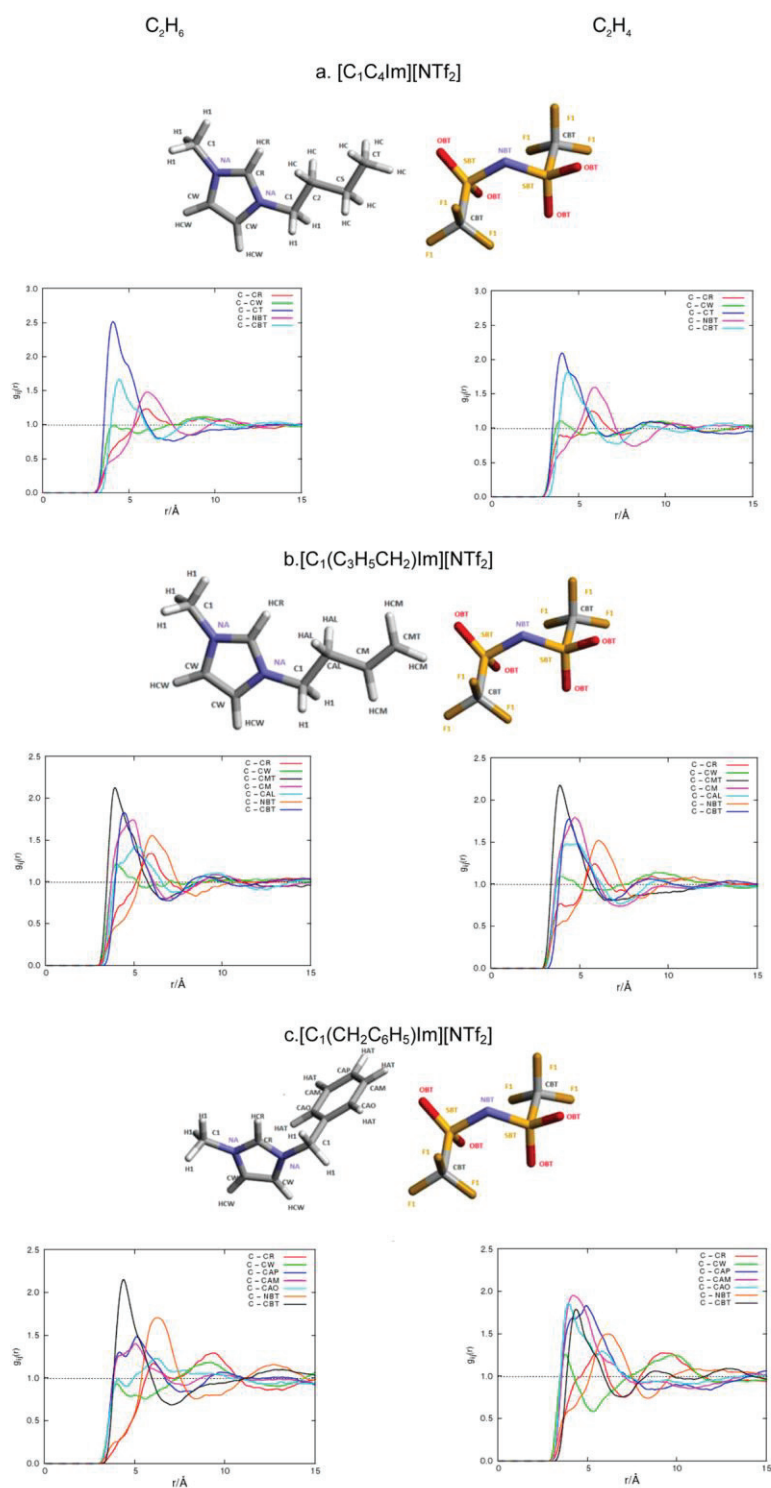


**Figure 5.** Site–site, solute–solvent radial distribution functions of ethane (plots on the left-hand side) and ethylene (plots on the right-hand side) for the three ionic liquids studied:  $[C_1C_4Im][NTf_2]$  (first row);  $[C_1(C_3H_5CH_2)Im][NTf_2]$  (second row) and  $[C_1(CH_2C_6H_5)Im][NTf_2]$  (third row).

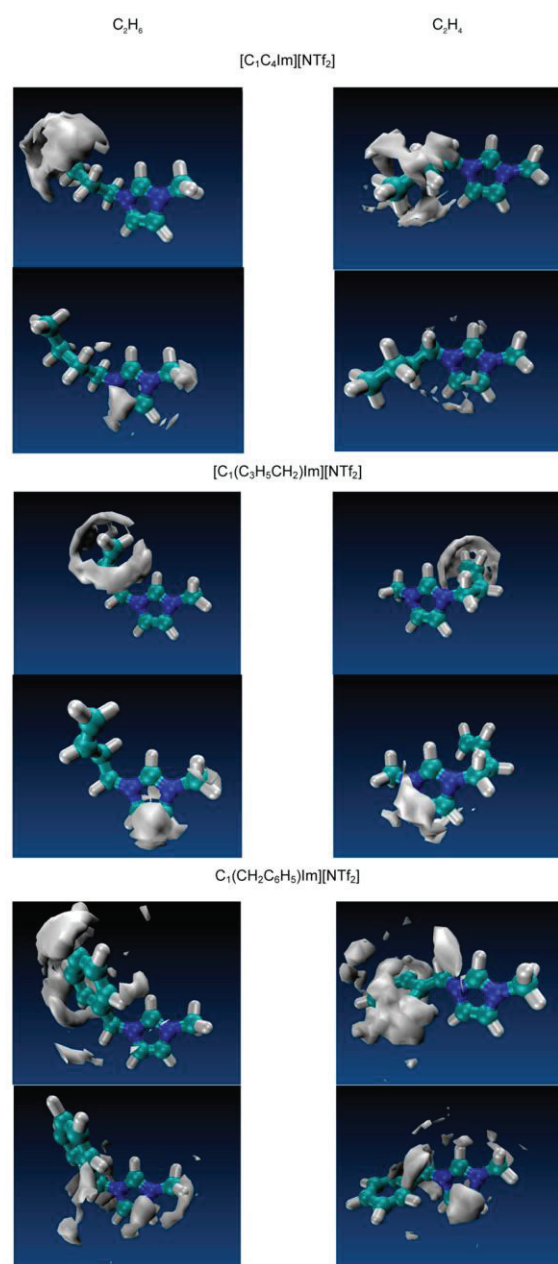


**Figure 6.** Spatial distribution functions of the center of mass of the two solutes around the terminal atoms of the alkyl-side chain of the cations or around the atoms of the imidazolium ring of the cation. The surface corresponds to an iso-probability density of 3.0 times the average density in the system.

liquids. For  $[\text{C}_1\text{C}_4\text{Im}][\text{NTf}_2]$ , both gases are solvated near the alkyl-side chain, but in the case of ethylene, the gas is preferentially solvated closer to the imidazolium ring. The interaction peak between the terminal atom of the alkyl-side chain and ethylene is wider than that with ethane, an observation indicating a larger mobility of the solute,

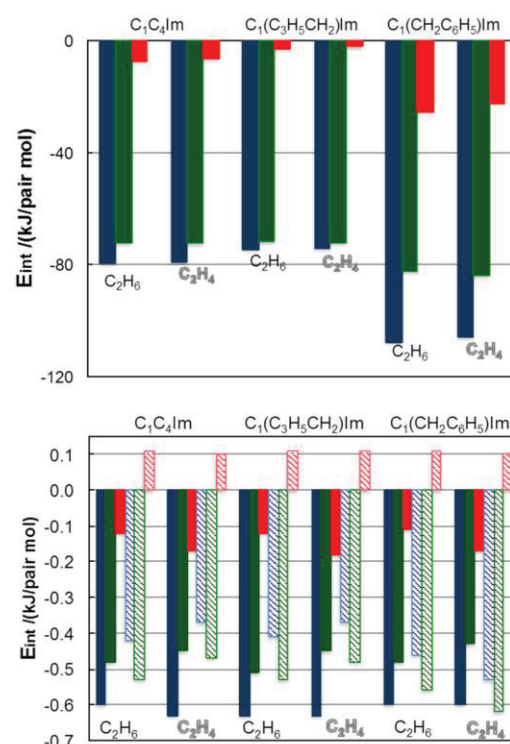


**Figure 7.** Energy decomposition calculated by molecular simulation. In blue, the total potential energy; in green, the dispersion interaction energy; and in red, the electrostatic contribution to the interaction energy. Upper plot: cation–anion interaction energy for the three ionic liquids in the presence of the two solutes. Lower plot: solute–ionic liquid interaction energies for the three ionic liquids. The filled bars represent the solute–anion interaction energy, and the patterned bars represent the solute–cation interaction energy.

compatible with the larger entropy of solvation found experimentally for this gas.

For the ionic liquid  $[\text{C}_1(\text{C}_3\text{H}_5\text{CH}_2)\text{Im}][\text{NTf}_2]$ , no significant differences are observed on the site–site solute–solvent radial distribution functions of the two gases (Figure 5b). In Figure 6, we can nevertheless observe a slight difference on the solvation of the two gases near the terminal atom of the alkyl side chain, with ethylene being more probably found on the extremity of the chain and ethane around the double bond.

## CONCLUSIONS

From the study of the absorption of ethane and ethylene in different ionic liquids as a function of temperature, it was possible to determine the influence of the presence of unsaturated bonds on the cation on the solubility of the two gases. It was observed that the solubility of both ethane and ethylene decreases when the side-chain of the cation in the ionic liquid is functionalized with a double bond or a benzyl ring. This decrease of the solubility can be explained by a less favorable enthalpy of solvation.

The difference in solubility between ethane and ethylene is similar for the cation with the saturated alkyl side-chain and for the cation containing the benzyl ring but decreases for the cation with the double bond in the side chain. This behavior

results from a balance of enthalpic and entropic factors: for the two first ionic liquids ( $[\text{C}_1\text{C}_4\text{Im}][\text{NTf}_2]$  and  $[\text{C}_1(\text{CH}_2\text{C}_6\text{H}_5)\text{Im}][\text{NTf}_2]$ ), it is the favorable entropy of solvation that is responsible for the selectivity of the absorption of the two gases (ethylene always being the more soluble). For the ionic liquid containing a double bond on the side chain of the cation,  $[\text{C}_1(\text{C}_3\text{H}_5\text{CH}_2)\text{Im}][\text{NTf}_2]$ , it is the more favorable enthalpy that explains the larger ethylene solubility.

Computer simulations allow an interpretation at the molecular level of the observed solvation behaviors. Although the differences in solubility are similar, and attributed to favorable entropic contributions, for the ionic liquids  $[\text{C}_1\text{C}_4\text{Im}][\text{NTf}_2]$  and  $[\text{C}_1(\text{CH}_2\text{C}_6\text{H}_5)\text{Im}][\text{NTf}_2]$ , the molecular reasons behind them are quite distinct. In the case of the ionic liquid with a benzyl substitution in the alkyl side-chain of the cation, the presence of ethylene decreases the cation–anion interaction, making the dissolution of  $\text{C}_2\text{H}_4$  entropically more favorable. For the ionic liquid with the saturated alkyl side-chain, several solvation sites compete for the solvation of ethylene, probably contributing to a larger mobility of the solute and so a more positive entropy of solvation.

In the case of the ionic liquid with a double bond on the side chain of the cation, a more favorable interaction  $\text{C}_2\text{H}_4$ – $[\text{C}_1(\text{C}_3\text{H}_5\text{CH}_2)\text{Im}][\text{NTf}_2]$  explains the larger solubility of this gas.

## ■ ASSOCIATED CONTENT

### Supporting Information

Details of the synthesis of the ionic liquids together with the NMR and the mass spectrometry analysis of the samples and the force field parameters for 1-methyl-3-(buten-3-yl)-imidazolium bis(trifluorosulfonyl)imide. This material is available free of charge via the Internet at <http://pubs.acs.org>.

## ■ AUTHOR INFORMATION

### Corresponding Author

\*E-mail: [Margarida.c.gomes@univ-bpclermont.fr](mailto:Margarida.c.gomes@univ-bpclermont.fr).

### Notes

The authors declare no competing financial interest.

## ■ ACKNOWLEDGMENTS

The authors thank Dr. A. Podgorssek and Mr. F. Jacquet for the measurement of the viscosity of the ionic liquid  $[\text{C}_1(\text{C}_3\text{H}_5\text{CH}_2)\text{Im}][\text{NTf}_2]$ . L.M. is financed by a Cluster Excellence of the Rhone Alpes region, France with the participation of IFPEN, France. V.B. acknowledges CONICYT for the PhD fellowship and CONICYT-BECAS CHILE for supporting the research visit to Blaise Pascal University in France. Support by FONDECYT through Grant 11090013, Financiamiento Basal Para Centros Científicos y Tecnológicos de Excelencia and also by Millennium Nucleus CILIS, Project ICM-P10-003-F is acknowledged.

## ■ REFERENCES

- (1) Eldrige, R. B. Olefin/Paraffin Separation Technology: A Review. *Ind. Eng. Chem. Res.* **1993**, *32*, 2208–2212.
- (2) Safarik, D. J.; Eldridge, R. B. Olefin/Paraffin Separations by Reactive Absorption: A Review. *Ind. Eng. Chem. Res.* **1998**, *37*, 2571–2581.
- (3) Faiz, R.; Li, K. Olefin/Paraffin Separation Using Membrane Based Facilitated Transport/Chemical Absorption Techniques. *Chem. Eng. Sci.* **2012**, *73*, 261–284.
- (4) Mokrushin, V.; Assenbaum, D.; Paape, N.; Gerhard, D.; Mokrushina, L.; Wasserscheid, P.; Arlt, W.; Kistenmacher, H.; Neuendorf, S.; Goeke, V. Ionic Liquids for Propene–Propane Separation. *Chem. Eng. Technol.* **2010**, *33*, 63–73.
- (5) Sikavitsas, V. I.; Yang, R. T.; Burns, M. A.; Langenmayr, E. J. Magnetically Stabilized Fluidized Bed for Gas Separations: Olefin–Paraffin Separations by  $\pi$ -Complexation. *Ind. Eng. Chem. Res.* **1995**, *34*, 2873–2880.
- (6) Dewitt, A.; Herwig, K.; Lombardo, S. Adsorption and Diffusion Behavior of Ethane and Ethylene in Sol-Gel Derived Microporous Silica. *Adsorption* **2005**, *11*, 491–499.
- (7) Khan, A.; Riaz, M.; Butt, S. B.; Zaidi, J. H. Novel Modified Alumina: Synthesis, Characterization and Application for Separation of Hydrocarbons. *Sep. Purif. Technol.* **2007**, *55*, 396–399.
- (8) van Miltenburg, A.; Zhu, W.; Kapteijn, F.; Moulijn, J. A. Adsorptive Separation of Light Olefin/Paraffin Mixtures. *Chem. Eng. Res. Des.* **2006**, *84*, 350–354.
- (9) Xu, L.; Rungta, M.; Brayden, M. K.; Martinez, M. V.; Stears, B. A.; Barbay, G. A.; Koros, W. J. Olefins-Selective Asymmetric Carbon Molecular Sieve Hollow Fiber Membranes for Hybrid Membrane-Distillation Processes for Olefin/Paraffin Separations. *J. Membr. Sci.* **2012**, *423–424*, 314–323.
- (10) Gucuyener, C.; van den Bergh, J.; Gascon, J.; Kapteijn, F. Ethane/Ethene Separation Turned on Its Head: Selective Ethane Adsorption on the Metal-Organic Framework ZIF-7 through a Gate-Opening Mechanism. *J. Am. Chem. Soc.* **2010**, *132*, 17704–17706.
- (11) Ravanchi, M. T.; Kaghazchi, T.; Kargari, A. Application of Membrane Separation Processes in Petrochemical Industry: A Review. *Desalination* **2009**, *235*, 199–244.
- (12) Kanezashi, M.; Kawano, M.; Yoshioka, T.; Tsuru, T. Organic–Inorganic Hybrid Silica Membranes with Controlled Silica Network Size for Propylene/Propane Separation. *Ind. Eng. Chem. Res.* **2011**, *51*, 944–953.
- (13) Chen, L.; Liu, X. Q.  $\pi$ -Complexation Mesoporous Adsorbents Cu-MCM-48 for Ethylene–Ethane Separation. *Chinese J. Chem. Eng.* **2008**, *16*, 570–574.
- (14) Kim, J.; Kang, S. W.; Mun, S. H.; Kang, Y. S. Facile Synthesis of Copper Nanoparticles by Ionic Liquids and Its Application to Facilitated Olefin Transport Membranes. *Ind. Eng. Chem. Res.* **2009**, *48*, 7437–7441.
- (15) Azhin, M.; Kaghazchi, T.; Rahmani, M. A Review on Olefin/Paraffin Separation Using Reversible Chemical Complexation Technology. *J. Ind. Eng. Chem.* **2008**, *14*, 622–638.
- (16) Costa Gomes, M. F.; Husson, P. Ionic Liquids: Promising Media for Gas Separations, Ionic Liquids: From Knowledge to Application; *ACS Symposium Series*; American Chemical Society: Washington DC, **2009**, *1030*, 223–237.
- (17) Gan, Q.; Zou, Y.; Rooney, D.; Nancarrow, P.; Thompson, J.; Liang, L.; Lewis, M. Theoretical and Experimental Correlations of Gas Dissolution, Diffusion, and Thermodynamic Properties in Determination of Gas Permeability and Selectivity in Supported Ionic Liquid Membranes. *Adv. Colloid Interfac.* **2011**, *164*, 45–55.
- (18) Malik, M. A.; Hashima, M. A.; Nabi, F. Ionic Liquids in Supported Liquid Membrane Technology. *Chem. Eng. J.* **2011**, *171*, 242–254.
- (19) Jung, S.; Palgunadi, J.; Kim, J. H.; Lee, H.; Ahn, B. S.; Cheong, M.; Kim, H. S. Highly Efficient Metal-Free Membranes for the Separation of Acetylene/Olefin Mixtures: Pyrrolidinium-Based Ionic Liquids as Acetylene Transport Carriers. *J. Membr. Sci.* **2010**, *354*, 63–67.
- (20) Costa Gomes, M. F.; Padua, A. A. H. Gas–Liquid Interactions in Solution. *Pure Appl. Chem.* **2005**, *77*, 653–665.
- (21) Campbell, P. S.; Santini, C. C.; Bouchu, D.; Fenet, B.; Philippot, K.; Chaudret, B.; Padua, A. A. H.; Chauvin, Y. A Novel Stabilisation Model for Ruthenium Nanoparticles in Imidazolium Ionic Liquids: In Situ Spectroscopic and Labelling Evidence. *Phys. Chem. Chem. Phys.* **2010**, *12*, 4217–4223.
- (22) Gutel, T.; Santini, C. S.; Philippot, K.; Padua, A.; Pelzer, K.; Chaudret, B.; Chauvin, Y.; Basset, J. Organized 3D-Alkyl Imidazolium

Ionic Liquids Could be Used to Control the Size of in Situ Generated Ruthenium Nanoparticles? *J. Mat. Chem.* **2009**, *19*, 3624–3631.

(23) Stracke, M. P.; Ebeling, G.; Cataluna, R.; Dupont, J. Hydrogen-Storage Materials Based on Imidazolium Ionic Liquids. *Energy Fuels* **2007**, *21*, 1695–1698.

(24) Almantariotis, D.; Gefflaut, T.; Padua, A. A. H.; Coxam, J. Y.; Costa Gomes, M. F. Effect of Fluorination and Size of the Alkyl Side-Chain on the Solubility of Carbon Dioxide in 1-Alkyl-3-methylimidazolium Bis(trifluoromethylsulfonyl)amide Ionic Liquids. *J. Phys. Chem. B* **2010**, *114*, 3608–3617.

(25) Hong, G.; Jacquemin, J.; Deetlefs, M.; Hardacre, C.; Husson, P.; Costa Gomes, M. F. Correlations for Describing Gas-to-Ionic Liquid Partitioning at 323 K Based on Ion-Specific Equation Coefficient and Group Contribution Versions of the Abraham Model. *Fluid Phase Equilib.* **2007**, *257*, 27–34.

(26) Jacquemin, J.; Costa Gomes, M. F.; Husson, P.; Majer, V. Solubility of Carbon Dioxide, Ethane, Methane, Oxygen, Nitrogen, Hydrogen, Argon, and Carbon Monoxide in 1-Butyl-3-Methylimidazolium Tetrafluoroborate Between Temperatures 283 and 343 K and at Pressures Close to Atmospheric. *J. Chem. Thermodyn.* **2006**, *38*, 490–502.

(27) Costa Gomes, M. F.; Pison, L.; Pensado, A. S.; Padua, A. A. H. Using Ethane and Butane as Probes to the Molecular Structure of 1-Alkyl-3-Methylimidazolium Bis(trifluoromethylsulfonyl)imide Ionic Liquids. *Faraday Discuss.* **2012**, *154*, 41–52.

(28) Smith, W. F.; Todorov, T. R. *The DL POLY Molecular Simulation Package*, 2.20; STFC Daresbury Laboratories: Warrington, UK, 2007.

(29) Jorgensen, W. L.; Maxwell, D. S.; Tirado-Rives, J. Development and Testing of the OPLS All-Atom Force Field on Conformational Energetics and Properties of Organic Liquids. *J. Am. Chem. Soc.* **1996**, *118*, 11225–11236.

(30) (a) Chipot, C.; Jaffe, R.; Maignet, B.; Pearlman, D. A.; Kollman, P. A. Benzene Dimer: A Good Model for  $\pi$ - $\pi$  Interactions in Proteins? A Comparison Between the Benzene and the Toluene Dimers in the Gas Phase and in an Aqueous Solution. *J. Am. Chem. Soc.* **1996**, *118*, 11217–11224. (b) Udier-Blagović, M.; Morales De Tirado, P.; Pearlman, S. A.; Jorgensen, W. L. Accuracy of Free Energies of Hydration Using CM1 and CM3 Atomic Charges. *J. Comput. Chem.* **2004**, *25*, 1322–1332.

(31) Canongia Lopes, J. N.; Padua, A. A. H. *J. Phys. Chem. B* **2004**, *108*, 16893–16898.

(32) Canongia Lopes, J. N.; Deschamps, J.; Padua, A. A. H. Molecular Force Field for Ionic Liquids Composed of Triflate or Bistriflylimide Anions. *J. Phys. Chem. B* **2004**, *108*, 2038–2047.

(33) Kaminski, G.; Jorgensen, W. L. Performance of the AMBER94, MMFF94, and OPLS-AA Force Fields for Modeling Organic Liquids. *J. Phys. Chem.* **1996**, *100*, 18010–18013.

(34) Fandiño, O.; Pensado, A. S.; Lugo, L.; Comuñas, M. J. P.; Fernandez, J. Compressed Liquid Densities of Squalane and Pentaerythritol Tetra(2-ethylhexanoate). *J. Chem. Eng. Data* **2005**, *50*, 939–946.

(35) Mahurin, S. M.; Dai, T.; Yeary, J. S.; Luo, H.; Dai, S. Benzyl-Functionalized Room Temperature Ionic Liquids for CO<sub>2</sub>/N<sub>2</sub> Separation. *Ind. Eng. Chem. Res.* **2011**, *50*, 14061–14069.

(36) Mandai, T.; Matsumura, A.; Imanari, M.; Nishikawa, K. Effects of Cyclic-Hydrocarbon Substituents and Linker Length on Physicochemical Properties and Reorientational Dynamics of Imidazolium-Based Ionic Liquids. *J. Phys. Chem. B* **2012**, *116*, 2090–2095.

(37) Orita, A.; Kamijima, K.; Yoshida, M. Allyl-Functionalized Ionic Liquids as Electrolytes for Electric Double-Layer Capacitors. *J. Power Sources* **2010**, *195*, 7471–7479.

(38) Jacquemin, J.; Husson, P.; Padua, A. A. H.; Majer, V. Density and Viscosity of Several Pure and Water-Saturated Ionic Liquids. *Green Chem.* **2006**, *8*, 172–180.

(39) Tokuda, H.; Tsuzuki, S.; Susan, A. B. H., Md.; Hayamizu, K.; Watanabe, M. How Ionic Are Room-Temperature Ionic Liquids? An Indicator of the Physicochemical Properties. *J. Phys. Chem. B* **2006**, *110*, 19593–19600.

(40) Dymond, J. H.; Marsh, K. N.; Wilhoit, R. C.; Wong, K. C. *The Virial Coefficients of Pure Gases and Mixtures, Landolt-Börnstein: Numerical Data and Functional Relationships in Science and Technology New Series, Subseries Physical Chemistry*; Springer: New York, 2003; 21B.

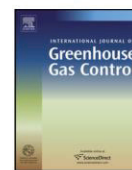
(41) Jacquemin, J.; Husson, P.; Majer, V.; Padua, A. A. H.; Costa Gomes, M. F. Thermophysical Properties, Low Pressure Solubilities and Thermodynamics of Solvation of Carbon Dioxide and Hydrogen in Two Ionic Liquids Based on the Alkylsulfate Anion. *Green Chem.* **2008**, *10*, 944–950.

(42) Almantariotis, D.; Fandino, O.; Coxam, J. Y.; Costa Gomes, M. F. Direct Measurement of the Heat of Solution and Solubility of Carbon Dioxide in 1-Hexyl-3-Methylimidazolium Bis(trifluoromethylsulfonyl)amide and 1-Octyl-3-Methylimidazolium Bis(trifluoromethylsulfonyl)amide. *Int. J. Greenhouse Gas Control* **2012**, *10*, 329–340.

(43) Anderson, J. L.; Dixon, J. K.; Brennecke, J. F. Solubility of CO<sub>2</sub>, CH<sub>4</sub>, C<sub>2</sub>H<sub>6</sub>, C<sub>2</sub>H<sub>4</sub>, O<sub>2</sub>, and N<sub>2</sub> in 1-Hexyl-3-Methylpyridinium Bis(trifluoromethylsulfonyl)imide: Comparison to Other Ionic Liquids. *Acc. Chem. Res.* **2007**, *40*, 1208–1216.

(44) Camper, D.; Becker, C.; Koval, C.; Noble, R. Low Pressure Hydrocarbon Solubility in Room Temperature Ionic Liquids Containing Imidazolium Rings Interpreted Using Regular Solution Theory. *Ind. Eng. Chem. Res.* **2005**, *44*, 1928–1933.

(45) Chirico, R. D.; Diky, V.; Magee, J. W.; Frenkel, M.; Marsh, K. N. Thermodynamic and Thermophysical Properties of the Reference Ionic Liquid: 1-Hexyl-3-Methylimidazolium Bis(trifluoromethylsulfonyl)imide (Including Mixtures). Part 2. Critical Evaluation and Recommended Property Values. *Pure Appl. Chem.* **2009**, *81*, 791–828.



## Absorption of carbon dioxide by ionic liquids with carboxylate anions



S. Stevanovic<sup>a,b</sup>, A. Podgorsek<sup>a</sup>, L. Moura<sup>a,b,c</sup>, C.C. Santini<sup>c</sup>, A.A.H. Padua<sup>a,b</sup>,  
M.F. Costa Gomes<sup>a,b,\*</sup>

<sup>a</sup> Institut de Chimie de Clermont-Ferrand, Equipe Thermodynamique et Interactions Moléculaires, Clermont Université, Université Blaise Pascal, BP 80026, 63171 Aubière, France

<sup>b</sup> CNRS, UMR 6296 ICCF, BP 80026, 63171 Aubière, France

<sup>c</sup> Université de Lyon, Institut de Chimie de Lyon, UMR 5265 CNRS-Université de Lyon 1-ESPE Lyon, C2P2, Equipe Chimie Organométallique de Surface, ESCPE 43 Boulevard du 11 Novembre 1918, 69616 Villeurbanne, France

### ARTICLE INFO

#### Article history:

Received 7 November 2012

Received in revised form 22 March 2013

Accepted 9 April 2013

#### Keywords:

Absorption

Carbon dioxide

Carboxylate ionic liquids

Water

Molecular simulations

Solubility mechanism

### ABSTRACT

Experimental values of the absorption of carbon dioxide in two ionic liquids with carboxylate anions – the 1-butyl-3-methylimidazolium levulinate [ $C_1C_4Im][LEV]$ ] and the 1-butyl-1-methylpyrrolidinium acetate [ $C_1C_4Pyrro][OAc]$ ] – are reported as a function of temperature and at pressures close to atmospheric. Mole fraction absorption of carbon dioxide in [ $C_1C_4Im][LEV]$ ] and [ $C_1C_4Pyrro][OAc]$ ] is equal to  $0.93 \times 10^{-2}$  and  $1.10 \times 10^{-2}$  at 303.15 K and 89.2 kPa and 353.15 K and 67.1 kPa, respectively. The effect of the presence of controlled amounts of water on the absorption of carbon dioxide was measured for [ $C_1C_4Pyrro][OAc]$ . The presence of a 0.35 mole fraction of water in [ $C_1C_4Pyrro][OAc]$ ] decreases the viscosity of the ionic liquid phase and dramatically increases the amount of carbon dioxide absorbed, pointing toward a chemical reaction between the gas and the liquid absorbent. Increasing the amounts of water lowers the viscosity further but also the absorption capacity of the ionic liquid. Molecular dynamics simulations were used to interpret the molecular mechanism of solvation of carbon dioxide in [ $C_1C_4Pyrro][OAc]$ . Results show that carbon dioxide is solvated preferentially in the non-polar domain of the solvent, and that the  $CO_2$ -anion interactions dominate over the  $CO_2$ -cation interactions. Molecular simulations could reproduce the experimental solubility of  $CO_2$  in [ $C_1C_4Im][TFA]$ ] (known to be a physical process), but not in [ $C_1C_4Pyrro][OAc]$ ] and reinforcing the conclusion that the higher solubility of carbon dioxide in the acetate based ionic liquid can be ascribed to a chemical reaction.

© 2013 Elsevier Ltd. All rights reserved.

### 1. Introduction

Ionic liquids are considered as promising media for gas separations (Costa Gomes and Husson, 2010) as they are able to selectively and efficiently absorb one gas in a mixture. In particular, they have been indicated as possible alternatives for carbon dioxide removal from flue-gas streams (Ramdin et al., 2012) by chemical (Bates et al., 2002) or physical absorption (Shiflett et al., 2010). Several properties are significant for the evaluation of ionic liquids as liquid absorbers for gaseous solutes – the absorption capacity, the selectivity and the mass transfer – as they will determine the design and cost of possible industrial processes (Henley et al., 2011).

We are interested in exploring the use of ionic liquids having carboxylate anions for the absorption of carbon dioxide, as they seem

to be capable of chemically coordinating this gas hence showing a high absorption capacity (Maginn, 2005; Shiflett et al., 2008). This chemical reaction, evidenced by several authors for acetate based ionic liquids (Stevanovic et al., 2012; Gurau et al., 2011; Besnard et al., 2012), seems to be reversible and so it is possible to recycle the absorbent at a relatively low energy cost. Nevertheless, ionic liquids based on the acetate anions and on the imidazolium cations have shown some drawbacks linked to the possibility of proton transfer between the anion and the cation (due to the acidity of the hydrogen in the position  $C_2$  of the imidazolium ring). Although the equilibrium constant of this reaction seems relatively unimportant, submitting the ionic liquid to repeated pressure cycles displaces the equilibrium in the sense of the formation of acetic acid, a volatile product. This means that these ionic liquids can, to some extent, be considered as protic ionic liquids (Greaves and Brummond, 2008) and so they are in reality a liquid mixture of different molecular compounds and ions, the composition of the mixture depending on the conditions at which it has been kept.

In this work, we have studied the absorption of carbon dioxide by two ionic liquids having carboxylate anions. Firstly, we have considered the 1-butyl-1-methylpyrrolidinium acetate

\* Corresponding author at: Institut de Chimie de Clermont-Ferrand, Equipe Thermodynamique et Interactions Moléculaires, UMR 6296 CNRS/Université Blaise Pascal, BP 80026, 63171 Aubière, France. Tel.: +33 4 73 40 72 05; fax: +33 4 73 40 71 85.

E-mail address: [margarida.c.gomes@univ-bpclermont.fr](mailto:margarida.c.gomes@univ-bpclermont.fr) (M.F. Costa Gomes).

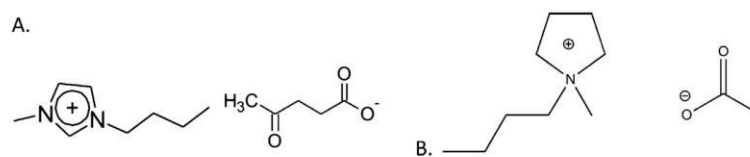


Fig. 1. Ionic liquids used in this work. (A) 1-butyl-3-methylimidazolium levulinate [ $C_1C_4Im][LEV]$ ] and (B) 1-butyl-1-methylpyrrolidinium acetate [ $C_1C_4Pyrro][OAc]$ ].

[ $C_1C_4Pyrro][OAc]$ , an ionic liquid based on the acetate anion but having no acidic proton in the cation. Due to its low fluidity we have studied the absorption capacity of the mixtures of this ionic liquid with water. Secondly, we have studied an ionic liquid with a heavier carboxylic anion, the 1-butyl-3-methylimidazolium levulinate [ $C_1C_4Im][LEV]$ ], in order to check if the absorption mechanism was the same as in the case of the acetate-based imidazolium ionic liquids. We predict a considerable advantage on the use of this ionic liquid linked to the fact that, if the cation–anion proton transfer occurs, a molecular species of low volatility is formed (as levulinic acid is much less volatile than acetic acid).

In order to contribute to the understanding of the mechanisms of solvation of carbon dioxide in this family of ionic liquids, the absorption of carbon dioxide in [ $C_1C_4Pyrro][OAc]$ ] was compared with the solvation of  $CO_2$  by 1-butyl-3-methylimidazolium trifluoroacetate [ $C_1C_4Im][TFA]$ ]. In this last ionic liquid, the absorption of carbon dioxide is purely physical and so linked to the gas–liquid molecular interactions and to the molecular structure of the solution.

Absorption of carbon dioxide by [ $C_1C_4Im][LEV]$ ] was first studied by Yokozeki et al. (2008) and the value of absorption was found to be equal to 0.245 at 298.1 K and at 100.2 kPa, when expressed in mole fraction of gas. Absorption of gas in [ $C_1C_4Pyrro][OAc]$ ] was not yet reported but a cation–anion proton transfer has been suggested (transfer of a proton from the butyl chain of the cation to the anion) with the release of acetic acid, methyl pyrrolidine and butane (Yoshizawa-Fujita et al., 2006). It seems then that the low acidity of the protons in the alkyl side-chain in the pyrrolidinium cation is sufficient to cause a cation–anion proton transfer.

Values of absorption of carbon dioxide in [ $C_1C_4Im][TFA]$ ] are available in the literature and were found to be significantly lower than in ionic liquids based on the acetate anion and an imidazolium cation (Shiflett et al., 2009; Carvalho et al., 2009; Cabaco et al., 2011). Many explanations have been proposed to interpret this difference in solubility mainly based on the stronger  $CO_2-OAc^-$  interaction than  $CO_2-TFA^-$  which can be attributed to the lower electron density, and therefore lower donor ability, of the trifluoroacetate anion when compared with the acetate anion. The exact mechanism of carbon dioxide absorption by these ionic liquids is, nevertheless, still not well understood.

We investigate the absorption of carbon dioxide and its solubility in [ $C_1C_4Pyrro][OAc]$ ] and the [ $C_1C_4Im][TFA]$ ] by molecular dynamic simulations. The comparison of the molecular structures and interactions of the solutions of carbon dioxide in the two ionic liquids ([ $C_1C_4Im][TFA]$ ] and [ $C_1C_4Pyrro][OAc]$ ]) is expected to clarify the molecular mechanism of the  $CO_2$  absorption.  $^1H$  and  $^{13}C$  NMR spectroscopy provided further experimental evidence for the solvation mechanism proposed.

## 2. Materials

The [ $C_1C_4Pyrro][OAc]$ ] was purchased from Solvionic with mole fraction purities of 0.995. The [ $C_1C_4Im][LEV]$ ] samples were synthesized at the laboratory of Chemistry, Catalysis, Polymers and Processes of Lyon.

During the synthesis of 1-butyl-3-methylimidazolium levulinate, [ $C_1C_4Im][LEV]$ ], all the operations were performed in the absence of oxygen and of water and under a purified argon atmosphere using glove box (Jacomex or MBraun) or vacuum-line techniques. 1-Methylimidazole (>99%, Aldrich) was distilled prior to use. Chlorobutane (>99%, Aldrich) was used without further purification. Sodium levulinate was previously synthesized at the laboratory LMOPS, Lyon, France and was used without further purification.

For the synthesis of the 1-butyl-3-methylimidazolium chloride, [ $C_1C_4Im][Cl]$ ], the first operation consisted on the slowly addition of 1-chlorobutane (106 mL, 1.01 mol) to 1-methylimidazole (50 mL, 0.63 mol) under strong stirring. The mixture was left stirring for 2 days at 343.15 K. The hot solution was then transferred drop wise via a cannula into dry toluene (200 mL) at 273.15 K under vigorous mechanical stirring. The white precipitate formed was then filtered and washed repeatedly with dry toluene ( $3 \times 200$  mL) and dried overnight under vacuum giving a white solid (95.6 g, 0.55 mol, 87%) (Magna et al., 2003).

To obtain the final product, 1-butyl-3-methylimidazolium levulinate, [ $C_1C_4Im][LEV]$ ], sodium levulinate (32.9 g, 0.24 mol) was dissolved in water (60 mL). 1-Butyl-3-methylimidazolium chloride, [ $C_1C_4Im][Cl]$ ] (34.4 g, 0.20 mol), was dissolved in dichloromethane (170 mL). The aqueous phase was added drop wise to the organic phase under strong stirring, at 303.15 K. The mixture was left stirring during 60–70 h at 303.15 K. After separating the two phases and drying the aqueous one, a dark viscous fluid was obtained (4.2 g, 0.08 mol, 41%).

The water contents of the degassed sample were determined, with a precision of  $\pm 5$  ppm, using a coulometric Karl Fisher titrator (Mettler Toledo DL31). The ionic liquids were kept under vacuum for 72 h at 303 K before each measurement. The water content of the degassed samples was found to be 365 ppm for [ $C_1C_4Im][LEV]$ ].

The temperature of decomposition of the ionic liquids used herein (represented in Fig. 1) was determined using a modulated DSC 2920 from TA Instruments and was found to be 448 K for [ $C_1C_4Im][LEV]$ ] and 518 K for [ $C_1C_4Pyrro][OAc]$ ], respectively. The temperature of fusion for [ $C_1C_4Pyrro][OAc]$ ], an ionic liquid which is solid at room temperature, was found to be 353 K.

Mixtures of [ $C_1C_4Pyrro][OAc]$ ] and water of different compositions were prepared gravimetrically. The [ $C_1C_4Pyrro][OAc]$ ] was first introduced in a glass vial and then the appropriate amount of water was added and the glass vial was sealed. The vial was completely filled with the liquid mixture in order to minimize the volume of the vapor phase in equilibrium with the liquid solution and so reduce the error in composition due to differential evaporation. The uncertainty of the mole fraction is estimated at  $\pm 0.0001$ . The molar fraction of water in the prepared mixtures was 0.35–0.85.

The gases used for this study were used as received from the manufacturer. Carbon dioxide was obtained from AGA/Linde Gas with mole fraction purity of 0.99995.

## 3. Density measurements

Densities were measured using a U-shape vibrating-tube densimeter (Anton Paar, model DMA 512) operating in a static

mode, following the procedure described in previous publications (Jacquemin et al., 2006a, 2007). Measurements for [C<sub>1</sub>C<sub>4</sub>Im][LEV] and [C<sub>1</sub>C<sub>4</sub>Pyrrro][OAc] + water were performed for pressures up to 25 MPa and at temperatures from 293 to 343 K.

The temperature in the densimeter was maintained constant to within ±0.01 K by means of a recirculating bath equipped with a PID temperature controller (Julabo FP40-HP). For measuring the temperature, a 100 Ω platinum resistance thermometer (precision of ±0.02 K and accuracy of ±0.04 K) was used. Its calibration was performed by verifying a water triple point (triple point cell by Hart Scientific) and by comparison against a 100 Ω platinum resistance Hart Scientific model 1502A.

The measured period of vibration ( $\tau$ ) of a U tube is related to the density ( $\rho$ ) according to:  $\rho = A\tau^2 + B$  where  $A$  and  $B$  are parameters that are function of temperature and pressure determined by calibration between temperatures of 293 and 343 K (and pressures of 0.1 and 25 MPa), using as calibration fluids *n*-heptane, bromobenzene and 2,4-dichlorotoluene following the recommendations by Schilling et al. (Schilling et al., 2008). Density measurements were performed in steps of 10 K. The uncertainty of the density measurements is estimated as  $10^{-4} \text{ g cm}^{-3}$ .

The density of the pure [C<sub>1</sub>C<sub>4</sub>Pyrrro][OAc] was calculated using a group contribution model developed by Jacquemin et al. (Jacquemin et al., 2008a,b).

#### 4. Viscosity measurements

The dynamic viscosities of the two systems, [C<sub>1</sub>C<sub>4</sub>Im][LEV] previously dried under vacuum and [C<sub>1</sub>C<sub>4</sub>Pyrrro][OAc] + water were measured using an Anton Paar AMVn rolling ball viscometer, as a function of the temperature from 293.15 K to 363.15 K (controlled to within 0.01 K and measured with an accuracy better than 0.05 K) and at atmospheric pressure. Before starting the measurements, the 3 mm diameter capillary tube was calibrated as a function of temperature and angle of measurement using standard viscosity oil from Cannon (N35). The overall uncertainty in the viscosity is estimated as ±1.5%.

#### 5. Gas-absorption measurements

The experimental method used for the gas absorption measurements in pure ionic liquids is based on an isochoric saturation technique and has been described in previous publications (Jacquemin et al., 2006b,c). In this technique, a known quantity of gaseous solute is put in contact with a precisely determined quantity of degassed solvent at a constant temperature inside an accurately known volume. When thermodynamic equilibrium is attained, the pressure above the liquid solution is constant and is directly related to the absorption of the gas in the liquid.

The quantity of ionic liquid introduced in the equilibration cell is determined gravimetrically. This quantity is equal to the amount of solvent present in the liquid solution,  $n_1^{\text{liq}}$ , as the ionic liquid does not present a measurable vapour pressure. The amount of solute present in the liquid solution,  $n_2^{\text{liq}}$  (subscripts 1 and 2 stand for solvent and solute, respectively), is calculated by the difference between two, pressure, volume, temperature,  $pVT$ , measurements: first when the gas is introduced in a calibrated bulb with volume  $V_{\text{GB}}$  and second after thermodynamic equilibrium is reached:

$$n_2^{\text{liq}} = \frac{p_{\text{ini}}V_{\text{GB}}}{[Z_2(p_{\text{ini}}, T_{\text{ini}})RT_{\text{ini}}]} - \frac{p_{\text{eq}}(V_{\text{tot}} - V_{\text{liq}})}{[Z_2(p_{\text{eq}}, T_{\text{eq}})RT_{\text{eq}}]} \quad (1)$$

where  $p_{\text{ini}}$  and  $T_{\text{ini}}$  are the pressure and temperature in the first  $pVT$  determination, respectively and  $p_{\text{eq}}$  and  $T_{\text{eq}}$  are the pressure and temperature at the equilibrium, respectively.  $V_{\text{tot}}$  is the total volume of the equilibration cell,  $V_{\text{liq}}$  is the volume of the liquid

solution and  $Z_2$  is the compression factor for the pure gas. The solubility can then be expressed in mole fraction, which is calculated from the following equation:

$$x_2 = \frac{n_2^{\text{liq}}}{n_1^{\text{liq}} + n_2^{\text{liq}}} \quad (2)$$

where  $n_2^{\text{liq}}$  is the amount of solute dissolved in the ionic liquid and  $n_1^{\text{liq}} = n_1^{\text{tot}}$  is the total amount of ionic liquid. We consider that the volume of the ionic liquid does not change when the gas is solubilized and so the volume of the liquid solution is equal to the molar volume of the pure ionic liquid.

A second experimental method is used for the gas absorption measurements in the mixtures ionic liquid + water. This one is also based on an isochoric saturation technique and has been described in previous publications (Hong et al., 2006; Husson et al., 2010).

In this technique a known quantity of gaseous solute is put into contact with a precisely determined quantity of degassed solvent at constant temperature inside an accurately known volume. As previously, when thermodynamic equilibrium is attained the pressure above the liquid solution is constant and directly related to the solubility of the gas in the liquid.

The gas absorption can be expressed as mole fraction of the gas in the liquid mixture,  $x_2$  calculated through:

$$x_2 = \frac{n_2^{\text{liq}}}{n_{\text{solv}}^{\text{liq}} + n_2^{\text{liq}}} \quad (3)$$

where  $n_{\text{solv}}^{\text{liq}} = n_1^{\text{liq}} + n_3^{\text{liq}}$  is the amount of solvent in the liquid phase with  $n_1^{\text{liq}}$  being the amount of ionic liquid which due to its negligible vapour pressure is equal to the total quantity of ionic liquid introduced in the equilibrium cell and  $n_3^{\text{liq}}$  the amount of water in the liquid solution.

#### 6. Molecular simulations

The microscopic structures and interactions in the mixtures of ionic liquids ([C<sub>1</sub>C<sub>4</sub>Im][TFA] and [C<sub>1</sub>C<sub>4</sub>Pyrrro][OAc]) and carbon dioxide were investigated by molecular dynamics simulations. Ionic liquids were represented by an all-atom force field, which is based on the AMBER/OPLS-AA framework (Smith and Todorov, 2007; Jorgensen et al., 1996). For imidazolium cation force field parameters were developed specifically (Canongia Lopes et al., 2004), meanwhile for the pyrrolidinium cation they were retrieved from the force field for amines (Rizzo and Jorgensen, 1999). Acetate (Jorgensen et al., 1996; Yu et al., 2004) and trifluoroacetate (Liu et al., 2006) were represented with the potential models existing in the literature, whereas the potential model of Harris and Yung (Mallet et al., 2008) was used for carbon dioxide.

The ionic liquids [C<sub>1</sub>C<sub>4</sub>Im][TFA] and [C<sub>1</sub>C<sub>4</sub>Pyrrro][OAc] were simulated in periodic cubic boxes containing 127 ion pairs, using the molecular dynamics method implemented in the DL-POLY package (Smith and Todorov, 2007). Initial low-density configurations, with ions placed at random in periodic cubic boxes, were equilibrated to attain liquid-like densities and structures at 373 K and 1 bar. Temperature and pressure were maintained using a Nosé–Hoover thermostat and barostat, respectively. Once the equilibrium density attained, simulations runs of 1 ns were performed, with an explicit cutoff distance of 16 Å for non-bonded interactions, from which 5000 configurations were stored. Structural quantities such as radial and spatial distribution functions were calculated from configurations generated during the production runs. Additionally, simulation boxes containing 200 ion pairs and 12 carbon dioxide molecules were prepared in the same manner, to calculate solute–solvent radial distribution functions between the gas and

the ionic liquid and the cation–anion interaction energy in the presence of carbon dioxide.

The chemical potentials of carbon dioxide at 373 K in the two ionic liquids were calculated in a two-step procedure, as already described by Almantariotis et al. (2010). First, for carbon dioxide, a reduced-size version of the molecule was made by subtracting 0.8 Å from the C–O bond length and also from the Lennard–Jones diameters  $\sigma_O$  and  $\sigma_C$ . The resulting molecule is small enough so that its chemical potential can be calculated using the Widom test-particle insertion method with efficient statistics (100,000 insertions into each of 5000 stored configurations of pure ionic liquids). Second, a stepwise finite difference thermodynamic integration procedure was followed to calculate the free-energy difference between the initial, reduced versions of the carbon dioxide molecule and the final full-size model. The free energy calculation was performed on six intermediate steps along a linear path connecting the intermolecular parameters (bonds and diameters) of the reduced-size to those of the full-size molecule. This relatively modest number of intermediate steps is adequate because the starting point of the thermodynamic integration route is not too far from the final state. In the finite-difference thermodynamic integration scheme, derivatives (finite differences) of the total energy of the system with respect to the activation parameter were evaluated by a free-energy perturbation expression in the  $NpT$  ensemble using a three-point formula with increments of  $2 \times 10^{-3}$ .

## 7. NMR measurements

$^1\text{H}$  and  $^{13}\text{C}$  NMR data were collected at 298.15 K or 313.15 K on a Bruker AC 400 MHz spectrometer. Spectra of  $[\text{C}_1\text{C}_4\text{Im}][\text{LEV}]$  and  $[\text{C}_1\text{C}_4\text{Pyrro}][\text{OAc}]$  samples were recorded in solution using acetone- $d_6$  and  $\text{CDCl}_3$  as solvents, respectively. A coaxial capillary tube loaded with  $\text{DMSO-}d_6$  was inserted into the 5 mm NMR tube filled with the  $[\text{C}_1\text{C}_4\text{Pyrro}][\text{OAc}]$ +water sample to avoid any contact between the deuterated solvent and the analyzed mixture. The deuterium in  $\text{DMSO-}d_6$  was used for the external lock of the NMR magnetic field and the residual proton in  $\text{DMSO-}d_6$  was used as the  $^1\text{H}$  NMR external reference at 2.5 ppm.

## 8. Results and discussion

The experimental values obtained for the density of  $[\text{C}_1\text{C}_4\text{Im}][\text{LEV}]$  and  $[\text{C}_1\text{C}_4\text{Pyrro}][\text{OAc}]$ +water as a function of pressure and at temperatures from 293 to 353 K are reported in Table S2 of Supplementary information. The values of density at atmospheric pressure (necessary for the calculation of the gas solubility) were adjusted to linear functions of temperature:

$$\rho_{[\text{C}_1\text{C}_4\text{Im}][\text{LEV}]} (\text{kg m}^{-3}) = 1281.7 - 0.6112 (T/\text{K}) \quad (4)$$

$$\rho_{[\text{C}_1\text{C}_4\text{Pyrro}][\text{OAc}]+\text{H}_2\text{O}(x=0.4)} (\text{kg m}^{-3}) = 1186.3 - 0.5669 (T/\text{K}) \quad (5)$$

$$\rho_{[\text{C}_1\text{C}_4\text{Pyrro}][\text{OAc}]+\text{H}_2\text{O}(x=0.6)} (\text{kg m}^{-3}) = 1198.7 - 0.5858 (T/\text{K}) \quad (6)$$

$$\rho_{[\text{C}_1\text{C}_4\text{Pyrro}][\text{OAc}]+\text{H}_2\text{O}(x=0.8)} (\text{kg m}^{-3}) = 1233.0 - 0.6689 (T/\text{K}) \quad (7)$$

the standard deviation of the fits is always better than 0.1%. The density of  $[\text{C}_1\text{C}_4\text{Im}][\text{LEV}]$  was compared to both the acetate based ionic liquids with imidazolium cations studied in our previous work (Stevanovic et al., 2012) and was found to be lower than  $[\text{C}_1\text{C}_2\text{Im}][\text{OAc}]$  and higher than  $[\text{C}_1\text{C}_4\text{Im}][\text{OAc}]$ . Mixtures of  $[\text{C}_1\text{C}_4\text{Pyrro}][\text{OAc}]$ +water present, as expected, lower densities than mixtures of  $[\text{C}_1\text{C}_2\text{Im}][\text{OAc}]$ +water or  $[\text{C}_1\text{C}_4\text{Im}][\text{OAc}]$ +water (Stevanovic et al., 2012) for an equivalent mole fraction of water. The density increases when the quantity of water increases as it was observed previously for the systems  $[\text{C}_1\text{C}_2\text{Im}][\text{OAc}]$ +water and

$[\text{C}_1\text{C}_4\text{Im}][\text{OAc}]$ +water. The densities measured herein as a function of pressure were correlated using the Tait equation:

$$\rho(T, P) = \left[ \frac{\rho^0(T, p^0)}{1 - C \ln((B(T) + p)/(B(T) + p^0))} \right] \quad (8)$$

where  $\rho^0(T, p^0)$  is the density value at a reference temperature  $T$  and at the pressure  $p^0 = 0.1$  MPa;  $C$  is an adjustable parameter and  $B(T)$  a polynomial defined by:

$$B(T) = \sum_{i=0}^2 B_i(T)^i \quad (9)$$

The parameters found for the present data are listed in Table 1.

The dynamic viscosity was measured for the systems  $[\text{C}_1\text{C}_4\text{Im}][\text{LEV}]$  and  $[\text{C}_1\text{C}_4\text{Pyrro}][\text{OAc}]$ +water, and is listed in Table 2 as a function of temperature from 293 to 373 K. The Vogel–Fulcher–Tamman (VFT) equation was used to correlate the experimental viscosities as a function of temperature:

$$\eta_{[\text{C}_1\text{C}_4\text{Im}][\text{LEV}]} (\text{mPa s}) = (2.07 \times 10^{-3}) (T/\text{K})^{1/2} \exp \left[ \frac{1197}{(T/\text{K}) - 190} \right] \quad (10)$$

$$\eta_{[\text{C}_1\text{C}_4\text{Pyrro}][\text{OAc}]+\text{H}_2\text{O}(x=0.4)} (\text{mPa s}) = (2.54 \times 10^{-3}) (T/\text{K})^{1/2} \times \exp \left[ \frac{985}{(T/\text{K}) - 183} \right] \quad (11)$$

$$\eta_{[\text{C}_1\text{C}_4\text{Pyrro}][\text{OAc}]+\text{H}_2\text{O}(x=0.6)} (\text{mPa s}) = (1.01 \times 10^{-3}) (T/\text{K})^{1/2} \times \exp \left[ \frac{1173}{(T/\text{K}) - 164} \right] \quad (12)$$

$$\eta_{[\text{C}_1\text{C}_4\text{Pyrro}][\text{OAc}]+\text{H}_2\text{O}(x=0.8)} (\text{mPa s}) = (1.97 \times 10^{-3}) (T/\text{K})^{1/2} \times \exp \left[ \frac{868}{(T/\text{K}) - 177} \right] \quad (13)$$

As expected, the viscosities of the ionic liquids depend both on the nature of the anion and the cation. Values of viscosity, at 303.15 K, of  $[\text{C}_1\text{C}_4\text{Im}][\text{LEV}]$  are equal to 1441 mPa s, so 3.6 and 13.7 times higher than values of  $[\text{C}_1\text{C}_4\text{Im}][\text{OAc}]$  and  $[\text{C}_1\text{C}_2\text{Im}][\text{OAc}]$ , respectively (Stevanovic et al., 2012). The system  $[\text{C}_1\text{C}_4\text{Pyrro}][\text{OAc}]$ +water (for a mole fraction of water equal to 0.4) presents a viscosity of 330.4 mPa s at 293.15 K, a value 1.1 and 3.7 times higher than those of  $[\text{C}_1\text{C}_4\text{Im}][\text{OAc}]$ +water and  $[\text{C}_1\text{C}_2\text{Im}][\text{OAc}]$ +water. The viscosity of the mixture  $[\text{C}_1\text{C}_4\text{Pyrro}][\text{OAc}]$ +water decreases with the addition of water, the viscosity, for a mole fraction of water equal to 0.8 being as low as 45.43 mPa s at 293 K, 2.1 and 7.3 times lower than for mole fractions of water equal to 0.6 and 0.4, respectively.

For both  $[\text{C}_1\text{C}_4\text{Im}][\text{LEV}]$ ,  $[\text{C}_1\text{C}_4\text{Pyrro}][\text{OAc}]$  and for the mixtures of  $[\text{C}_1\text{C}_4\text{Pyrro}][\text{OAc}]$ +water, multiple experimental data points on the absorption of carbon dioxide were obtained in the temperature interval between 303.15 K and 343.15 K in steps of approximately 10 K. The pure ionic liquid  $[\text{C}_1\text{C}_4\text{Pyrro}][\text{OAc}]$  was only studied at 353 K. For the  $[\text{C}_1\text{C}_4\text{Pyrro}][\text{OAc}]$ +water mixtures, measurements of the  $\text{CO}_2$  absorption were made at 303.15 and 313.15 K for mole fractions of water equal to 0.35, 0.6 and 0.85. The experimental values are reported in Table 3.

The absorption of carbon dioxide in pure  $[\text{C}_1\text{C}_4\text{Im}][\text{LEV}]$  is represented in Fig. 2 as a function of pressure for the different temperatures studied. The gas is absorbed up to a  $0.93 \times 10^{-2}$  mole fraction at 303.15 K and 67.1 kPa. Absorption of carbon dioxide in  $[\text{C}_1\text{C}_4\text{Im}][\text{LEV}]$  increases when the partial pressure of gas increases

**Table 1**

Tait parameters  $C$ ,  $B_0$ ,  $B_1$  and  $B_2$  used to smooth the experimental densities as a function of pressure (to 25 MPa) and temperature (from 293 to 353 K). AAD indicated the percent average absolute deviation of the fit.

Ionic liquid	$10^2 \times C$	$B_0$ (MPa)	$B_1$ (MPa K <sup>-1</sup> )	$10^3 \times B_2$ (MPa K <sup>-2</sup> )	AAD (%)
[C <sub>1</sub> C <sub>4</sub> Pyrrro][OAc] + water ( $x_{\text{water}} = 0.4077$ )	-2.137	+278.999	-2.339	+3.808	0.016
[C <sub>1</sub> C <sub>4</sub> Pyrrro][OAc] + water ( $x_{\text{water}} = 0.6028$ )	-1.527	-107.704	+0.136	+0.007	0.016
[C <sub>1</sub> C <sub>4</sub> Pyrrro][OAc] + water ( $x_{\text{water}} = 0.8027$ )	-2.005	-136.864	+0.230	-0.158	0.020

**Table 2**

Experimental dynamic viscosities,  $\eta$ , of the ionic liquids [C<sub>1</sub>C<sub>4</sub>Im][LEV] and [C<sub>1</sub>C<sub>4</sub>Pyrrro][OAc] + water mixtures as a function of temperature at atmospheric pressure.

$T$ (K)	$\eta^{\text{exp}}$ (mPa s)	$\delta$ (%)	$T$ (K)	$\eta^{\text{exp}}$ (mPa s)	$\delta$ (%)
<b>[C<sub>1</sub>C<sub>4</sub>Im][LEV]</b>			<b>[C<sub>1</sub>C<sub>4</sub>Pyrrro][OAc] + water (<math>x_{\text{water}} = 0.4077</math>)</b>		
303.15	1441	+0.0	293.15	330.4	+0.0
313.15	619.6	-0.2	303.15	160.12	-0.2
323.15	300.2	+0.7	313.15	86.23	+0.4
333.15	165.0	-0.9	323.15	51.09	+0.4
			333.15	32.67	-0.2
			343.15	22.10	-0.5
			353.15	15.73	-1.2
			363.15	11.52	-0.8
			373.15	8.644	+0.6
<b>[C<sub>1</sub>C<sub>4</sub>Pyrrro][OAc] + water (<math>x_{\text{water}} = 0.6028</math>)</b>			<b>[C<sub>1</sub>C<sub>4</sub>Pyrrro][OAc] + water (<math>x_{\text{water}} = 0.8027</math>)</b>		
293.15	152.7	+0.1	293.15	45.43	+0.0
303.15	81.31	-0.6	303.15	26.05	+0.2
313.15	45.97	+1.5	313.15	16.32	-0.2
323.15	29.13	-0.7	323.15	10.90	-0.3
333.15	18.89	+0.5	333.15	7.665	-0.2
343.15	13.23	-1.1			
353.15	9.512	-1.3			

and when the temperature decreases. It is observed in Fig. 2 that the carbon dioxide absorption progress linearly with the pressure for all temperatures studied, indicating that Henry's law is verified and that carbon dioxide is only physically dissolved in that case. Compared to the imidazolium acetate ionic liquids studied previously by our research group (Stevanovic et al., 2012), which are able to both chemically and physically absorb carbon dioxide, absorption in the [C<sub>1</sub>C<sub>4</sub>Im][LEV] was found to be one order of magnitude lower.

The results presented herein on the absorption of CO<sub>2</sub> in the mixtures [C<sub>1</sub>C<sub>4</sub>Pyrrro][OAc] + water are presented in Fig. 3. The absorption of carbon dioxide decreases when the mole fraction of water increases, the absorbed quantity of gas varying from  $10.9 \times 10^{-2}$  to  $0.9 \times 10^{-2}$  at 303.15 K and 9.4 kPa and 303.15 K and 63.8 kPa for water mole fractions equal to 0.35 and 0.85, respectively.

In order to compare the absorption of carbon dioxide in all studied systems, experimental data were extrapolated linearly to

**Table 3**

Experimental values of carbon dioxide in [C<sub>1</sub>C<sub>4</sub>Pyrrro][LEV], [C<sub>1</sub>C<sub>4</sub>Pyrrro][OAc] and [C<sub>1</sub>C<sub>4</sub>Pyrrro][OAc] + water expressed as carbon dioxide mole fraction,  $x_2$ .  $p$  is the experimental equilibrium pressure,  $K_H$  the Henry's law constants and dev is the estimation of the precision of the experimental data.

$T$ (K)	$p$ (10 <sup>2</sup> Pa)	$x_2^{\text{exp}}$	$K_H$ (10 <sup>5</sup> Pa)	$x_2^2$ (10 <sup>-2</sup> )	dev (%)
<b>[C<sub>1</sub>C<sub>4</sub>Pyrrro][LEV]</b>					
303.16	670.78	0.0093	72.2	1.38	-0.1
313.28	633.60	0.0078	81.4	1.22	+1.9
313.28	691.26	0.0083	82.9	1.20	+0.1
313.31	696.99	0.0082	84.4	1.18	-1.7
323.32	658.57	0.0066	99.5	1.00	+0.1
323.34	717.90	0.0073	97.4	1.02	+2.3
323.34	723.84	0.0070	102.5	0.97	-2.7
333.35	683.20	0.0056	122.3	0.82	+1.4
333.36	750.17	0.0060	124.1	0.80	+0.0
333.41	747.00	0.0059	125.7	0.79	-1.2
<b>[C<sub>1</sub>C<sub>4</sub>Pyrrro][OAc]</b>					
353.55	891.8	0.011	84.5	0.012	
353.18	434.26	0.005	88.8	0.011	
<b>[C<sub>1</sub>C<sub>4</sub>Pyrrro][OAc] + water (<math>x_{\text{water}} = 0.35</math>)</b>					
303.34	94.00	0.109			
313.35	147.00	0.103			
<b>[C<sub>1</sub>C<sub>4</sub>Pyrrro][OAc] + water (<math>x_{\text{water}} = 0.6</math>)</b>					
303.32	154.00	0.057			
313.72	221.00	0.053			
<b>[C<sub>1</sub>C<sub>4</sub>Pyrrro][OAc] + water (<math>x_{\text{water}} = 0.85</math>)</b>					
303.35	638	0.009			
313.36	709	0.008			

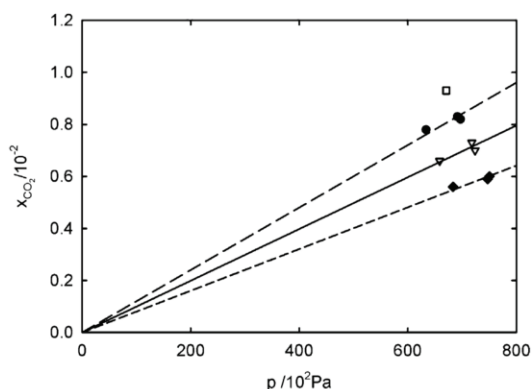


Fig. 2. Mole fraction absorption of carbon dioxide in the  $[C_1C_4Im][LEV]$  as a function of the temperature: (□), 303.15 K; (●), 313.15 K; (▽), 323.15 K; and (◆), 333.15 K.

353.15 K for all systems except for  $[C_1C_4PyrrO][OAc]$ . In that case, it is assumed that the pressure differences do not affect significantly the values of absorption of carbon dioxide in the different systems studied and so they can be compared at the different temperatures studied. Results are presented in Fig. 4. The absorption of carbon dioxide in the mixtures  $[C_1C_4PyrrO][OAc]$  + water for water mole fractions equal to 0.35 and 0.60 is one order of magnitude higher than in the three other systems. Values are comparable to these found for the systems  $[C_1C_2Im][OAc]$  + water and  $[C_1C_4Im][OAc]$  + water studied previously (Stevanovic et al., 2012). It implies that the system  $[C_1C_4PyrrO][OAc]$  + water can react chemically with carbon dioxide when the amount of water present is sufficient. Absorption of carbon dioxide in pure  $[C_1C_4PyrrO][OAc]$  was found to be lower than in mixtures of  $[C_1C_4PyrrO][OAc]$  + water for water mole fraction equal to 0.35 and 0.60. Absorption of carbon dioxide in pure  $[C_1C_4PyrrO][OAc]$  is also one order of magnitude lower than in  $[C_1C_2Im][OAc]$  and  $[C_1C_4Im][OAc]$ . It appears that pure  $[C_1C_4PyrrO][OAc]$  is only able to physically absorb carbon dioxide and the mechanism of chemical reaction between  $[C_1C_4PyrrO][OAc]$  + water and carbon dioxide is different from that of the systems with the ionic liquids  $[C_1C_2Im][OAc]$  and  $[C_1C_4Im][OAc]$ , these two ionic liquids reacting chemically with carbon dioxide with and without water present.

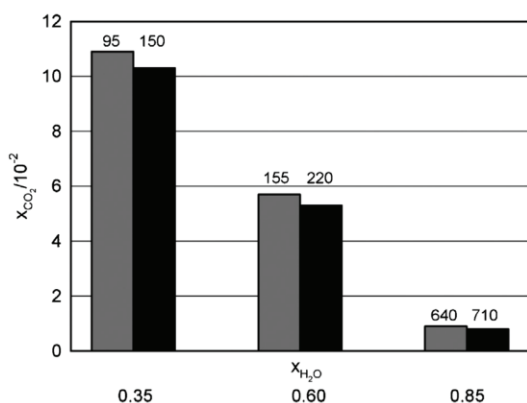


Fig. 3. Mole fraction absorption of carbon dioxide in the systems  $[C_1C_4PyrrO][OAc]$  + water as a function of the temperature: (■) 303.15 K and (■) 313.15 K. The number above each bar represents the equilibrium pressure in  $10^2$  Pa.

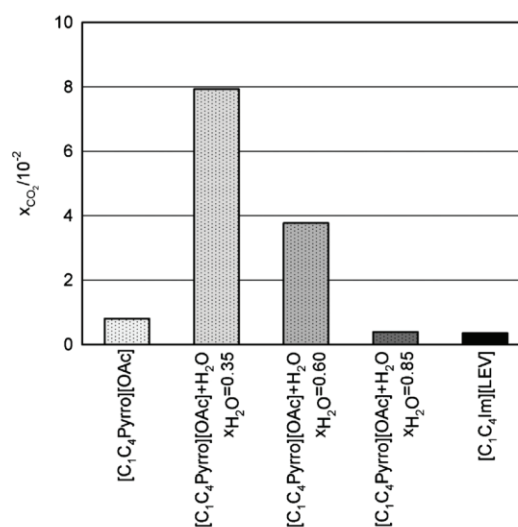


Fig. 4. Mole fraction absorption of carbon dioxide in the ionic liquids and ionic liquids + water systems studied herein, at 353.15 K: (□),  $[C_1C_4PyrrO][OAc]$ ; (■),  $[C_1C_4PyrrO][OAc]$  + water ( $x_{H_2O} = 0.35$ ); (■),  $[C_1C_4PyrrO][OAc]$  + water ( $x_{H_2O} = 0.60$ ); (■),  $[C_1C_4PyrrO][OAc]$  + water ( $x_{H_2O} = 0.80$ ); (■),  $[C_1C_4Im][LEV]$ . Values are obtained by extrapolating linearly experimental data to 353.15 K for all systems except for  $[C_1C_4PyrrO][OAc]$ .

Absorption of carbon dioxide in  $[C_1C_4Im][LEV]$  is comparable to the absorption in pure  $[C_1C_4PyrrO][OAc]$  or in the mixture  $[C_1C_4PyrrO][OAc]$  + water for water molar fraction equal to 0.85.

In order to explain the difference in carbon dioxide absorption in the studied ionic liquids as well as the effect of water on the microscopic structure of the pure ionic liquids and in their mixtures with carbon dioxide, we have used molecular dynamics simulations. Two ionic liquids were considered, the 1-butyl-3-methyl trifluoroacetate  $[C_1C_4Im][TFA]$  and the  $[C_1C_4PyrrO][OAc]$ . In the first case, it is well known that the absorption of  $CO_2$  is purely physical (Carvalho et al., 2009) and we expect that the comparison between the behaviors of the two ionic liquids will contribute to the understanding of the mechanisms of gas absorption in  $[C_1C_4PyrrO][OAc]$ .

Molecular dynamics simulations were done in a condensed-phase and took into account all the two-body interactions from the environment of each molecule or ion, labeled as depicted in Fig. 5.

Initially, the microscopic structure of the pure ionic liquids  $[C_1C_4Im][TFA]$  and  $[C_1C_4PyrrO][OAc]$ , was perceived by the analysis of the site-site radial distribution function – probability of finding two selected atomic sites at a certain distance is represented in Fig. 6 for several representative atomic sites in the pure ionic liquids. From the plots in Fig. 6 it can be observed that in the imidazolium ionic liquid, the cation and the anion interact preferentially through the  $H_{2Im}$  hydrogen of the  $C_1C_4Im^+$  and the  $O_{TFA}$  oxygen of  $TFA^-$ , where negative charge is concentrated. The oxygen atom of the anion  $TFA^-$  is also found with significant probability in the vicinity of the nitrogen  $N_{Im}$  of imidazolium cation. This result was expected and is consistent with other imidazolium liquids reported in literature.

Likewise, in the pyrrolidinium ionic liquid the interaction between the partially positive  $N_{PYRRO}$  (as well as  $C1_{PYRRO}$ ) and the oxygen of the  $OAc^-$  are of the most importance. The other interaction sites between the cation and the anion are present, but less expressed. However, the distance between these cation and anion atomic sites are shorter for the imidazolium ionic liquid (Stevanovic et al., 2012) than for the pyrrolidinium based one, in accordance

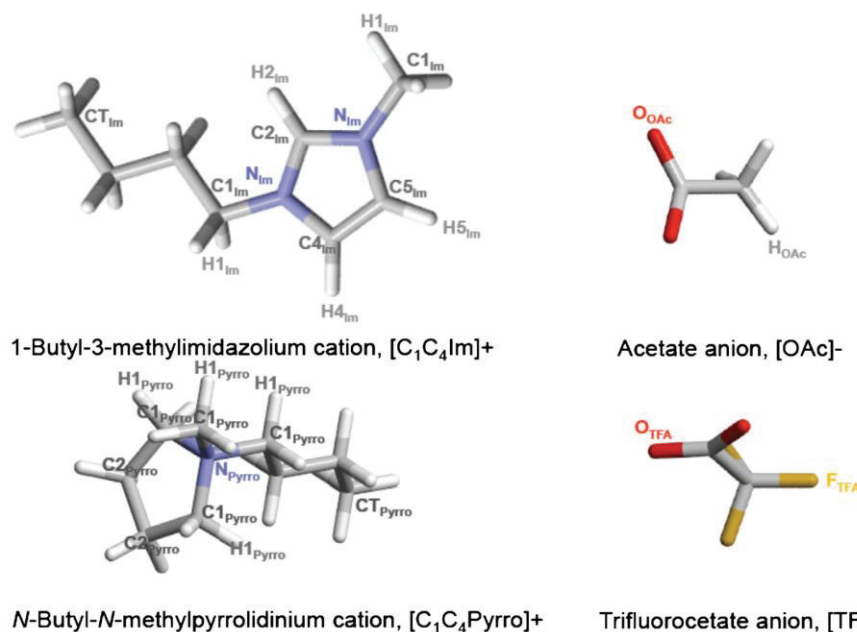


Fig. 5. Atom labeling in 1-butyl-3-methylimidazolium and N-butyl-N-methylpyrrolidinium cations and acetate and trifluoroacetate anions.

with accessibility and acidity of imidazolium  $H2_{im}$  and therefore stronger acid-base interactions in the former case.

The molecular simulation results indicate that the presence of carbon dioxide does not affect the most significant interaction sites present in the pure ionic liquids. This can be also deduced from the plots in Fig. 6, where solid lines refer to the pure ionic liquid and dotted lines to the mixture ( $CO_2$  + ionic liquid). In the  $[C_1C_4Im][TFA]$ , both peaks, one corresponding to the interactions of the terminal carbon atoms of the alkyl chain of the cation  $CT_{im}$  and the oxygen of  $CO_2$  ( $O_{CO_2}$ ), and the other between the oxygen of the anion ( $O_{OAc}$ ) and carbon of carbon dioxide ( $C_{CO_2}$ ) are of significant importance. This indicates that carbon dioxide is solvated preferentially in the vicinity of the anion and in the non-polar region of imidazolium ionic liquids. Carbon dioxide was found to be solvated similarly in  $[C_1C_4Im][TFA]$  and in  $[C_1C_4Im][OAc]$  as demonstrated in our previous work (Stevanovic et al., 2012). Analogously in  $[C_1C_4Pyrro][OAc]$ , there is a high probability of finding carbon dioxide near oxygen of  $OAc^-$  and  $CT_{pyrro}$ . No significant difference in solvation of carbon dioxide in both types of ionic

liquid, imidazolium (Stevanovic et al., 2012) and pyrrolidinium, was observed.

These structural features of the mixture of ( $CO_2$  + ionic liquid) can be perceived and confirmed also in 3 dimensional spatial distribution functions in Fig. 7. In Fig. 7a and d is represented the distribution of the local density of the cationic and the anionic atomic sites around carbon dioxide in  $[C_1C_4Im][TFA]$  and  $[C_1C_4Pyrro][OAc]$ , respectively. As already deduced from the radial distribution functions, for the two ionic liquids studied the spatial distribution function shows that carbon dioxide is mainly solvated by the anion ( $O_{OAc}$  or  $O_{TFA}$ , red) and the terminal carbon atoms of  $CT_{im}$  or  $CT_{pyrro}$  (gray). Looking at distribution of atomic density around acetate or trifluoroacetate (Fig. 7b and e) is expected to find  $C_{CO_2}$  (cyan) and  $C2_{im}$  or  $N_{pyrro}$  (blue) interacting with the oxygen atoms of the anion. From Fig. 7c and f we can observe that the presence of the oxygen of carbon dioxide around the cation is minor.

Calculations of the free energy of solvation of carbon dioxide in  $[C_1C_4Im][TFA]$  and  $[C_1C_4Pyrro][OAc]$  at 373 K give access

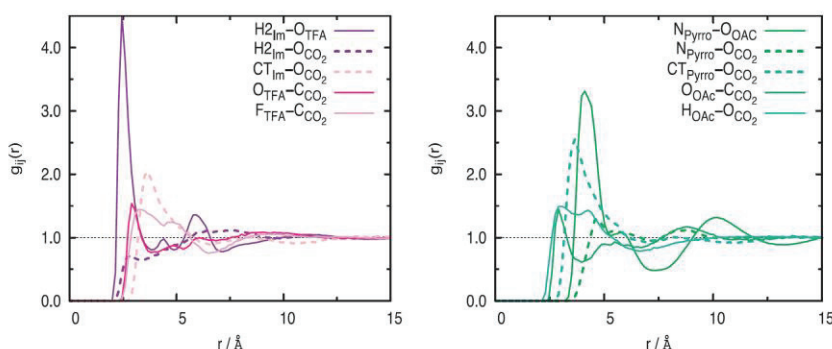
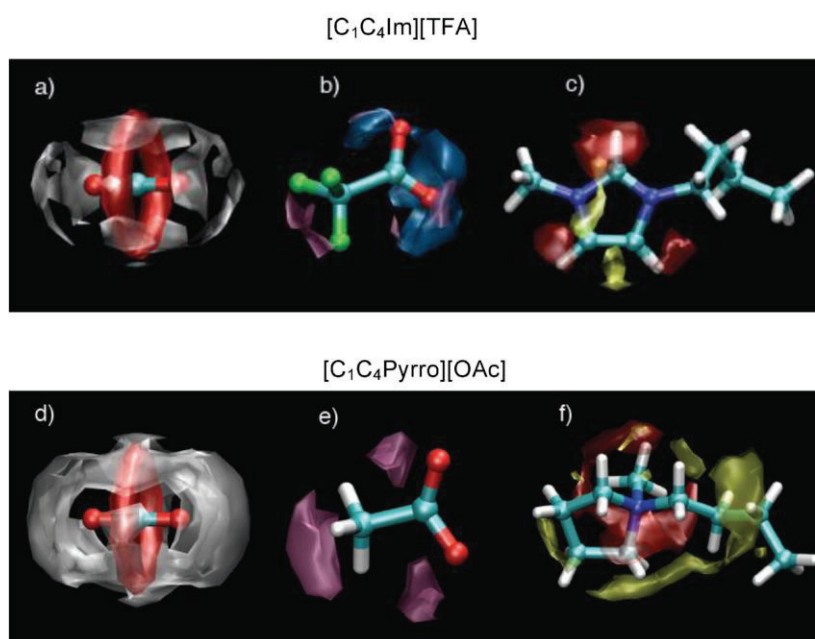


Fig. 6. Preferential interaction sites between ionic liquid and carbon dioxide. On the left-hand side:  $[C_1C_4Im][TFA]$  and on the right-hand side:  $[C_1C_4Pyrro][OAc]$ .



**Fig. 7.** Spatial distribution functions between selected atomic sites in [C<sub>1</sub>C<sub>4</sub>Im][TFA], [C<sub>1</sub>C<sub>4</sub>Pyrro][OAc] and carbon dioxide. (a and d) Around carbon dioxide: iso-surface corresponding to a local density of twice the average density of the C<sub>TIm</sub> or C<sub>TPyrro</sub> (gray) and of the O<sub>OAc</sub> or O<sub>TFA</sub> (red). (b and e) Around OAc<sup>-</sup> or TFA<sup>-</sup>. Iso-surface corresponding to a local density of 3-times the average density of the H<sub>2Im</sub> (blue) and C<sub>CO2</sub> (purple). Figure c and f: around C<sub>1</sub>C<sub>4</sub>Im<sup>+</sup> or C<sub>1</sub>C<sub>4</sub>Pyrro<sup>+</sup>. Iso-surface corresponding to a local density of twice the average density of the O<sub>CO2</sub> (yellow) and of 4-times of the O<sub>OAc</sub> or O<sub>TFA</sub> (red). (For interpretation of the references to color in this figure legend, the reader is referred to the web version of the article.)

to the Henry's law constants,  $K_H$ , that allow us to calculate the gas solubility at a partial pressure of gas  $p_{\text{gas}} = 1$  bar. The results are summarized in Table 4, where a comparison with the experimental values is also reported. The results of the simulations agree with the experiments for [C<sub>1</sub>C<sub>4</sub>Im][TFA]. Whereas, simulations made previously (Stevanovic et al., 2012) did not reproduce experimental trends for [C<sub>1</sub>C<sub>4</sub>Im][OAc]. Solubilities calculated for [C<sub>1</sub>C<sub>4</sub>Im][TFA] were found to be the same than for [C<sub>1</sub>C<sub>4</sub>Im][OAc] studied previously (Stevanovic et al., 2012), within the incertitude of simulations. This implies that the nature of the cation does not affect the solubility of carbon dioxide significantly.

The disparity in the solubility of carbon dioxide in the studied ionic liquids can be ascribed either to the structural difference in ionic liquids or/and different strength and nature of interactions. As the structural analysis showed no significant difference between [C<sub>1</sub>C<sub>4</sub>Im][TFA] and [C<sub>1</sub>C<sub>4</sub>Pyrro][OAc], the strength of interactions CO<sub>2</sub>-solute must be of significant importance.

In order to explain such a difference in the solubility of carbon dioxide the simulation results were examined in detail. The overall system configuration energy of the mixtures (CO<sub>2</sub> + ionic liquid) was decomposed to the energy between each pair of species,

represented in Fig. 8. The overall cation-anion interactions are stronger for the pair [C<sub>1</sub>C<sub>4</sub>Im]<sup>+</sup>[TFA]<sup>-</sup> than for [C<sub>1</sub>C<sub>4</sub>Pyrro]<sup>+</sup>[OAc]<sup>-</sup>. These observations were already made from the analysis of the site-site radial distribution functions in Fig. 6. The presence of carbon dioxide increases the cation-anion interactions thus favoring the ion pair association. No significant difference in the interaction energy between carbon dioxide and cation/anion was observed for the two ionic liquids. Surprisingly, carbon dioxide was found to have a more favorable energy of interaction with the cation than with the anion of the ionic liquids.

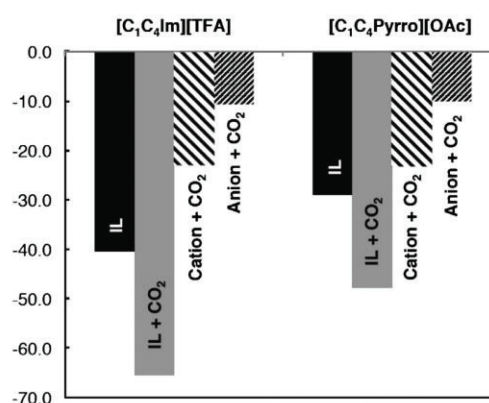


**Fig. 8.** Comparison of the cation-anion, cation-CO<sub>2</sub> and anion-CO<sub>2</sub> interaction energies in pure ionic liquids and in the mixtures with carbon dioxide. The values are normalized by a number of the amount of substance of ionic liquid in moles. In the mixtures IL + CO<sub>2</sub> interaction energies are normalized by number of CO<sub>2</sub> molecules. Exact values are reported in Table S1 (ESI).

**Table 4**

Comparison of experimental solubilities of carbon dioxide in ionic liquids and calculated by molecular dynamic simulations expressed in mole fraction: [C<sub>1</sub>C<sub>4</sub>Im][TFA] and [C<sub>1</sub>C<sub>4</sub>Pyrro][OAc].

Ionic liquid	Calculated, $x_{\text{sim}}^a$	Experimental, $x_{\text{exp}}$
[C <sub>1</sub> C <sub>4</sub> Im][TFA]	0.004 ± 0.001	0.005 <sup>c</sup>
[C <sub>1</sub> C <sub>4</sub> Pyrro][OAc]	0.002 ± 0.001 <sup>b</sup>	0.012 <sup>d</sup>

<sup>a</sup> 373 K.

<sup>b</sup> Extrapolated to 373 K.

<sup>c</sup> 298 K.

<sup>d</sup> 353 K.

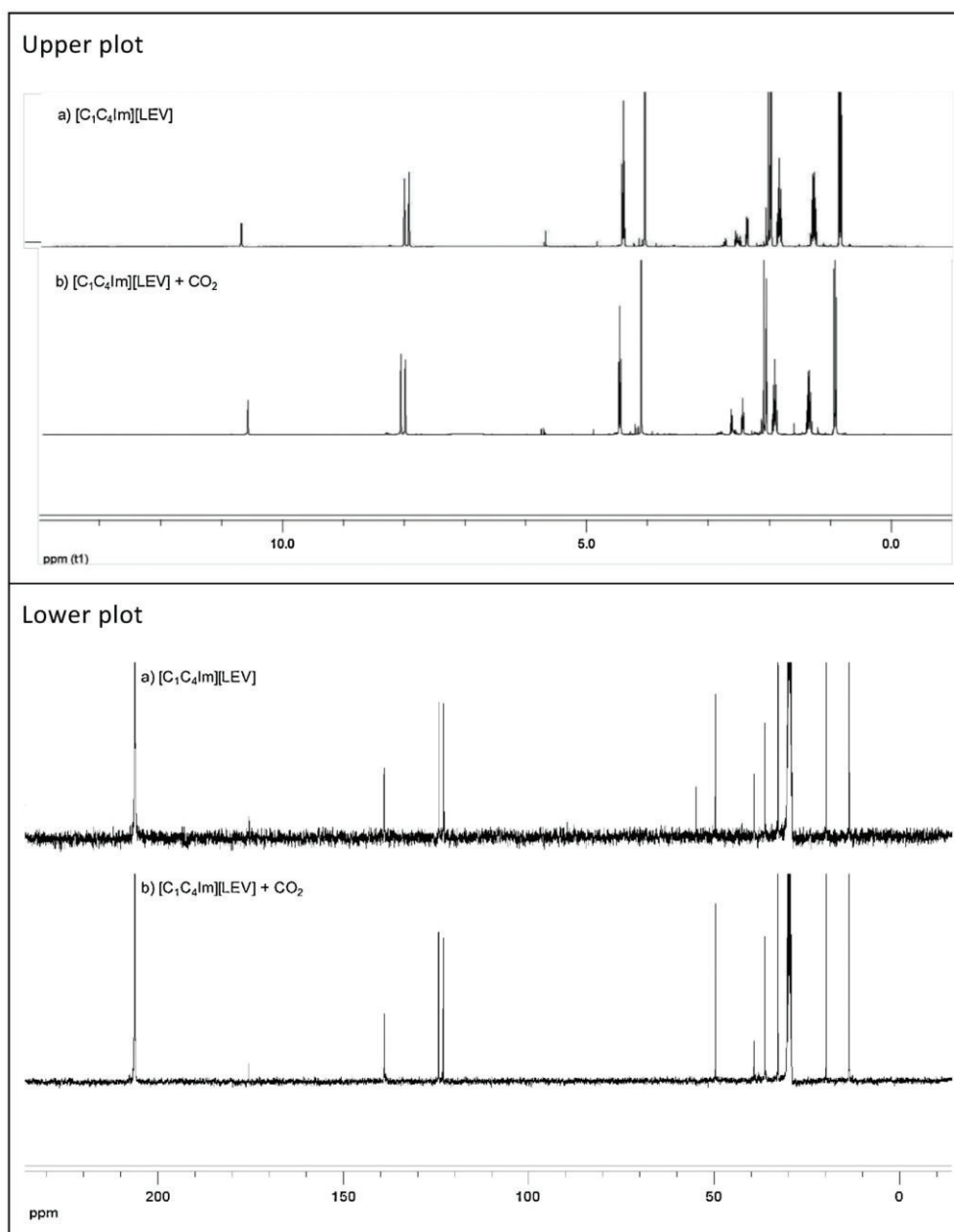
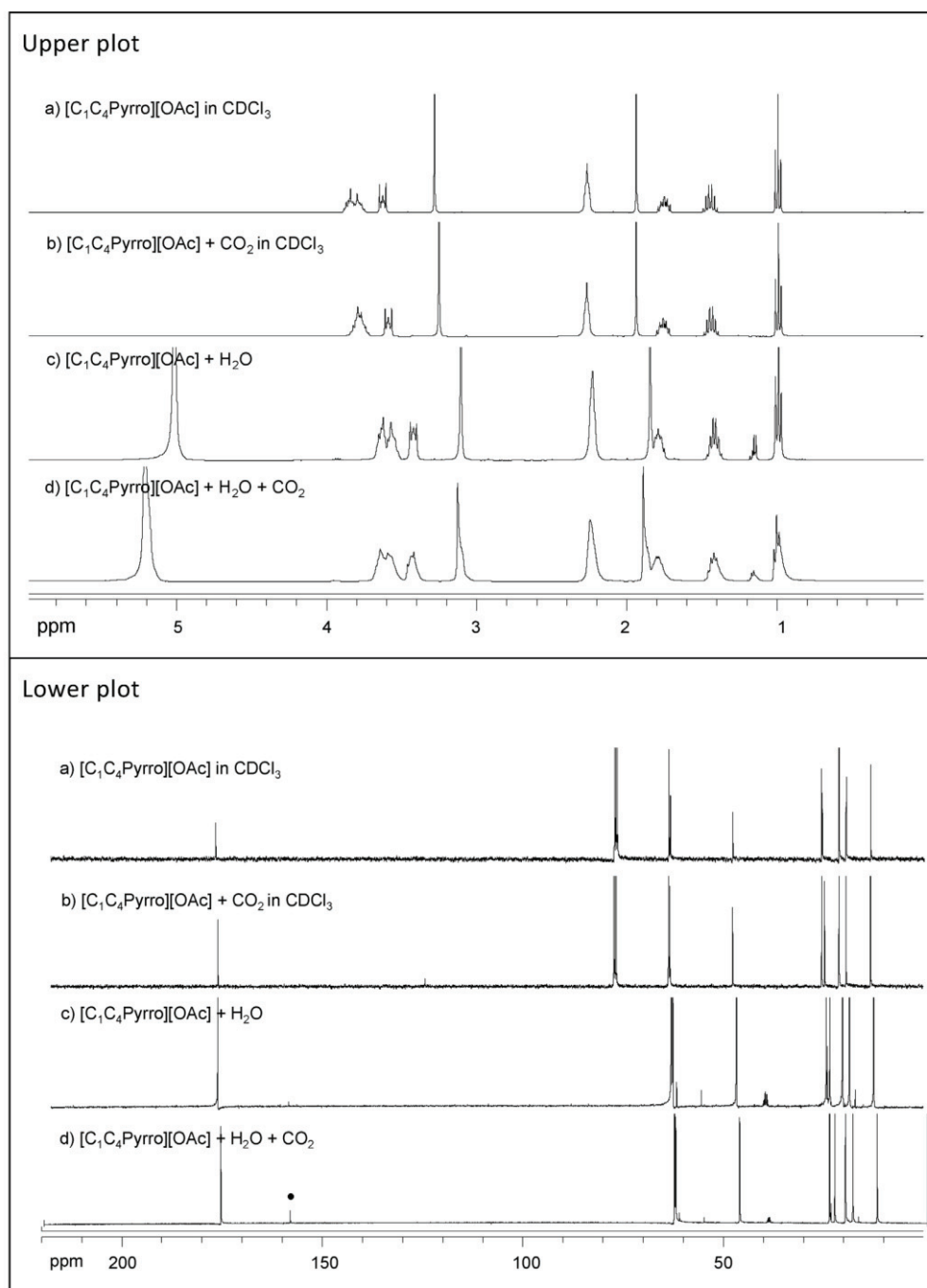


Fig. 9.  $^1\text{H}$  NMR (upper plot) and  $^{13}\text{C}$  NMR spectra (lower plot) of various samples of  $[\text{C}_1\text{C}_4\text{Im}][\text{LEV}]$  in acetone- $d_6$ .

Molecular simulation reproduces the correct carbon dioxide solubility in  $[\text{C}_1\text{C}_4\text{Im}][\text{TFA}]$ , but not in  $[\text{C}_1\text{C}_4\text{Pyrro}][\text{OAc}]$ , meaning that in the later case some mechanism of gas absorption other than physical absorption (the only implemented in the molecular simulations), prevails.

To obtain further information about the interaction of carbon dioxide and the ionic liquids, which could help to interpret the trends of the experimental values of carbon dioxide absorption,  $^1\text{H}$  and  $^{13}\text{C}$  NMR spectra of pure and carbon dioxide-saturated ionic liquids were recorded at atmospheric pressure. Fig. 9 shows NMR spectra of pure  $[\text{C}_1\text{C}_4\text{Im}][\text{LEV}]$  and  $[\text{C}_1\text{C}_4\text{Im}][\text{LEV}]$  saturated

with carbon dioxide. Comparison of the spectra (a) and (b) in the upper and lower plots of Fig. 9 shows no noticeable changes neither in  $^1\text{H}$  or in  $^{13}\text{C}$  chemical shifts upon saturation of the ionic liquid with carbon dioxide. This observation proves that no chemical reaction is involved in the carbon dioxide absorption by  $[\text{C}_1\text{C}_4\text{Im}][\text{LEV}]$ , in agreement with the lower values of absorption found compared to the imidazolium acetate based ionic liquids (Stevanovic et al., 2012). Furthermore, the small peak in spectrum (b) of the lower plot in Fig. 9 at around 175 ppm is the clear signature of free  $\text{CO}_2$  in solution (Tomizaki et al., 2010).



**Fig. 10.** <sup>1</sup>H NMR spectra (upper plot) and <sup>13</sup>C NMR spectra (lower plot) of various samples of [C<sub>1</sub>C<sub>4</sub>Pyrro][OAc]. Samples (a) and (b) were recorded in solution in CDCl<sub>3</sub> while samples (c) and (d) were recorded in a coaxial tube loaded with DMSO-d<sub>6</sub>.

To obtain further insight into the mechanism of carbon dioxide absorption by pyrrolidinium acetate, <sup>1</sup>H and <sup>13</sup>C NMR spectra of pure [C<sub>1</sub>C<sub>4</sub>Pyrro][OAc], of the [C<sub>1</sub>C<sub>4</sub>Pyrro][OAc] + H<sub>2</sub>O mixtures and of the solutions containing CO<sub>2</sub> in these liquids were recorded and are depicted in Fig. 10. Since [C<sub>1</sub>C<sub>4</sub>Pyrro][OAc] is a solid at

room conditions with a melting point at 353 K, the pure ionic liquid was dissolved in CDCl<sub>3</sub> before the NMR spectra of the solution were recorded. Comparison of the spectra (a) and (b) in the upper and lower plots of Fig. 10 shows no noticeable changes, neither in <sup>1</sup>H or in <sup>13</sup>C chemical shifts upon saturation of the mixture

with carbon dioxide. This indicates that, without the presence of water, the mechanism of absorption is different from the mechanism in  $[C_1C_4Im][OAc]$  in which chemical reactions with acetate were observed previously (Stevanovic et al., 2012). Contrary to  $[C_1C_4Im][OAc]$ , solubility measurements showed that the presence of water in  $[C_1C_4Pyrro][OAc]$  increases dramatically the absorption of gas when compared with that in the pure ionic liquid. This is another evidence that the mechanism of absorption of the gas is different in the two ionic liquids containing the acetate anion. An additional peak appears in the  $^{13}C$  NMR spectrum at 158.5 ppm (● in the lower plot labeled d) in Fig. 10) when the ionic liquid + water mixture is saturated with  $CO_2$ . Most probably, this peak corresponds to the formed  $HCO_3^-$ , as proved independently by dissolving  $NaHCO_3$  in the ionic liquid (Fig. S1 in Supplementary information). This observation is in agreement with previously established results, which showed that solubility of carbon dioxide in triethylbutylammonium acetate is excluded by chemical reaction involving cation (Wang et al., 2011), but instead involves the acetate anion. Although the reaction is possible only in the presence of water, excess water displaces equilibrium toward the reactants and decreases the absorption, as proved by the experimental measurements herein. This work shows that there should be an optimum concentration of water around mole fraction concentrations of 0.35.

## 9. Conclusions

This work presents an original study of the physico-chemical properties of the ionic liquids  $[C_1C_4Im][LEV]$ ,  $[C_1C_4Pyrro][OAc]$  and  $[C_1C_4Pyrro][OAc]$  + water. Our aim is to study the absorption mechanisms of carbon dioxide in these solvents. These mechanisms are relevant to propose alternative processes for carbon dioxide capture.

We have observed that the ionic liquid  $[C_1C_4Im][LEV]$  presents a higher viscosity than the imidazolium acetate based ionic liquids, which can constitute a disadvantage for industrial processes needing high fluidities. The mixtures  $[C_1C_4Pyrro][OAc]$  + water present also higher values of absorption than  $[C_1C_2Im][OAc]$  + water and  $[C_1C_4Im][OAc]$  + water for the same water molar composition.

We have observed that absorption of carbon dioxide in the pure ionic liquids is of the order of  $10^{-2}$  when expressed in mole fraction of gas, indicating that no chemical reaction between carbon dioxide and ionic liquids are involved unlike in the case of imidazolium acetate based ionic liquids. Absence of chemical reaction is confirmed by comparison between the NMR spectra of pure ionic liquids and those of carbon dioxide saturated ionic liquids.

The mixtures  $[C_1C_4Pyrro][OAc]$  + water present values for the carbon dioxide absorption one order of magnitude higher than that in the pure ionic liquids. These values, comparable to those that can be found in the systems  $[C_1C_2Im][OAc]$  + water and  $[C_1C_4Im][OAc]$  + water, point toward the existence of chemical reaction between  $[C_1C_4Pyrro][OAc]$  and carbon dioxide but only in the presence of water. The NMR study reported here proves that, in the case of  $[C_1C_4Pyrro][OAc]$  + water, the mechanism of  $CO_2$  absorption is different from that previously reported for  $[C_1C_4Im][OAc]$  + water mixtures.

## Acknowledgements

The FUI ACACIA project is acknowledged for financing part of this work and the PhD grant of S.S. The authors thank D. Pic from LMOPS, Lyon, France, for his help in the synthesis of one of the products used. A.P. was financed by the *Contrat d'Objectifs Partagés*,

CNRS-UBP, Région Auvergne, France. L.M. is financed by a *Cluster Excellence* of the Rhone Alpes region, France with the participation of IFPEN, France.

## Appendix A. Supplementary data

Supplementary data associated with this article can be found, in the online version, at <http://dx.doi.org/10.1016/j.ijggc.2013.04.017>.

## References

- Almantariotis, D., Gefflaut, T., Padua, A.A.H., Coxam, J.Y., Costa Gomes, M.F., 2010. *Journal of Physical Chemistry B* 114, 3608.
- Bates, E.D., Mayton, R.D., Ntai, I., Davis, J.H.J., 2002. *Journal of American Chemical Society* 124, 926.
- Besnard, M., Cabaço, M.I., Chavez, F.V., Pinaud, N., Sebastiao, P.J., Coutinho, J.A.P., Danten, Y., 2012. *Chemical Communications*, 1245.
- Cabaco, M.I., Besnard, M., Danten, Y., Coutinho, J.A.P.C.B., 2011. *Journal of Physical Chemistry B* 115, 3538.
- Canongia Lopes, J.N., Deschamps, J., Padua, A.A.H., 2004. *Journal of Physical Chemistry B* 108, 2038.
- Carvalho, P.J., Alvarez, V.H., Schroder, B., Gil, A.M., Marrucho, I.M., Aznar, M., Santos, L.M.N.B.F., Coutinho, J.A.P., 2009. *Journal of Physical Chemistry B* 113, 6803.
- Costa Gomes, M.F., Husson, P., 2010. *ACS Symposium Series* 1030 (16), 223.
- Greaves, T.L., Brummond, C.J., 2008. *Chemical Reviews* 108, 206.
- Gurau, G., Rodriguez, H., Kelley, S.P., Janiczek, P., Kalb, R.S., Rogers, R.D., 2011. *Angewandte Chemie International Edition* 123, 12230–12232.
- Henley, E.J., Seader, J.D., Roper, D.K., 2011. *Separation Process Principles*, 3rd ed. John Wiley & Sons, Hoboken, NJ, USA.
- Hong, G., Jacquemin, J., Husson, P., Costa Gomes, M.F., Deetlefs, M., Nieuwenhuyzen, M., Sheppard, O., Hardacre, C., 2006. *Industrial and Engineering Chemistry Research* 45, 8180–8188.
- Husson, P., Pison, L., Jacquemin, J., Costa Gomes, M.F., 2010. *Fluid Phase Equilibria* 294, 98.
- Jacquemin, J., Husson, P., Padua, A.A.H., Majer, V., 2006a. *Green Chemistry* 8, 172.
- Jacquemin, J., Costa Gomes, M.F., Husson, P., Majer, V., 2006b. *Journal of Chemical Thermodynamics* 38, 490.
- Jacquemin, J., Husson, P., Majer, V., Costa Gomes, M.F., 2006c. *Fluid Phase Equilibria* 240, 87.
- Jacquemin, J., Husson, P., Majer, V., Cibulka, I., 2007. *Journal of Chemical and Engineering Data* 52, 2204.
- Jacquemin, J., Ge, R., Nancarrow, P., Rooney, D.W., Costa Gomes, M.F., Padua, A.A.H., Hardacre, C., 2008a. *Journal of Chemical and Engineering Data* 53, 716.
- Jacquemin, J., Nancarrow, P., Rooney, D.W., Costa Gomes, M.F., Husson, P., Majer, V., Padua, A.A.H., Hardacre, C., 2008b. *Journal of Chemical and Engineering Data* 53, 2133.
- Jorgensen, W.L., Maxwell, D.S., TiradoRives, J., 1996. *Journal of American Chemical Society* 118, 11225.
- Liu, X.M., Zhang, S.J., Zhou, G.H., Wu, G.W., Yuan, X.L., Yao, X.Q., 2006. *Journal of Physical Chemistry B* 110, 12062.
- Maginn, E.J., 2005. *Quarterly Technical Report to DOE*. USA.
- Magna, L., Chauvin, Y., Nicolai, G.P., Basset, J.-M., 2003. *Organometallics* 22, 4418.
- Mallet, J., Molinari, M., Martineau, F., Delavoie, F., Fricoteaux, P., Troyon, M., 2008. *Nano Letters* 8, 3468.
- Ramdin, M., de Loos, T.W., Vlucht, T.J.H., 2012. *Industrial and Engineering Chemistry Research* 51, 8149–8177.
- Rizzo, R.C., Jorgensen, W.L., 1999. *Journal of American Chemical Society* 121, 4827.
- Schilling, G., Kleinrahm, R., Wagner, W., 2008. *Journal of Chemical Thermodynamics* 40, 1095.
- Shiflett, M.B., Kasprzak, D.J., Junk, C.P., et al., 2008. *Journal of Chemical Thermodynamics* 40, 25.
- Shiflett, M.B., Yokozeki, A., Junk, C.P., Grieco, L.M., Foo, T., 2009. *Journal of Chemical and Engineering Data* 54, 108.
- Shiflett, M., Drew, D.W., Cantini, R.A., Yokozeki, A., 2010. *Energy and Fuels* 24, 5781.
- Smith, W.F., Todorov, T.R., 2007. *The DL-POLY Molecular Simulation Package*, 2. 20. STFC Daresbury Laboratory, Warrington, UK.
- Stevanovic, S., Podgorsek, A., Padua, A.A.H., Costa Gomes, M.F., 2012. *Journal of Physical Chemistry B* 116, 14416–14425.
- Tomizaki, K., Kanakubo, M., Nanjo, H., Shimizu, S., Onoda, M., Fujioka, Y., 2010. *Industrial and Engineering Chemistry Research* 49, 1222–1228.
- Wang, G., Hou, W., Xiao, F., Geng, J., Wu, Y., Zhang, Z., 2011. *Journal of Chemical and Engineering Data* 56, 1125–1133.
- Yokozeki, A., Shiflett, M.B., Junk, C.P., Grieco, L.M., Foo, T., 2008. *Journal of Physical Chemistry B* 112, 16654.
- Yoshizawa-Fujita, M., Johansson, K., Newman, P., MacFarlane, D.R., Forsyth, M., 2006. *Tetrahedron Letters* 47, 2755–2758.
- Yu, Z.Y., Jacobson, M.P., Josovitz, J., Rapp, C.S., Friesner, R.A., 2004. *Journal of Physical Chemistry B* 108, 6643.

**Submitted RCS book chapter in “CHEMICAL PROCESS TECHNOLOGY FOR A SUSTAINABLE FUTURE”,** *Editors: Trevor M Letcher, Janet L Scott and Darrell A Paterson*

## Chapter 23

### *Gas separations using ionic liquids*

LEILA MOURA<sup>1,2</sup>, CATHERINE C. SANTINI<sup>2</sup>, AND MARGARIDA F. COSTA GOMES<sup>1</sup>

<sup>1</sup> *Institut de Chimie de Clermont-Ferrand, UMR 6296 CNRS and Université Blaise Pascal, équipe Thermodynamique et Interactions Moléculaires, BP 80026, 63171 Aubière, France.*

<sup>2</sup> *LC2P2, UMR 5265 CNRS and Université de Lyon 1, CPE LYON 43 Bd du 11 Novembre 1918, 69616 Villeurbanne, France.*

#### 23.1 Introduction

Separation processes explore differences in the properties of the species, either molecular (molar mass, dipole moment or dielectric constant), thermodynamic (vapour pressure or solubility) or transport (diffusivity). Common separation techniques rely on creating or adding a new phase, on introducing a barrier or a solid agent, or on using a force field or a gradient.<sup>1</sup>

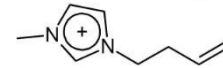
Distillation, crystallization, liquid-liquid extraction and absorption are the most common examples of separation techniques based on the creation or on the addition of a new phase that require an energy transfer or the use of a mass-transfer agent, respectively. The latter is usually less energy demanding but technologically more challenging, as the mass-transfer agent needs to be effectively separated and then recycled with reasonable purity. Membrane separation processes are based on the use of liquid or solid (often polymeric) barriers<sup>2</sup> that have different permeability to the components of a mixture. Membranes can be used in small, compact and clean units that require low energy to achieve separation but are still difficult to scale-up. Adsorption consists on the use of a solid agent, often a porous material with a large

surface area, capable of selectively retaining at its surface (by physical or chemical adsorption) the constituents of a mixture. Because the active separating agents (e.g. alumina, ion exchanging resins, high-surface-area SiO<sub>2</sub>, zeolites or molecular sieves) eventually become saturated and need to be regenerated, the separation by adsorption is seldom conducted continuously. Centrifugation, electrolysis, electro dialysis or electrophoresis are examples of separation techniques that exploit the differences in the responses of the constituents of a feed to an external force or gradient. These techniques are used to separate both liquid and gaseous mixtures and are especially useful and versatile for separating biochemicals.

Cryogenic distillation is the most used separation process for mixtures of gases. For ethane/ethylene and propane/propylene separation,<sup>1,3</sup> it has been in use industrially since the 1960's, ethylene and propylene being used in large quantities (demand of  $25 \times 10^{12}$  tons of ethylene per annum)<sup>4</sup> as precursors for the production of polymers, lubricants, rubbers, solvents and fuel components.<sup>4,5,6</sup> These separations require large distillation towers (120–180 trays), low temperatures (–114°C) and high pressures (15–30 bar), resulting in a high capital and energy demanding processes needing up to  $120 \times 10^{12}$  BTU/year.<sup>7,8</sup> The implementation of alternative processes with improved economic and environmental performance would represent a major advance in the sector

Ionic liquids have been suggested as separating agents for olefin/paraffin gas separation, as absorbents or as solvents for the chemical complexation of olefins with silver or copper salts. Ionic liquids are composed uniquely of ions and have a melting point below 100°C. Many present unique properties such as negligible vapour pressure, high thermal, chemical and electrochemical stability, non-flammability, high ionic conductivity. Ionic liquid can be synthesized in a large variety of combination of cations and anions, leading to tuneable physical chemical properties. The cations and anions that constitute the ionic liquids proposed for gaseous olefin/paraffin separations are listed in tables 23.1 and 23.2.

Table 23.1 - Abbreviation, full designation and structure of some cations of ionic liquids. C<sub>n</sub>/m represent alkyl chains of variable size

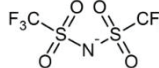
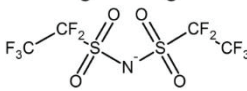
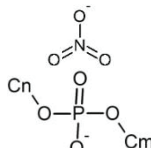
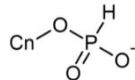
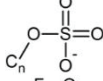
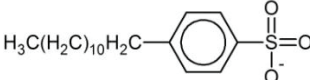
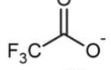
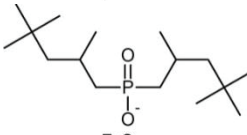
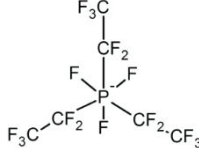
Abbreviation	Full designation	Structure
C <sub>n</sub> C <sub>m</sub> Im <sup>+</sup>	1-C <sub>n</sub> -3-C <sub>m</sub> Imidazolium	
C <sub>1</sub> (C <sub>3</sub> H <sub>5</sub> CH <sub>2</sub> )Im <sup>+</sup>	1-(buten-3-yl)-3-methylImidazolium	

$C_1(CH_2C_6H_5)Im^+$	1-benzyl-3-methylimidazolium	
$(C_2SO_2C_2)C_1Im^+$	1-diethylsulfonyl-3-methylimidazolium	
$C_1C_3CNIm^+$	1-(3-cyanopropyl)-3-methylimidazolium	
$C_1C_1C_3CNIm^+$	1-(3-cyanopropyl)-2,3-dimethylimidazolium	
$(C_3CN)_2Im^+$	1,3-(3-cyanopropyl)imidazolium	
$C_1C_1COOC_5Im^+$	-1-(pentoxycarbonylmethyl)-3-methylimidazolium	
$C_1C_1COOC_2OC_2Im^+$	1-(ethoxyethoxycarbonylmethyl)-3-methylimidazolium	
$C_1C_1COOC_2OC_2OC_4Im^+$	1-(2-(2-butoxyethoxy)ethoxycarbonylmethyl)-3-methylimidazolium	
$C_nC_mPyr^+$	$C_nC_m$ Pyrrolidinium	
$C_nPyr^+$	$C_n$ Pyridinium	
$P_{n m p q}^+$	$C_nC_mC_pC_q$ Phosphonium	
$N_{n m p q}^+$	$C_nC_mC_pC_q$ Ammonium	
$N_{1132-OH}$	Propylcholinium	

Unsaturated hydrocarbons usually present a higher solubility in ionic liquids than their saturated counterparts as can be seen in Figure 23.1 where the Henry's law constants of different gases in one ionic liquid are represented. The exact reasons for the observed trends are still poorly known, but are essential for the development of new alkane/alkene/alkyne separation processes.<sup>9</sup> Herein, we present the current knowledge on the solubility of ethane, ethylene, acetylene, propane, propylene and methyl acetylene in pure ionic liquids. Whenever possible we calculate the ionic liquid absorption capacity and ideal selectivity (solubility ratio) for ethane/ethylene, ethylene/acetylene, propane/propylene and propylene/methyl

acetylene mixtures and so assess the potential of a particular ionic liquid as separating agent.

Table 23.2 - Abbreviation, full designation and structure of some anions of ionic liquids. R<sub>n</sub> represents alkyl chains of variable size

Abbreviation	Full designation	Structure
NTf <sub>2</sub> <sup>-</sup>	Bis(trifluoromethylsulfonyl)imide	
BETf <sup>-</sup>	Bis(perfluoroethylsulfonyl)imide	
DCA <sup>-</sup>	Dicyanamide	
NO <sub>3</sub> <sup>-</sup>	Nitrate	
C <sub>n</sub> C <sub>m</sub> PO <sub>4</sub> <sup>-</sup>	C <sub>n</sub> C <sub>m</sub> Phosphate	
C <sub>n</sub> HPO <sub>3</sub> <sup>-</sup>	C <sub>n</sub> Phosphite	
PF <sub>6</sub> <sup>-</sup>	Hexafluorophosphate	
C <sub>n</sub> SO <sub>4</sub> <sup>-</sup>	C <sub>n</sub> Sulfate	
CF <sub>3</sub> SO <sub>3</sub> <sup>-</sup>	Trifluoromethanesulfonate	
DBS <sup>-</sup>	Dodecylbenzenesulfonate	
C <sub>n</sub> CO <sub>2</sub> <sup>-</sup>	Carboxylate	
OAc <sup>-</sup>	Acetate	
TFA <sup>-</sup>	Trifluoroacetate	
AlCl <sub>4</sub> <sup>-</sup>	Tetrachloroaluminate	
BF <sub>4</sub> <sup>-</sup>	Tetrafluoroborate	
TMPP <sup>-</sup>	Bis(2,4,4-trimethylpentyl) phosphinate	
FAP <sup>-</sup>	Tris(pentafluoroethyl)trifluorophosphate	

The absorption capacity of gaseous hydrocarbons by pure ionic liquids is relatively low because, in most cases, it is only a physical process. The use of silver(I) and copper(I) salts can significantly improve the amount of the unsaturated hydrocarbon absorbed by the ionic liquid phase as these metal cations are capable of selectively and reversibly reacting with it. This concept has been explored for the separation of ethane from ethylene and propane from propylene.

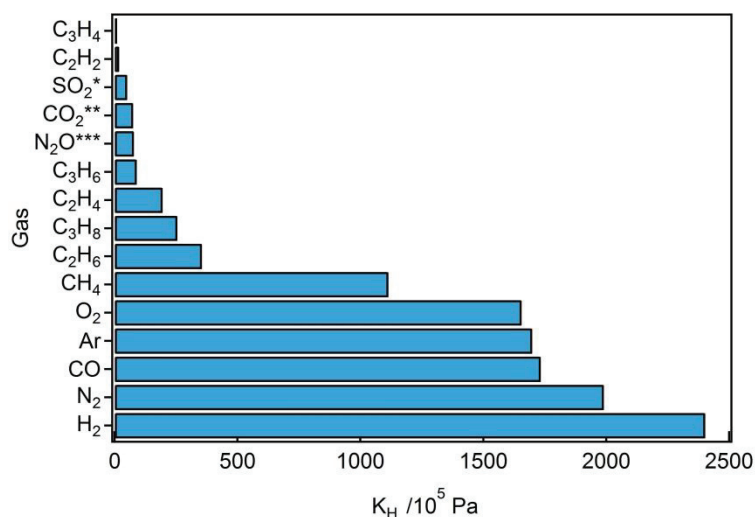


Figure 23.1 - Henry's law constant,  $K_H$ , for several gases in ionic liquid  $[C_1C_4Im][BF_4]$ <sup>10, 11, 12, 13, 14</sup> at 313 K. \* - 293 K; \*\* - 314 K; \*\*\* - 298 K.

## 23.2 Gas solubility

The chemical potential of component  $i$  in a mixture is defined as<sup>15,16</sup>

$$\mu_i = \mu_i^{\text{ref}} + RT \ln(\gamma_i x_i) \quad (1)$$

where  $\mu_i^{\text{ref}}$  is the chemical potential of component  $i$  in a chosen reference state and  $\gamma_i$  its activity coefficient. Two conventions are usually adopted to choose the appropriate combination of the reference state chemical potential and the activity coefficient, the choice depending on the physical state of the pure components at the thermodynamic conditions of the mixture.

The asymmetric convention is usually applied to solutions where the solute(s) or the solvent are not in the physical state of the solution at a given temperature and pressure, as in the case of the solutions of gases in ionic liquids considered herein. For the solvent, the activity coefficient approaches unity when its mole fraction is approximately unity and for the solute its activity coefficient becomes unity when the solute is present at very low concentrations,  $\gamma_i^H \rightarrow 1$  when  $x_i \rightarrow 0$ . In this case the solute is present in the limit of infinite dilution and the solution approaches ideal behaviour in the sense of Henry's law. The reference state adopted for the calculation of the chemical potential in this case is that of the pure solute at infinite dilution:<sup>15,17</sup>

$$\mu_i = \mu_i^{*H} + RT \ln(\gamma_i^H x_i) \quad x_i \rightarrow 0 \Rightarrow \gamma_i^H \rightarrow 1 \quad (2)$$

the activity coefficient in the asymmetric convention,  $\gamma_i^H$ , being a measure of the solute intermolecular interactions, the solvent and solute-solvent interactions being accounted for in the reference state.

The Gibbs energy of solution is defined as the difference in chemical potential when the solute is transferred, at constant pressure and temperature, from its pure state into the infinitely dilute solution. If the solute remains pure at equilibrium with the solution<sup>1</sup> and the solubility is low enough that  $\gamma_i^H \ll 1$ , the following, approximate relation can be used:

$$\Delta_{\text{sol}} G_i \approx RT \ln x_i \quad (3)$$

The Gibbs energy of solution expresses the difference between the solute-solute interactions in the pure species, which may be a condensed phase, and the solute-solvent interactions in an infinitely dilute solution. In order to isolate the role of the solute-solvent interactions in the process of dissolution, a thermodynamic transformation called solvation<sup>18</sup> can be defined as the difference in chemical potential when the solute is transferred from an ideal gas at standard pressure into the reference state at infinite dilution, equation (3) leading to:

---

<sup>1</sup> This is the case for the solutions of gases in ionic liquids because the solvent does not have any measurable vapour pressure at moderate temperatures.

$$\Delta_{\text{solv}}G_i = RT \ln \left( \frac{K_{H,i}}{p^o} \right) \quad (4)$$

in which  $K_{H,i}$  is the Henry's law constant defined as:

$$K_{H,i} \equiv \lim_{x_i \rightarrow 0} (f_i/x_i) \quad (5)$$

From the behaviour with temperature or with pressure of the Gibbs energy of solvation it is possible to calculate the other thermodynamic properties:<sup>19</sup>

$$\begin{aligned} \Delta_{\text{solv}}H_i &= -T^2 \frac{\partial}{\partial T} \left( \frac{\Delta_{\text{solv}}G_i}{T} \right)_p \\ \Delta_{\text{solv}}S_i &= - \left( \frac{\partial \Delta_{\text{solv}}G_i}{\partial T} \right)_p \\ \Delta_{\text{solv}}V_i &= \left( \frac{\partial \Delta_{\text{solv}}G_i}{\partial p} \right)_T \end{aligned} \quad (6)$$

The thermodynamic properties of solvation provide insights into the molecular mechanisms determining the solution behaviour – the enthalpy of solvation reflects the energy of solute-solvent interactions and the entropic contribution is related to structural organization in the solution. These thermodynamic properties of solvation are approximately equal to the thermodynamic properties of solution in the case of gaseous solutes at low pressure, the differences becoming more important for liquid or solid solutes<sup>20</sup>. These solvation properties can be determined through experimentally accessible quantities namely from solubility measurements and the calculation of the Henry's law constants.

### 23.3 Ethane and propane solubility

The ethane and propane mole fraction solubility<sup>2</sup> in different ionic liquids at 313 K is depicted in Figure 23.2. For ethane, 27 different ionic liquids were studied (20 based in imidazolium cations) and the mole fraction gas solubility ranges from  $1.50 \times 10^{-3}$  in  $[\text{C}_1\text{C}_2\text{Im}][\text{DCA}]$  to  $52.6 \times 10^{-3}$  in  $[\text{P}_{(14)666}][\text{TMPP}]$ . For propane, 8 ionic

---

<sup>2</sup> Calculated for a 1 bar partial pressure of gas.

liquids were studied (6 based in imidazolium cations and 2 based in phosphonium cations) and the mole fraction gas solubility varies from  $3.24 \times 10^{-3}$  in  $[\text{C}_1\text{C}_2\text{Im}][\text{DCA}]$  to  $156 \times 10^{-3}$  in  $[\text{P}_{(14)666}][\text{TMPP}]$ .

For both gases, the solubility is higher in phosphonium based ionic liquids followed by imidazolium bis(trifluoromethylsulfonyl)imide ionic liquids and imidazolium tris(pentafluoroethyl)trifluorophosphate ionic liquids, the latter having been studied only with ethane. Phosphonium based ionic liquids are capable of dissolving three times more ethane and eight times more propane than imidazolium based ones, these differences being less pronounced when the solubility is expressed in mass fraction, as can be observed in figure 23.3.

For both imidazolium and phosphonium based ionic liquids, the gas solubility increases with the increase of the size of the alkyl side-chains. For example, for imidazolium bis(trifluoromethylsulfonyl)imide ionic liquids, the mole fraction solubility of ethane increases, at 313 K, from  $6.73 \times 10^{-3}$  for  $[\text{C}_1\text{C}_2\text{Im}][\text{NTf}_2]$  to  $16.4 \times 10^{-3}$  for  $[\text{C}_1\text{C}_{10}\text{Im}][\text{NTf}_2]$  and the solubility of propane increases from  $12.0 \times 10^{-3}$  (at 313 K) for  $[\text{C}_1\text{C}_2\text{Im}][\text{NTf}_2]$  to  $16.9 \times 10^{-3}$  (at 320 K) for  $[\text{C}_1\text{C}_4\text{Im}][\text{NTf}_2]$ . The increase in ethane solubility for the ionic liquids  $[\text{C}_1\text{C}_n\text{Im}][\text{NTf}_2]$  can be explained by a more favourable entropy of solvation when the alkyl side-chain of the cation increases. Using molecular simulation, it was observed that ethane is solvated in the non-polar domains of the ionic liquid, preferentially near the terminal carbon of the alkyl chain and it becomes more mobile when the alkyl side-chain becomes longer.<sup>23</sup> The same variation of ethane solubility is found for  $[\text{C}_1\text{C}_n\text{Im}][\text{PF}_6]$  ionic liquids but is much smaller for  $[\text{C}_1\text{C}_n\text{Im}][\text{FAP}]$  ( $n = 4, 6$ ) for which a more moderate increase of the ethane solubility is observed. This is attributed to a balancing effect between a more favourable enthalpy and less favourable entropy, resulting in similar Gibbs energies of solvation for  $[\text{C}_1\text{C}_n\text{Im}][\text{FAP}]$  ( $n = 4, 6$ ).<sup>21</sup>

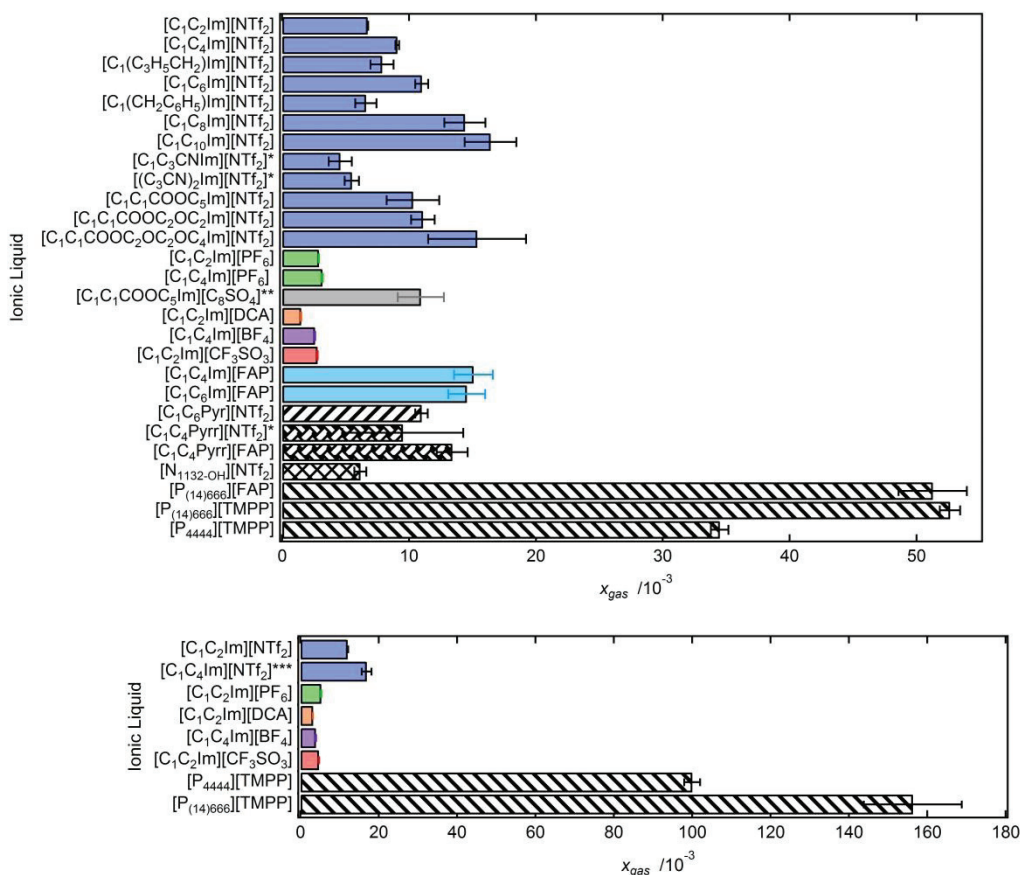


Figure 23.2 - Mole fraction solubility for ethane (top) and propane (bottom) in several ionic liquids at 313 K.

\* - values at 303 K; \*\* - values at 323 K; \*\*\* - values at 320 K.  $[C_1C_2Im][NTf_2]$ <sup>22, 33</sup>;  $[C_1C_4Im][NTf_2]$ <sup>23, 24</sup>;  $[C_1(C_3H_5CH_2)Im][NTf_2]$ <sup>25</sup>;  $[C_1C_6Im][NTf_2]$ <sup>26</sup>;  $[C_1(CH_2C_6H_5)Im][NTf_2]$ <sup>25</sup>;  $[C_1C_8Im][NTf_2]$ <sup>23</sup>;  $[C_1C_{10}Im][NTf_2]$ <sup>23</sup>;  $[C_1C_3CNIm][NTf_2]$ <sup>27</sup>;  $[(C_3CN)_2Im][NTf_2]$ <sup>27</sup>;  $[C_1C_1COOC_5Im][NTf_2]$ <sup>28</sup>;  $[C_1C_1COOC_2OC_2Im][NTf_2]$ <sup>28</sup>;  $[C_1C_1COOC_2OC_2OC_4Im][NTf_2]$ <sup>28</sup>;  $[C_1C_2Im][PF_6]$ <sup>13, 29</sup>;  $[C_1C_4Im][PF_6]$ <sup>30</sup>;  $[C_1C_1COOC_5Im][C_8SO_4]$ <sup>28</sup>;  $[C_1C_2Im][DCA]$ <sup>30</sup>;  $[C_1C_4Im][BF_4]$ <sup>14, 29</sup>;  $[C_1C_2Im][CF_3SO_3]$ <sup>30</sup>;  $[C_1C_4Im][FAP]$ <sup>21</sup>;  $[C_1C_6Im][FAP]$ <sup>21</sup>;  $[C_1C_6Pyr][NTf_2]$ <sup>31</sup>;  $[C_1C_4Pyr][NTf_2]$ <sup>22</sup>;  $[C_1C_4Pyr][FAP]$ <sup>32</sup>;  $[N_{1132-OH}][NTf_2]$ <sup>22</sup>;  $[P_{(14)666}][FAP]$ <sup>32</sup>;  $[P_{(14)666}][TMPP]$ <sup>33, 34</sup>;  $[P_{4444}][TMPP]$ <sup>33</sup>.

In the case of phosphonium based ionic liquids, a large increase in the solubility of ethane and propane was observed when the size of the alkyl chains increases in the cation, independently of the anions studied.

The functionalization of the alkyl side-chains in imidazolium based ionic liquids with cyano, ether or ester groups, does not improve the solubility of ethane and propane for the ionic liquids studied so far. Furthermore, when ester or ether functions are included in the side-chain of the imidazolium cations, the solubility increases more slowly with the increase of the chain when compared with non-functionalised alkyl chains.

Imidazolium-based ionic liquids containing large anions such as  $FAP^-$ ,  $C_8SO_4^-$  and  $NTf_2^-$  present higher ethane and propane solubility, followed by  $PF_6^-$ ,  $CF_3SO_3^-$ ,  $BF_4^-$  and  $DCA^-$ .

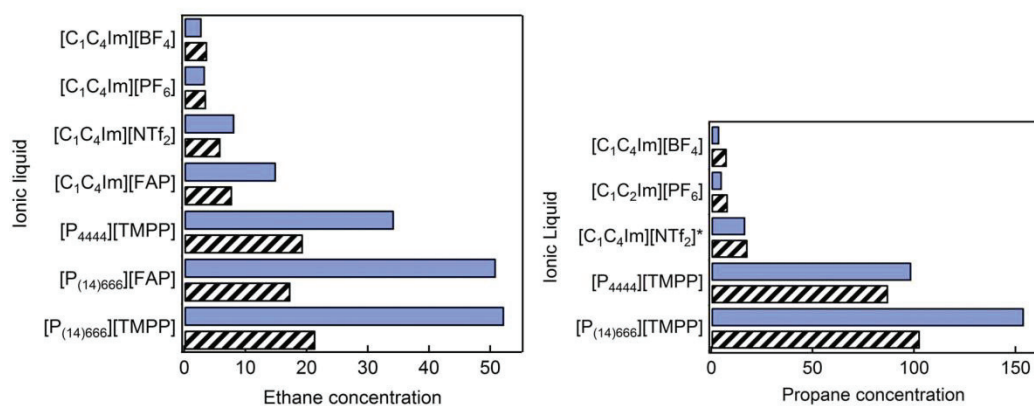


Figure 23.3 - Mole fraction ( $\times 10^3$ , full bars) and mass fraction ( $\times 10^4$ , patterned bars) of ethane (on the left) or propane (on the right) in several ionic liquids at 1 bar partial pressure of gas and 313 K (\* values at 320 K).

## 23.4 Ethylene and propylene solubility

The ethylene and propylene mole fraction solubility in different ionic liquids at 313 K is depicted in Figures 23.4 and 23.5, respectively. For ethylene, 53 different ionic liquids were studied (30 based on the imidazolium cation and 23 based on other cations) and the mole fraction gas solubility ranges from  $1.78 \times 10^{-3}$  in [C<sub>1</sub>C<sub>3</sub>CNIIm][DCA] to  $38.5 \times 10^{-3}$  in [P<sub>(14)666</sub>][TMPP]. For propylene, 40 ionic liquids were studied (25 based on the imidazolium cation and 15 based on other cations) and the mole fraction gas solubility varies from  $4.14 \times 10^{-3}$  in [C<sub>1</sub>C<sub>1</sub>Im][C<sub>1</sub>SO<sub>4</sub>] to  $133 \times 10^{-3}$  in [P<sub>(14)666</sub>][TMPP]. Both ethylene and propylene solubility is less affected when changing from [C<sub>1</sub>C<sub>2</sub>Im][DCA] to [P<sub>(14)666</sub>][TMPP] than the solubility of ethane or propane.

For both ethylene and propylene, the solubility is higher in phosphonium based ionic liquids followed by ammonium, pyridinium, pyrrolidinium and imidazolium ionic liquids. In the case of phosphonium based ionic liquids, several anions were studied and both ethylene and propylene solubility follow the order: [P<sub>(14)666</sub>][DCA] < [P<sub>(14)666</sub>][Cl] < [P<sub>4444</sub>][TMPP] < [P<sub>(14)444</sub>][DBS] < [P<sub>(14)666</sub>][TMPP]. In the case of imidazolium and ammonium based ionic liquids, ethylene is more soluble in [C<sub>1</sub>C<sub>4</sub>Im][NTf<sub>2</sub>] than in [N<sub>(4)111</sub>][NTf<sub>2</sub>] but significantly less soluble than in [N<sub>(1)888</sub>][NTf<sub>2</sub>], at 303K.

As for ethane and propane, the solubility of ethylene and propylene increases with the increase of the alkyl chain of the cation for imidazolium ionic liquids based in the  $\text{NTf}_2^-$ ,  $\text{BF}_4^-$ , phosphate and phosphite anions. An outlier is found ethylene in  $[\text{C}_1\text{C}_6\text{Im}][\text{NTf}_2]$  with a strangely low solubility. Ethylene solubility also increases with the increase of the alkyl chains in phosphonium and ammonium based ionic liquids but no precise contribution can be attributed to each supplementary  $-\text{CH}_2-$  group. The ethylene solubility also increases with the increase of the alkyl chain in the anion of imidazolium based ionic liquids as can be evaluated by comparing the gas solubility in  $[\text{C}_1\text{C}_4\text{Im}][\text{OAc}]$  and in  $[\text{C}_1\text{C}_4\text{Im}][n\text{-C}_{15}\text{H}_{31}\text{COO}]$  or in  $[\text{C}_1\text{C}_4\text{Im}][n\text{-C}_{15}\text{H}_{31}\text{COO}]$  and in  $[\text{C}_1\text{C}_4\text{Im}][n\text{-C}_{17}\text{H}_{35}\text{COO}]$ . The same effect is observed when the alkyl chain in the anion is fluorinated, the solubility of ethylene being larger in  $[\text{C}_1\text{C}_n\text{Im}][\text{BETI}]$  than in  $[\text{C}_1\text{C}_n\text{Im}][\text{NTf}_2]$  ionic liquids.

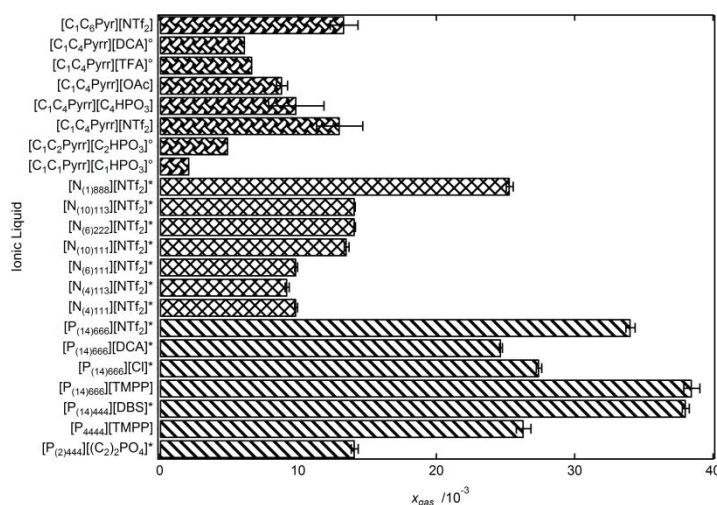
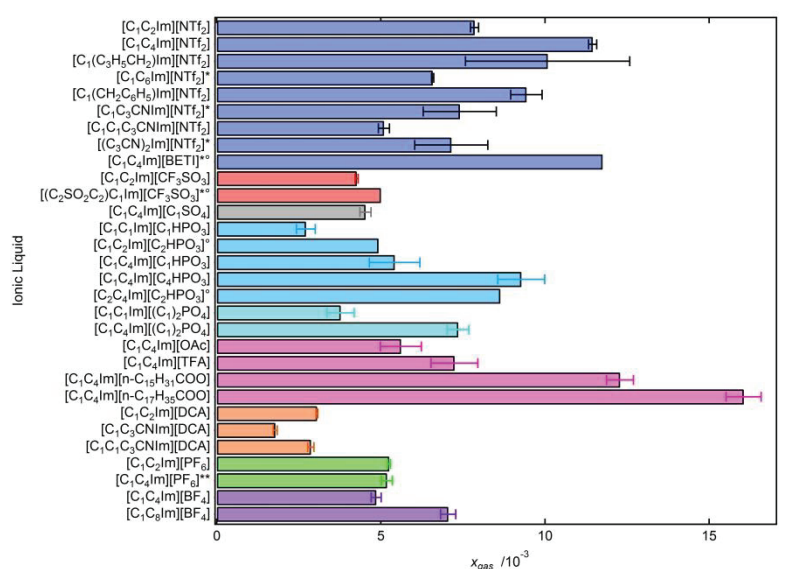


Figure 23.4 - Mole fraction solubility for ethylene in imidazolium based ionic liquids (top) and in pyridinium, pyrrolidinium, ammonium and phosphonium based ionic liquids (bottom) at 313 K. \* - at 303 K; \*\* - at 323 K; ° - Uncertainty not indicated by the authors.

[C<sub>1</sub>C<sub>2</sub>Im][NTf<sub>2</sub>]<sup>33</sup>; [C<sub>1</sub>C<sub>4</sub>Im][NTf<sub>2</sub>]<sup>25</sup>; C<sub>1</sub>(C<sub>3</sub>H<sub>5</sub>CH<sub>2</sub>)Im][NTf<sub>2</sub>]<sup>25</sup>; [C<sub>1</sub>C<sub>6</sub>Im][NTf<sub>2</sub>]<sup>35, 36</sup>; [C<sub>1</sub>(CH<sub>2</sub>C<sub>6</sub>H<sub>5</sub>)Im][NTf<sub>2</sub>]<sup>25</sup>; [C<sub>1</sub>C<sub>3</sub>CNIm][NTf<sub>2</sub>]<sup>27</sup>; [C<sub>1</sub>C<sub>1</sub>C<sub>3</sub>CNIm][NTf<sub>2</sub>]<sup>37, 38</sup>; [(C<sub>3</sub>CN)<sub>2</sub>Im][NTf<sub>2</sub>]<sup>27</sup>; [C<sub>1</sub>C<sub>4</sub>Im][BETI]<sup>35</sup>; [C<sub>1</sub>C<sub>2</sub>Im][CF<sub>3</sub>SO<sub>3</sub>]<sup>13</sup>; [(C<sub>2</sub>SO<sub>2</sub>C<sub>2</sub>)C<sub>1</sub>Im][CF<sub>3</sub>SO<sub>3</sub>]<sup>35, 36</sup>; [C<sub>1</sub>C<sub>4</sub>Im][C<sub>1</sub>SO<sub>4</sub>]<sup>10</sup>; [C<sub>1</sub>C<sub>1</sub>Im][C<sub>1</sub>HPO<sub>3</sub>]<sup>10</sup>; [C<sub>1</sub>C<sub>2</sub>Im][C<sub>2</sub>HPO<sub>3</sub>]<sup>39</sup>; [C<sub>1</sub>C<sub>4</sub>Im][C<sub>1</sub>HPO<sub>3</sub>]<sup>10</sup>; [C<sub>1</sub>C<sub>4</sub>Im][C<sub>4</sub>HPO<sub>3</sub>]<sup>10</sup>; [C<sub>2</sub>C<sub>4</sub>Im][C<sub>2</sub>HPO<sub>3</sub>]<sup>39</sup>; [C<sub>1</sub>C<sub>1</sub>Im][(C<sub>1</sub>)<sub>2</sub>PO<sub>4</sub>]<sup>10</sup>; [C<sub>1</sub>C<sub>4</sub>Im][(C<sub>1</sub>)<sub>2</sub>PO<sub>4</sub>]<sup>10</sup>; [C<sub>1</sub>C<sub>4</sub>Im][OAc]<sup>10</sup>; [C<sub>1</sub>C<sub>4</sub>Im][TFA]<sup>10</sup>; [C<sub>1</sub>C<sub>4</sub>Im][n-C<sub>15</sub>H<sub>31</sub>COO]<sup>38</sup>; [C<sub>1</sub>C<sub>2</sub>Im][DCA]<sup>13</sup>; [C<sub>1</sub>C<sub>3</sub>CNIm][DCA]<sup>37, 38</sup>; [C<sub>1</sub>C<sub>1</sub>C<sub>3</sub>CNIm][DCA]<sup>37, 38</sup>; [C<sub>1</sub>C<sub>2</sub>Im][PF<sub>6</sub>]<sup>13</sup>; [C<sub>1</sub>C<sub>4</sub>Im][PF<sub>6</sub>]<sup>30, 40</sup>; [C<sub>1</sub>C<sub>4</sub>Im][BF<sub>4</sub>]<sup>10</sup>; [C<sub>1</sub>C<sub>8</sub>Im][BF<sub>4</sub>]<sup>38</sup>; [C<sub>1</sub>C<sub>6</sub>Pyrr][NTf<sub>2</sub>]<sup>31</sup>; [C<sub>1</sub>C<sub>4</sub>Pyrr][NTf<sub>2</sub>]<sup>10</sup>; [C<sub>1</sub>C<sub>4</sub>Pyrr][DCA]<sup>41</sup>; [C<sub>1</sub>C<sub>4</sub>Pyrr][OAc]<sup>10, 41</sup>; [C<sub>1</sub>C<sub>4</sub>Pyrr][TFA]<sup>41</sup>; [C<sub>1</sub>C<sub>1</sub>Pyrr][C<sub>1</sub>HPO<sub>3</sub>]<sup>41</sup>; [C<sub>1</sub>C<sub>2</sub>Pyrr][C<sub>2</sub>HPO<sub>3</sub>]<sup>41</sup>; [C<sub>1</sub>C<sub>4</sub>Pyrr][C<sub>4</sub>HPO<sub>3</sub>]<sup>10</sup>; [N<sub>(4)111</sub>][NTf<sub>2</sub>]<sup>35, 36, 42</sup>; [N<sub>(4)113</sub>][NTf<sub>2</sub>]<sup>35, 36, 42</sup>; [N<sub>(6)111</sub>][NTf<sub>2</sub>]<sup>35, 36, 42</sup>; [N<sub>(6)222</sub>][NTf<sub>2</sub>]<sup>35, 36, 42</sup>; [N<sub>(10)111</sub>][NTf<sub>2</sub>]<sup>35, 36, 42</sup>; [N<sub>(10)113</sub>][NTf<sub>2</sub>]<sup>35, 36, 42</sup>; [N<sub>(1)888</sub>][NTf<sub>2</sub>]<sup>35, 36, 42</sup>; [P<sub>(14)666</sub>][NTf<sub>2</sub>]<sup>35, 36, 43</sup>; [P<sub>(14)666</sub>][DCA]<sup>35, 36, 43</sup>; [P<sub>(2)444</sub>][(C<sub>2</sub>)<sub>2</sub>PO<sub>4</sub>]<sup>35, 36, 43</sup>; [P<sub>(14)666</sub>][Cl]<sup>35, 36, 43, 44</sup>; [P<sub>(14)444</sub>][DBS]<sup>35, 43</sup>; [P<sub>4444</sub>][TMPP]<sup>33</sup>; [P<sub>(14)666</sub>][TMPP]<sup>33, 34</sup>.

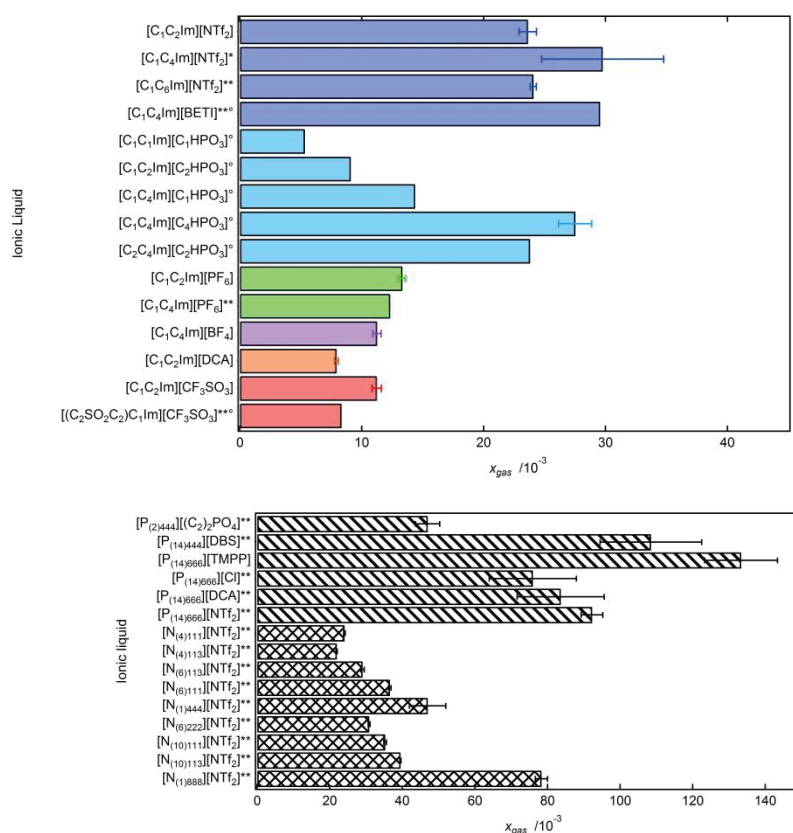


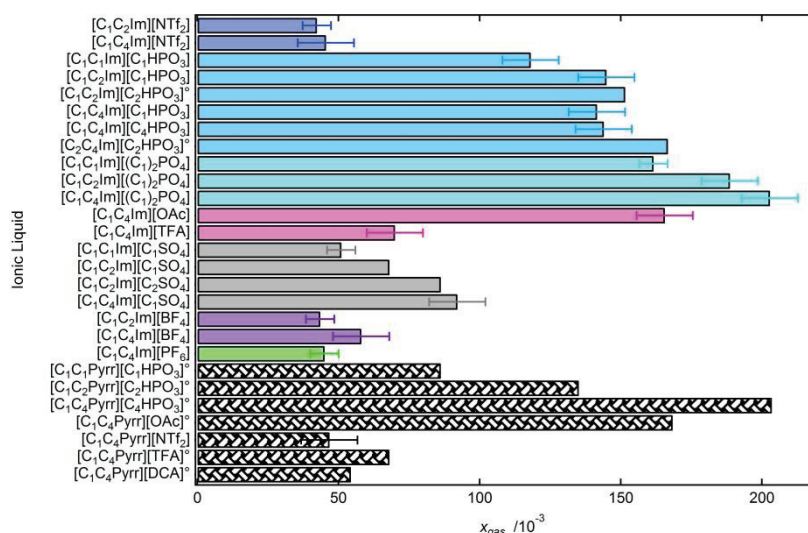
Figure 23.5 - Mole fraction solubility for propylene in imidazolium based ionic liquids (top) and in ammonium and phosphonium based ionic liquids (bottom) at 313 K. \* - at 320 K; \*\* - at 303 K; ° - Uncertainty not indicated by the authors.

[C<sub>1</sub>C<sub>2</sub>Im][NTf<sub>2</sub>]<sup>13</sup>; [C<sub>1</sub>C<sub>4</sub>Im][NTf<sub>2</sub>]<sup>24</sup>; [C<sub>1</sub>C<sub>6</sub>Im][NTf<sub>2</sub>]<sup>35, 36</sup>; [C<sub>1</sub>C<sub>4</sub>Im][BETI]<sup>35</sup>; [C<sub>1</sub>C<sub>1</sub>Im][C<sub>1</sub>HPO<sub>3</sub>]<sup>39</sup>; [C<sub>1</sub>C<sub>2</sub>Im][C<sub>2</sub>HPO<sub>3</sub>]<sup>39</sup>; [C<sub>1</sub>C<sub>4</sub>Im][C<sub>1</sub>HPO<sub>3</sub>]<sup>39</sup>; [C<sub>1</sub>C<sub>4</sub>Im][C<sub>4</sub>HPO<sub>3</sub>]<sup>39</sup>; [C<sub>2</sub>C<sub>4</sub>Im][C<sub>2</sub>HPO<sub>3</sub>]<sup>39</sup>; [C<sub>1</sub>C<sub>2</sub>Im][PF<sub>6</sub>]<sup>13</sup>; [C<sub>1</sub>C<sub>4</sub>Im][PF<sub>6</sub>]<sup>35, 36, 44</sup>; [C<sub>1</sub>C<sub>4</sub>Im][BF<sub>4</sub>]<sup>13</sup>; [C<sub>1</sub>C<sub>2</sub>Im][DCA]<sup>13</sup>; [C<sub>1</sub>C<sub>2</sub>Im][CF<sub>3</sub>SO<sub>3</sub>]<sup>13</sup>; [(C<sub>2</sub>SO<sub>2</sub>C<sub>2</sub>)C<sub>1</sub>Im][CF<sub>3</sub>SO<sub>3</sub>]<sup>35, 36</sup>; [N<sub>(4)111</sub>][NTf<sub>2</sub>]<sup>35, 36, 42</sup>; [N<sub>(4)113</sub>][NTf<sub>2</sub>]<sup>35, 36, 42</sup>; [N<sub>(6)111</sub>][NTf<sub>2</sub>]<sup>35, 36, 42</sup>; [N<sub>(6)113</sub>][NTf<sub>2</sub>]<sup>35, 36, 42</sup>; [N<sub>(1)444</sub>][NTf<sub>2</sub>]<sup>42</sup>; [N<sub>(6)222</sub>][NTf<sub>2</sub>]<sup>35, 36, 42</sup>; [N<sub>(10)111</sub>][NTf<sub>2</sub>]<sup>35, 36, 42</sup>; [N<sub>(10)113</sub>][NTf<sub>2</sub>]<sup>35, 36, 42</sup>; [N<sub>(1)888</sub>][NTf<sub>2</sub>]<sup>35, 36, 42</sup>; [P<sub>(14)666</sub>][NTf<sub>2</sub>]<sup>35, 36, 43</sup>; [P<sub>(2)444</sub>][(C<sub>2</sub>)<sub>2</sub>PO<sub>4</sub>]<sup>35, 36, 43</sup>; [P<sub>(14)666</sub>][Cl]<sup>35, 36, 43</sup>; [P<sub>(14)666</sub>][DCA]<sup>35, 36, 43</sup>; [P<sub>(14)444</sub>][DBS]<sup>35, 43</sup>; [P<sub>(14)666</sub>][TMPP]<sup>34</sup>.

Functionalizing the alkyl side-chains of the ionic liquid can have very different effects on the ethylene or propylene solubility. For example, ethylene solubility is lower in  $[C_1C_2Im][CF_3SO_3]$  than in  $[(C_2SO_2C_2)C_1Im][CF_3SO_3]$  while significantly higher than in  $[C_1C_3CNIm][DCA]$ . The presence of polar groups in the side chain of the cation of the ionic liquid can increase or decrease ethylene solubility, while it was observed that it always seems to decrease ethane solubility. The absence of the imidazolium acidic proton in  $[C_1C_1C_3CNIm][DCA]$  seems to significantly increase the solubility of ethylene as can be observed by comparing  $[C_1C_3CNIm][DCA]$  and  $[C_1C_1C_3CNIm][DCA]$ .

### 23.5 Acetylene and methyl acetylene solubility

The acetylene and methyl acetylene mole fraction solubility in different ionic liquids at 313 K is depicted in Figure 23.6. For acetylene, 27 different ionic liquids were studied (20 based in the imidazolium cation and 7 based in pyrrolidinium cations), the mole fraction gas solubility ranging from  $42.4 \times 10^{-3}$  in  $[C_1C_2Im][NTf_2]$  to  $204 \times 10^{-3}$  in  $[C_1C_4Im][(C_1)_2PO_4]$  and  $[C_1C_4Pyrr][(C_4HPO_3)]$ . For methyl acetylene, 17 imidazolium based ionic liquids were studied and the mole fraction gas solubility varies in this case from  $58.5 \times 10^{-3}$  in  $[C_1C_1Im][C_1SO_4]$  to  $156 \times 10^{-3}$  in  $[C_1C_4Im][(C_4)_2PO_4]$ . Both gases, acetylene and methyl acetylene, are much more soluble in the ionic liquids studied than the four lighter gases reviewed above.



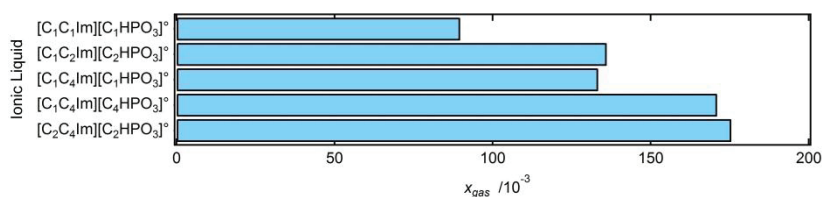


Figure 23.6 - Mole fraction solubility for acetylene (top) and methyl acetylene (bottom) in different ionic liquids at 313 K. ° - Uncertainty not indicated by the authors.

[C<sub>1</sub>C<sub>2</sub>Im][NTf<sub>2</sub>]<sup>45</sup>; [C<sub>1</sub>C<sub>4</sub>Im][NTf<sub>2</sub>]<sup>45</sup>; [C<sub>1</sub>C<sub>1</sub>Im][C<sub>1</sub>HPO<sub>3</sub>]<sup>39, 45</sup>; [C<sub>1</sub>C<sub>2</sub>Im][C<sub>1</sub>HPO<sub>3</sub>]<sup>45</sup>; [C<sub>1</sub>C<sub>2</sub>Im][C<sub>2</sub>HPO<sub>3</sub>]<sup>39</sup>; [C<sub>1</sub>C<sub>4</sub>Im][C<sub>1</sub>HPO<sub>3</sub>]<sup>39, 45</sup>; [C<sub>1</sub>C<sub>4</sub>Im][C<sub>4</sub>HPO<sub>3</sub>]<sup>10, 39</sup>; [C<sub>2</sub>C<sub>4</sub>Im][C<sub>2</sub>HPO<sub>3</sub>]<sup>39</sup>; [C<sub>1</sub>C<sub>1</sub>Im][(C<sub>1</sub>)<sub>2</sub>PO<sub>4</sub>]<sup>45</sup>; [C<sub>1</sub>C<sub>2</sub>Im][(C<sub>1</sub>)<sub>2</sub>PO<sub>4</sub>]<sup>45</sup>; [C<sub>1</sub>C<sub>4</sub>Im][(C<sub>1</sub>)<sub>2</sub>PO<sub>4</sub>]<sup>45</sup>; [C<sub>1</sub>C<sub>4</sub>Im][OAc]<sup>45</sup>; [C<sub>1</sub>C<sub>4</sub>Im][TFA]<sup>45</sup>; [C<sub>1</sub>C<sub>1</sub>Im][C<sub>1</sub>SO<sub>4</sub>]<sup>45</sup>; [C<sub>1</sub>C<sub>1</sub>Im][C<sub>1</sub>SO<sub>4</sub>]<sup>45</sup>; [C<sub>1</sub>C<sub>1</sub>Im][C<sub>1</sub>SO<sub>4</sub>]<sup>45</sup>; [C<sub>1</sub>C<sub>2</sub>Im][BF<sub>4</sub>]<sup>45</sup>; [C<sub>1</sub>C<sub>4</sub>Im][BF<sub>4</sub>]<sup>45</sup>; [C<sub>1</sub>C<sub>4</sub>Im][PF<sub>6</sub>]<sup>45</sup>; [C<sub>1</sub>C<sub>1</sub>Pyrr][C<sub>1</sub>HPO<sub>3</sub>]<sup>41</sup>; [C<sub>1</sub>C<sub>2</sub>Pyrr][C<sub>2</sub>HPO<sub>3</sub>]<sup>41</sup>; [C<sub>1</sub>C<sub>4</sub>Pyrr][C<sub>4</sub>HPO<sub>3</sub>]<sup>41</sup>; [C<sub>1</sub>C<sub>4</sub>Pyrr][OAc]<sup>41</sup>; [C<sub>1</sub>C<sub>4</sub>Pyrr][NTf<sub>2</sub>]<sup>45</sup>; [C<sub>1</sub>C<sub>4</sub>Pyrr][TFA]<sup>41</sup>; [C<sub>1</sub>C<sub>4</sub>Pyrr][DCA]<sup>41</sup>.

Contrary to what was found for ethane, ethylene, propane and propylene, the solubility of acetylene does not always increase when the side alkyl chain of the cation or of the anion increases. For example, almost no change in acetylene solubility is observed when comparing [C<sub>1</sub>C<sub>2</sub>Im][NTf<sub>2</sub>] and [C<sub>1</sub>C<sub>4</sub>Im][NTf<sub>2</sub>], [C<sub>1</sub>C<sub>2</sub>Im][C<sub>1</sub>HPO<sub>3</sub>] and [C<sub>1</sub>C<sub>2</sub>Im][C<sub>2</sub>HPO<sub>3</sub>], [C<sub>1</sub>C<sub>2</sub>Im][C<sub>1</sub>HPO<sub>3</sub>] and [C<sub>1</sub>C<sub>4</sub>Im][C<sub>1</sub>HPO<sub>3</sub>], [C<sub>1</sub>C<sub>4</sub>Im][C<sub>1</sub>HPO<sub>3</sub>] and [C<sub>1</sub>C<sub>4</sub>Im][C<sub>4</sub>HPO<sub>3</sub>], or [C<sub>1</sub>C<sub>2</sub>Im][(C<sub>1</sub>)<sub>2</sub>PO<sub>4</sub>] and [C<sub>1</sub>C<sub>4</sub>Im][(C<sub>1</sub>)<sub>2</sub>PO<sub>4</sub>]. For pyrrolidinium based ionic liquids, a systematic increase of the solubility of acetylene with the alkyl size of the cation or anion of the ionic liquid is observed.

For all the cations studied, the solubility of acetylene generally follows the order for the anions: C<sub>n</sub>C<sub>m</sub>PO<sub>4</sub><sup>-</sup> > OAc > C<sub>n</sub>HPO<sub>3</sub><sup>-</sup> > C<sub>n</sub>SO<sub>4</sub><sup>-</sup> > BF<sub>4</sub><sup>-</sup> > TFA<sup>-</sup> > PF<sub>6</sub><sup>-</sup> = NTf<sub>2</sub><sup>-</sup>. Some exceptions are observed as for example no change in acetylene solubility was found between [C<sub>1</sub>C<sub>2</sub>Im][NTf<sub>2</sub>] and [C<sub>1</sub>C<sub>2</sub>Im][BF<sub>4</sub>].

## 23.6 Selectivity and performance

The ideal selectivity of an ionic liquid for a particular gas in a mixture,  $\square$ , can be defined as a ratio of Henry's law constants:

$$\square = \frac{K_H^1}{K_H^2} \quad (7)$$

where,  $K_H^1$  is the Henry's law constant of the lightest gas. The calculated ideal selectivity is plotted as a function of the absorption of the unsaturated gas for the

pairs ethane/ethylene, ethylene/acetylene, propane/propylene and propylene/methyl acetylene, in Figures 23.7 and 23.8, respectively.

In general, the highest ideal selectivities are found for the separation of unsaturated gases and the increase of the ionic liquid unsaturated gas absorption corresponds to a lower selectivity for this gas.

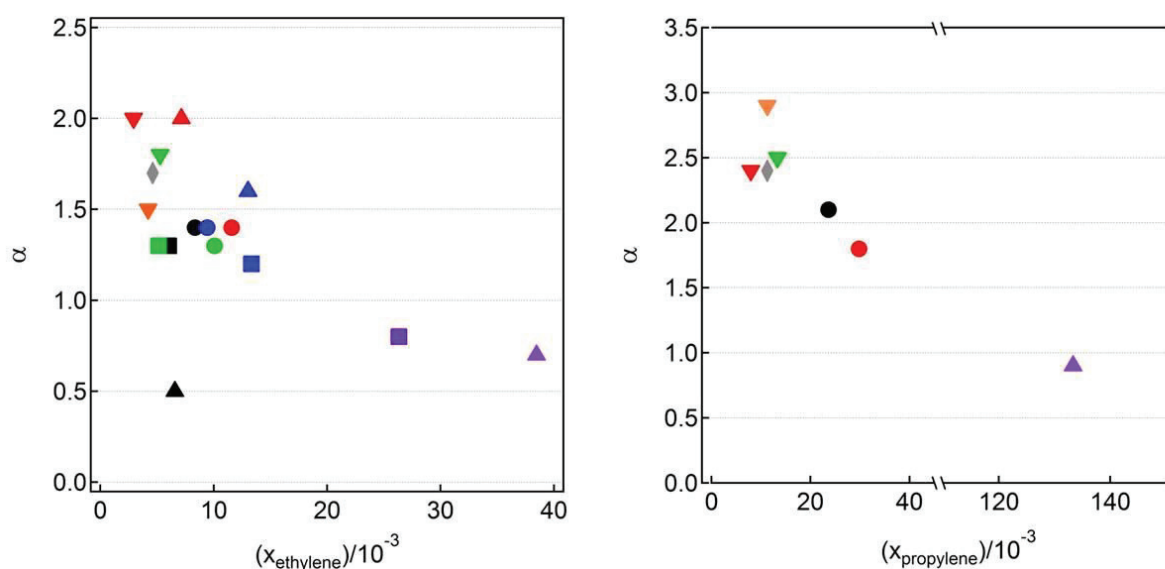


Figure 23.7 - Ethane/ethylene ideal selectivity versus ethylene absorption (left-hand side) and propane/propylene ideal selectivity versus propylene absorption (right-hand side) in the ionic liquids: ●, [C<sub>1</sub>C<sub>2</sub>Im][NTf<sub>2</sub>]; ●, [C<sub>1</sub>C<sub>4</sub>Im][NTf<sub>2</sub>]; ●, [C<sub>1</sub>(C<sub>3</sub>H<sub>5</sub>CH<sub>2</sub>)Im][NTf<sub>2</sub>]; ▲, [C<sub>1</sub>C<sub>6</sub>Im][NTf<sub>2</sub>]\*; ●, [C<sub>1</sub>(CH<sub>2</sub>C<sub>6</sub>H<sub>5</sub>)Im][NTf<sub>2</sub>]; ■, [C<sub>1</sub>C<sub>3</sub>CNIIm][NTf<sub>2</sub>]\*; ▲, [(C<sub>3</sub>CN)<sub>2</sub>Im][NTf<sub>2</sub>]\*; ▼, [C<sub>1</sub>C<sub>2</sub>Im][PF<sub>6</sub>]; ■, [C<sub>1</sub>C<sub>4</sub>Im][PF<sub>6</sub>]\*; ▼, [C<sub>1</sub>C<sub>2</sub>Im][DCA]; ▼, [C<sub>1</sub>C<sub>4</sub>Im][BF<sub>4</sub>]; ◆, [C<sub>1</sub>C<sub>2</sub>Im][CF<sub>3</sub>SO<sub>3</sub>]; ■, [P<sub>4444</sub>][TMPP]; ▲, [P<sub>(14)666</sub>][TMPP]; ▲, [C<sub>1</sub>C<sub>4</sub>Pyrr][NTf<sub>2</sub>] and ■, [C<sub>1</sub>C<sub>6</sub>Pyr][NTf<sub>2</sub>] at 313 K. \* at 303 K for the ethane/ethylene separation.

[C<sub>1</sub>C<sub>1</sub>Im][C<sub>1</sub>HPO<sub>3</sub>] and [C<sub>1</sub>C<sub>1</sub>Pyrr][C<sub>1</sub>HPO<sub>3</sub>] present the highest ethylene/acetylene ideal selectivities, 43 and 40, respectively. Ionic liquids containing NTf<sub>2</sub><sup>-</sup>, DCA<sup>-</sup>, TFA<sup>-</sup>, BF<sub>4</sub><sup>-</sup> or PF<sub>6</sub><sup>-</sup> anions present both low acetylene absorption capacities and low ideal selectivity for the ethylene/acetylene separation.

The maximum values for the ideal selectivities for propylene/acetylene separation are half of the values observed for ethylene/acetylene separation. As for ethylene/acetylene, they are observed for ionic liquids based in imidazolium cations having short alkyl chains associated to phosphorous anions – [C<sub>1</sub>C<sub>1</sub>Im][C<sub>1</sub>HPO<sub>3</sub>] and [C<sub>1</sub>C<sub>1</sub>Im][(C<sub>1</sub>)<sub>2</sub>PO<sub>4</sub>], with selectivities of 17 and 16, respectively.

With the lowest values for the ideal selectivity and absorption capacity, the ethane/ethylene separation seems to be the most difficult to perform with ionic liquids as far as these criteria are concerned. The ionic liquids [C<sub>1</sub>C<sub>2</sub>Im][DCA], [(C<sub>3</sub>CN)<sub>2</sub>Im][NTf<sub>2</sub>] and [C<sub>1</sub>C<sub>2</sub>Im][PF<sub>6</sub>] present the highest ideal selectivity for the

ethane/ethylene separation, 2 for the two first and 1.8 for the third. The presence of a CN group seems to have a positive effect in the ideal selectivity however leading to lower absorption capacities.

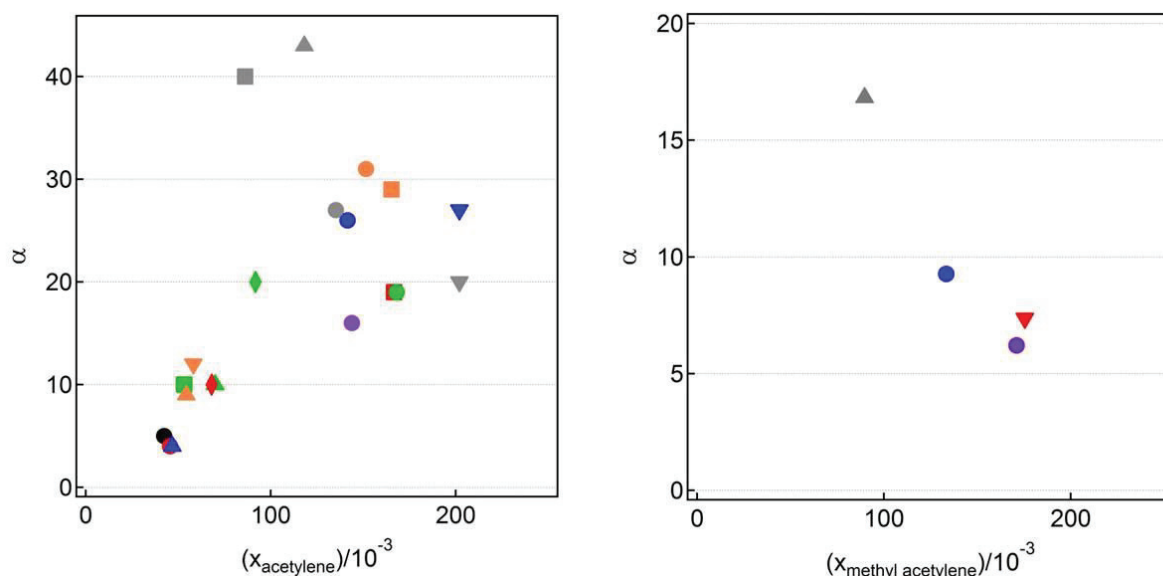


Figure 23.8 - Ethylene/acetylene ideal selectivity versus acetylene absorption (left-hand side) and propylene/methyl acetylene ideal selectivity versus methyl acetylene absorption (right-hand side) in the ionic liquids ●, [C<sub>1</sub>C<sub>2</sub>Im][NTf<sub>2</sub>]; ●, [C<sub>1</sub>C<sub>4</sub>Im][NTf<sub>2</sub>]; ■, [C<sub>1</sub>C<sub>4</sub>Im][PF<sub>6</sub>]\*; ◆, [C<sub>1</sub>C<sub>2</sub>Im][BF<sub>4</sub>]; ▼, [C<sub>1</sub>C<sub>4</sub>Im][BF<sub>4</sub>]; ▲, [C<sub>1</sub>C<sub>4</sub>Im][TFA]; ■, [C<sub>1</sub>C<sub>4</sub>Im][OAc]; ▲, [C<sub>1</sub>C<sub>1</sub>Im][C<sub>1</sub>HPO<sub>3</sub>]; ◆, [C<sub>1</sub>C<sub>2</sub>Im][C<sub>1</sub>HPO<sub>3</sub>]; ●, [C<sub>1</sub>C<sub>2</sub>Im][C<sub>2</sub>HPO<sub>3</sub>]; ●, [C<sub>1</sub>C<sub>4</sub>Im][C<sub>1</sub>HPO<sub>3</sub>]; ●, [C<sub>1</sub>C<sub>4</sub>Im][C<sub>4</sub>HPO<sub>3</sub>]; ▼, [C<sub>2</sub>C<sub>4</sub>Im][C<sub>2</sub>HPO<sub>3</sub>]; ▼, [C<sub>1</sub>C<sub>1</sub>Im][(C<sub>1</sub>)<sub>2</sub>PO<sub>4</sub>]; ◆, [C<sub>1</sub>C<sub>2</sub>Im][(C<sub>1</sub>)<sub>2</sub>PO<sub>4</sub>]; ▲, [C<sub>1</sub>C<sub>2</sub>Im][(C<sub>2</sub>)<sub>2</sub>PO<sub>4</sub>]; ▼, [C<sub>1</sub>C<sub>4</sub>Im][(C<sub>1</sub>)<sub>2</sub>PO<sub>4</sub>]; ■, [C<sub>1</sub>C<sub>4</sub>Im][(C<sub>2</sub>)<sub>2</sub>PO<sub>4</sub>]; ◆, [C<sub>1</sub>C<sub>1</sub>Im][C<sub>1</sub>SO<sub>4</sub>]; ▼, [C<sub>1</sub>C<sub>2</sub>Im][C<sub>1</sub>SO<sub>4</sub>]; ●, [C<sub>1</sub>C<sub>2</sub>Im][C<sub>2</sub>SO<sub>4</sub>]; ◆, [C<sub>1</sub>C<sub>4</sub>Im][C<sub>1</sub>SO<sub>4</sub>]; ■, [C<sub>1</sub>C<sub>1</sub>Pyrr][C<sub>1</sub>HPO<sub>3</sub>]; ●, [C<sub>1</sub>C<sub>2</sub>Pyrr][C<sub>2</sub>HPO<sub>3</sub>]; ▼, [C<sub>1</sub>C<sub>4</sub>Pyrr][C<sub>4</sub>HPO<sub>3</sub>]; ●, [C<sub>1</sub>C<sub>4</sub>Pyrr][OAc]; ▲, [C<sub>1</sub>C<sub>4</sub>Pyrr][NTf<sub>2</sub>]; ◆, [C<sub>1</sub>C<sub>4</sub>Pyrr][TFA] and ▲, [C<sub>1</sub>C<sub>4</sub>Pyrr][DCA] at 313 K. \* at 303 K for the ethylene/acetylene separation

For all separations, the increase of the alkyl chain in the cation or in the anion, leads to a decrease in the values of the ideal selectivity, and to an increase of the absorption capacity of the ionic liquid. This increase seems to be less important for the case of ethane/ethylene.

## 23.7 Conclusions

The solubilities of ethane, ethylene, acetylene, propane, propylene and methyl acetylene in pure ionic liquids were presented. The potential of the use of different ionic liquids as separating agents for gaseous mixtures of saturated and unsaturated gases was analysed on the basis of their ideal selectivities as absorption capacities.

The highest gas solubilities are observed for acetylene in  $[C_1C_4Im][(C_1)_2PO_4]$  and  $[C_1C_4Pyr][C_4HPO_3]$  with a 0.20 mole fraction at 313 K and 1 bar. The maximum mole fraction solubilities reported for propane and propylene in the same conditions, are 0.15 and 0.13 in  $[P_{(14)666}][TMPP]$ , respectively. For ethane and ethylene the maximum mole fraction solubilities are much lower – 0.052 and 0.038 in  $[P_{(14)666}][TMPP]$ , respectively.

If the cations forming the ionic liquids are considered, the solubility of ethane and propane follows the order:  $P_{nmpq}^+ > C_nC_mIm^+ > C_nPyr^+ > C_nC_mPyr^+ > N_{nmpq}^+$ . For ethylene and propylene the solubility order is:  $P_{nmpq}^+ > N_{nmpq}^+ > C_nPyr^+ > C_nC_mPyr^+ > C_nC_mIm^+$ . The solubility of acetylene has been reported only in imidazolium and pyrrolidinium based ionic liquids and the solubility order is confirmed. For methyl acetylene, only imidazolium based ionic liquids were studied.

Imidazolium-based ionic liquids containing large anions such as large carboxylates,  $BETI^-$ ,  $FAP^-$ ,  $C_8SO_4^-$ ,  $NTf_2^-$ , heavy phosphates and phosphites present higher ethane, ethylene, propane and propylene solubility, followed by  $PF_6^-$ ,  $CF_3SO_3^-$ ,  $BF_4^-$  and  $DCA^-$  based ionic liquids. The order of solubility of acetylene and methyl acetylene relative to the anions in the ionic liquids is:  $C_nC_mPO_4^- > OAc^- > C_nHPO_3^- > C_nSO_4^- > BF_4^- > TFA^- > PF_6^- = NTf_2^-$ .

Ionic liquids present great potential for light hydrocarbon separation, especially in the case of ethylene/acetylene and propylene/methyl acetylene separations, with ideal selectivities of over 40 in the first case and over 15 in the second and corresponding mole fraction absorptions between 0.1 and 0.2.

## 23.8 References

- <sup>1</sup>. E. J. Henley; J. D. Seader and D. K. Roper, *Separation Process Principles*. 3rd Ed., John Wiley & Sons, 2011.
- <sup>2</sup>. M. S. Avgidou; S. P. Kaldis; G. P. Sakellariopoulos, *J. Membrane Sci.*, 2004, **233**, 21-37
- <sup>3</sup>. R. B. Eldrige, *Ind. Eng. Chem. Res.*, 1993, **32**, 2208-2212
- <sup>4</sup>. R. W. Baker, *Ind. Eng. Chem. Res.*, 2002, **41**, 1393-1411
- <sup>5</sup>. K. Keyvanloo; J. Towfighi; S. M. Sadrameli; A. Mohamadalizadeh, *J. Anal. Appl. Pyrol.*, 2010, **87**, 224-230
- <sup>6</sup>. E. J. Henley, J. D. Seader and D. K. Roper, *Separation Process Principles: 3rd Edition*, John Wiley & Sons, 2011
- <sup>7</sup>. D. J. Safarik; R. B. Eldridge, *Ind. Eng. Chem. Res.*, 1998, **37**, 2571-2581

- 
- <sup>8</sup>. M. F. Asaro, Sorbents and Processes for Separation of Olefins from Paraffins. US2009 0143632A1
- <sup>9</sup>. Y. Hu, Z. Liu, C. Xu, and X. Zhang, **Chem. Soc. Rev.**, 2011, **40**, 3802-3823
- <sup>10</sup>. J. Palgunadi, H. S. Kim, J. M. Lee and S. Jung, *Chem. Eng. Process.* 2010, **49**, 192-198
- <sup>11</sup>. M. Jin, Y. Hou, W. Wu, S. Ren, S. Tian, L. Xiao and Z. Lei, *J. Phys. Chem. B*, 2011, **115**, 6585-6591
- <sup>12</sup>. M. B. Shiflett, A. M. S. Niehaus and A. Yokozeki, *J. Phys. Chem. B*, 2011, **115**, 3478-3487
- <sup>13</sup>. D. Camper, C. Becker, C. Koval and R. Noble, *Ind. Eng. Chem. Res.*, 2005, **44**, 1928-1933
- <sup>14</sup>. J. Jacquemin, M. F. Costa Gomes, P. Husson and V. Majer, *J. Chem. Thermodyn.*, 2006, **38**, 490-502
- <sup>15</sup>. K. Denbigh, "The Principles of Chemical Equilibrium", 4th edition, CUP, Cambridge, 1981.
- <sup>16</sup>. J. M. Smith, H. C. Van Ness, M. M. Abbott, "Introduction to Chemical Engineering Thermodynamics", 5th edition, McGraw Hill, NY, 1996.
- <sup>17</sup>. J. M. Prausnitz, R. N. Lichtenthaler, E. Gomes de Azevedo, "Molecular Thermodynamics of Fluid-Phase Equilibria", 3rd edition, Prentice Hall, NJ, 1999.
- <sup>18</sup>. A. Ben-Naim, "Statistical Thermodynamics for Chemists and Biochemists", Plenum Press, New York, 1992.
- <sup>19</sup>. V. Majer, J. Sedlbauer, R.H. Wood, in "Aqueous Systems at Elevated Temperatures and Pressures: Physical Chemistry in Water, Steam and Hydrothermal Solutions", ed. D.A. Palmer, R. Fernandez-Prini and A.H. Harvey, Elsevier, Amsterdam, 2004.
- <sup>20</sup>. B. B. Benson, D. Krause Jr., *J. Solution Chem.*, 1989, **18**, 803.
- <sup>21</sup>. D. Almantariotis, S. Stevanovic, O. Fandiño, A. S. Pensado, A. A. H. Padua, J.-Y. Coxam and M. F. Costa Gomes, *J. Phys. Chem. B*, 2012, **116**, 7728-7738
- <sup>22</sup>. G. Hong, J. Jacquemin, M. Deetlefs, C. Hardacre, P. Husson, M. F. Costa Gomes, *Fluid Phase Equilib.*, 2007, **257**, 27-34
- <sup>23</sup>. M. F. Costa Gomes, L. Pison, A. S. Pensado and A. A. H. Padua, *Faraday Discuss.*, 2012, **154**, 41-52
- <sup>24</sup>. B. Lee and S. L. Outcalt, *J. Chem. Eng. Data*, 2006, **51**, 892-897
- <sup>25</sup>. L. Moura, M. Mishra, V. Bernalles, P. Fuentealba, A. A. H. Padua, C. C. Santini and M. F. Costa Gomes, *J. Phys. Chem. B*, 2013, **117**, 7416-7425
- <sup>26</sup>. M. F. Costa Gomes, *J. Chem. Eng. Data* 2007, **52**, 472-475
- <sup>27</sup>. H. Xing, X. Zhao, R. Li, Y. Yang, B. Su, Z. Bao, Y. Yang and Q. Ren, *ACS Sustainable Chem. Eng.*, 2013, **1**, 1357-1363
- <sup>28</sup>. Y. Deng, S. Morrissey, N. Gathergood, A. Delort, P. Husson, and M. F. Costa Gomes, *ChemSusChem* 2010, **3**, 377-385
- <sup>29</sup>. D. Camper, C. Becker, C. Koval and R. Noble, *Ind. Eng. Chem. Res.*, 2005, **44**, 1928-1933
- <sup>30</sup>. J. L. Anthony, E. J. Maginn and J. F. Brennecke, *J. Phys. Chem. B*, 2002, **106**, 7315-7320
- <sup>31</sup>. J. L. Anderson, J. K. Dixon and J. F. Brennecke, *Acc. Chem. Res.*, 2007, **40**, 1208-1216
- <sup>32</sup>. S. Stevanovic, M. F. Costa Gomes, *J. Chem. Thermodyn.*, 2013, **59**, 65-71
- <sup>33</sup>. X. Liu, W. Afzal, and J. M. Prausnitz, *Ind. Eng. Chem. Res.*, 2013, **52**, 14975-14978
- <sup>34</sup>. X. Liu, W. Afzal, G. Yu, M. He, and J. M. Prausnitz, *J. Phys. Chem. B*, 2013, **117**, 10534-10539

- 
- <sup>35</sup>. P. K. Kilaru and P. Scovazzo, *Ind. Eng. Chem. Res.*, 2008, **47**, 910-919
- <sup>36</sup>. P. K. Kilaru, R. A. Condemarin and P. Scovazzo, *Ind. Eng. Chem. Res.*, 2008, **47**, 900-909
- <sup>37</sup>. Q. Zhang, Z. Li, J. Zhang, S. Zhang, L. Zhu, J. Yang, X. Zhang, and Y. Deng, *J. Phys. Chem. B*, 2007, **111**, 2864-2872
- <sup>38</sup>. J. Zhang, Q. Zhang, B. Qiao and Y. Deng, *J. Chem. Eng. Data*, 2007, **52**, 2277-2283
- <sup>39</sup>. J. M. Lee, J. Palgunadi, J. H. Kim, S. Jung, Y. Choi, M. Cheong and H. S. Kim, *Phys. Chem. Chem. Phys.*, 2010, **12**, 1812-1816
- <sup>40</sup>. J. L. Anthony, J. L. Anderson, E. J. Maginn and J. F. Brennecke, *J. Phys. Chem. B*, 2005, **109**, 6366-6374
- <sup>41</sup>. S. Jung, J. Palgunadi, J.H. Kim, H. Lee, B.S. Ahn, M. Cheong, H.S. Kim, *J. Membrane Sci.*, 2010, **354**, 63-67
- <sup>42</sup>. R. Condemarin, P. Scovazzo, *Chem. Eng. J.*, 2009, **147**, 51-57
- <sup>43</sup>. L. Ferguson and P. Scovazzo, *Ind. Eng. Chem. Res.* 2007, **46**, 1369-1374
- <sup>44</sup>. D. Morgan, L. Ferguson and P. Scovazzo, *Ind. Eng. Chem. Res.*, 2005, **44**, 4815-4823
- <sup>45</sup>. J. Palgunadi, S. Y. Hong, J. K. Lee, H. Lee, S. D. Lee, M. Cheong and H. S. Kim, *J. Phys. Chem. B*. 2011, **115**, 1067-1074